PHASE 2 INITIAL BOREHOLE DRILLING AND TESTING, IGNACE AREA

WP04C Data Report: Porewater Extraction and Analysis for IG_BH05

APM-REP-01332-0488 **December 2024**

WSP Canada Ltd. (and Hydroisotop GmbH)

nwmo
NUCLEAR WASTE MANAGEMENT ORGANIZATION
SOCIÉTÉ DE GESTION DES DÉCHETS NUCLÉAIRES

This report has been prepared under contract to NWMO. The report has been reviewed by NWMO, but the views and conclusions are those of the authors and do not necessarily represent those of the NWMO.

All copyright and intellectual property rights belong to NWMO.

Nuclear Waste Management Organization
22 St. Clair Avenue East, 4th Floor
Toronto, Ontario
M4T 2S3
Canada

Tel: 416-934-9814
Web: www.nwmo.ca

REPORT

PHASE 2 INITIAL BOREHOLE DRILLING AND TESTING AT IG_BH04/05/06

WP04C Data Report - Porewater Extraction and Analysis for IG_BH05

Submitted to:

Nuclear Waste Management Organization

4th Floor
22 St. Clair Avenue East
Toronto, Ontario, M4T 2S3

Submitted by:

WSP Canada Inc.
6925 Century Avenue, Suite #600, Mississauga, Ontario, L5N 7K2, Canada

+1 (905) 567 4444

NWMO Document: APM-REP-01332-0488

2001102 / 20253946

December 2024

Distribution List

e-copy - NWMO

e-copy - WSP

e-copy - Hydroisotop

WP4C DATA REPORT
POREWATER EXTRACTION AND ANALYSIS FOR IG_BH05

CLIENT INFORMATION

Project Name: Phase 2 Initial Borehole Drilling and Testing at IG_BH04/05/06, Ignace Area
Project Number: 20253946
Client PO Number: 2000141
Document Name: 20253946 IG_BH05 WP04C Rpt_Dec2024_R9a

Client:	Nuclear Waste Management Organization (NWMO)	
Address:	22 St. Clair Avenue East, 4th Floor	
City:	Toronto	
Province:	Ontario	
Postal Code:	M4T 2S3	
Client Contact:	Laura Kennell-Morrison	Warwick Watt
Telephone:	647-259-3737	437-972-3669
Email:	lkennell@nwmo.ca	wwatt@nwmo.ca

ISSUE/REVISION INDEX

Issue Code	Revision					Revision Details
	No.	By	Revd.	App.	Date	
RI	0	JI/FE	GWS	-	16.11.2022	Preliminary draft for information
RI	1a	JI/FE	GWS	-	17.05.2023	Internal draft for information
RR	1b	JI/FE	GWS	-	20.06.2023	Draft released for review and comment
RR	2a	JI/FE	GWS	-	07.07.2023	Revised draft for review and comment
RR	3b	JI/FE	GWS	-	05.12.2023	Revised draft for review and comment
RR	4a	JI/FE	GWS	-	05.03.2024	Final report for NWMO acceptance
RR	5a	FE	GWS	KDV	03.06.2024	Revised report for NWMO acceptance
RR	6a	FE	GWS	KDV	19.07.2024	Revised report for NWMO acceptance
RR	7a	FE	GWS		03.08.2024	Revised report for internal use
RI	8a	FE	GWS	KDV	18.11.2024	Revised report for NWMO acceptance
RI	9a	FE	GWS	KDV	09.12.2024	Final report released for information

Issue Codes: RR = Released for Review and Comments, RI = Released for Information

SIGNATURES

Prepared by: _____

Dr. Florian Eichinger
Hydroisotop GmbH

Reviewed by: _____

George Schneider, M.Sc., P.Geo.
Senior Geoscientist

Approved by: _____

Ken DeVos, M.Sc., P.Geo.
Senior Hydrogeochemist

Table of Contents

1.0 INTRODUCTION 1

1.1 Geological Setting 2

1.2 Technical Objectives 4

2.0 SAMPLING AND SAMPLE PREPARATION 6

2.1 Porewater Samples 6

2.2 Porewater Gas Samples 11

2.3 Core Logging Depth Correction 12

3.0 EXPERIMENTAL SET-UPS AND ANALYTICAL METHODS 12

3.1 Water Content and Water-Loss Porosity 12

3.2 Porewater Extraction Methods 14

3.2.1 Aqueous Extraction Experiments 14

3.2.2 Out-Diffusion Experiments 14

3.2.3 Isotope Diffusive Exchange Technique 16

3.3 Out-gassing Experiments to Extract Gases Dissolved in Porewater 17

3.3.1 Extraction and Quantification of Non-Inert gases (DG) Dissolved in Porewater 17

3.3.1.1 Quantification of Extracted Non-Inert Gases 17

3.3.1.2 Stable Isotope Analyses on Non-Inert Gases 19

3.3.2 Determination of Noble Gases (NG) Dissolved in Porewater 19

4.0 RESULTS OF WATER CONTENT AND WATER-LOSS POROSITY INVESTIGATIONS 20

4.1 Water Contents 20

4.1.1 Gravimetric Water Contents Determined on Aqueous Extraction Core Samples 20

4.1.2 Gravimetric Water Contents Determined on Porewater Cores 24

4.1.2.1 Gravimetric Water Contents Determined on End Pieces 24

4.1.3 Gravimetric Water Contents Determined on Out-Diffusion Cores 25

4.1.4 Gravimetric Water Contents Determined by Isotope Diffusive Exchange 28

4.1.5 Gravimetric Water Contents Determined on Out-Gassing Cores 32

4.1.6 Summary and Depth Profiles of Water Content Results 32

4.2 Bulk Dry/Wet Density and Water-Loss Porosity....34

5.0 RESULTS OF CHEMICAL COMPOSITION OF EXPERIMENT SOLUTIONS OF AQUEOUS EXTRACTION AND OUT-DIFFUSION EXPERIMENTS....37

5.1 Chemical Composition of Aqueous Extraction Solutions....38

5.2 Chemical Composition of Out-Diffusion Experiment Solutions....44

6.0 RESULTS FROM ELEMENTAL TIME SERIES AND PORE DIFFUSION COEFFICIENT OF CHLORIDE....51

6.1 Elemental Elution Curves....51

6.2 Modelling of Pore Diffusion Coefficients....85

7.0 RESULTS FROM CHLORIDE, BROMIDE AND CHLORIDE ISOTOPES IN POREWATER OF CORE SAMPLES FROM BOREHOLE IG_BH05....95

7.1 Porewater Chloride Concentrations Estimated by Aqueous Extraction Experiments....95

7.2 Porewater Chloride Concentrations and Bromide Concentrations and $\delta^{37}Cl$ Isotope Ratios Determined by Out-Diffusion Experiments....97

8.0 RESULTS FROM $\delta^{18}O$ AND $\delta^{2}H$ OF POREWATER OF CORE SAMPLES FROM IG_BH05....101

9.0 RESULTS FROM DISSOLVED GASES IN MATRIX POREWATER OF CORE SAMPLES FROM IG_BH05....105

9.1 Non-Inert Gases....107

9.1.1 Concentrations of Non-Inert Gases Dissolved in Porewater....107

9.1.1.1 Porewater Nitrogen-, Hydrogen- and Carbon Dioxide Concentrations....107

9.1.1.2 Porewater Hydrocarbon Gas Concentrations....108

9.1.2 Stable Isotope Signatures of Non-Inert Gases Dissolved in Porewater....110

9.2 Noble Gases....116

10.0 REFERENCES....121

TABLES

Table 2-1: Overview of the core samples taken from IG_BH05 for porewater investigations (PW = porewater samples, AQ = cores dedicated for aqueous extraction experiments, AR = retained samples, decided to be investigated after borehole completion)....7

Table 2-2: Overview of the analytical porewater program conducted on core samples from IG_BH05 (PW: porewater extraction, AQ: aqueous extraction)....9

Table 2-3: Overview of the core samples taken from IG_BH05 for porewater gas investigations (NG = noble gas; DG = non-inert dissolved gas; Hydro = HI = Hydroisotop; UoO = University of Oxford). 11

Table 2-4: Overview of the analytical porewater gas program conducted on core samples from IG_BH05 (NG = noble gas; DG = non-inert dissolved gas). 12

Table 4-1: Gravimetric water contents (WC) of aliquots of AQ core samples from IG_BH05 used for aqueous extraction experiments using wet (WC_{wet}) and dry masses (WC_{dry}) of the individual core pieces. The weighed values are calculated by using the individual masses; (G / T: granodiorite / tonalite, D: diabase). 22

Table 4-2: Gravimetric water contents (WC) of aliquots of PW core samples from IG_BH05 used for out-diffusion experiments using wet (WC_{wet}) and dry masses (WC_{dry}) of the individual core pieces. The weighed values are calculated by using the individual masses; (G / T: granodiorite / tonalite, D: diabase, A: amphibolite). 24

Table 4-3: Gravimetric water contents of out-diffusion core samples from IG_BH05 calculated by the mass of cores determined before (b.e.) and after (a.e.) experiments using wet (WC_{wet}) and dry masses (WC_{dry}) of the individual core pieces; the error of the water content is determined by Gaussian error propagation (Appendix C); (G / T: granodiorite / tonalite, D: diabase, A: amphibolite). 26

Table 4-4: Gravimetric water contents determined on core samples from IG_BH05 used for isotope diffusive exchange experiments ($WC_{IsoEx,\ grav}$); Water contents are corrected for weight changes during experiments (b.e. = before experiment, a.e. = after experiment); the gravimetric water contents determined on the rock pieces used in the experiments with LAB – and ICE water are weighed taking their weights into account; the error of the water content is determined by Gaussian error propagation (Appendix C). 29

Table 4-5: Water contents of core samples from IG_BH05 calculated by isotope diffusive exchange method (eq. 7); the error of the water content is determined by Gaussian error propagation (Appendix C). 30

Table 4-7: Weighed gravimetric water contents of aqueous extraction and porewater core samples taken from borehole IG_BH05 and their corresponding total masses; the uncertainties of the water content values are the weighed standard deviations of the individual aliquots showing the density of water contents in one entire sample; (G / T: granodiorite / tonalite, D: diabase, A: amphibolite). 33

Table 4-8: Bulk wet and dry density and water-loss (=WL-) porosity determined by water contents calculated for dry ($\Phi_{WL,dry}$) and wet ($\Phi_{WL,wet}$) core samples from borehole IG_BH05; the errors are calculated by Gaussian error propagation (Appendix C); (G / T: granodiorite / tonalite, D: diabase, A: amphibolite). 35

Table 5-1: Analytical results of the aqueous extraction solutions of crushed core samples from borehole IG_BH05; Test solution types are classified after Jäckli (1970). 39

Table 5-2: Analytical results of test solutions of out-diffusion experiments using core samples from borehole IG_BH05 46

Table 6-1: Minimum (min), maximum (max) and average (avg) pore and effective diffusion coefficients determined by 1-dimensional modelling of Cl elution curves of out-diffusion experiments on core samples from IG_BH05 at 45 °C and calculated by the Stoke-Einstein-equation for 10 °C and 25 °C; (G / T: granodiorite / tonalite, D: diabase, A: amphibolite). 94

Table 7-1: Porewater Cl and Br concentrations and Br*1000/Cl mass ratios estimated using aqueous extraction experiments; the errors of porewater Cl and Br concentrations and Br*1000/Cl mass ratios are calculated by Gaussian error propagation (Appendix C). 95

Table 7-2: Porewater Cl and Br concentrations, Br*1000/Cl mass ratios and $\delta^{37}Cl$ isotope signatures. Cl concentrations are determined by out-diffusion experiments; the errors of porewater Cl and Br concentrations and Br*1000/Cl mass ratios are calculated by Gaussian error propagation (Appendix C); the errors of $\delta^{37}Cl$ values are the standard deviation of triplicate analyses; (G / T: granodiorite / tonalite, D: diabase). 98

Table 8-1: $\delta^{18}O$ and $\delta^{2}H$ values of porewater of core samples from borehole IG_BH05; the errors are calculated by Gaussian error propagation; (G / T: granodiorite / tonalite, D: diabase, A: amphibolite). 103

Table 9-1: Concentrations of gases dissolved in porewater of core samples from borehole IG_BH05; the volumes in NmL/L_{PW} are given normalised to standard conditions (273 K = 0°C, 1 bar); the errors are estimated to be ±20%. 110

Table 9-2: Stable isotope signatures of gases dissolved in porewater of core samples from borehole IG_BH05. 115

Table 9-3: Noble gas concentrations and ratios dissolved in porewater of cores taken from borehole IG_BH05. 117

FIGURES

Figure 1-1: Location of IG_BH05 in relation to the Revell Site. 1

Figure 1-2: Geological Setting and Location of Boreholes IG_BH04, IG_BH05, and IG_BH06 in the Northern Portion of the Revell Batholith. 3

Figure 4-1: Mass of core samples from IG_BH05 before and after the out-diffusion experiments; the uncertainty of the core mass is ± 0.05g. 27

Figure 4-2: Water content calculated from the wet mass (dry surface) before and after the out-diffusion experiments of core sections from IG_BH05; the error of the water content is determined by Gaussian error propagation (Appendix C). 28

Figure 4-3: Comparison of water contents determined by isotope diffusive exchange (WC_{IsoEx}) and gravimetrically ($WC_{IsoEx,\ grav,\ corr.}$ by wet weight, corrected for weight change during experiments) on the same core pieces; the error of the water content is determined by Gaussian error propagation (Appendix C). 31

Figure 4-4: Water content and water-loss porosity of core samples from IG_BH05. 37

Figure 5-1: Schoeller diagram of experiment solutions from aqueous extraction experiments conducted with core samples from Borehole IG_BH05. 42

Figure 5-2: Schoeller diagram of experiment solutions from out-diffusion experiments. 49

Figure 6-1: Elution curves of anions and cations set-up by the periodic sampling of the test solutions from out-diffusion experiments using core samples from borehole IG_BH05; the errors are the analytical uncertainty of ± 5%. 53

Figure 6-2: Maximum (Dp(max)) and minimum (Dp(min)) pore diffusion coefficients (45 °C) determined ba a best fit of Cl elution curves in linear and logarithmic time and concentration scale; the solid lines mark the average diffusion coefficients (45 °C, Dp (avg)). 86

Figure 7-1: Borehole IG_BH05: Estimated porewater Cl and Br concentrations and Br*1000/Cl mass ratios versus depth by aqueous extraction experiments. 96

Figure 7-2: Porewater chloride, bromide, Br*1000/Cl mass ratios and $\delta^{37}Cl$ isotope signatures from cores from borehole IG_BH05 as function of depth. 99

Figure 7-3: Porewater Cl versus Br concentrations determined by out-diffusion experiments on core samples from IG_BH05. 100

Figure 7-4: Porewater $\delta^{37}Cl$ isotope signatures versus porewater Cl concentrations 100

Figure 8-1: $\delta^{18}O$ and $\delta^{2}H$ porewater signatures as function of depth along borehole IG_BH05; errors are calculated by Gaussian error propagation (depth in mbgs (downhole)). 102

Figure 8-2: $\delta^{18}O$ versus $\delta^{2}H$ values of porewater; the blue line marks the global meteoric water line; the errors of the stable isotope ratios are calculated by Gaussian error propagation. 103

Figure 8-3: Errors of the determination of the $\delta^{18}O$ (left) and $\delta^{2}H$ (right) porewater isotope signatures versus the mass ratio of test water and porewater (R(tw/pw)). 104

Figure 9-1: Diffusive equilibration of gases dissolved in porewater. The model calculations show that the equilibration time in days is sufficient to achieve equilibrium with respect to the analysed gases. The diffusive exchange in the experiments of the non-inert gases and noble gases with the lowest (Butane, Xenon) and the highest diffusion coefficient in free water (Methane, Helium) were modelled ($D_{(He)}$ = 7.2*10^{-9} m^2/s, $D_{(Xe)}$ = 1.5*10^{-9} m^2/s, $D_{(CH4)}$ = 1.9*10^{-9} m^2/s, $D_{(C4H10)}$ = 9.6*10^{-10} m^2/s at 20°C, Jähne et al. 1987). The conversion of these diffusion coefficients in free water to pore diffusion coefficients of the single gases in the rock samples was done according to Equation 14 using an average geometry factor of 0.04 as estimated for chloride (cf. Section 6.2)..... 106

Figure 9-2: Porewater nitrogen (N_2, left) and hydrogen (H_2, right) concentrations as function of depth along borehole IG_BH05; errors are ± 20% (depth in mbgs (downhole)). 108

Figure 9-3: Porewater methane (CH_4, top, left), saturated (C_2-C_5, bottom left) and unsaturated (C_2-C_4, bottom right) higher hydrocarbon concentrations and hydrocarbon ratios (top, right) as function of depth along borehole IG_BH05; errors are ± 20%..... 109

Figure 9-4: Stable isotope signatures of nitrogen ($\delta^{15}N$-N_2, left) and methane ($\delta^{13}C$-CH_4, center, $\delta^{2}H$-CH_4, right) dissolved in porewater as function of depth along borehole IG_BH05; errors are ± 0.1 ‰ for $\delta^{15}N$-N_2, ± 2.0 ‰ for $\delta^{13}C$-CH_4 and ± 10.0 ‰ for $\delta^{2}H$-CH_4. 111

Figure 9-5: Stable carbon isotope signatures of higher hydrocarbons dissolved in porewater as function of depth along borehole IG_BH05; errors are ± 2.0‰. 112

Figure 9-6: Isotopic classification of methane dissolved in porewater from core samples from borehole IG_BH05. The porewater results are compared to end-member signatures according to Whiticar (2020). 113

Figure 9-7: Carbon isotope signature patterns of hydrocarbons dissolved in porewater of cores from borehole IG_BH05 versus carbon numbers compared to patters of hydrocarbons produced by abiogenic processes (Sherwood Lollar et al. 2002) and thermogenic processes (Sherwood Lollar et al. 1994). 114

Figure 9-8: Carbon isotope signatures of methane versus the hydrocarbon ratio of methane over ethane plus propane (C1/C2+C3) dissolved in porewater of cores from borehole IG_BH05 compared to end-member fields according to Faber (1987), Whiticar (1999) and Kietäväinen et al. (2017) and references therein. 115

Figure 9-9: Helium (left) and argon concentrations of porewater as function of depth along borehole IG_BH05; errors are ± 20.0%..... 118

Figure 9-10: $^{40}Ar/^{36}Ar$ and $^{3}He/^{4}He$ isotope ratios dissolved in porewater as function of depth along borehole IG_BH05 compared to end-members of air and crustal and mantle He..... 119

Figure 9-11: $^{3}He/^{4}He$ isotope ratios versus helium concentrations dissolved in porewater of cores taken from borehole IG_BH05 compared to end-member concentration of air saturated water (ASW), crust and mantle signature and potential mantle mixing paths (Osenbrück 1996)..... 120

APPENDICES

APPENDIX A
Core Logging Depth Correction and Photo Documentation

APPENDIX B
Analytical Raw Data

APPENDIX C
Error Calculations

1.0 INTRODUCTION

The Initial Borehole Drilling and Testing project in the Wabigoon Lake Ojibway Nation (WLON) – Ignace Area, Ontario is part of Phase 2 Geoscientific Preliminary Field Investigations of the Nuclear Waste Management Organization's (NWMO) Adaptive Phased Management Site Selection Phase. This project includes the drilling and testing of six deep boreholes at the Revell site, as well as additional on-going studies, located within the northern portion of the Revell batholith.

This project involves testing of deep borehole IG_BH04 and the drilling and testing of deep boreholes IG_BH05 and IG_BH06 in the Revell site within the identified Potential Repository Area (PRA) as shown on Figure 1-1. The work comprises a total of eleven work packages and was carried out by a team led by WSP Canada Inc. (WSP) on behalf of the NWMO. The IG_BH05 program is described in a Borehole Characterization Plan (BCP) for IG_BH05.

This data report describes the methodology, activities, and results for Work Package 4C (WP04C): Porewater Extraction and Analysis for IG_BH05.

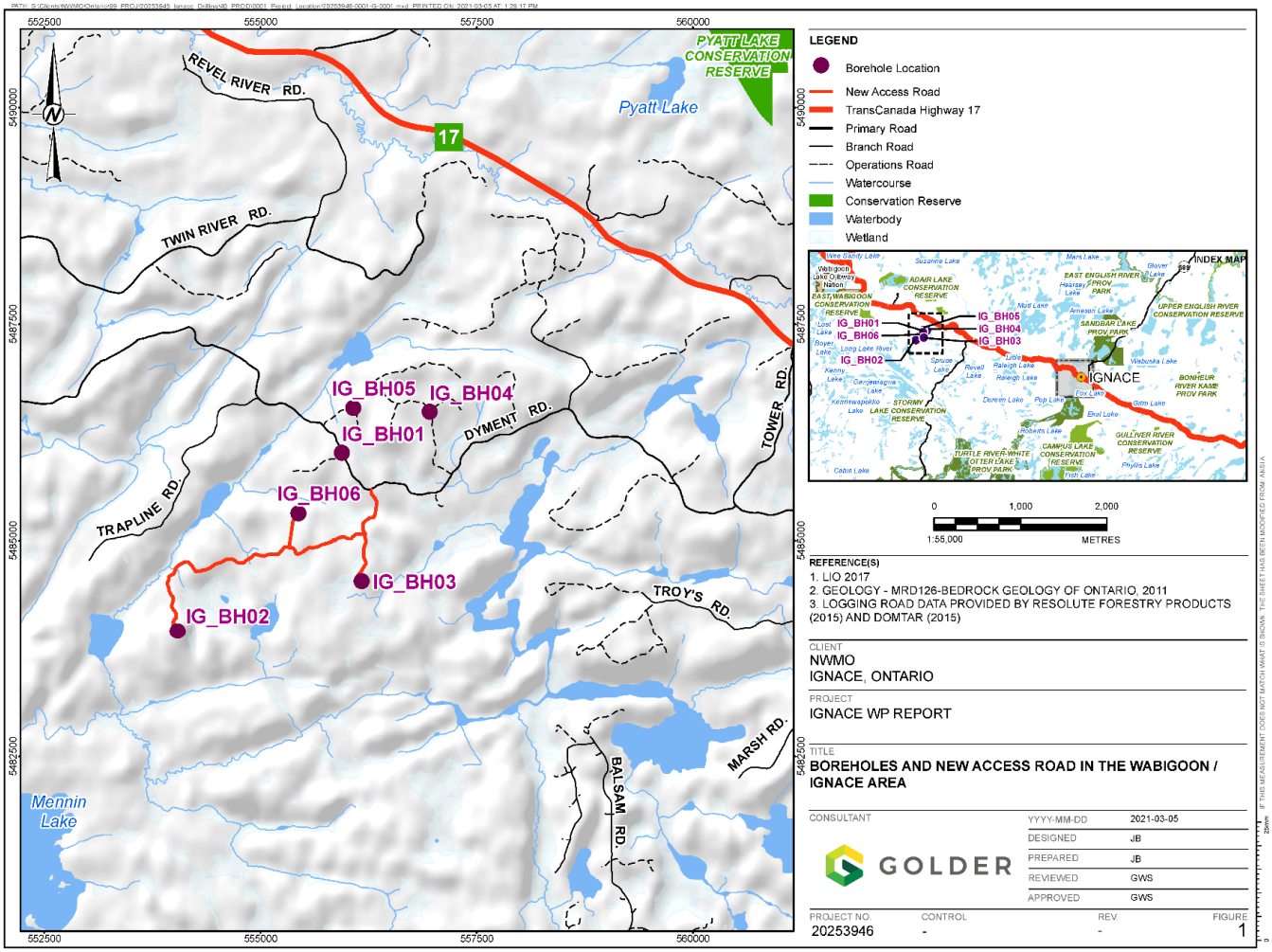


Figure 1-1: Location of IG_BH05 in relation to the Revell Site.

Given that the permeability of the crystalline rock units being characterized is expected to be very low, it is unlikely that groundwater can be sampled beyond a few opportunistic groundwater samples from conductive fractures. As such, core samples were collected and preserved on site and sent for porewater extraction and analysis. Core samples were taken with the overall objective of characterizing porewater geochemistry and gas composition at depth. The geochemical results provide information about the paleohydrogeological evolution of the bedrock system in the crystalline rock units at depth. Sampling depths and intervals were selected based on the geological and structural conditions of the bedrock and on the observations and investigation results gained from previous boreholes.

Thin section petrographic analyses will be carried out in the same core sample intervals on adjacent core sections to characterize mineralogy and support the evaluation of the porewater chemistry, which is obtained by indirect extraction methods, requiring the determination of both the in situ water content and the connected porosity. The evaluation of the petrophysical parameters requires a correlation with the petrographic and mineralogical characteristics of the investigated lithologies. Thin section petrographic analysis was completed under WP04D (WSP 2024).

1.1 Geological Setting

The approximately 2.7 billion year old Revell batholith is located in the western part of the Wabigoon Subprovince of the Archean Superior Province. The batholith is roughly elliptical in shape trending northwest, is approximately 40 km in length, 15 km in width, and covers an area of approximately 455 km^2. Based on geophysical modelling, the batholith is approximately 2 km to 3 km thick through the center of the northern portion (SGL 2015). The batholith is surrounded by supracrustal rocks of the Raleigh Lake (to the north and east) and Bending Lake (to the southwest) greenstone belts (Figure 1-2).

IG_BH05 is located within an investigation area of approximately 19 km^2 in size, situated in the northern portion of the Revell batholith. Bedrock exposure in the area is generally very good due to minimal overburden, few water bodies, and relatively recent logging activities. Ground elevations generally range from 400 to 450 m above sea level. The ground surface broadly slopes towards the northwest as indicated by the flow direction of the main rivers in the area. Local water courses tend to flow to the southwest towards Mennin Lake (Figure 1-1).

Four main rock units are identified in the supracrustal rock group: mafic metavolcanic rocks, intermediate to felsic metavolcanic rocks, metasedimentary rocks, and mafic intrusive rocks (Figure 1-2). Sedimentation within the supracrustal rock assemblage was largely synvolcanic, although sediment deposition in the Bending Lake area may have continued past the volcanic period (Stone 2009; Stone 2010a; Stone 2010b). All supracrustal rocks are affected, to varying degrees, by penetrative brittle-ductile to ductile deformation under greenschist- to amphibolite-facies metamorphic conditions (Blackburn and Hinz 1996; Stone et al. 1998). In some locations, primary features, such as pillow basalt or bedding in sedimentary rocks are preserved, in other locations, primary relationships are completely masked by penetrative deformation. Uranium-lead (U-Pb) geochronological analysis of the supracrustal rocks produced ages that range between 2734.6 +/-1.1 Ma and 2725 +/-5 Ma (Stone et al. 2010).

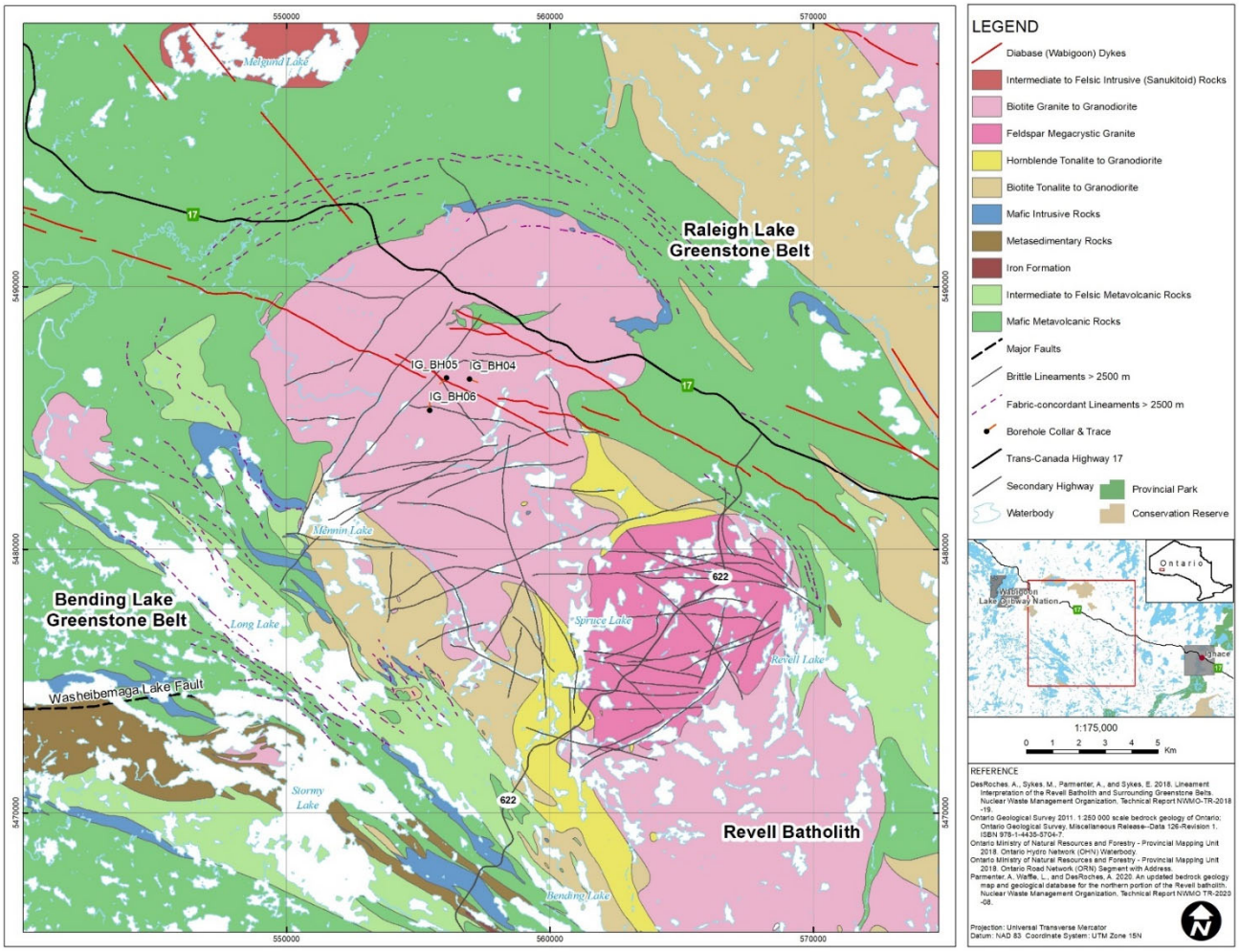


Figure 1-2: Geological Setting and Location of Boreholes IG_BH04, IG_BH05, and IG_BH06 in the Northern Portion of the Revell Batholith.

Three main suites of plutonic rock are recognized in the Revell batholith, including, from oldest to youngest: a Biotite Tonalite to Granodiorite suite, a Hornblende Tonalite to Granodiorite suite, and a Biotite Granite to Granodiorite suite (Figure 1-2). Plutonic rocks of the Biotite Tonalite to Granodiorite suite occur along the southwestern and northeastern margins of the Revell batholith. The principal type of rock within this suite is a white to grey, medium-grained, variably massive to foliated or weakly gneissic, biotite tonalite to granodiorite. One sample of foliated and medium-grained biotite tonalite produced a U-Pb age of 2734.2+/-0.8 Ma (Stone et al. 2010). The Hornblende Tonalite to Granodiorite suite occurs in two irregularly-shaped zones surrounding the central core of the Revell batholith. Rocks of the Hornblende Tonalite to Granodiorite suite range compositionally from tonalite through granodiorite to granite, and include significant proportions of quartz diorite and quartz monzodiorite. One sample of coarse-grained grey mesocratic hornblende tonalite produced a U-Pb age of 2732.3+/-0.8 Ma (Stone et al. 2010). Rocks of the Biotite Granite to Granodiorite suite underlie most of the northern, central and southern portions of the Revell batholith. Rocks of this suite are typically coarse-grained, massive to weakly foliated, and white to pink in colour. The Biotite Granite to Granodiorite suite ranges compositionally from granite through granodiorite to tonalite. A distinct potassium (K)-Feldspar Megacrystic

Granite phase of the Biotite Granite to Granodiorite suite occurs as an oval-shaped body in the central portion of the Revell batholith (Figure 1-2). One sample of coarse-grained, pink, massive K-feldspar megacrystic biotite granite produced a U-Pb age of 2694.0+/-0.9 Ma (Stone et al. 2010).

The bedrock surrounding IG_BH05 is composed mainly of massive to weakly foliated felsic intrusive rocks that vary in composition between granodiorite and tonalite, and together form a relatively homogeneous intrusive complex. Bedrock identified as tonalite transitions gradationally into granodiorite and no distinct contact relationships between these two rock types are typically observed (SRK and Golder 2015; Golder and PGW 2017). Massive to weakly foliated granite is identified at the ground surface to the northwest of the feldspar-megacrystic granite. The granite is observed to intrude into the granodiorite-tonalite bedrock, indicating it is distinct from, and younger than, the intrusive complex (Golder and PGW 2017).

West-northwest trending mafic dykes interpreted from aeromagnetic data extend across the northern portion of the Revell batholith and into the surrounding greenstone belts. One mafic dyke occurrence, located to the northwest of IG_BH01, is approximately 15-20 m wide (Figure 1-2). All of these mafic dykes have a similar character and are interpreted to be part of the Wabigoon dyke swarm. One sample from the same Wabigoon swarm produced a U-Pb age of 1887+/-13 Ma (Stone et al. 2010), indicating that these mafic dykes are Proterozoic in age. It is assumed based on surface measurements that these mafic dykes are sub-vertical (Golder and PGW 2017).

Long, narrow valleys are located along the western and southern limits of the investigation area (Figure 1-1). These local valleys host creeks and small lakes that drain to the southwest and may represent the surface expression of structural features that extend into the bedrock. A broad valley is located along the eastern limits of the investigation area and hosts a more continuous, un-named water body that flows to the south. The linear and segmented nature of this waterbody's shorelines may also represent the surface expression of structural features that extend into the bedrock.

Regional observations from mapping have indicated that structural features are widely spaced (typical 30 to 500 cm spacing range) and dominantly comprised of sub-vertical joints with two dominant orientations, northeast and northwest trending (Golder and PGW 2017). Interpreted bedrock lineaments generally follow these same dominant orientations in the northern portion of the Revell batholith (Figure 1-2; DesRoches et al. 2018). Minor sub-horizontal joints have been observed with minimal alteration, suggesting they are younger and perhaps related to glacial unloading. One mapped regional-scale fault, the Washeibemaga Lake fault, trends east and is located to the west of the Revell batholith (Figure 1-2). Ductile lineaments, also shown on Figure 2, follow the trend of foliation mapped in the surrounding greenstone belts. Additional details of the lithological units and structures found at surface within the investigation area are reported in Golder and PGW (2017).

1.2 Technical Objectives

The technical objectives of the porewater testing program are to assess the key chemical and transport properties of the crystalline host rock with depth and within the repository horizon (presently assumed to be at depths of > 600 m). The geochemical results will provide information about the palaeohydrogeological evolution of the bedrock system. The porewater chemistry will be evaluated using indirect extraction methods which require the determination of the in situ water content and connected porosity.

The associated work tasks include:

- Aqueous extraction experiments to determine initial estimates of pore fluid composition and Total Dissolved Solids (TDS);
- Isotope diffusive exchange experiments, for the determination of stable water isotopes ($\delta^{18}O$ and $\delta^{2}H$);
- Out-diffusion experiments, for determination of porewater stable ion concentrations (Cl and Br), as well as the determination of pore and effective diffusion coefficients, D_p, D_e, for Cl;
- Determination of elemental elution curves during out-diffusion experiments;
- $\delta^{37}Cl$ analyses; and
- Determination of density, water content and porosity for the various subsamples used in the above-listed analytical suites.

Further objectives within this study are to extract and characterise gases dissolved in porewater. This includes:

- The extraction of non-inert gases (N_2, CO_2, H_2, O_2, CH_4, C_xH_x) from porewater by out-gassing experiments;
- Quantification of the gas concentrations dissolved in porewater using the water content of the naturally saturates core samples;
- The isotopic characterisation of non-inert gases ($\delta^{13}C$-CO_2, -CH_4, -C_xH_x, $\delta^{2}H$-CH_4, $\delta^{15}N$-N_2) dissolved in porewater;
- The extraction of noble gases (He, Ar, Ne, Kr, Xe) from porewater by out-gassing experiments;
- Quantification of the noble-gas concentrations dissolved in porewater using the water content of the naturally saturated core samples; and
- The isotopic characterisation of noble gases ($^{3}He/^{4}He$, $^{40}Ar/^{36}Ar$, ^{132}Xe, ^{84}Kr) dissolved in porewater

The characterization of porewater composition, including gases and the solute transport processes in the rock matrix, contribute important information for the long-term safety assessment of deep geological repositories for radioactive waste. Thus, knowledge of the porewater composition will allow better constraints on the processes affecting the near-field of a repository. In designs where repository construction is restricted to bedrock of low permeability, the first water to interact with the repository barrier materials (e.g., bentonite, Cu-canister) will be the porewater. This interaction could result in changes of the physical and chemical properties of the various barrier materials. Knowledge of the porewater composition and its evolution over recent geological time – particularly during the last thousand to hundreds of thousands of years, in accordance with the expected lifespan of a geologic repository – is considered to be of high importance.

In combination with the knowledge gained about solute transport in the rock matrix, characterization of porewater also contributes to a better understanding of processes related to the far-field environment around the repository. Thus, it provides valuable information about matrix diffusion as a potential retardation factor for radionuclides, and allows better constraints to be placed on the palaeohydrogeological history of a repository site. Due to the exchange by diffusion between fracture groundwater and matrix porewater, released radionuclides may be temporally immobilized by matrix diffusion, and possible subsequent sorption onto mineral surfaces. For radionuclides susceptible to sorption, the accessible surface areas are greatly enhanced by matrix diffusion when

compared to the accessible surface area on fracture surfaces alone. Matrix diffusion therefore has the potential to increase solute transport times.

The chemical and isotopic characterisation and quantification of gases dissolved in porewater is important to estimate the potential gas flow in the bedrock. It gives first information about the gas behaviour in the bedrock, which can act as sink or source for gases occurring during the deposition of radioactive waste.

The combination of the characterisation of non-inert and noble gases allows for the source characterisation of detected gases. Additionally, the noble gas investigations allow an estimate of the residence times of porewater to be made.

In contrast to fracture groundwater, porewater cannot be sampled by conventional groundwater sampling techniques; it has to be derived by indirect extraction techniques. In most of these indirect extraction techniques – especially in case of rocks of a porosity below about 2 vol.% – the original porewater concentrations are diluted and need to be back-calculated to in situ concentrations. This requires a well-defined value for the connected porosity – accessible to different solutes under in situ conditions. The derivation of connected porosity values, as well as solute concentrations, is prone to various perturbations during drilling, core sampling, storage, and experiments in the laboratory. The obtained data have to be carefully evaluated for potential perturbations induced by drilling activities, rock stress release and sample treatment in the laboratory in order to derive values that are representative of in situ conditions. This requires detailed characterization of the rock composition, the rock texture, and the local stress field.

Matrix porewater of 32 core samples taken from 166 to 982 mbgs, (downhole) in the borehole IG_BH05, were investigated for their chemical and isotopic composition. Additionally, the same set of core samples were characterised for their petrophysical properties, including water content, water-loss porosity, bulk density and chloride pore diffusion coefficients. Additionally, 10 core samples taken from 431 to 834 mbgs (downhole) were investigated for their non-inert and noble gas composition. These cores were also characterised for their water contents and water-loss porosities.

2.0 SAMPLING AND SAMPLE PREPARATION

2.1 Porewater Samples

A total of 32 samples from 32 depth intervals were taken from borehole IG_BH05 between June 5, 2021 and August 6, 2021 for the porewater characterization program (Table 2-1). Sampling was conducted by WSP according to the instructions provided by Hydroisotop GmbH (Hydroisotop) via personnel training. After recovery from the borehole, the individual core sections (two per depth interval, 32 intervals in total) were photographed and immediately packed in a plastic (PE) bag, evacuated and sealed airtight. This procedure was repeated for a second PE bag and a final Al-coated plastic layer. The samples were stored in a refrigerator on site and then sent to Hydroisotop, Germany, in a cooler.

The samples arrived in the lab between June 24 and August 17, 2021. Three additional archived core samples (IG_BH05_AR033, IG_BH05_AR052 and IG_BH05_AR059) arrived on January 24, 2022. All samples were well packed and arrived in the lab with preserved vacuum. At Hydroisotop, the samples were stored in the refrigerator at 4°C and prepared between June 25 and September 2, 2021. The three additional archived core samples were prepared on March 14, 2022.

The assigned samples were unpacked and immediately wrapped into Parafilm™ and cut by dry-sawing into full-diameter sections. After sawing, the surfaces of the obtained pieces were cleaned with paper towels and again wrapped into Parafilm™. The entire sample preparation was conducted as rapidly as possible (within 10 minutes) after opening the sealed bags, in order to minimize evaporation. During sample preparation it was observed that four of the porewater core samples (IG_BH05_PW004, IG_BH05_AR033, IG_BH05_AR052 and IG_BH05_AR059) and one of the aqueous extraction core samples (IG_BH05_AQ004) show a different lithology (PW004 and AQ004 - diabase; AR033, AR052 and AR059 - amphibolite) compared to the other core samples (granodiorite / tonalite).

The analytical program conducted on each sample is summarized in Table 2-2.

Table 2-1: Overview of the core samples taken from IG_BH05 for porewater investigations (PW = porewater samples, AQ = cores dedicated for aqueous extraction experiments, AR = retained samples, decided to be investigated after borehole completion)

Interval	Sample ID	Hydro Lab Nr.	Depth from	Depth To	Depth Mid-point depth	Length	Test Type	Date sampled	Time recovered	Date sent	Date arrived
			mbgs*	mbgs*	mbgs*	m			hh:mm		
1	IG_BH05_AQ001	364838	166.22	166.48	166.4	0.26	AQ	05. Jun	04:55	11.06.2021	24.06.2021
	IG_BH05_PW001	364835	171.18	171.61	171.4	0.43	PW	06. Jun	01:17	11.06.2021	24.06.2021
2	IG_BH05_PW002	364836	218.92	219.29	219.1	0.37	PW	08. Jun	18:27	11.06.2021	24.06.2021
	IG_BH05_AQ002	364839	221.06	221.23	221.1	0.17	AQ	09. Jun	01:04	11.06.2021	24.06.2021
3	IG_BH05_AQ003	364840	253.13	253.31	253.2	0.18	AQ	11. Jun	04:59	11.06.2021	24.06.2021
	IG_BH05_PW003	364837	253.32	253.68	253.5	0.36	PW	11. Jun	04:52	11.06.2021	24.06.2021
4	IG_BH05_AQ004	365845	289.90	290.06	290.0	0.16	AQ	14. Jun	16:09	11.06.2021	24.06.2021
	IG_BH05_PW004	365844	290.06	290.43	290.3	0.37	PW	14. Jun	16:02	11.06.2021	24.06.2021
5	IG_BH05_PW005	365847	341.50	341.87	341.7	0.37	PW	17. Jun	17:25	11.06.2021	24.06.2021
	IG_BH05_AQ005	365846	343.14	343.35	343.3	0.21	AQ	17. Jun	17:28	11.06.2021	24.06.2021
6	IG_BH05_PW006	366656	386.48	386.88	386.7	0.40	PW	28. Jun	02:14	01.07.2021	19.07.2021
	IG_BH05_AQ006	366658	387.14	387.56	387.4	0.42	AQ	28. Jun	02:19	01.07.2021	19.07.2021
7	IG_BH05_PW007	366657	398.29	398.70	398.5	0.41	PW	29. Jun	11:10	01.07.2021	19.07.2021
	IG_BH05_AQ007	366659	399.85	400.04	400.0	0.19	AQ	29. Jun	11:19	01.07.2021	19.07.2021
8	IG_BH05_PW008	366660	426.09	426.51	426.3	0.42	PW	01. Jul	02:28	01.07.2021	19.07.2021
	IG_BH05_AQ008	366661	426.89	427.09	427.0	0.20	AQ	01. Jul	02:19	01.07.2021	19.07.2021
9	IG_BH05_AQ009	366664	453.53	453.72	453.6	0.19	AQ	02. Jul	12:46	04.07.2021	12.07.2021
	IG_BH05_PW009	366662	454.08	454.49	454.3	0.41	PW	02. Jul	12:39	04.07.2021	12.07.2021
10	IG_BH05_PW010	366663	479.25	479.62	479.4	0.37	PW	03. Jul	11:15	04.07.2021	12.07.2021
	IG_BH05_AQ010	366665	480.00	480.19	480.1	0.19	AQ	03. Jul	11:20	04.07.2021	12.07.2021
11	IG_BH05_PW011	366666	506.24	506.65	506.5	0.41	PW	04. Jul	05:54	04.07.2021	12.07.2021
	IG_BH05_AQ011	366667	507.04	507.23	507.1	0.19	AQ	04. Jul	05:49	04.07.2021	12.07.2021
12	IG_BH05_PW012	368207	524.85	525.25	525.1	0.40	PW	04. Jul	23:44	09.07.2021	05.08.2021
	IG_BH05_AQ012	368209	525.63	525.82	525.7	0.19	AQ	04. Jul	23:52	09.07.2021	05.08.2021
13	IG_BH05_PW013	368208	559.89	560.26	560.1	0.37	PW	06. Jul	18:15	09.07.2021	05.08.2021
	IG_BH05_AQ013	368210	560.62	560.81	560.4	0.36	AQ	06. Jul	18:22	09.07.2021	05.08.2021
14	IG_BH05_PW014	368211	586.92	587.30	587.1	0.38	PW	08. Jul	22:02	09.07.2021	05.08.2021
	IG_BH05_AQ014	368212	588.12	588.36	588.2	0.24	AQ	08. Jul	22:12	09.07.2021	05.08.2021
15	IG_BH05_PW015	366879	611.93	612.31	612.1	0.38	PW	09. Jul	15:43	13.07.2021	26.07.2021
	IG_BH05_AQ015	366881	612.68	612.85	612.8	0.17	AQ	09. Jul	15:48	13.07.2021	26.07.2021
16	IG_BH05_PW016	366880	637.26	637.63	637.5	0.37	PW	11. Jul	16:15	13.07.2021	26.07.2021

Interval	Sample ID	Hydro Lab Nr.	Depth from	Depth To	Depth Mid-point depth	Length	Test Type	Date sampled	Time recovered	Date sent	Date arrived
			mbgs*	mbgs*	mbgs*	m			hh:mm		
	IG_BH05_AQ016	366882	640.32	640.52	640.4	0.20	AQ	11. Jul	17:52	13.07.2021	26.07.2021
17	IG_BH05_AQ017	368213	664.49	664.71	664.6	0.22	AQ	13. Jul	11:16	19.07.2021	09.08.2021
	IG_BH05_PW017	368214	665.05	665.49	665.3	0.44	PW	13. Jul	13:22	19.07.2021	09.08.2021
18	IG_BH05_PW018	368216	692.17	692.56	692.4	0.39	PW	15. Jul	01:08	19.07.2021	09.08.2021
	IG_BH05_AQ018	368215	694.07	694.30	694.2	0.23	AQ	15. Jul	01:02	19.07.2021	09.08.2021
19	IG_BH05_AQ019	368217	720.62	720.85	720.7	0.23	AQ	16. Jul	16:26	19.07.2021	09.08.2021
	IG_BH05_PW019	368218	721.98	722.38	722.2	0.40	PW	17. Jul	03:49	19.07.2021	09.08.2021
20	IG_BH05_PW020	367662	749.38	749.79	749.6	0.41	PW	19. Jul	12:56	23.07.2021	29.07.2021
	IG_BH05_AQ020	367661	750.19	750.41	750.3	0.22	AQ	19. Jul	12:58	23.07.2021	29.07.2021
21	IG_BH05_AQ021	367663	773.15	773.47	773.3	0.32	AQ	21. Jul	00:09	23.07.2021	29.07.2021
	IG_BH05_PW021	367664	774.29	774.72	774.5	0.43	PW	21. Jul	00:13	23.07.2021	29.07.2021
22	IG_BH05_PW022	367666	801.55	801.95	801.8	0.28	AQ	22. Jul	14:55	23.07.2021	29.07.2021
	IG_BH05_AQ022	367665	797.16	797.44	797.3	0.40	PW	22. Jul	23:46	23.07.2021	29.07.2021
23	IG_BH05_PW023	368219	827.01	827.38	827.2	0.37	PW	24. Jul	23:36	28.07.2021	11.08.2021
	IG_BH05_AQ023	368220	827.74	827.96	827.9	0.22	AQ	24. Jul	23:43	28.07.2021	11.08.2021
24	IG_BH05_PW024	368221	848.51	848.86	848.7	0.35	PW	26. Jul	02:01	28.07.2021	11.08.2021
	IG_BH05_AQ024	368222	849.22	849.39	849.3	0.17	AQ	26. Jul	02:08	28.07.2021	11.08.2021
25	IG_BH05_PW025	368223	881.36	881.73	881.5	0.37	PW	27. Jul	22:56	28.07.2021	11.08.2021
	IG_BH05_AQ025	368224	881.73	881.91	881.6	0.18	AQ	27. Jul	22:59	28.07.2021	11.08.2021
26	IG_BH05_PW026	369738	905.93	906.27	906.1	0.34	PW	29. Jul	04:45	09.08.2021	17.08.2021
	IG_BH05_AQ026	369739	906.66	906.82	906.7	0.16	AQ	29. Jul	04:51	09.08.2021	17.08.2021
27	IG_BH05_PW027	369740	936.13	936.51	936.3	0.38	PW	31. Jul	17:14	09.08.2021	17.08.2021
	IG_BH05_AQ027	369741	936.89	937.09	937.0	0.20	AQ	31. Jul	17:18	09.08.2021	17.08.2021
28	IG_BH05_PW028	369742	962.72	963.07	962.9	0.35	PW	02. Aug	05:46	09.08.2021	17.08.2021
	IG_BH05_AQ028	369743	963.07	963.22	963.1	0.15	AQ	02. Aug	05:50	09.08.2021	17.08.2021
29	IG_BH05_PW029	369744	986.30	986.68	986.5	0.38	PW	06. Aug	09:59	09.08.2021	17.08.2021
	IG_BH05_AQ029	369745	982.24	982.44	982.3	0.20	AQ	06. Aug	12:01	09.08.2021	17.08.2021
AR	IG_BH05_AR033	378923	717.28	717.48	717.4	0.20	PW (AR)	16. Jul	12:56	17.01.2022	24.01.2022
	IG_BH05_AR052	378924	855.93	856.16	856.1	0.23	PW (AR)	26. Jul	11:59	17.01.2022	24.01.2022
	IG_BH05_AR059	378925	978.81	979.10	979.0	0.29	PW (AR)	03. Aug	10:38	17.01.2022	24.01.2022

*mbgs (downhole)

Table 2-2: Overview of the analytical porewater program conducted on core samples from IG_BH05 (PW: porewater extraction, AQ: aqueous extraction).

					Experimental and analytical programme													
					Aqueous Extraction			Diffusive isotope exchange experiments			Out-diffusion experiments							Grav. WC
Sample ID	Hydro Lab Nr.	Ave. Depth	Date prepared	Experiment	Exp. Set-Up	Chemical analyses	Grav. WC	Exp. Set-Up	Isotope Analyses	Grav. WC	Exp. Set-Up	Time Series	Analyses ions	Analyses $\delta^{37}Cl$	Grav. WC	Density	Modelling D_P	Extra Pieces
		m BHL																
IG_BH05_AQ001	364838	166,4	25.06.2021	AQ	X	X	X											
IG_BH05_PW001	364835	171,4	25.06.2021	PW				X	X	X	X	X	X	X	X	X	X	X
IG_BH05_PW002	364836	219,1	25.06.2021	PW				X	X	X	X	X	X	X	X	X	X	X
IG_BH05_AQ002	364839	221,1	25.06.2021	AQ	X	X	X											
IG_BH05_AQ003	364840	253,2	25.06.2021	AQ	X	X	X											
IG_BH05_PW003	364837	253,5	25.06.2021	PW				X	X	X	X	X	X	X	X	X	X	X
IG_BH05_AQ004	365845	290,0	06.07.2021	AQ	X	X	X					X						
IG_BH05_PW004	365844	290,3	06.07.2021	PW				X	X	X	X	X	X	X	X	X	X	X
IG_BH05_PW005	365847	341,7	06.07.2021	PW				X	X	X	X	X	X	X	X	X	X	X
IG_BH05_AQ005	365846	343,3	06.07.2021	AQ	X	X	X											
IG_BH05_PW006	366656	386,7	19.07.2021	PW				X	X	X	X	X	X	o	x	x	X	X
IG_BH05_AQ006	366658	387,4	19.07.2021	AQ	X	X	X											
IG_BH05_PW007	366657	398,5	19.07.2021	PW				X	X	X	X	X	X	o	X	X	X	X
IG_BH05_AQ007	366659	400,0	19.07.2021	AQ	X	X	X											
IG_BH05_PW008	366660	426,3	19.07.2021	PW				X	X	X	X	X	X	o	X	X	X	X
IG_BH05_AQ008	366661	427,0	19.07.2021	AQ	X	X	X											
IG_BH05_AQ009	366664	453,6	19.07.2021	AQ	X	X	X											
IG_BH05_PW009	366662	454,3	19.07.2021	PW				X	X	X	X	X	X	o	X	X	X	X
IG_BH05_PW010	366663	479,4	19.07.2021	PW				X	X	X	X	X	X	o	X	X	X	X
IG_BH05_AQ010	366665	480,1	19.07.2021	AQ	X	X	X											
IG_BH05_PW011	366666	506,5	19.07.2021	PW				X	X	X	X	X	X	o	X	X	X	X
IG_BH05_AQ011	366667	507,1	19.07.2021	AQ	X	X	X											
IG_BH05_PW012	368207	525,1	09.08.2021	PW				X	X	X	X	X	X	o	X	X	X	X
IG_BH05_AQ012	368209	525,7	09.08.2021	AQ	X	X	X											
IG_BH05_PW013	368208	560,1	09.08.2021	PW				X	X	X	X	X	X	o	X	X	X	X
IG_BH05_AQ013	368210	560,7	09.08.2021	AQ	X	X	X											
IG_BH05_PW014	368211	587,1	09.08.2021	PW				X	X	X	X	X	X	o	X	X	X	X
IG_BH05_AQ014	368212	588,2	09.08.2021	AQ	X	X	X											
IG_BH05_PW015	366879	612,1	29.07.2021	PW				X	X	X	X	X	X	o	X	X	X	X
IG_BH05_AQ015	366881	612,8	29.07.2021	AQ	X	X	X											
IG_BH05_PW016	366880	637,5	29.07.2021	PW				X	X	X	X	X	X	o	X	X	X	X
IG_BH05_AQ016	366882	640,4	29.07.2021	AQ	X	X	X											

*mbgs (downhole)

Table 2-2: Continued

					Experimental and analytical programme													
					Aqueous Extraction			Diffusive isotope exchange experiments			Out-diffusion experiments							Grav. WC
Sample ID	Hydro Lab Nr.	Ave. Depth	Date prepared	Experiment	Exp. Set-Up	Chemical analyses	Grav. WC	Exp. Set-Up	Isotope Analyses	Grav. WC	Exp. Set-Up	Time Series	Analyses ions	Analyses $\delta^{37}Cl$	Grav. WC	Density	Modelling D_P	Extra Pieces
		m BHL																
IG_BH05_AQ017	368213	664,6	13.08.2021	AQ				X	X	X	X	X	X	X	X	X	X	X
IG_BH05_PW017	368214	665,3	13.08.2021	PW	X	X	X											
IG_BH05_PW018	368216	692,4	13.08.2021	PW				X	X	X	X	X	X	X	X	X	X	X
IG_BH05_AQ018	368215	694,2	13.08.2021	AQ	X	X	X											
IG_BH05_AQ019	368217	720,7	13.08.2021	AQ				X	X	X	X	X	X	X	X	X	X	X
IG_BH05_PW019	368218	722,2	13.08.2021	PW	X	X	X											
IG_BH05_PW020	367662	749,6	09.08.2021	PW				X	X	X	X	X	X	X	X	X	X	X
IG_BH05_AQ020	367661	750,3	09.08.2021	AQ	X	X	X											
IG_BH05_AQ021	367663	773,3	09.08.2021	AQ	X	X	X											
IG_BH05_PW021	367664	774,5	09.08.2021	PW				X	X	X	X	X	X	X	X	X	X	X
IG_BH05_PW022	367666	801,8	09.08.2021	PW				X	X	X	X	X	X	X	X	X	X	X
IG_BH05_AQ022	367665	797,6	09.08.2021	AQ	X	X	X											
IG_BH05_PW023	368219	827,2	10.08.2021	PW				X	X	X	X	X	X	X	X	X	X	X
IG_BH05_AQ023	368220	827,9	11.08.2021	AQ	X	X	X											
IG_BH05_PW024	368221	848,7	12.08.2021	PW				X	X	X	X	X	X	X	X	X	X	X
IG_BH05_AQ024	368222	849,3	13.08.2021	AQ	X	X	X											
IG_BH05_PW025	368223	881,5	14.08.2021	PW				X	X	X	X	X	X	X	X	X	X	X
IG_BH05_AQ025	368224	881,6	15.08.2021	AQ	X	X	X											
IG_BH05_PW026	369738	906,1	09.08.2021	PW				X	X	X	X	X	X	X	X	X	X	X
IG_BH05_AQ026	369739	906,7	09.08.2021	AQ	X	X	X											
IG_BH05_PW027	369740	936,8	10.08.2021	PW				X	X	X	X	X	X	X	X	X	X	X
IG_BH05_AQ027	369741	937,0	11.08.2021	AQ	X	X	X											
IG_BH05_PW028	369742	963,0	12.08.2021	PW				X	X	X	X	X	X	X	X	X	X	X
IG_BH05_AQ028	369743	963,4	13.08.2021	AQ	X	X	X											
IG_BH05_PW029	369744	986,5	14.08.2021	PW				X	X	X	X	X	X	X	X	X	X	X
IG_BH05_AQ029	369745	982,3	15.08.2021	AQ	X	X	X											
IG_BH05_AR033	378923	717,4	16.08.2021	PW							X	X	X	o	X	X	X	X
IG_BH05_AR052	378924	856,1	17.08.2021	PW							X	X	X	o	X	X	X	X
IG_BH05_AR059	378925	979,0	18.08.2021	PW				X	X	X	X	X	X	o	X	X	X	X

*mbgs (downhole)

2.2 Porewater Gas Samples

A total of 15 samples from 5 depth intervals were taken from borehole IG_BH05 between July 1, 2021 and July 27, 2021 for the porewater gas characterization program (Table 2-3). Sampling was conducted by WSP according to the instructions provided by Hydroisotop GmbH (Hydroisotop) via video and video tutorial training. After recovery from the borehole, the individual core sections were photographed, weighed, and immediately placed in stainless-steel cylinders.

The cylinders were closed vacuum tight and repeatedly flushed with nitrogen (for the noble gas (NG) samples) or helium (for the non-inert dissolved gas (DG) samples) and evacuated.

Afterward, the samples were stored at room temperature and sent in one batch to Hydroisotop GmbH and to the University of Oxford. At Hydroisotop, the cylinders were stored at room temperature. The samples were allowed to equilibrate for 415 to 441 days for DG samples and 734 to 759 days for NG samples, respectively.

The analytical program conducted on each sample is summarized in Table 2-4.

Table 2-3: Overview of the core samples taken from IG_BH05 for porewater gas investigations (NG = noble gas; DG = non-inert dissolved gas; Hydro = HI = Hydroisotop; UoO = University of Oxford).

Sample ID	Lab	Depth		Mid-point depth	Core length	Sampling Date	m (cyl)	m (core)
		From	To					
		mbgs*	mbgs*	mbgs*	m		Kg	kg
IG_BH05_NG001	Hydro	428.43	428.63	428.5	0.20	01.07.2021	4.98419	1.59134
IG_BH05_NG002	UoO	428.63	428.84	428.7	0.21	01.07.2021	5.04249	1.65761
IG_BH05_DG001	Hydro	431.14	431.35	431.3	0.21	01.07.2021	5.03765	1.64244
IG_BH05_NG003	Hydro	533.15	533.35	533.3	0.20	05.07.2021	4.97605	1.58875
IG_BH05_NG004	UoO	533.35	533.57	533.5	0.22	05.07.2021	5.14795	1.75629
IG_BH05_DG002	Hydro	536.24	536.47	536.4	0.23	05.07.2021	5.51352	1.76277
IG_BH05_NG005	Hydro	630.13	630.35	630.2	0.22	10.07.2021	5.19238	1.79400
IG_BH05_NG006	UoO	631.54	631.76	631.7	0.22	10.07.2021	4.93992	1.54684
IG_BH05_DG003	Hydro	634.11	634.33	634.2	0.22	10.07.2021	5.14315	1.75405
IG_BH05_DG004	Hydro	744.22	744.43	744.3	0.21	18.07.2021	5.00981	1.62037
IG_BH05_NG007	Hydro	747.15	747.37	747.3	0.22	18.07.2021	5.10550	1.71669
IG_BH05_NG008	UoO	747.37	747.58	747.5	0.21	18.07.2021	4.99598	1.60612
IG_BH05_NG009	Hydro	872.08	872.3	872.2	0.22	27.07.2021	5.11355	1.72037
IG_BH05_NG010	UoO	873.03	873.24	873.1	0.21	27.07.2021	5.09511	1.71177
IG_BH05_DG005	Hydro	879.21	879.44	879.3	0.23	27.07.2021	5.17146	1.77830

*mbgs (downhole)

Table 2-4: Overview of the analytical porewater gas program conducted on core samples from IG_BH05 (NG = noble gas; DG = non-inert dissolved gas).

					Experimental and analytical programme					
Sample ID	Hydro Lab Nr.	Depth mbgs	Test Type	Date analysed	Exp. Set-Up	DG analyses	DG isotope analyses	NG analyses	isotope analyses	Water content
IG_BH05_DG001	378510	431.2	DG	15.09.2022	x	x	x			x
IG_BH05_DG002	378510	536.4	DG	15.09.2022	x	x	x			x
IG_BH05_DG003	378510	634.2	DG	15.09.2022	x	x	x			x
IG_BH05_DG004	378510	744.3	DG	15.09.2022	x	x	x			x
IG_BH05_DG005	378510	879.3	DG	15.09.2022	x	x	x			x
IG_BH05_NG001	378515	428.5	NG	27.07.2023	x	x	x	x	x	x
IG_BH05_NG002	378516	533.3	NG	03.08.2023	x	x	x	x	x	x
IG_BH05_NG003	378517	630.2	NG	07.08.2023	x	x	x	x	x	x
IG_BH05_NG004	378518	747.3	NG	31.07.2023	x	x	x	x	x	x
IG_BH05_NG005	378519	872.2	NG	31.07.2023	x	x	x	x	x	x

*mbgs (downhole)

2.3 Core Logging Depth Correction

During the core logging of borehole IG_BH05, the logged depths were not reconciled with the depths obtained by the drilling supervisor calculated from measurement of the drill string and drill rod stick-up. This resulted in the WP03 core logging depths and core sample depths to be recorded as being slightly deeper than the actual sample depths. Refer to the WP03 Report for IG_BH05 for details of the correction applied to the core logging data.

All sample depths referred to in this report and appendices are the original, uncorrected sample depths in metres below ground surface (mbgs) downhole.

An Addendum to the Laboratory Report summarizing the original and corrected core depths for each sample is provided in Appendix A.

3.0 EXPERIMENTAL SET-UPS AND ANALYTICAL METHODS

Porewater investigations included: 1) the determination of the water content and water-loss porosity on the respective samples, 2) aqueous extraction and out-diffusion experiments to characterise porewater using chemical tracers, 3) isotope diffusive exchange experiments used to determine the porewater $\delta^{18}O$ and $\delta^{2}H$ composition, 4) out-gassing experiments to determine the composition and volume as well as isotopic signatures and ratios of non-inert gases and noble gases dissolved in porewater.

Unless otherwise specified, the analytical work has been conducted at Hydroisotop GmbH, Germany.

3.1 Water Content and Water-Loss Porosity

The water content was determined on core material used for aqueous extraction and out-diffusion experiments, as well as on the core pieces used for the isotope diffusive exchange experiments and out-gassing experiments.

Water contents also were determined on extra pieces of core available from those used for the out-diffusion experiments.

The quality of sample preservation upon arrival in the laboratory was assessed by the condition of the sample bags and of the core surface (wet vs. dry). Core pieces used for out-gassing experiments were weighed directly in the field before placing them in the cylinders and after the experiments.

For water content measurements, drill-core pieces were placed in a crystallization dish, weighed and subsequently dried at 105 °C until stable weight conditions. According to the experience and knowledge gained from the investigations of cores from boreholes IG_BH01 to IG_BH03, the first drying step at 45 °C was considered unnecessary. Before taking the initial wet weight of the full diameter core sections, the surface was allowed to dry on the balance until stable weight was achieved for ≈10 sec. During the following drying process, weighing was carried out every 14 days until the sample weight remained constant (±0.002 g) for at least 14 days.

Water contents were determined on core samples used for aqueous extraction experiments (Table 2-2). Therefore, one half of the full disc core (348 – 571 g) was broken by a mortar to an edge length of approximately 1 cm, placed in a crystallization dish, weighed and put in the oven at 105 °C for drying. Additionally, the two end-cut pieces with weights between 130 and 755 g were also weighed and put in the oven to determine the water content. Drying times varied between 35 and 156 days for crushed pieces, and 25 to 114 days for full core discs.

Water contents also were determined on core pieces used for out-diffusion experiments, with weights between 1354 and 1640 g and drying times between 36 and 258 days. Two extra pieces of the core sample used for out-diffusion and isotope exchange experiments were also taken for the determination of the water content. These sections had weights between 106 and 616 g and drying times between 35 and 149 days.

Gravimetric water contents were further determined on crushed core sections used for the single isotope diffusive exchange experiments after equilibration. The crushed core material (348 and 555 g) was placed in a crystallizing dish and put in the oven at 105 °C. These samples had weights between 354 g and 480 g and drying times between 22 and 104 days.

Water contents were determined on the full-size cores used for out-gassing experiments (NG and DG) with weights between 1591 and 1794 g also in the oven at 105°C. Drying to constant weight needed between 79 and 133 days.

The calculation of the water-loss porosity (i.e., the connected porosity) from the gravimetric water content requires a measure of the grain density. In rocks of low porosity, the bulk wet density can be used as a proxy for the grain density. A measure for the bulk wet density of the rocks used for out-diffusion and aqueous extraction experiments was obtained from the volume and saturated mass of the core samples. The volume was calculated from measurements of height and diameter of the core samples using a Vernier Caliper, with an error of ± 0.01 mm.

Core lengths varied between 5.0 and 7.2 cm for aqueous extraction cores, and between 12.2 and 19.2 cm for out-diffusion cores.

From known sample volume and wet mass, the bulk, wet and dry density is obtained by

$$\rho_{bulk,wet} = \frac{m_{rock,wet}}{V_{rock}}, \qquad \rho_{bulk,dry} = \frac{m_{rock,dry}}{V_{rock}} \tag{1}$$

and the water-loss (connected) porosity, ϕWL, can be calculated according to

$$\emptyset_{WL} = WC_{wet} \times \frac{\rho_{bulk,wet}}{\rho_{water}} \quad \emptyset_{WL} = \frac{m_{pw} \times 100}{r^2 \times h \times \pi \times \rho_{water}} \tag{2}$$

where WC_{wet} is the water content based on the wet weight of the rock sample and $\rho_{bulk,wet}$ the bulk wet density of the rock. In a first approximation, the density of water, ρ_{water}, is assumed to be 1 g/cm^3. Due to the low water content of the investigated crystalline rocks, the water content and water-loss porosity determined by the wet weight and bulk, wet density of the sample is essentially equal to those values calculated using the dry weight and bulk, dry density.

As shown by Gaussian error propagation (Appendix C), the error of the water content and the water-loss porosity depends predominately on the accuracy of the determination of the mass of porewater measured after unpacking (i.e., on the measured initial wet weight) and the final dry weight of the cores.

3.2 Porewater Extraction Methods

3.2.1 Aqueous Extraction Experiments

Aqueous extraction experiments were conducted prior to out-diffusion and isotope exchange experiments to estimate the salinity of the investigated porewaters.

Saturated full disc core sections were crushed by a mortar and sieved by an analytical sieve to a grain size of < 2 mm and 82 to 124 g of rock material were put in a polyethylene (PE) bottle, where 46 to 76 ml of deionized water was added. Subsequently the bottle was gently shaken for 24 hours. Afterward, the elution was decanted, filtered (0.45 µm) and immediately analysed for alkalinity, pH and specific electrical conductivity (EC) using a Metrohm Titrino 785 and WTW LF 325 system.

The main anion and cation concentrations were analysed by ion chromatography (IC) using a Dionex ICS 1500 system. The analytical error of the ion concentration analyses is ±5 %. Aluminium concentrations were analysed using a ContrAA800 G graphite tube atomic absorption spectrometer (AAS) from ThermoFischer with an analytical error of ±10 % and silica concentrations were determined photometrically with an analytical error of ±5 %. DOC concentrations were analysed using a Shimazu TOC-VCSH analyser (analytical error of 3-5 % depending on the concentration range).

The porewater Cl concentration was further calculated according to

$$C_{i,pw} = \frac{C_{i,sol} \times V_{sol} \times 0.001}{m_{pw}} \tag{3}$$

where $C_{i,pw}$ = porewater elemental concentration, $C_{i,sol}$ = analyzed elemental concentration in the aqueous extraction solution, V_{sol} = Volume of aqueous extraction solution, and m_{pw} = mass of porewater.

3.2.2 Out-Diffusion Experiments

Out-diffusion experiments were performed on intact full disc cores by immersion into ultrapure water. The volume of test water varied between 118 and 164 ml, resulting in test water to core mass ratios between 0.08 and 0.12. During the experiments the two water reservoirs, i.e., porewater and test water, were allowed to exchange until equilibrium. Equilibrium with respect to chloride is reached when the Cl concentration has been constant within the analytical error range (= ±5 %) over a minimum of 14 days.

After placing the core sample in the PE-vessel, the vessel was sealed and put in a vibrating water bath (40 rpm) at a constant temperature of 45 °C to accelerate diffusion. The PE-vessels were covered by a vapour-tight lid,

which is equipped with two Swagelok™ valves and PEEK™ sampling lines. The core, the experiment container and the test water were weighed before and after the experiment to ensure that no loss of test water occurred during the entire experiment. At specific time intervals of initially a few days, and later a few weeks, 0.5 ml of solution were sampled using a PVC-syringe to determine the chloride concentration as a function of time. The experimental time depended on the equilibration grade in the individual experiments. All out-diffusion experiments were ended between 113 and 156 days.

After equilibrium with respect to chloride was achieved, the vessels were removed from the water bath and cooled to room temperature. Subsequently, the cylinder, the core and the remaining test water were weighed, and the supernatant solution was filtered (0.45 µm) and analysed immediately for pH, EC and alkalinity (total alkalinity (pH 4.3) and base capacity 8.2), and later for major cations and anions and certain trace elements and isotopes.

The major cations (Na^+, K^+, Ca^{2+}, Mg^{2+}, Sr^{2+}) and anions (F^-, Cl^-, NO_3^-, Br^-, SO_4^{2-}) of the 0.5 ml time series and final test solutions of the out-diffusion experiments were analysed by IC using a Dionex ICS 1500 system or a Thermo Scientific Dionex Aquion and Integrion IC system. The relative analytical error of these analyses is ±5 % based on multiple measurements of external check standard solutions (1σ). The final test solutions with a volume of approximately 100 ml were analysed undiluted and in different dilutions (1:10 and, if necessary, 1:20). The time series samples were analysed timely after sampling. Due to the low volume, the samples could only be measured once in a 1:10 dilution. As such, the detection limit is different for each element in the two different solutions.

The alkalinity titration, pH-value and specific electrical conductivity measurements were performed using Metrohm titration systems and a WTW LF325 probe. TOC and TIC concentrations were analysed on the final solutions using a Shimadzu VCSH analyser with a relative analytical error of ±5 % based on multiple measurements of external check standard solutions (1σ). Aluminium and lithium concentrations were analysed using a ContrAA800G graphite tube atomic absorbtion spectrometer (AAS) from ThermoFischer and silica concentrations were determined photometrically. Boron of out-diffusion test solutions was analysed at Analytik Institut Rietzler GmbH, Germany, using an ICP-MS system with a detection limit of 0.0001 mg/l and an analytical uncertainty of ±5 %.

The $^{37}Cl/^{35}Cl$ isotope ratio, expressed as $\delta^{37}Cl$ relative to SMOC, was measured by a GC-MS-IRMS system (ThermoFischer Delta S), according to the method described in Ertl et al. (2024). Analytical errors were determined by the standard deviation of triplicate analyses of every sample. Strontium isotope signatures were analysed at Iso Analysis UG, Germany, by a ThermoFischer MC-ICP-MS system with an analytical uncertainty of 0.0005.

Chloride and bromide concentrations of the experiment solution can be converted to porewater concentrations by applying mass balance calculations if equilibrium between test water and porewater is achieved. With knowledge of the mass of porewater in the rock sample, the chloride and bromide concentration of the porewater can be calculated according to:

$$C_{pw} = \frac{(m_{pw}+m_{TWi}-\sum^n m_s)\times C_{TW\infty}-(m_{TWi}\times C_{TWi})+\sum^n m_s\times C_s}{m_{pw}} \quad (4)$$

where C_{pw} = porewater concentration, m_{pw} = mass of porewater, m_{TWi} = initial mass of test water, C_{TWi} = initial Cl concentration of test water, m_s = mass of sub sample used for time series, and C_s = Cl concentration of sub sample used for time series.

The term $\sum m_s{*}C_s$ (Equation 4) describes the amount of Cl removed from the initial experiment solution for Cl time-series samples. A correction for chloride and bromide in the initial experiment solution ($m_{TWi}{*}C_{TWi}$) is necessary if this solution is not entirely free of chloride and bromide.

The unit for the porewater concentration is given in mg/kg H_2O (and not mg/l) because it is derived on a mass basis rather than a volumetric basis. This is due to the fact that the density of the porewater is not known beforehand, because it depends on the in situ salinity of the water (which is unknown).

3.2.3 Isotope Diffusive Exchange Technique

The isotope diffusive exchange technique to determine the water isotope composition, $\delta^{18}O$ and $\delta^{2}H$, of the porewater and the mass of porewater was originally developed by Rogge (1997) and Rübel et al. (2002) for sedimentary rocks and later adapted for crystalline rocks by Waber and Smellie (2005, 2006) and Eichinger et al. (2006). In this method, initially saturated rock material is placed into two vapour-tight containers together with different test waters of known isotope composition. The porewater and test water are then allowed to isotopically equilibrate via the vapour phase without any direct contact between the core material and the test water. The porewater isotope composition and the water content of the rock sample can then be derived by isotope mass balance relationships. It has been shown that the uncertainty of the derived isotope composition largely depends on the ratio of porewater to test water used in the experiments (e.g., Rübel et al. 2002). For crystalline rocks, this ratio was optimised by using larger volumes of rock and smaller volumes of test water in the experiments (e.g., Waber and Smellie 2005, 2006; Eichinger et al. 2006).

For the present samples, 1.8 ml of test water were placed in a Petri dish in the centre of a glass vessel and surrounded by hand crushed core pieces 4-6 cm^3 in size and with a total mass of 301 to 555 g. After an equilibration time of 60 days, the two test waters were removed and analysed by Cavity Ring Down Spectroscopy using a Picarro L 2130-I Analyser. The results for the test waters are reported relative to the V-SMOW (Vienna Standard Mean Ocean Water) standard with a precision of ±0.15 ‰ for $\delta^{18}O$ and ±1.5 ‰ for $\delta^{2}H$.

Test water and core material were weighed before and after the experiment to assess if test water was lost on the container walls and/or rock material due to evaporation and/or condensation. To minimise condensation, about 0.3 mol of NaCl were dissolved in the test water to lower its water vapour pressure. For every sample, two experiments were performed, one using test water with an isotope composition close to that expected in the porewater ("LAB-sample") and one using test water with an isotope composition far from that expected for the porewater ("ICE-sample").

The test water used for the LAB-sample was normal laboratory tap water ($\delta^{18}O$ = -10.30 to -10.00 ‰ V-SMOW; $\delta^{2}H$ = -74.0 to -72.1 ‰ V-SMOW), while that for the ICE-sample was water from an ice core drilled in the Antarctic ($\delta^{18}O$ = -31.685 to -31.42 ‰ V-SMOW; $\delta^{2}H$ = -248.4 to -245.4 ‰ V-SMOW). The equilibration time in the three reservoirs – rock porewater, test water, and the air inside the container as a diaphragm – depends on the volume of the container, the size of the rock pieces and the distance of the rock pieces to the test water (see Rogge 1997). Based on the estimations of the minimum time period required for complete isotopic equilibration (Eichinger et al. 2006) an experimental time of 60 days was chosen.

The isotope diffusive exchange technique can be used to determine porewater $\delta^{18}O$ and $\delta^{2}H$ values and the mass of the porewater present in the connected pore space of the rock sample. These parameters are calculated from the analytical results obtained for the two test water solutions, using mass balance relationships, according to

$$m_{pw} * c_{pw}\Big|_{t=0} + m_{tw} * c_{tw}\Big|_{t=0} = (m_{pw} + m_{tw}) * c_{tw}\Big|_{t=\infty} \quad (5)$$

where m = mass, c = isotope ratios expressed in the δ notation, *pw* = porewater, *tw* = test water, $t = 0$ represents the isotope concentrations at the beginning of the experiment, and $t = \infty$ represents the isotope concentrations at the end of the experiment.

The water content of the applied samples is calculated by transformation of Equation 5 to

$$WC_{IsoEx} = \left[\frac{m_{TW(Std2)} \times m_{Rock(Std1)} \times (C_{TW^0(Std2)} - C_{TW\infty(Std2)}) + m_{TW(Std1)} \times m_{Rock(Std2)} \times (C_{TW\infty(Std1)} - C_{TW^0(Std1)})}{m_{Rock(Std1)} \times m_{Rock(Std2)} \times (C_{TW\infty(Std2)} - C_{TW\infty(Std1)})} \right] \times 100 \quad (6)$$

where m_{Rock} = mass of rock, *Std 1* = test solution 1 and *Std 2* = test solution 2.

Equation 6 can be set up for oxygen and hydrogen isotope ratios of the test water, resulting in two independent values for the mass of porewater.

The $\delta^{18}O$- and $\delta^{2}H$- values of the porewater are calculated by transformation of Equation 5 to

$$C_{PW} = \frac{C_{TW\infty(Std1)} \times m_{TW(Std2)} \times m_{Rock(Std1)} \times (C_{TW\infty(Std2)} - C_{TW^0(Std2)}) - C_{TW\infty(Std2)} \times m_{TW(Std1)} \times m_{Rock(Std2)} \times (C_{TW\infty(Std1)} - C_{TW^0(Std1)})}{m_{TW(Std2)} \times m_{Rock(Std1)} \times (C_{TW\infty(Std2)} - C_{TW^0(Std2)}) - m_{TW(Std1)} \times m_{Rock(Std2)} \times (C_{TW\infty(Std1)} - C_{TW^0(Std1)})} \quad (7)$$

The errors of the calculated $\delta^{18}O$, $\delta^{2}H$ and the mass of porewater are computed for each sample using Gauss' law of error propagation (Appendix C).

3.3 Out-gassing Experiments to Extract Gases Dissolved in Porewater

3.3.1 Extraction and Quantification of Non-Inert gases (DG) Dissolved in Porewater

Gases in porewater were allowed to outgas into the void volume of the gas tight cylinder during sampling over a time period of 415 to 441 days at room temperature. Non-inert dissolved gases include oxygen, hydrogen, nitrogen and carbon dioxide as well as saturated and unsaturated hydrocarbons. These were analysed at Hydroisotop GmbH, Germany. The experimental set-up and the analytical gas programme performed on the core samples is given in Table 2-3 and Table 2-4.

Non-inert gases were also analysed on the samples dedicated for noble gas analyses, after the analyses of noble gases was completed.

3.3.1.1 Quantification of Extracted Non-Inert Gases

Prior to gas analyses, the cylinders were brought to a constant temperature of 21°C to guarantee controlled water vapour conditions. Afterward, the cylinder was plugged directly onto the gas chromatograph, the attached valve was opened, and the total gas pressure in the cylinder was measured by a connected pressure gauge (Druck Limited) with a determination range of 0.1 to 1100 mbar. The total pressures in the cylinders varied between 31 and 35 mbar. The gas composition was then analysed by a Shimadzu GC 17A gas chromatograph, equipped with a GC-WLD detector for the detection of gaseous O_2, N_2, H_2 and CO_2, and a GC-FID detector for the detection of saturated and unsaturated hydrocarbon gases. The gas chromatograph was calibrated with control standards before each group of measurements was conducted. The detection limits of these methods vary for the different gas species and are listed in Appendix B. The errors of the gas analyses are calculated by Gaussian error propagation and depend on the gas pressure and composition. The control of the quality of the total gas analyses is given by the sum of the gases, which should sum to ~100 %.

For the calculation of the exact volume of the liberated gas mixture and the individual gas species, the void volume in the gas cylinder had to be determined. This void volume corresponds to the sum of the cylinder volume and the copper tube volume minus the volume of the rock sample. All cylinders, including the valve, have a constant volume of 860 ml. The volume of the cores was determined by taking the weight of the individual cores and density determined on adjacent pieces.

Possible air-contamination due to leakage of the cylinder or valve during equilibration and/or during measurement was corrected based on the analysed O_2 concentrations in the extracted gas, based on the assumption that the in situ porewater is O_2-free. Where necessary, a correction was applied to the measured concentrations of N_2, CO_2 and CH_4 in the extracted gas. The concentrations of higher hydrocarbons in air are very low and even a large air contamination will not alter the measured concentrations. The gas composition of atmospheric air, as used for any required corrections, is shown in Appendix B.

The original volume of a gas in the cylinder is corrected for air contamination according to:

$$V_{X,Sample,corrected} = V_{X,Sample,measured} - \frac{C_{O_2,Sample,measured} * C_{X,air}}{C_{O_2,air}} \quad (8),$$

where V_X is the volume of a gas species X in vpm (volume per million = 10^{-5} Vol.%) and V_{O2} is the volume of oxygen in vpm.

The volumetric proportion of the single gas species of the total extracted gas volume is calculated according to:

$$V_X = \frac{V_{x,tot}}{V_{gas,tot}} \text{ with } V_{gas,tot} = P_{gas} * V_{Void} \quad (9),$$

where V_x is the volume of a certain gas species X in ml, $V_{x,tot}$ the concentration of the gas species X in ml/L of the total amount of gas, $V_{gas,tot}$ the total volume of the extracted gas in mL, P_{gas} the final gas pressure in the cylinder in mbar and V_{void} the void volume in the cylinder in ml.

The gas pressure measured in the cylinder after equilibration is a mixture of the gases liberated from the porewater and the water vapour pressure at a certain temperature, here 21°C. Therefore, the gas pressure measured in each cylinder after equilibration was corrected according to:

$$P_{WV} = 5.268721 + 0.663623 * T - 0.002364 * T^2 + 0.000716 * T^3 \quad (10)$$

where P_{WV} is the water vapour pressure at a temperature T in mbar (Lide, 1994).

All given gas concentrations are related to standard temperature and pressure conditions (STP = 0°C, 1.013 bar; referred to by 'N' in the units NmL/L for the reported gas concentrations) according to:

$$V_{gas,tot,STP} = \frac{V_{gas,corr} * 273K}{(273K + T_{anal.})} \quad (11)$$

Where $V_{gas,tot,STP}$ is the standardized total gas volume, $V_{gas,corr}$ is the measured and corrected (air contamination and water vapour) gas volume and $T_{anal.}$ Is the temperature during analyses (=21°C).

Finally, the gas contents of the single gas species dissolved in matrix porewater is calculated according to:

$$V_{X,PW} = \frac{V_X}{V_{PW}} * 1000 \quad (12)$$

where $V_{x,PW}$ is the gas content of a gas species X dissolved in porewater in ml_{gas}/kg_{PW}, V_X the volume of a certain gas species X in ml_{gas} and V_{PW} the volume of porewater in the used drillcore segment in kg_{H2O}.

The volume of porewater was determined gravimetrically by drying as described in Section 3.1.

3.3.1.2 Stable Isotope Analyses on Non-Inert Gases

Carbon stable isotope ratios ($\delta^{13}C$) of CH_4, higher hydrocarbons and CO_2, hydrogen stable isotope ratios ($\delta^{2}H$) of CH_4, and nitrogen stable isotope ratios ($\delta^{15}N$) of N_2 could be determined on all five DG samples and on all five NG samples.

For the gas isotope analyses, the gas cylinders with the remaining sample gas were filled with He as a carrier gas to a pressure of 1.5 to 2 bar. Before an aliquot of the gas was transferred to gas tight GC-IRMS glass vials, the gas mixture was allowed to equilibrate for about an hour at a temperature of about 60 °C. Afterward, the carbon and hydrogen isotope ratios of hydrocarbons and CO_2, as well as nitrogen isotope signatures of N_2, were determined by a Thermo V GC-IRMS, which is equipped with a purge and trap system and a direct dual inlet system. The results are reported relative to the V-PDB and V-SMOW standards. The analytical error of $\delta^{13}C$ in hydrocarbons and CO_2 is ± 2 ‰, that of $\delta^{2}H$ ± 10 ‰, and that of $\delta^{15}N$-N_2 ± 0.1 ‰

3.3.2 Determination of Noble Gases (NG) Dissolved in Porewater

The porewater noble gas method is based on the quantitative release of the noble gases from the rock sample by out-gassing from the porewater into the void volume of the stainless-steel container (Eichinger et al. 2011, 2013, 2018; Rufer et al., 2019; Osenbrück et al. 1998). This assumption is based on the chemical inertness and the low solubility of noble gases in water (Weiss 1971).

After sealing the sample in an evacuated steel container, the noble gases are quantitatively released from the porewater by molecular diffusion into the container void volume. The time required to reach equilibrium conditions depends on the transport properties of the rock material as well as the sample size and geometry. The equilibration time was estimated according to diffusive scoping calculations (cf. Section 9.0).

In order to allow equilibration with respect to all noble gases (cf. Section 9.0 and Eichinger et al. 2013), the noble gases dissolved in porewater of the IG_BH05 drill core samples were allowed to outgas into the void volume of the He-tight sample cylinders for 734 to 759 days at room temperature (approximately 20 °C).

All noble gas analyses were conducted at the Institute of Environmental Physics, University of Heidelberg, Germany according to the procedure described in detail in Friedrich (2007). The concentrations of the noble gas isotopes, ^{3}He, ^{4}He, ^{20}Ne, ^{22}Ne, ^{36}Ar and ^{40}Ar, in the gas mixture were measured by a GV 5400He Noble Gas Mass Spectrometer. The analytical errors of the single noble gases were determined by multiple measurements of atmospheric air. The volume of an individual noble gas species in mL/L_{PW} was calculated according to Equations 9, 10 and 12, ensuring the correction for water vapour and the normalisation to standard temperature and pressure conditions (reported as NmL/L_{PW}).

The degree of air contamination of the extracted gas was monitored by the measured neon content (= ^{20}Ne+^{22}Ne). As outlined in Section 9.2, there is negligible in situ production of ^{20}Ne and ^{22}Ne, even over a geological time span of more than 1 Ga. Consequently, the Ne isotope concentrations in matrix porewater cannot exceed that of the air

saturated water (i.e. the concentrations brought into the system by surface-derived water). The time of such infiltration is unknown and could have taken place under different climatic conditions. To account for the temperature dependent solubility of Ne, the Ne content in air saturated water was taken as a range ($[Ne]_{asw}$ = (1.9 ± 0.2)*10^{-7} cc STP Ne/g_{H2O}, Weiss 1971) corresponding to an infiltration temperature between 5 and 25 °C. An air contamination is present in the gas samples once the measured total Ne (^{20}Ne+^{22}Ne) content in the gas sample exceeds that range. The excess of the single noble gas species ($C(X)_{ex}$), introduced to the gas samples by air contamination is calculated using the measured Ne isotope contents, the Ne/C(X) ratio in air, and the range of Ne ($[Ne]_{asw}$) during infiltration according to:

$$C(X)_{ex} = \frac{(C_{Ne_{tot}} - 1.9*10^{-7})}{\frac{C_{Ne_{air}}}{C(X)_{air}}} \quad (13)$$

Where $C(X)_{ex}$ is the excess of the single noble gas species, C_{Neair} the concentration of Ne in air in cc/cc_{air}, and $C(X)_{air}$ the concentration of the single noble gas species in air in cc/cc_{gas}.

4.0 RESULTS OF WATER CONTENT AND WATER-LOSS POROSITY INVESTIGATIONS

Water content, bulk density and water-loss porosity were determined on originally saturated segments of the core samples from borehole IG_BH05. The water content was determined by two independent methods, i.e., gravimetrically by drying rock sections at 105 °C to stable weight conditions, and by using the isotope diffusive exchange technique (see Section 3). The gravimetric water content (WC_{grav}) was determined on different segments of the core samples used for the individual experiments. The initial saturated weight of all these samples was recorded directly after unpacking and preparation of the samples in the laboratory. This ensures that the calculation of the porewater mass is not affected by any possible changes induced during the experiments. Such possible changes were monitored as well by recording the sample weight right after termination of the experiment and before the drying process began. The water loss was calculated using the initial wet weight measured in the lab and the final weight after drying.

The exact determination of the in situ mass of porewater is of particular importance when using indirect extraction methods because porewater tracer concentrations are calculated by mass balance equations using the mass of porewater (Section 3). Knowledge of the water-loss porosity (calculated from the water content and density) is further required for the derivation of diffusion coefficients (Section 6.2).

4.1 Water Contents

Gravimetric water contents were determined on different segments used for individual experiments (see Section 3).

4.1.1 Gravimetric Water Contents Determined on Aqueous Extraction Core Samples

The gravimetric water contents were determined on different aliquots of the 29 aqueous extraction core samples (AQ) taken between 166 and 982 mbgs (downhole). These values were used for the estimation of porewater Cl and Br concentrations derived from the aqueous extraction experiments (cf. Section 6.1).

The gravimetric water contents determined on individual aliquots of the AQ samples vary between 0.09 wt.% and 0.52 wt.%, with weighed values ranging between 0.09 ± 0.01 and 0.46 ± 0.08 wt.% (Table 4-1).

The water contents determined by taking the wet (WC_{wet}) and dry weight (WC_{dry}) are similar within the first two decimal places due to the low water masses in the investigated cores.

The water contents determined on the individual aliquots of the different AQ samples can vary significantly, which is interpreted to be due to mineralogical heterogeneities.

Table 4-1: Gravimetric water contents (WC) of aliquots of AQ core samples from IG_BH05 used for aqueous extraction experiments using wet (WC_{wet}) and dry masses (WC_{dry}) of the individual core pieces. The weighed values are calculated by using the individual masses; (G / T: granodiorite / tonalite, D: diabase).

Sample	Depth	Lithology	Aq.ex. subsample A			Aq.ex. subsample B			Aq.ex. subsample C			WC weighed		
	mbgs*		mass	WC_{wet}	WC_{dry}	mass	WC_{wet}	WC_{dry}	mass	WC_{wet}	WC_{dry}	WC_{wet}	WC_{dry}	Stdev
			g	wt.%	wt.%	g	wt.%	wt.%	g	wt.%	wt.%	wt.%	wt.%	wt.%
IG_BH05_AQ001	166.4	G / T	437.253	0.21	0.21	192.867	0.20	0.20	755.701	0.22	0.22	**0.21**	**0.21**	**0.01**
IG_BH05_AQ002	221.1	G / T	346.389	0.15	0.15	276.458	0.17	0.17	211.169	0.17	0.17	**0.16**	**0.16**	**0.01**
IG_BH05_AQ003	253.2	G / T	382.415	0.20	0.20	188.290	0.18	0.18	199.075	0.22	0.22	**0.20**	**0.20**	**0.02**
IG_BH05_AQ004	290.0	D	435.567	0.52	0.53	190.654	0.38	0.38	160.908	0.40	0.40	**0.46**	**0.47**	**0.08**
IG_BH05_AQ005	343.2	G / T	394.831	0.15	0.15	191.464	0.16	0.16	246.244	0.16	0.16	**0.16**	**0.16**	**0.01**
IG_BH05_AQ006	387.4	G / T	571.320	0.17	0.17	221.437	0.19	0.19	294.755	0.18	0.18	**0.18**	**0.18**	**0.01**
IG_BH05_AQ007	399.9	G / T	544.605	0.17	0.17	294.755	0.18	0.18	210.768	0.19	0.19	**0.17**	**0.17**	**0.01**
IG_BH05_AQ008	427.0	G / T	459.566	0.12	0.12	210.768	0.19	0.19	171.173	0.18	0.18	**0.15**	**0.15**	**0.01**
IG_BH05_AQ009	453.6	G / T	439.705	0.15	0.15	171.173	0.18	0.18	217.735	0.13	0.13	**0.15**	**0.15**	**0.01**
IG_BH05_AQ010	480.1	G / T	487.194	0.14	0.14	217.735	0.13	0.13	238.379	0.12	0.12	**0.13**	**0.13**	**0.01**
IG_BH05_AQ011	507.1	G / T	509.261	0.13	0.13	238.379	0.12	0.12	252.625	0.15	0.15	**0.13**	**0.13**	**0.01**
IG_BH05_AQ012	525.7	G / T	480.132	0.13	0.13	272.243	0.13	0.13	169.541	0.13	0.13	**0.13**	**0.13**	**0.01**
IG_BH05_AQ013	560.7	G / T	422.542	0.13	0.13	169.541	0.13	0.13	216.002	0.13	0.13	**0.13**	**0.13**	**0.01**
IG_BH05_AQ014	588.2	G / T	405.145	0.13	0.13	216.002	0.13	0.13	325.164	0.12	0.12	**0.13**	**0.13**	**0.01**
IG_BH05_AQ015	612.8	G / T	377.051	0.15	0.15	209.513	0.16	0.16	196.685	0.16	0.16	**0.16**	**0.16**	**0.01**
IG_BH05_AQ016	640.4	G / T	434.201	0.12	0.12	196.685	0.16	0.16	431.100	0.12	0.12	**0.13**	**0.13**	**0.01**
IG_BH05_AQ017	664.6	G / T	415.749	0.13	0.13	409.264	0.13	0.14	292.620	0.13	0.13	**0.13**	**0.13**	**0.01**
IG_BH05_AQ018	694.2	G / T	474.545	0.18	0.18	292.620	0.13	0.13	276.595	0.20	0.20	**0.17**	**0.17**	**0.01**
IG_BH05_AQ019	720.7	G / T	478.685	0.16	0.16	276.595	0.20	0.20	399.162	0.18	0.18	**0.18**	**0.18**	**0.01**
IG_BH05_AQ020	750.3	G / T	432.434	0.14	0.14	314.640	0.14	0.14	361.441	0.14	0.14	**0.14**	**0.14**	**0.01**
IG_BH05_AQ021	773.3	G / T	370.490	0.16	0.16	361.441	0.14	0.14	237.389	0.15	0.15	**0.15**	**0.15**	**0.01**
IG_BH05_AQ022	797.6	G / T	415.974	0.23	0.23	237.389	0.15	0.15	324.731	0.16	0.16	**0.18**	**0.18**	**0.04**
IG_BH05_AQ023	827.9	G / T	412.942	0.16	0.16	359.605	0.18	0.18	403.948	0.18	0.18	**0.18**	**0.18**	**0.01**
IG_BH05_AQ024	849.3	G / T	464.189	0.11	0.11	403.948	0.18	0.18	175.391	0.15	0.15	**0.15**	**0.15**	**0.02**
IG_BH05_AQ025	881.8	G / T	474.254	0.10	0.10	175.391	0.15	0.15	169.773	0.14	0.14	**0.12**	**0.12**	**0.02**

Sample	Depth	Lithology	Aq.ex. subsample A			Aq.ex. subsample B			Aq.ex. subsample C			WC weighed		
	mbgs*		mass	WC_{wet}	WC_{dry}	mass	WC_{wet}	WC_{dry}	mass	WC_{wet}	WC_{dry}	WC_{wet}	WC_{dry}	Stdev
			g	wt.%	wt.%	g	wt.%	wt.%	g	wt.%	wt.%	wt.%	wt.%	wt.%
IG_BH05_AQ026	906.7	G / T	366.067	0.10	0.10	185.607	0.14	0.14	130.056	0.13	0.13	**0.11**	**0.11**	**0.02**
IG_BH05_AQ027	936.3	G / T	436.288	0.09	0.09	130.056	0.13	0.13	243.247	0.09	0.09	**0.09**	**0.09**	**0.01**
IG_BH05_AQ028	963.1	G / T	348.196	0.12	0.12	243.247	0.09	0.09	210.845	0.09	0.09	**0.10**	**0.10**	**0.02**
IG_BH05_AQ029	982.3	G / T	376.157	0.14	0.14	210.845	0.09	0.09	183.373	0.15	0.15	**0.13**	**0.13**	**0.02**

* mbgs (downhole)

4.1.2 Gravimetric Water Contents Determined on Porewater Cores

Gravimetric water contents were determined on different aliquots of the 32 PW samples taken between 171 and 986 mbgs (downhole).

4.1.2.1 Gravimetric Water Contents Determined on End Pieces

During sample preparation, the end pieces with weights between 106 and 616 g were cut, weighed and dried at 105 °C to obtain a first estimate about the water contents of the investigated core samples.

The gravimetric water contents determined on the end pieces of the PW core samples vary between 0.02 wt.% and 0.34 wt.%, with weighed WC_{grav} values between 0.03 ± 0.01 wt.% and 0.30 ± 0.03 wt.% (Table 4-2).

The water contents determined by taking the wet (WC_{wet}) and dry weight (WC_{dry}) are similar within the first two decimal places due to the low water masses in the investigated cores.

The water contents determined on the two end pieces of the different PW samples vary, which is attributed to mineralogical heterogeneities.

Table 4-2: Gravimetric water contents (WC) of aliquots of PW core samples from IG_BH05 used for out-diffusion experiments using wet (WC_{wet}) and dry masses (WC_{dry}) of the individual core pieces. The weighed values are calculated by using the individual masses; (G / T: granodiorite / tonalite, D: diabase, A: amphibolite).

Sample	Depth	Litho-logy	Subsample A			Subsample B			WC weighed		
			mass	WC_{wet}	WC_{dry}	mass	WC_{wet}	WC_{dry}	WC_{wet}	WC_{dry}	Stdev
	mbgs*		g	wt.%	wt.%	g	wt.%	wt.%	wt.%	wt.%	wt.%
IG_BH05_PW001	171.4	G / T	266.501	0.23	0.23	615.987	0.23	0.23	**0.23**	**0.23**	**0.01**
IG_BH05_PW002	219.1	G / T	178.501	0.16	0.16	151.922	0.18	0.18	**0.17**	**0.17**	**0.01**
IG_BH05_PW003	253.5	G / T	227.343	0.19	0.19	199.911	0.20	0.20	**0.20**	**0.20**	**0.01**
IG_BH05_PW004	290.2	D	153.211	0.34	0.34	482.521	0.29	0.29	**0.30**	**0.30**	**0.03**
IG_BH05_PW005	341.7	G / T	224.537	0.17	0.17	127.565	0.16	0.16	**0.17**	**0.17**	**0.01**
IG_BH05_PW006	386.7	G / T	222.916	0.20	0.20	199.274	0.20	0.20	**0.20**	**0.20**	**0.01**
IG_BH05_PW007	398.5	G / T	192.601	0.16	0.16	276.321	0.18	0.18	**0.17**	**0.17**	**0.02**
IG_BH05_PW008	426.3	G / T	362.828	0.14	0.14	258.447	0.12	0.12	**0.13**	**0.13**	**0.01**
IG_BH05_PW009	454.3	G / T	276.321	0.17	0.17	206.091	0.17	0.17	**0.17**	**0.17**	**0.01**
IG_BH05_PW010	479.4	G / T	225.827	0.13	0.13	124.059	0.13	0.13	**0.13**	**0.13**	**0.01**
IG_BH05_PW011	506.4	G / T	281.167	0.13	0.13	223.809	0.14	0.14	**0.14**	**0.14**	**0.01**
IG_BH05_PW012	525.1	G / T	164.244	0.13	0.13	272.632	0.13	0.13	**0.13**	**0.13**	**0.01**
IG_BH05_PW013	560.1	G / T	181.586	0.13	0.13	203.490	0.14	0.14	**0.14**	**0.14**	**0.01**
IG_BH05_PW014	587.1	G / T	158.536	0.12	0.12	160.103	0.12	0.12	**0.12**	**0.12**	**0.01**
IG_BH05_PW015	612.1	G / T	152.786	0.17	0.17	105.873	0.17	0.17	**0.17**	**0.17**	**0.01**
IG_BH05_PW016	637.4	G / T	244.830	0.14	0.14	146.224	0.14	0.14	**0.14**	**0.14**	**0.01**
IG_BH05_PW017	665.3	G / T	238.392	0.14	0.14	170.551	0.13	0.13	**0.14**	**0.14**	**0.01**
IG_BH05_PW018	692.4	G / T	224.328	0.19	0.19	173.288	0.19	0.19	**0.19**	**0.19**	**0.01**
IG_BH05_AR033	717.4	A	226.480	0.20	0.20	376.999	0.21	0.21	**0.20**	**0.20**	**0.01**
IG_BH05_PW019	722.2	G / T	285.865	0.18	0.18	196.566	0.17	0.17	**0.17**	**0.17**	**0.01**
IG_BH05_PW020	749.6	G / T	204.604	0.12	0.12	202.287	0.13	0.13	**0.12**	**0.12**	**0.01**

Sample	Depth	Litho-logy	Subsample A			Subsample B			WC weighed		
			mass	WC_{wet}	WC_{dry}	mass	WC_{wet}	WC_{dry}	WC_{wet}	WC_{dry}	Stdev
	mbgs*		g	wt.%	wt.%	g	wt.%	wt.%	wt.%	wt.%	wt.%
IG_BH05_PW021	774.5	G / T	548.149	0.13	0.13	198.738	0.15	0.15	**0.13**	**0.13**	**0.01**
IG_BH05_PW022	801.8	G / T	232.210	0.21	0.21	256.689	0.31	0.31	**0.26**	**0.26**	**0.07**
IG_BH05_PW023	827.2	G / T	139.629	0.15	0.15	133.248	0.14	0.14	**0.15**	**0.15**	**0.01**
IG_BH05_PW024	848.7	G / T	152.606	0.22	0.22	164.370	0.16	0.16	**0.19**	**0.19**	**0.04**
IG_BH05_AR052	856.0	A	192.251	0.02	0.02	135.558	0.03	0.03	**0.03**	**0.03**	**0.01**
IG_BH05_PW025	881.5	G / T	187.783	0.10	0.10	116.634	0.10	0.10	**0.10**	**0.10**	**0.01**
IG_BH05_PW026	906.1	G / T	167.513	0.15	0.15	129.632	0.13	0.13	**0.14**	**0.14**	**0.01**
IG_BH05_PW027	936.3	G / T	227.077	0.09	0.09	138.084	0.10	0.10	**0.09**	**0.09**	**0.01**
IG_BH05_PW028	962.9	G / T	212.555	0.14	0.14	130.414	0.14	0.14	**0.14**	**0.14**	**0.01**
IG_BH05_AR059	979.0	A	175.005	0.06	0.03	275.875	0.04	0.04	**0.05**	**0.04**	**0.01**
IG_BH05_PW029	986.5	G / T	223.648	0.19	0.19	144.155	0.18	0.18	**0.18**	**0.18**	**0.01**

* mbgs (downhole)

4.1.3 Gravimetric Water Contents Determined on Out-Diffusion Cores

Gravimetric water contents determined on the large sized 1,033 to 1,640 g heavy core pieces were determined by the weights taken before and after their long-term immersion in deionised water during the out-diffusion experiments. For 13 samples, the weights of cores were higher, beyond the assumed error of 0.05 g (uncertainty in the determination of the weight with dry surface) after the experiment than before the experiment (Table 4-3, Figure 4-1). The weight gain and hence intake of water during the experiments, which is between 0.113 and 0.335 g can be caused by:

- The filling of pore space created post drilling by stress release;
- The filling of pore space that was desaturated during the time period between core recovery (during drilling) and packaging; or
- Uncertainty of the determination of the initial wet weight during drying of the surface water.

Major evaporation effects in the period between the recovery out of the borehole and sample packing can, in principle, be excluded, because most of the samples arrived with moist surfaces in the lab.

Seven samples showed lower (>0.05 g) weights after the experiments than before (0.053 – 0.100 g, negative Δ-values in Table 4-3). The differences are presumed to be due to the fact that determination of the initial weight is done after drying the surfaces of the cores.

The gravimetric water contents determined on the out-diffusion cores vary between 0.04 ± 0.01 wt.% and 0.25 ± 0.01 wt.%, as calculated using the wet weight (dry surface) of the core before the experiment (b.e.), and between 0.06 ± 0.01 wt.% and 0.26 ± 0.01 wt.%, as calculated using the wet weight (dry surface) of the core after the experiment (a.e.) (Table 4-3). The weight differences of the core samples determined before (b.e.) and after the experiments (a.e.) result in water content variations of 0.01-0.03 wt.% (Table 4-3, Figure 4-2). These differences are within the error ranges determined by Gaussian error propagation (Table 4-3, Figure 4-2). The weight differences before and after the experiments, and the corresponding differences in porewater masses expressed as water content, are considered for the calculation of the porewater Cl and Br concentrations.

The water contents determined by taking the wet (WC_{wet}) and dry weight (WC_{dry}) are similar within the first two decimal places due to the low water masses in the investigated cores (Table 4-3).

Table 4-3: Gravimetric water contents of out-diffusion core samples from IG_BH05 calculated by the mass of cores determined before (b.e.) and after (a.e.) experiments using wet (WC_{wet}) and dry masses (WC_{dry}) of the individual core pieces; the error of the water content is determined by Gaussian error propagation (Appendix C); (G / T: granodiorite / tonalite, D: diabase, A: amphibolite).

Sample	Depth	Lith-ology	mass core			mass porewater		$WC_{grav,wet}$		$WC_{grav,dry}$		error WC_{grav}
			wet b.e.	wet a.e.	Δm_{core}	m_{core} b.e.	m_{core} a.e.	m_{core} b.e.	m_{core} a.e.	m_{core} b.e.	m_{core} a.e.	
	mbgs*		g	g	g	g	g	wt.%	wt.%	wt.%	wt.%	wt.%
IG_BH05_PW001	171.4	G / T	1433.079	1433.082	0.003	2.717	2.720	0.19	0.19	0.19	0.19	0.01
IG_BH05_PW002	219.1	G / T	1439.895	1439.823	-0.072	2.483	2.411	0.17	0.17	0.17	0.17	0.01
IG_BH05_PW003	253.5	G / T	1423.929	1423.880	-0.049	2.868	2.819	0.20	0.20	0.20	0.20	0.01
IG_BH05_PW004	290.2	D	1639.730	1639.631	-0.099	3.700	3.601	0.23	0.22	0.23	0.22	0.01
IG_BH05_PW005	341.7	G / T	1427.080	1427.027	-0.053	2.281	2.228	0.16	0.16	0.16	0.16	0.01
IG_BH05_PW006	386.7	G / T	1427.555	1427.455	-0.100	2.754	2.654	0.19	0.19	0.19	0.19	0.01
IG_BH05_PW007	398.5	G / T	1394.110	1394.155	0.045	2.278	2.323	0.16	0.17	0.16	0.17	0.01
IG_BH05_PW008	426.3	G / T	1465.295	1465.301	0.006	1.840	1.846	0.13	0.13	0.13	0.13	0.01
IG_BH05_PW009	454.3	G / T	1473.535	1473.780	0.245	2.765	3.010	0.19	0.20	0.19	0.20	0.01
IG_BH05_PW010	479.4	G / T	1449.520	1449.735	0.215	2.009	2.224	0.14	0.15	0.14	0.15	0.01
IG_BH05_PW011	506.4	G / T	1464.205	1464.318	0.113	2.033	2.146	0.14	0.15	0.14	0.15	0.01
IG_BH05_PW012	525.1	G / T	1511.659	1511.800	0.141	2.039	2.180	0.13	0.14	0.14	0.14	0.02
IG_BH05_PW013	560.1	G / T	1467.202	1467.530	0.328	2.270	2.598	0.15	0.18	0.15	0.18	0.02
IG_BH05_PW014	587.1	G / T	1485.270	1485.471	0.201	1.877	2.078	0.13	0.14	0.13	0.14	0.01
IG_BH05_PW015	612.1	G / T	1477.510	1477.475	-0.035	2.307	2.272	0.16	0.15	0.16	0.15	0.01
IG_BH05_PW016	637.4	G / T	1447.505	1447.525	0.020	2.077	2.097	0.14	0.14	0.14	0.15	0.03
IG_BH05_PW017	665.3	G / T	1428.345	1428.314	-0.031	2.009	1.978	0.14	0.14	0.14	0.14	0.02
IG_BH05_PW018	692.4	G / T	1353.657	1353.561	-0.096	2.273	2.177	0.17	0.16	0.17	0.16	0.01
IG_BH05_AR033	717.4	A	1032.790	1032.822	0.032	2.203	2.235	0.21	0.22	0.21	0.22	0.01
IG_BH05_PW019	722.2	G / T	1446.155	1446.070	-0.085	2.508	2.423	0.17	0.17	0.17	0.17	0.01
IG_BH05_PW020	749.6	G / T	1402.924	1403.086	0.162	1.922	2.084	0.14	0.15	0.14	0.15	0.01
IG_BH05_PW021	774.5	G / T	1427.565	1427.729	0.164	1.978	2.142	0.14	0.15	0.14	0.15	0.01
IG_BH05_PW022	801.8	G / T	1423.230	1423.247	0.017	3.623	3.640	0.25	0.26	0.26	0.26	0.01
IG_BH05_PW023	827.2	G / T	1405.170	1405.331	0.161	2.245	2.406	0.16	0.17	0.16	0.17	0.01
IG_BH05_PW024	848.7	G / T	1460.094	1460.027	-0.067	2.158	2.091	0.15	0.14	0.15	0.14	0.01
IG_BH05_AR052	856.0	A	1523.566	1524.016	0.450	0.534	0.984	0.04	0.06	0.04	0.06	0.01
IG_BH05_PW025	881.5	G / T	1420.928	1420.948	0.020	1.311	1.331	0.09	0.09	0.09	0.09	0.01
IG_BH05_PW026	906.1	G / T	1445.630	1445.920	0.290	1.494	1.784	0.10	0.12	0.10	0.12	0.01
IG_BH05_PW027	936.3	G / T	1450.818	1450.782	-0.036	1.293	1.257	0.09	0.09	0.09	0.09	0.01

Sample	Depth	Lith-ology	mass core			mass porewater		$WC_{grav,wet}$		$WC_{grav,dry}$		error WC_{grav}
			wet b.e.	wet a.e.	Δm_{core}	m_{core} b.e.	m_{core} a.e.	m_{core} b.e.	m_{core} a.e.	m_{core} b.e.	m_{core} a.e.	
	mbgs*		g	g	g	g	g	wt.%	wt.%	wt.%	wt.%	wt.%
IG_BH05_PW028	962.9	G / T	1465.130	1465.145	0.015	2.122	2.137	0.14	0.15	0.15	0.15	0.01
IG_BH05_AR059	979.0	A	1173.639	1173.950	0.311	0.653	0.964	0.06	0.08	0.06	0.08	0.01
IG_BH05_PW029	986.5	G / T	1440.235	1440.570	0.335	2.796	3.131	0.19	0.22	0.19	0.22	0.01

* mbgs (downhole)

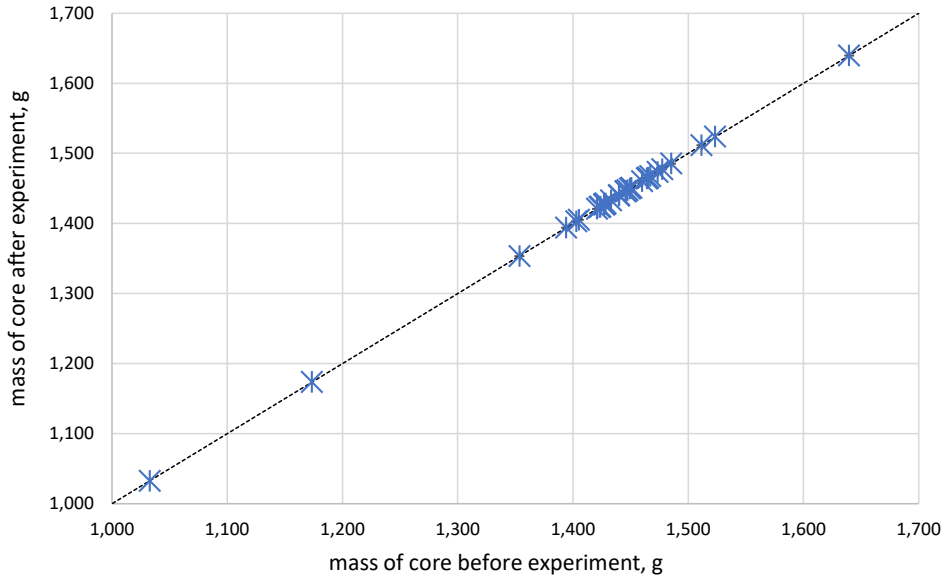


Figure 4-1: Mass of core samples from IG_BH05 before and after the out-diffusion experiments; the uncertainty of the core mass is ± 0.05g.

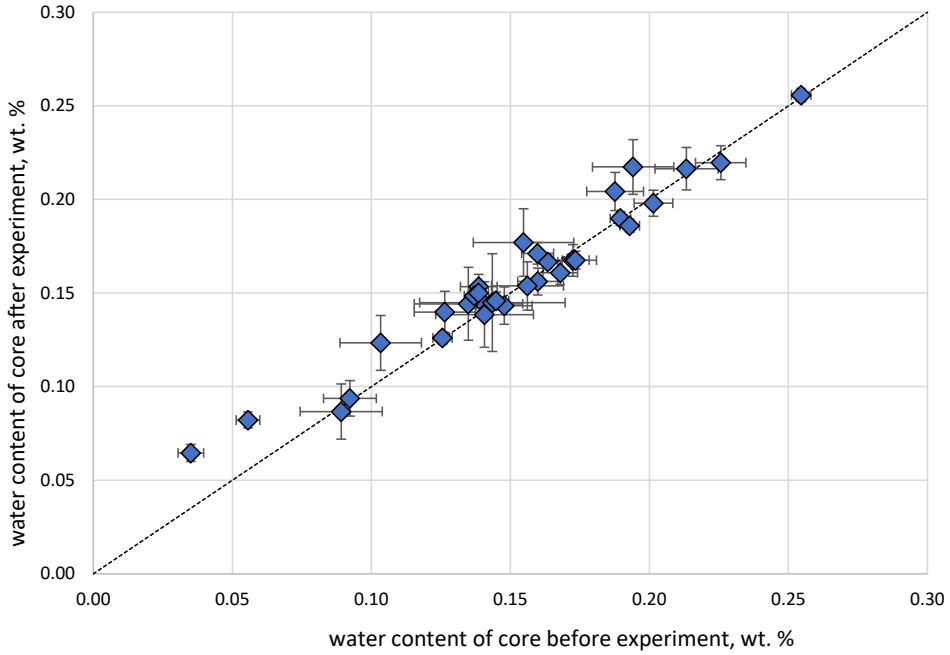


Figure 4-2: Water content calculated from the wet mass (dry surface) before and after the out-diffusion experiments of core sections from IG_BH05; the error of the water content is determined by Gaussian error propagation (Appendix C).

4.1.4 Gravimetric Water Contents Determined by Isotope Diffusive Exchange

Gravimetric water contents were determined on crushed core pieces used for the isotope diffusive exchange experiments. The masses of the used rock material were measured before and after the experiments. During the experiments the rocks remained saturated. A weight change of the rocks above the analytical uncertainty of ± 0.05 g at constant total weight was observed in all experiments (Table 4-4). Therefore, the water contents were corrected for the weight loss or gain.

The gravimetric water contents determined on rock pieces used for isotope diffusive exchange experiments ($WC_{IsoEx,grav,corr.}$) vary between 0.04 wt.% and 0.30 wt.% with weighed $WC_{IsoEx,grav}$ values ranging from 0.05 ± 0.01 wt.% to 0.30 ± 0.01 wt.% (Table 4-4).

The water contents determined by the isotope diffusive exchange technique ($WC_{IsoEx,average}$) for core samples from borehole IG_BH05 vary between 0.07 ± 0.01 wt.% and 0.37 ± 0.2 wt.% (Table 4-5).

During the isotope diffusive exchange experiment water uptake of 0.07 to 0.31 g was observed for almost all individual experiments. For two individual experiments the rock mass was 0.04 g (IG_BH05_PW009 ICE) and 0.11 g (IG_BH05_PW009 LAB) lower after the experiment.

Hence, the gravimetric water content of crushed rock samples used for isotope diffusive exchange experiments were corrected by calculating the mass difference ($\Delta m_{(rock,wet)}$ = $m_{(rock,wet)}$ after experiment – $m_{(rock,wet)}$ before experiment) of the crushed rock sample in the container. The porewater mass was then corrected by this mass difference and the gravimetric water contents were calculated using the corrected porewater mass values.

The water contents determined by the isotope diffusive exchange technique are slightly higher compared to gravimetric values determined on the same core pieces (Table 4-4 and Table 4-5, Figure 4-3). For the samples

IG_BH05_PW001, PW003, PW004 and PW022 the water contents determined by isotope diffusive exchange are >0.05 wt% higher than those determined gravimetrically (Table 4-4). Based on the experimental quality check, it was decided to classify these values as reliable.

It is known from many sites, that generally the water contents determined by the isotope diffusive exchange (WC_{IsoEx}) technique are slightly higher than those determined gravimetrically ($WC_{IsoEx, grav}$) (e.g., Eichinger et al. 2010, 2018; Eichinger 2021). This can be observed in argillaceous and crystalline rocks and is explained by the isotopic exchange of the test water with interlayer and bound water, which is generally more pronounced in argillaceous rocks and altered crystalline rocks (e.g., Pearson et al. 2003; Gimmi et al. 2022).

For the further use of the values, it is recommended to take the weighed gravimetric water contents (Table 4-7).

Table 4-4: Gravimetric water contents determined on core samples from IG_BH05 used for isotope diffusive exchange experiments ($WC_{IsoEx, grav}$); Water contents are corrected for weight changes during experiments (b.e. = before experiment, a.e. = after experiment); the gravimetric water contents determined on the rock pieces used in the experiments with LAB – and ICE water are weighed taking their weights into account; the error of the water content is determined by Gaussian error propagation (Appendix C).

	LAB				ICE				
Sample	mass	Δm (a.e.-b.e.)	$WC_{IsoEx, grav}$	$WC_{IsoEx, grav,corr.}$	mass	Δm (a.e.-b.e.)	$WC_{IsoEx, grav}$	$WC_{IsoEx, grav,corr.}$	$WC_{IsoEx,grav}$ weighed
	g	g	wt.%	wt.%	g	g	wt.%	wt.%	wt. %
IG_BH05_PW001	348.1	0.123	0.17	0.14	347.9	0.146	0.17	0.13	**0.13**
IG_BH05_PW002	401.9	0.076	0.14	0.12	400.1	0.076	0.14	0.12	**0.12**
IG_BH05_PW003	403.5	0.107	0.16	0.14	400.9	0.094	0.18	0.15	**0.15**
IG_BH05_PW004	367.2	0.119	0.33	0.30	371.7	0.119	0.33	0.30	**0.30**
IG_BH05_PW005	398.1	0.072	0.15	0.14	398.6	0.074	0.15	0.13	**0.13**
IG_BH05_PW006	458.4	0.088	0.15	0.13	458.7	0.086	0.15	0.13	**0.13**
IG_BH05_PW007	507.5	0.110	0.15	0.13	507.7	0.101	0.15	0.13	**0.13**
IG_BH05_PW008	474.5	0.059	0.11	0.10	475.6	0.128	0.11	0.09	**0.09**
IG_BH05_PW009	523.7	-0.106	0.19	0.21	524.3	-0.041	0.16	0.19	**0.19**
IG_BH05_PW010	444.7	0.108	0.14	0.11	446.8	0.114	0.14	0.11	**0.11**
IG_BH05_PW011	468.4	0.106	0.13	0.11	470.5	0.115	0.14	0.11	**0.11**
IG_BH05_PW012	484.0	0.147	0.12	0.09	473.2	0.142	0.12	0.09	**0.09**
IG_BH05_PW013	399.7	0.093	0.12	0.10	397.4	0.127	0.13	0.10	**0.10**
IG_BH05_PW014	433.7	0.143	0.12	0.09	432.3	0.180	0.12	0.09	**0.09**
IG_BH05_PW015	482.0	0.113	0.15	0.12	483.5	0.140	0.15	0.12	**0.12**
IG_BH05_PW016	394.6	0.102	0.12	0.10	396.0	0.118	0.12	0.10	**0.10**
IG_BH05_PW017	454.8	0.119	0.12	0.09	452.1	0.129	0.12	0.09	**0.09**
IG_BH05_PW018	464.9	0.069	0.12	0.11	466.8	0.093	0.12	0.11	**0.11**
IG_BH05_PW019	435.9	0.104	0.14	0.12	436.1	0.125	0.14	0.11	**0.11**
IG_BH05_PW020	553.2	0.137	0.12	0.09	554.6	0.178	0.12	0.09	**0.09**

Sample	LAB				ICE				
	mass	Δm (a.e.-b.e.)	$WC_{IsoEx,grav}$	$WC_{IsoEx,grav,corr.}$	mass	Δm (a.e.-b.e.)	$WC_{IsoEx,grav}$	$WC_{IsoEx,grav,corr.}$	$WC_{IsoEx,grav}$ weighed
	g	g	wt.%	wt.%	g	g	wt.%	wt.%	wt. %
IG_BH05_PW021	471.8	0.155	0.14	0.11	468.9	0.174	0.14	0.10	**0.10**
IG_BH05_PW022	446.2	0.084	0.19	0.17	448.1	0.092	0.16	0.16	**0.16**
IG_BH05_PW023	422.2	0.114	0.14	0.11	423.1	0.126	0.15	0.12	**0.12**
IG_BH05_PW024	353.3	0.121	0.16	0.12	358.0	0.141	0.17	0.12	**0.12**
IG_BH05_PW025	439.0	0.192	0.09	0.05	435.3	0.212	0.10	0.05	**0.05**
IG_BH05_PW026	381.4	0.118	0.09	0.06	378.4	0.157	0.10	0.06	**0.06**
IG_BH05_PW027	480.5	0.210	0.09	0.05	477.8	0.277	0.10	0.05	**0.05**
IG_BH05_PW028	383.2	0.151	0.13	0.09	384.8	0.193	0.14	0.09	**0.09**
IG_BH05_AR059	303.1	0.313	0.09	0.07	301.2	0.259	0.10	0.10	**0.08**
IG_BH05_PW029	469.7	0.237	0.20	0.15	467.1	0.288	0.21	0.15	**0.15**

Table 4-5: Water contents of core samples from IG_BH05 calculated by isotope diffusive exchange method (eq. 7); the error of the water content is determined by Gaussian error propagation (Appendix C).

Sample	WC_{IsoEx} ($\delta^{18}O$) wt.%	WC_{IsoEx} ($\delta^{2}H$) wt.%	WC_{IsoEx} average wt.%
IG_BH05_PW001	0.23±0.01	0.24±0.02	0.24±0.02
IG_BH05_PW002	0.14±0.01	0.14±0.01	0.14±0.01
IG_BH05_PW003	0.21±0.01	0.20±0.02	0.20±0.01
IG_BH05_PW004	0.37±0.02	0.37±0.02	0.37±0.02
IG_BH05_PW005	0.16±0.01	0.16±0.01	0.16±0.01
IG_BH05_PW006	0.18±0.01	0.18±0.01	0.18±0.01
IG_BH05_PW007	0.19±0.01	0.18±0.02	0.19±0.01
IG_BH05_PW008	0.12±0.01	0.11±0.01	0.11±0.01
IG_BH05_PW009	0.17±0.01	0.17±0.01	0.17±0.01
IG_BH05_PW010	0.12±0.01	0.12±0.01	0.12±0.01
IG_BH05_PW011	0.11±0.01	0.11±0.01	0.11±0.01
IG_BH05_PW012	0.12±0.01	0.11±0.01	0.11±0.01
IG_BH05_PW013	0.15±0.01	0.15±0.01	0.15±0.01
IG_BH05_PW014	0.11±0.01	0.11±0.02	0.11±0.01
IG_BH05_PW015	0.16±0.01	0.16±0.01	0.16±0.01
IG_BH05_PW016	0.13±0.01	0.13±0.02	0.13±0.01
IG_BH05_PW017	0.13±0.01	0.13±0.02	0.13±0.01
IG_BH05_PW018	0.14±0.01	0.14±0.01	0.14±0.01

Sample	WC_{IsoEx} ($\delta^{18}O$) wt.%	WC_{IsoEx} ($\delta^{2}H$) wt.%	WC_{IsoEx} average wt.%
IG_BH05_PW019	0.15±0.01	0.14±0.01	0.14±0.01
IG_BH05_PW020	0.11±0.01	0.11±0.02	0.11±0.01
IG_BH05_PW021	0.12±0.01	0.12±0.01	0.12±0.01
IG_BH05_PW022	0.22±0.01	0.21±0.01	0.22±0.01
IG_BH05_PW023	0.15±0.01	0.15±0.01	0.15±0.01
IG_BH05_PW024	0.16±0.01	0.15±0.01	0.16±0.01
IG_BH05_PW025	0.08±0.01	0.08±0.01	0.08±0.01
IG_BH05_PW026	0.10±0.01	0.10±0.01	0.10±0.01
IG_BH05_PW027	0.07±0.01	0.07±0.01	0.07±0.01
IG_BH05_PW028	0.13±0.01	0.12±0.01	0.13±0.01
IG_BH05_AR059	0.07±0.01	0.08±0.01	0.08±0.01
IG_BH05_PW029	0.18±0.01	0.17±0.01	0.17±0.01

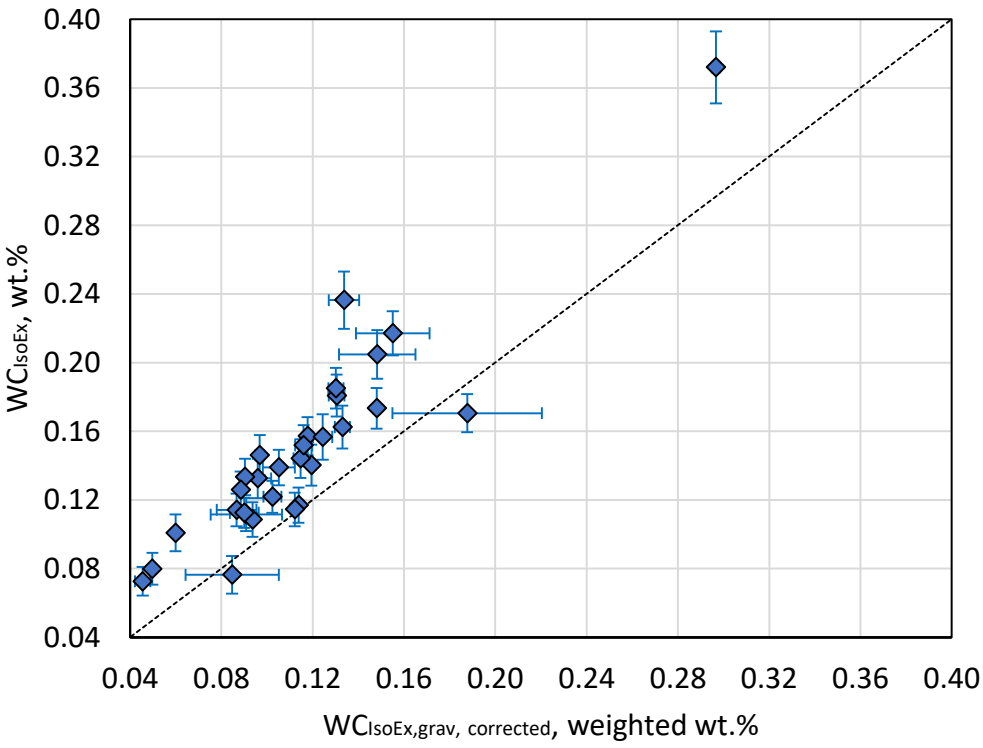


Figure 4-3: Comparison of water contents determined by isotope diffusive exchange (WC_{IsoEx}) and gravimetrically ($WC_{IsoEx,\ grav,\ corr.}$ by wet weight, corrected for weight change during experiments) on the same core pieces; the error of the water content is determined by Gaussian error propagation (Appendix C).

4.1.5 Gravimetric Water Contents Determined on Out-Gassing Cores

Gravimetric water contents were determined on the full-sized cores used for out-gassing experiments (NG and DF) with weights between 1,588 and 1,794 g by taking the weights determined after recovery on site. For all samples except IG_BH05_NG005 the weights of cores were lower after the experiment than before the experiment (Table 4-6) The weight loss during the experiments which is between 0.26 and 1.61 g is most likely caused by evacuating and flushing the cylinders with helium (DG samples) or nitrogen (NG samples) and by the outtake of various gas aliquots for the analyses.

The gravimetric water contents determined on the out-gassing cores vary between 0.09 ± 0.01 wt.% and 0.21 ± 0.01 wt.%, as calculated using the weight of the core before the experiment (b.e.) (Table 4-6).

Table 4-6: Gravimetric water contents of out-gassing core samples from IG_BH05 calculated by the mass of cores determined before experiments of the individual cores; the error of the water content is determined by Gaussian error propagation (Appendix C); (G / T: granodiorite / tonalite)

Sample	Depth	Lithology	m_{core} b.e.	m_{core} a.e.	Δm_{core}	m_{PW} (m_{core} b.e.)	WC (m_{core} b.e.)	error WC_{grav}
	mbgs*		g	g	g	g	wt.%	wt.%
IG_BH05_DG001	431.2	G / T	1642.44	1641.568	0.87	3.11	0.19	0.02
IG_BH05_DG002	536.4	G / T	1762.77	1762.514	0.26	3.31	0.19	0.02
IG_BH05_DG003	634.2	G / T	1754.05	1752.937	1.11	3.24	0.18	0.02
IG_BH05_DG004	744.3	G / T	1620.37	1619.689	0.68	2.78	0.17	0.02
IG_BH05_DG005	879.3	G / T	1778.30	1777.390	0.91	2.32	0.13	0.01
IG_BH05_NG001	428.5	G / T	1591.34	1590.391	0.85	2.86	0.18	0.02
IG_BH05_NG003	533.3	G / T	1588.75	1587.784	0.97	2.87	0.18	0.02
IG_BH05_NG005	630.2	G / T	1794.00	1794.421	-0.42	1.60	0.09	0.01
IG_BH05_NG007	747.3	G / T	1716.69	1715.083	1.61	3.55	0.22	0.03
IG_BH05_NG009	872.2	G / T	1720.37	1719.310	1.06	2.44	0.14	0.02

* mbgs (downhole)

4.1.6 Summary and Depth Profiles of Water Content Results

The gravimetric water contents determined on different portions of the core pieces for the AQ and the PW investigations are weighed using the masses of the individual rock pieces (Table 4-7). The weighed water contents represent the entire cores, with masses between 682 g and 1,386 g for AQ cores and between 1,636 g and 3,115 g for PW cores. As shown in the previous paragraphs, the water contents of the individual aliquots can vary significantly, and is inferred to be caused by mineralogical heterogeneities. This indicates that water content values cannot be extrapolated.

The weighed gravimetric water contents of the AQ- and PW-core samples taken between 166.4 and 979.0 mbgs (downhole) vary between 0.03±0.01 wt.% and 0.26 ±0.04 wt.% (Table 4-7, Figure 4-4).

The water contents of the individual sub-samples and of the AQ and PW samples, which are generally collected close, or adjacent, to one another (e.g. AQ001 and PW001), can differ significantly. This is demonstrated by the large error bars associated with the weighed water content values (Table 4-7, Figure 4-4). A clear trend in the water content values with depth cannot be observed.

Table 4-7: Weighed gravimetric water contents of aqueous extraction and porewater core samples taken from borehole IG_BH05 and their corresponding total masses; the uncertainties of the water content values are the weighed standard deviations of the individual aliquots showing the density of water contents in one entire sample; (G / T: granodiorite / tonalite, D: diabase, A: amphibolite).

Sample	Depth	Lithology	$m_{rock,tot}$	$WC_{grav,weighed}$	Bulk,wet density	$Vol._{core}$	$Porosity_{grav,weighed}$
	mbgs*		g	wt. %	g/cm³	cm³	Vol.%
IG_BH05_AQ001	166.4	G / T	1385.8	0.21±0.01	2.67	163.0	0.57±0.14
IG_BH05_AQ002	221.1	G / T	834.0	0.16±0.01	2.64	143.2	0.43±0.09
IG_BH05_AQ003	253.2	G / T	769.8	0.20±0.02	2.64	173.6	0.52±0.07
IG_BH05_AQ004	290.0	D	787.1	0.47±0.08	3.00	146.0	1.39±0.22
IG_BH05_AQ005	343.2	G / T	832.5	0.16±0.01	2.65	175.6	0.42±0.06
IG_BH05_AQ006	387.4	G / T	1087.5	0.18±0.01	2.63	196.0	0.47±0.07
IG_BH05_AQ007	399.9	G / T	1050.1	0.17±0.01	2.66	171.9	0.46±0.09
IG_BH05_AQ008	427.0	G / T	841.5	0.15±0.01	2.67	180.0	0.41±0.06
IG_BH05_AQ009	453.6	G / T	828.6	0.15±0.01	2.64	184.4	0.39±0.05
IG_BH05_AQ010	480.1	G / T	943.3	0.13±0.01	2.69	168.9	0.36±0.06
IG_BH05_AQ011	507.1	G / T	1000.3	0.13±0.01	2.68	159.9	0.35±0.07
IG_BH05_AQ012	525.7	G / T	921.9	0.13±0.02	2.70	157.2	0.35±0.07
IG_BH05_AQ013	560.7	G / T	808.1	0.13±0.01	2.67	162.0	0.34±0.06
IG_BH05_AQ014	588.2	G / T	946.3	0.13±0.01	2.64	209.7	0.34±0.04
IG_BH05_AQ015	612.8	G / T	783.2	0.16±0.01	2.64	167.5	0.42±0.06
IG_BH05_AQ016	640.4	G / T	1062.0	0.13±0.01	2.67	159.3	0.35±0.08
IG_BH05_AQ017	664.6	G / T	1117.6	0.13±0.01	2.68	171.9	0.35±0.07
IG_BH05_AQ018	694.2	G / T	1043.8	0.17±0.01	2.66	195.1	0.45±0.07
IG_BH05_AQ019	720.7	G / T	1154.4	0.18±0.01	2.65	188.7	0.47±0.08
IG_BH05_AQ020	750.3	G / T	1108.5	0.14±0.01	2.69	196.7	0.38±0.06
IG_BH05_AQ021	773.3	G / T	969.3	0.15±0.01	2.68	170.6	0.40±0.07
IG_BH05_AQ022	797.6	G / T	978.1	0.18±0.04	2.62	165.7	0.48±0.09
IG_BH05_AQ023	827.9	G / T	1176.5	0.18±0.01	2.66	144.8	0.47±0.13
IG_BH05_AQ024	849.3	G / T	1043.5	0.15±0.02	2.72	145.0	0.40±0.10
IG_BH05_AQ025	881.8	G / T	819.4	0.12±0.02	2.71	160.5	0.32±0.06
IG_BH05_AQ026	906.7	G / T	681.7	0.11±0.02	2.72	184.4	0.31±0.04
IG_BH05_AQ027	937.0	G / T	809.6	0.09±0.01	2.73	199.7	0.25±0.04
IG_BH05_AQ028	963.1	G / T	802.3	0.10±0.02	2.69	156.1	0.27±0.05
IG_BH05_AQ029	982.3	G / T	770.4	0.13±0.02	2.70	194.3	0.34±0.04
IG_BH05_PW001	171.4	G / T	3011.6	0.19±0.05	2.68	535.9	0.51±0.02
IG_BH05_PW002	219.1	G / T	2572.2	0.16±0.03	2.66	541.1	0.46±0.03
IG_BH05_PW003	253.5	G / T	2655.6	0.18±0.03	2.66	534.7	0.54±0.03

Sample	Depth mbgs*	Lithology	$m_{rock,tot}$ g	$WC_{grav,weighed}$ wt. %	Bulk,wet density g/cm³	$Vol._{core}$ cm³	$Porosity_{grav,weighed}$ Vol.%
IG_BH05_PW004	290.2	D	3014.2	0.26±0.05	3.01	544.5	0.66±0.04
IG_BH05_PW005	341.7	G / T	2575.8	0.15±0.02	2.68	533.4	0.43±0.03
IG_BH05_PW006	386.7	G / T	2766.8	0.17±0.04	2.64	541.5	0.51±0.02
IG_BH05_PW007	398.5	G / T	2878.4	0.15±0.02	2.64	527.8	0.43±0.02
IG_BH05_PW008	426.3	G / T	3036.6	0.12±0.02	2.66	551.5	0.33±0.02
IG_BH05_PW009	454.3	G / T	3004.2	0.18±0.01	2.65	557.1	0.50±0.03
IG_BH05_PW010	479.4	G / T	2691.1	0.13±0.01	2.65	538.0	0.37±0.03
IG_BH05_PW011	506.4	G / T	2908.2	0.13±0.01	2.69	543.9	0.37±0.02
IG_BH05_PW012	525.1	G / T	2905.9	0.12±0.03	2.69	560.2	0.36±0.02
IG_BH05_PW013	560.1	G / T	2649.8	0.13±0.03	2.70	547.9	0.42±0.05
IG_BH05_PW014	587.1	G / T	2670.1	0.11±0.02	2.68	554.7	0.34±0.05
IG_BH05_PW015	612.1	G / T	2701.6	0.14±0.03	2.68	550.5	0.42±0.03
IG_BH05_PW016	637.4	G / T	2629.2	0.13±0.03	2.68	547.1	0.39±0.04
IG_BH05_PW017	665.3	G / T	2744.2	0.12±0.03	2.65	538.6	0.37±0.07
IG_BH05_PW018	692.4	G / T	2682.9	0.15±0.04	2.65	509.5	0.45±0.05
IG_BH05_AR033	717.4	A	1636.3	0.21±0.01	2.67	350.4	0.57±0.04
IG_BH05_PW019	722.2	G / T	2800.6	0.16±0.03	2.66	540.9	0.46±0.02
IG_BH05_PW020	749.6	G / T	2917.8	0.12±0.02	2.67	522.8	0.36±0.02
IG_BH05_PW021	774.5	G / T	3115.3	0.13±0.02	2.68	534.5	0.37±0.02
IG_BH05_PW022	801.8	G / T	2806.5	0.22±0.06	2.67	540.4	0.68±0.02
IG_BH05_PW023	827.2	G / T	2523.5	0.14±0.02	2.63	533.0	0.42±0.03
IG_BH05_PW024	848.7	G / T	2488.4	0.15±0.03	2.64	538.6	0.39±0.02
IG_BH05_AR052	856.0	A	1851.8	0.03±0.01	2.95	521.1	0.10±0.04
IG_BH05_PW025	881.5	G / T	2599.6	0.08±0.03	2.71	527.2	0.25±0.03
IG_BH05_PW026	906.1	G / T	2502.8	0.09±0.04	2.70	532.8	0.28±0.03
IG_BH05_PW027	936.3	G / T	2774.2	0.07±0.03	2.53	533.9	0.23±0.04
IG_BH05_PW028	962.9	G / T	2576.1	0.13±0.03	2.72	545.9	0.39±0.04
IG_BH05_AR059	979.0	A	2229.1	0.06±0.02	2.92	424.6	0.16±0.01
IG_BH05_PW029	986.5	G / T	2745.2	0.18±0.02	2.68	538.9	0.52±0.02

* mbgs (downhole)

4.2 Bulk Dry/Wet Density and Water-Loss Porosity

The bulk dry and wet density are calculated according to Equation 1 (Section 3.2) using the dry and wet mass of the full diameter cylindrical cores and the volume of the core samples determined by measuring the height and core diameter by a Vernier Caliper. Bulk wet densities were determined for the cores used for out-diffusion and aqueous extraction experiments before crushing, and bulk dry density was determined only for out-diffusion cores.

Bulk dry and wet density values of the core samples from borehole IG_BH05 are similar, differing by a maximum of 0.01 g/cm^3, due to the low water content of the samples, and vary between 2.63 and 3.01 g/cm^3 (Table 4-8).

The water-loss (connected) porosity was calculated according to Equation 2 (Section 3.2) using the water content calculated by the dry and wet weight and the bulk dry/wet density of the samples. Water-loss porosities are calculated for core sections used for the out-diffusion and aqueous extraction experiments, for which the water content and the bulk dry/wet density were determined. Water-loss porosities calculated using the wet mass and density differ by a maximum of 0.01 Vol.% from those determined by the dry mass and density (Table 4-8).

Water-loss porosity values of core samples taken between 166 and 987 mbgs (downhole) from borehole IG_BH05 vary between 0.10 ± 0.04 Vol.% and 1.39 ± 0.22 Vol.% (Table 4-8, Figure 4-4). Trends in the porosity values for the samples follow the same trends as described by the water contents (Figure 4-4).

Table 4-8: Bulk wet and dry density and water-loss (=WL-) porosity determined by water contents calculated for dry ($\Phi_{WL,dry}$) and wet ($\Phi_{WL,wet}$) core samples from borehole IG_BH05; the errors are calculated by Gaussian error propagation (Appendix C); (G / T: granodiorite / tonalite, D: diabase, A: amphibolite).

Sample	Depth mbgs*	Litho-logy	bulk, wet density g/cm^3	bulk, dry density g/cm^3	water-loss porosity $\Phi_{WL,wet}$ Vol.%	water-loss porosity $\Phi_{WL,dry}$ Vol.%
IG_BH05_AQ001	166.4	G / T	2.67		0.57±0.014	
IG_BH05_AQ002	221.1	G / T	2.64		0.43±0.09	
IG_BH05_AQ003	253.2	G / T	2.64		0.52±0.07	
IG_BH05_AQ004	290.0	D	3.00		1.39±0.22	
IG_BH05_AQ005	343.2	G / T	2.65		0.42±0.06	
IG_BH05_AQ006	387.4	G / T	2.63		0.47±0.07	
IG_BH05_AQ007	399.9	G / T	2.66		0.46±0.09	
IG_BH05_AQ008	427.0	G / T	2.67		0.41±0.06	
IG_BH05_AQ009	453.6	G / T	2.64		0.39±0.05	
IG_BH05_AQ010	480.1	G / T	2.69		0.36±0.06	
IG_BH05_AQ011	507.1	G / T	2.68		0.35±0.07	
IG_BH05_AQ012	525.7	G / T	2.70		0.35±0.07	
IG_BH05_AQ013	560.7	G / T	2.67		0.34±0.06	
IG_BH05_AQ014	588.2	G / T	2.64		0.34±0.04	
IG_BH05_AQ015	612.8	G / T	2.64		0.42±0.06	
IG_BH05_AQ016	640.4	G / T	2.67		0.35±0.08	
IG_BH05_AQ017	664.6	G / T	2.68		0.35±0.07	
IG_BH05_AQ018	694.2	G / T	2.66		0.45±0.07	
IG_BH05_AQ019	720.7	G / T	2.65		0.47±0.08	
IG_BH05_AQ020	750.3	G / T	2.69		0.38±0.06	
IG_BH05_AQ021	773.3	G / T	2.68		0.40±0.07	
IG_BH05_AQ022	797.6	G / T	2.62		0.48±0.09	
IG_BH05_AQ023	827.9	G / T	2.66		0.47±0.13	
IG_BH05_AQ024	849.3	G / T	2.72		0.40±0.10	
IG_BH05_AQ025	881.8	G / T	2.71		0.32±0.06	
IG_BH05_AQ026	906.7	G / T	2.72		0.31±0.04	
IG_BH05_AQ027	937.0	G / T	2.73		0.25±0.04	
IG_BH05_AQ028	963.1	G / T	2.69		0.27±0.05	
IG_BH05_AQ029	982.3	G / T	2.70		0.34±0.04	

Sample	Depth mbgs*	Litho-logy	bulk, wet density g/cm³	bulk, dry density g/cm³	water-loss porosity $\Phi_{WL,wet}$ Vol.%	water-loss porosity $\Phi_{WL,dry}$ Vol.%
IG_BH05_PW001	171.4	G / T	2.68	2.67	0.51±0.02	0.51±0.02
IG_BH05_PW002	219.1	G / T	2.66	2.66	0.46±0.03	0.46±0.03
IG_BH05_PW003	253.5	G / T	2.66	2.66	0.54±0.03	0.54±0.03
IG_BH05_PW004	290.2	D	3.01	3.01	0.68±0.04	0.68±0.04
IG_BH05_PW005	341.7	G / T	2.68	2.68	0.43±0.03	0.43±0.03
IG_BH05_PW006	386.7	G / T	2.64	2.64	0.51±0.02	0.51±0.02
IG_BH05_PW007	398.5	G / T	2.64	2.64	0.43±0.02	0.43±0.02
IG_BH05_PW008	426.3	G / T	2.66	2.66	0.33±0.02	0.33±0.02
IG_BH05_PW009	454.3	G / T	2.65	2.65	0.50±0.03	0.50±0.03
IG_BH05_PW010	479.4	G / T	2.69	2.69	0.37±0.02	0.37±0.02
IG_BH05_PW011	506.4	G / T	2.69	2.69	0.37±0.02	0.37±0.02
IG_BH05_PW012	525.1	G / T	2.70	2.70	0.36±0.05	0.36±0.05
IG_BH05_PW013	560.1	G / T	2.68	2.68	0.42±0.05	0.42±0.05
IG_BH05_PW014	587.1	G / T	2.68	2.68	0.34±0.03	0.34±0.03
IG_BH05_PW015	612.1	G / T	2.68	2.68	0.42±0.04	0.42±0.04
IG_BH05_PW016	637.4	G / T	2.65	2.65	0.39±0.07	0.39±0.07
IG_BH05_PW017	665.3	G / T	2.65	2.65	0.37±0.05	0.37±0.05
IG_BH05_PW018	692.4	G / T	2.66	2.66	0.45±0.02	0.45±0.02
IG_BH05_AR033	717.4	A	2.95	2.95	0.57±0.04	0.57±0.04
IG_BH05_PW019	722.2	G / T	2.67	2.67	0.46±0.02	0.46±0.02
IG_BH05_PW020	749.6	G / T	2.68	2.68	0.37±0.02	0.37±0.02
IG_BH05_PW021	774.5	G / T	2.67	2.67	0.37±0.02	0.37±0.02
IG_BH05_PW022	801.8	G / T	2.64	2.63	0.68±0.03	0.68±0.03
IG_BH05_PW023	827.2	G / T	2.64	2.64	0.42±0.02	0.42±0.02
IG_BH05_PW024	848.7	G / T	2.71	2.71	0.39±0.03	0.39±0.03
IG_BH05_AR052	856.0	A	2.93	2.93	0.10±0.01	0.10±0.01
IG_BH05_PW025	881.5	G / T	2.70	2.70	0.25±0.03	0.25±0.03
IG_BH05_PW026	906.1	G / T	2.53	2.53	0.28±0.04	0.28±0.04
IG_BH05_PW027	936.3	G / T	2.72	2.72	0.23±0.04	0.23±0.04
IG_BH05_PW028	962.9	G / T	2.68	2.68	0.39±0.02	2
IG_BH05_AR059	979.0	A	2.77	7	0.16±0.01	0.16±0.01
IG_BH05_PW029	986.5	G / T	2.67	2.67	0.52±0.04	0.52±0.04

* mbgs (downhole)

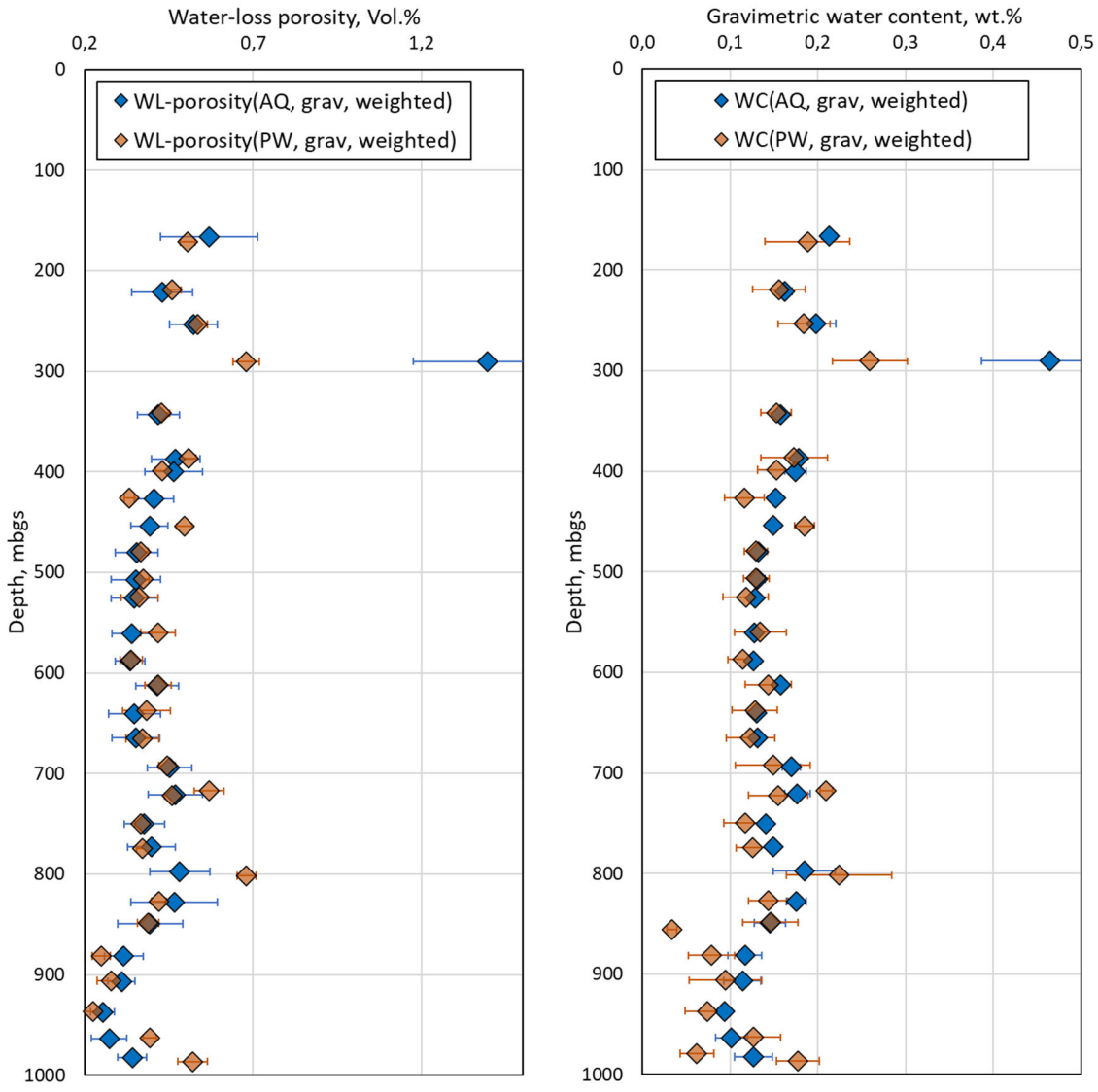


Figure 4-4: Water content and water-loss porosity of core samples from IG_BH05.

5.0 RESULTS OF CHEMICAL COMPOSITION OF EXPERIMENT SOLUTIONS OF AQUEOUS EXTRACTION AND OUT-DIFFUSION EXPERIMENTS

Out-diffusion and aqueous extraction experiments were performed on 32 PW and 29 AQ core samples taken from borehole IG_BH05, respectively. In both experiments the investigated rock samples were immersed in test water. The concentrations of dissolved constituents in the test solutions originate from:

- Porewater, which exchanges and mixes with test water;
- Water-rock interactions, releasing reactive elements in the test water; and

- Fluid inclusions (only aqueous extractions), which are liberated during crushing of the rocks.

5.1 Chemical Composition of Aqueous Extraction Solutions

The purpose of aqueous extraction experiments is to obtain an initial estimate of the porewater salinity, which is necessary for the adjustment of the ion concentration in the test waters for the indirect porewater extraction methods.

Crushing and grinding of the rock material additionally liberates fluid trapped in mineral fluid inclusions. During leaching, all salts will become dissolved in addition to the limited dissolution of the original mineral assemblage. The mineralization of a leach solution is therefore the sum of:

- The constituents originally dissolved in the porewater;
- The constituents present in fluid inclusions; and
- Water-rock interactions during the leaching process.

Aqueous leach solutions represent a complex composition in rocks with abundant fluid inclusions and/or rapidly reacting mineral phases. The aqueous extraction solutions produced by the immersion of crushed cores from borehole IG_BH05 in deionized water (procedure cf. Section 3.2.1) have pH values between 9.3 and 10.2, and a mineralization between 69 and 165 mg/L (EC = 105 – 301 µS/cm, Table 5-1).

The dissolved constituents consist predominately of Na^+, K^+, Ca^{2+}, HCO_3^-, Cl^-, SO_4^{2-} and Si in different concentrations and proportions (Table 5-1, Figure 5-1). Minor concentrations of Mg^{2+}, F^- and Br^- could be detected. Concentrations of Sr were below detection limit for most samples (Table 5-1). In samples IG_BH05_AQ026-AQ029 low Sr concentrations between 0.57 and 2.9 mg/L could be detected (Table 5-1). Silicon and aluminium could be detected in concentrations between 3.6 and 9.2 mg/L (Si) and between 0.14 and 11.5 mg/L (Al).

The estimated porewater Cl concentrations of core samples from IG_BH05, extracted by aqueous extraction experiments using the weighed water contents of the AQ samples (cf. Table 4-7), vary between 1,720 mg/kg_{PW} and 20,594 mg/kg_{PW} (Table 7-2).

Table 5-1: Analytical results of the aqueous extraction solutions of crushed core samples from borehole IG_BH05; Test solution types are classified after Jäckli (1970).

Sample		IG_BH05_AQ001	IG_BH05_AQ002	IG_BH05_AQ003	IG_BH05_AQ004	IG_BH05_AQ005	IG_BH05_AQ006	IG_BH05_AQ007	IG_BH05_AQ008	IG_BH05_AQ009	IG_BH05_AQ010
Interval	m BHL	166.4	221.1	253.2	290.0	343.2	387.4	399.9	427.0	453.6	480.1
Hydroisotop No.		365894	365895	365896	365897	365898	368156	368157	368158	368159	368160
MASTER VARIABLES											
pH (lab)	-log(H+)	9.7	9.5	9.6	10.2	9.6	9.7	9.7	9.5	9.6	9.5
Electr. Conductivity	µS/cm	129	137	125	254	130	106	107	130	135	143
Sample Temperature	°C	20	20	20	20	20	20	20	20	20	20
Alkalinity (pH 4,3) Lab.	mmol/l	0.87	0.66	0.71	1.56	0.77	0.8	0.8	0.6	0.72	0.5
Alkalinity (pH 8,2) Lab.	mmol/l	0.26	0.42	0.42	0.56	0.42	0.35	0.35	0.48	0.37	0.38
DISSOLVED CONSTITUENTS											
CATIONS	mg/l										
Sodium (Na+)	mg/l	23.5	21.1	21.1	44.9	20.6	16.7	17.1	15.6	18.6	15.1
Potassium (K+)	mg/l	2.6	5.4	6.3	0.68	6.7	4	3.5	9.3	8.8	10.5
Magnesium (Mg+2)	mg/l	< 0.2	< 0.2	< 0.2	< 0.2	< 0.2	< 0.2	< 0.2	< 0.2	0.21	< 0.2
Calcium (Ca+2)	mg/l	0.23	1.3	1.1	0	0.75	2.8	2.6	3.5	3.6	4.7
Strontium (Sr+2)	mg/l	< 0,05	< 0,05	< 0,05	< 0,05	< 0,05	< 0,05	< 0,05	< 0,05	< 0,05	< 0,05
Silicon (Si+4)	mg/l	9	8.5	8.2	8.6	7.1	9	8.5	7.3	7.7	7.2
Aluminium (Al+3)	mg/l	11.5	4.34	2.35	4.72	2.47	1.0	2.9	1.1	6.14	0.849
ANIONS											
Fluoride (F-)	mg/l	0.12	0.13	0.12	0.49	0.14	0.36	0.2	0.15	0.22	0.1
Chloride (Cl-)	mg/l	6.1	15.1	14.1	9.6	10.9	7	5.6	15.6	16.3	22.2
Bromide (Br-)	mg/l	0.6	0.27	0.63	0.11	0.22	0.17	0.12	2.1	0.32	0.49
Sulfate (SO4-2)	mg/l	2	1.8	1.7	5.5	1.5	1	2	1.1	1.8	1.3
Nitrate (NO3-)	mg/l	0.32	0.21	0.27	0.29	< 0,2	< 0,2	< 0,2	< 0,2	0.24	< 0,2
Total Alkalinity as HCO3	mg/l	53.0	40.5	43.2	95.2	47.0	45.5	46.4	37.5	43.9	30.8
PARAMETERS CALCULATED FROM ANALYTICAL DATA											
Sum of analysed constituents	mg/l	88	86	89	157	88	78	77	85	94	85
Charge balance	%	-0.11%	-0.72%	-1.21%	-0.17%	-0.63%	-1.07%	-0.44%	-0.73%	-0.23%	-0.20%
Water type		Na-HCO_3-(Cl)	Na-(K)-HCO_3-Cl	Na-(K)-HCO_3-Cl	Na-HCO_3-(Cl)	Na-(K)-HCO_3-Cl	Na-(Ca)-(K)-HCO_3-Cl	Na-(K)-HCO_3-(Cl)	Na-K-(Ca)-HCO_3-Cl	Na-(K)-(Ca)-HCO_3-Cl	Na-K-Ca-HCO_3-Cl

Note: m BHL is equivalent to mbgs (downhole).

Table 5-1: Continued

Sample		IG_BH05_AQ011	IG_BH05_AQ012	IG_BH05_AQ013	IG_BH05_AQ014	IG_BH05_AQ015	IG_BH05_AQ016	IG_BH05_AQ017	IG_BH05_AQ018	IG_BH05_AQ019	IG_BH05_AQ020
Interval	m BHL	507.1	525.7	560.7	588.2	612.8	640.4	664.6	694.2	720.7	750.3
Hydroisotop No.		368161	368198	368199	368200	367724	368201	368580	368581	368582	368886
MASTER VARIABLES											
pH (lab)	-log(H+)	9.6	9.6	9.6	9.6	9.4	9.6	9.7	9.5	9.6	9.6
Electr. Conductivity	µS/cm	140	149	160	156	126	105	175	205	195	151
Sample Temperature	°C	20	20	20	20	20	20	20	20	20	20
Alkalinity (pH 4,3) Lab.	mmol/l	0.51	0.53	0.54	0.57	0.66	0.6	0.8	0.7	0.72	0.59
Alkalinity (pH 8,2) Lab.	mmol/l	0.36	0.12	0.08	0.2	0.11	0.26	0.25	0.25	0.27	0.15
DISSOLVED CONSTITUENTS											
CATIONS	mg/l										
Sodium (Na+)	mg/l	14.5	15.2	18.7	16.2	17.1	13.3	27.3	29.2	28.3	17.3
Potassium (K+)	mg/l	10.5	12.1	11.4	12	7.1	5.4	7.2	9.7	8.7	10.4
Magnesium (Mg+2)	mg/l	< 0.2	< 0.2	< 0.2	< 0.2	0.2	< 0.2	< 0.2	< 0.2	< 0.2	0.22
Calcium (Ca+2)	mg/l	4.5	4.8	4.1	5.1	4.1	3.4	3.0	4.6	3.9	4.8
Strontium (Sr+2)	mg/l	< 0,05	< 0,05	< 0,05	< 0,05	0.06	< 0,05	< 0,05	< 0,05	< 0,05	< 0,05
Silicon (Si+4)	mg/l	7.3	8.3	6.7	8	7.3	6.4	9.1	9.2	9	7.2
Aluminium (Al+3)	mg/l	0.446	1.54	3.24	1.2	0.137	0.6	4.8	1.4	4.72	1.91
ANIONS											
Fluoride (F-)	mg/l	< 0,1	< 0,1	0.1	< 0,1	0.1	0.11	< 0,1	< 0,1	< 0,1	0.17
Chloride (Cl-)	mg/l	21.2	23.9	26.8	24.1	16.7	10.4	22.9	34	31.2	22.9
Bromide (Br-)	mg/l	0.5	0.56	0.62	0.52	1.1	0.83	2.2	3.5	2	0.74
Sulfate (SO4-2)	mg/l	1.4	0.99	1.2	1.3	1.5	1	1.4	1.9	2	1.8
Nitrate (NO3-)	mg/l	< 0,2	< 0,2	< 0,2	< 0,2	< 0,2	< 0,2	0.36	0.28	0.23	< 0,2
Total Alkalinity as HCO3	mg/l	31.1	32.3	33.0	35.0	40.0	34.9	51.4	44.4	43.8	36.1
PARAMETERS CALCULATED FROM											
Sum of analysed constituents	mg/l	84	90	96	94	88	69	116	128	120	94
Charge balance	%	-0.86%	-0.88%	-0.92%	-0.68%	-1.44%	-0.79%	-0.88%	-0.83%	-0.67%	-0.60%
Water type		Na-K-Ca-Cl-HCO_3	Na-K-(Ca)-Cl-HCO_3	Na-K-(Ca)-Cl-HCO_3	Na-K-Ca-Cl-HCO_3	Na-(Ca)-(K)-HCO_3-Cl	Na-(Ca)-(K)-HCO_3-Cl	Na-(K)-HCO_3-Cl	Na-(K)-(Ca)-Cl-HCO_3	Na-(K)-(Ca)-Cl-HCO_3	Na-K-(Ca)-Cl-HCO_3

Table 5-1: Continued

Sample		IG_BH05_AQ020	IG_BH05_AQ021	IG_BH05_AQ022	IG_BH05_AQ023	IG_BH05_AQ024	IG_BH05_AQ025	IG_BH05_AQ026	IG_BH05_AQ027	IG_BH05_AQ028	IG_BH05_AQ029
Interval	m BHL	750.3	773.3	797.6	827.9	849.3	881.8	906.7	937.0	963.4	982.3
Hydroisotop No.		368886	368887	368888	368889	368890	368891	369747	369748	369749	369750
MASTER VARIABLES											
pH (lab)	-log(H+)	9.6	9.5	9.5	9.4	9.4	9.3	9.8	9.6	9.6	9.3
Electr. Conductivity	µS/cm	151	155	123	196	216	190	192	164	227	301
Sample Temperature	°C	20	20	20	20	20	20	20	20	20	20
Alkalinity (pH 4,3) Lab.	mmol/l	0.59	0.59	0.5	0.66	0.57	0.5	0.7	0.6	0.5	0.31
Alkalinity (pH 8,2) Lab.	mmol/l	0.15	0.15	0.12	0.13	0.12	0.1	0.29	0.17	0.13	0.08
DISSOLVED CONSTITUENTS											
CATIONS	mg/l										
Sodium (Na+)	mg/l	17.3	19.1	15	26.7	24.8	20.3	23.4	18.4	27.2	36.5
Potassium (K+)	mg/l	10.4	8.8	4.0	10.7	16.3	14.2	15.4	14.5	15.2	7.8
Magnesium (Mg+2)	mg/l	0.22	0.21	< 0.2	0.21	0.25	0.21	0.32	0.38	0.39	0.86
Calcium (Ca+2)	mg/l	4.8	4.5	5.6	4.4	4.9	5.6	4.1	3.6	6.1	13.5
Strontium (Sr+2)	mg/l	< 0,05	< 0,05	< 0,05	< 0,05	< 0,05	< 0,05	1	0.57	1.36	2.94
Silicon (Si+4)	mg/l	7.2	7.2	6	8.3	6.7	5.8	7.3	5.9	5.5	3.6
Aluminium (Al+3)	mg/l	1.91	1.47	2.16	9.21	3.72	3.13	6.1	1.7	5.5	1.77
ANIONS											
Fluoride (F-)	mg/l	0.17	0.22	0.15	0.38	0.24	< 0,1	0.13	< 0,1	0.17	0.43
Chloride (Cl-)	mg/l	22.9	24.1	17.9	32.0	39.1	34.8	30.9	25.3	49.3	78.7
Bromide (Br-)	mg/l	0.74	0.81	1	1.5	1.5	1.7	2.7	0.93	0.89	2.3
Sulfate (SO4-2)	mg/l	1.8	1.8	1.4	2.7	1.8	0.88	1.8	2	2	2.6
Nitrate (NO3-)	mg/l	< 0,2	< 0,2	< 0,2	< 0,2	< 0,2	< 0,2	< 0,2	0.25	< 0,2	0.46
Total Alkalinity as HCO3	mg/l	36.1	35.8	30.5	40.1	35.0	30.2	43.9	36.1	29.8	18.9
PARAMETERS CALCULATED FROM											
Sum of analysed constituents	mg/l	94	95	76	119	124	108	124	102	132	165
Charge balance	%	-0.60%	-1.19%	-0.97%	0.43%	0.54%	0.71%	-0.13%	1.24%	-0.07%	-0.84%
Water type		Na-K-(Ca)-Cl-HCO_3	Na-(K)-(Ca)-Cl-HCO3	Na-Ca-Cl-HCO3	Na-(K)-(Ca)-Cl-HCO_3	Na-K-(Ca)-Cl-HCO_3	Na-K-(Ca)-Cl-HCO_3	Na-K-(Ca)-Cl-HCO_3	Na-K-(Ca)-Cl-HCO_3	Na-K-(Ca)-Cl-HCO_3	Na-Ca-Cl-(HCO_3)

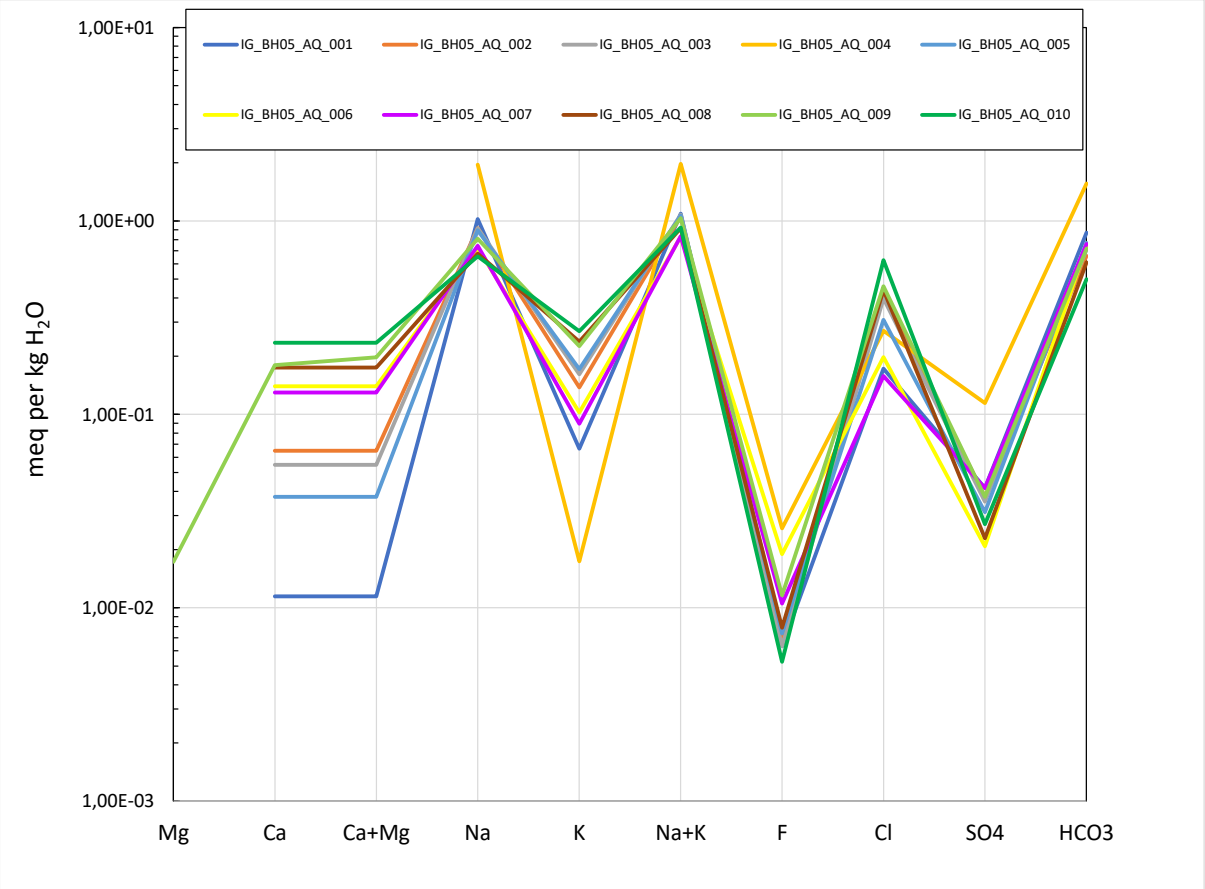


Figure 5-1: Schoeller diagram of experiment solutions from aqueous extraction experiments conducted with core samples from Borehole IG_BH05.

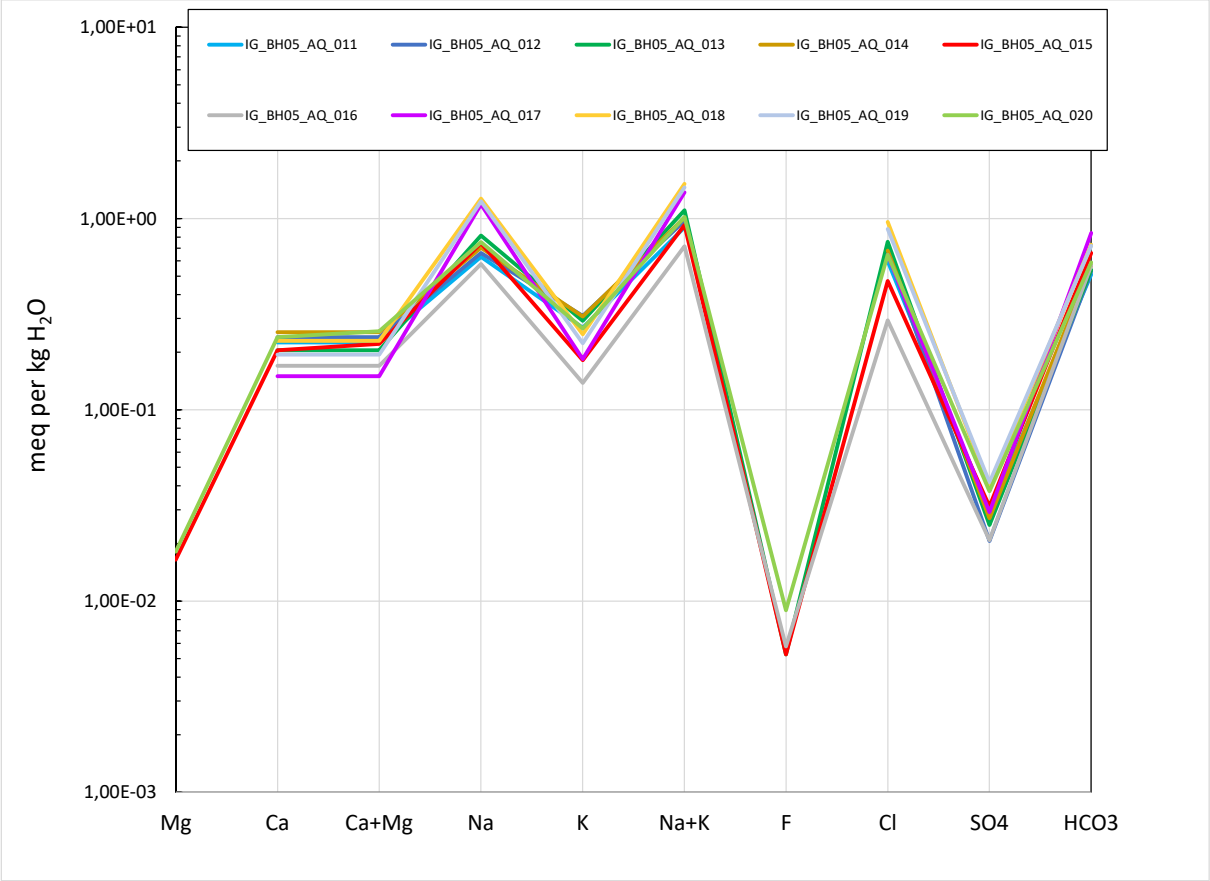


Figure 5-1 continued

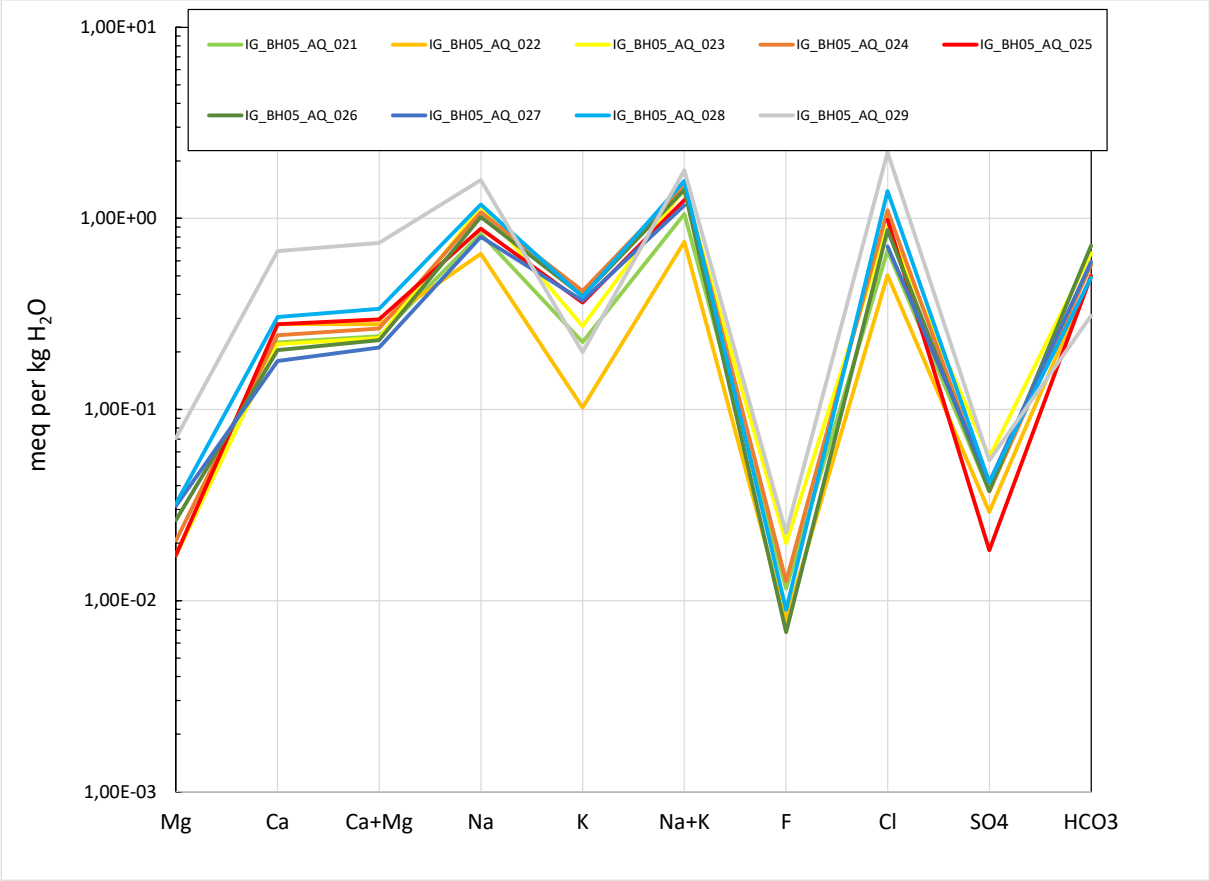


Figure 5-1 continued

5.2 Chemical Composition of Out-Diffusion Experiment Solutions

Out-diffusion experiments were performed on 32 core samples from borehole IG_BH05 to derive the porewater chloride and bromide concentrations, porewater $\delta^{37}Cl$ isotopic ratios, and chemical composition of the test solutions - which are the basis for the hydrogeochemical modelling of porewater chemical compositions. The core sections varied in diameter between 60.4 mm and 61.1 mm, with lengths between 122 mm and 192 mm. The corresponding volume of the sections varied between 350 cm^3 and 560 cm^3 and the saturated mass was between 1,033 and 1,640 g. In the out-diffusion experiments, the mass ratio of experiment solution to rock samples was between 0.084 and 0.122 (Table 5-2).

During the out-diffusion experiments, a continuous exchange between porewater and test water takes place until equilibrium conditions with respect to conservative, non-reactive compounds are achieved. The experiments use intact large-sized core pieces and so, there is no release and/or influence of fluids from within fluid inclusions. The exchange appears to occur mainly by diffusion (Section 6). For chemically conservative elements, such as chloride and bromide, for which the porewater is the only source, the porewater concentration can be calculated using the gravimetrically determined porewater mass of the rock sample. For reactive elements and compounds, such as Ca^{2+}, Mg^{2+}, Na^{+}, K^{+}, Sr^{2+}, Si, Al, SO_4^{2-} and HCO_3^{-}, the contribution of mineral dissolution reactions during

the experiment has to be accounted for. Those reactions are evaluated by the determination of the concentrations of the non-conservative elements taken in time-series (Section 6.1).

The pH of the experiment solutions varies between 7.1 and 9.8, with a total mineralization between 68 mg/L and 411 mg/L (EC = 74 - 1026 µS/cm, Table 5-2). It should be noted that the total mineralization obtained for the experiment solutions depends on the water content of the sample and the water/rock ratio used in the experiment (Table 4-3) and does not directly reflect differences in porewater salinity.

The experimental solutions contain Na^+ (16.0 – 53.7 mg/L), Ca^{2+} (1.2 – 121 mg/L), K^+ (0.80 – 10.4 mg/L), HCO_3^- (39.5 – 127 mg/L), Cl^- (0.9 – 269 mg/L), Br (<0.05 to 9.6 mg/L) and SO_4^{2-} (1.5 – 27.4 mg/L) in varying proportions and concentrations (Table 5-2, Figure 5-2).

Based on the out-diffusion test solutions, samples are characterized by Na^+ and HCO_3- dominated water between 171 and 387 mbgs (downhole), and transition to a Na-Cl dominated water between 399 and 587 mbgs (downhole). Between 612 and 665 mbgs (downhole) samples are again characterized by Na- and HCO_3-dominated water and further to a Na-, Ca- and Cl- dominated water between 692 and 987 mbgs (downhole) (Table 5-2).

Silicon (expressed as Si) is present in concentrations between 4.7 and 11.8 mg/L. Magnesium, strontium, aluminium, boron, fluoride, and nitrate are below detection limit or present in low or trace concentrations (Table 5-2).

The concentrations of dissolved organic carbon (DOC) vary between 4.2 and 14.2 mg/L (Table 5-2).

The DIC/TIC concentrations (DIC = TIC, because analyses are performed on filtered samples) determined by TIC analyser vary between 8.0 and 25.7 mg/L. The comparison of the TIC concentrations determined by direct analyses with those determined by acid titration (AC4.3) shows that the total alkalinity is mainly determined by HCO_3.

The strontium $^{87}Sr/^{86}Sr$ isotope ratios of the out-diffusion test solutions vary between 0.714518 and 0.740887 with Sr^{2+} concentrations below the detection limit of 0.1 mg/L or very low concentrations between 0.4 and 0.75 mg/L (Table 5-2).

Table 5-2: Analytical results of test solutions of out-diffusion experiments using core samples from borehole IG_BH05

Sample		IG_BH05_Blank	IG_BH05_PW001	IG_BH05_PW002	IG_BH05_PW003	IG_BH05_PW004	IG_BH05_PW005	IG_BH05_PW006	IG_BH05_PW007	IG_BH05_PW008	IG_BH05_PW009	IG_BH05_PW010
Hydroisotop Nr.		374595	374590	374591	374592	374593	374594	375609	375610	375611	375612	375613
Interval	mbgs		171.4	219.1	253.5	290.3	341.7	386.7	398.5	426.3	454.3	479.4
Ratio TW:PW			52.7	58.4	50.2	37.4	61.5	59.5	66.1	74.7	54.8	74.8
MISCELLANEOUS PROPERTIES												
pH (lab)	-log(H+)	4.7	7.1	8.1	8.3	9.8	7.3	7.8	7.6	7.4	7.7	7.4
sp. el. Conductivity	µS/cm	9	74	148	157	255	95	151	142	211	302	354
Acid Capacity (4.3)	mmol	< 0.1	0.7	1.27	1.48	2.09	0.79	1.19	0.94	0.99	0.9	0.9
Base Capacity (8.2)	mmol	-	-	-	0.1	0.62	-	-	-	-	-	-
Sample Temperature	ºC	18.8	23.9	24	24.1	24.2	24.3	24.5	25	24.6	24.6	24.6
DOC	mg/l	3.6	7.9	7.5	6.3	10.2	11.4	6	4.9	5.6	4.4	5.6
TIC	mg/l	< 1	9.4	15.6	18.7	19.5	9.9	14.5	11.8	10.4	10	11.2
DISSOLVED CONSTITUENTS												
CATIONS	mg/l											
Sodium (Na+)	mg/l	< 0.2	16	26.8	30.2	53.7	16.9	20.1	21.5	27.2	29.9	27.6
Potassium (K+)	mg/l	< 0.1	1.4	2.9	2.5	0.79	2	2.7	2.3	4.4	3.7	7.1
Calcium (Ca+2)	mg/l	0.72	1.2	6.3	6.1	2.7	4	10.6	6.6	12.6	25.7	32.5
Magnesium (Mg+2)	mg/l	< 0.2	< 0.2	< 0.2	< 0.2	< 0.2	< 0.2	<0.2	<0.2	< 0.2	< 0.2	< 0.2
Strontium (Sr+2)	mg/l	<0.002	0.012	0.036	0.044	0.018	0.031	0.088	0.070	0.138	0.199	0.298
Aluminium (Al+3)	mg/l	0.058	0.151	0.521	0.447	1.752	0.084	0.198	0.136	0.067	0.137	0.134
Silicon (Si+4)	mg/l	< 0.1	11.8	6.5	7.5	7	10.9	7.7	7.37	10.29	7.14	8.12
Boron (B)	mg/l	0.008	0.18	0.079	0.218	0.214	0.138	0.084	0.115	0.049	0.07	0.039
ANIONS												
Fluoride (F-)	mg/l	< 0.1	0.37	0.97	0.5	0.23	0.38	2.1	0.55	0.15	2.0	< 0.1
Chloride (Cl-)	mg/l	0.12	1	6.8	3.5	0.94	4.1	4.9	11	30.5	54.8	65.9
Bromide (Br-)	mg/l	< 0.05	< 0,05	0.06	0.08	< 0.05	< 0.05	<0.05	0.16	1.4	0.95	1.4
Nitrate (NO3-)	mg/l	< 0.2	< 0.2	< 0.2	1.3	< 0.2	< 0.2	< 0.2	< 0.2	< 0.2	< 0.2	< 0.2
Sulphate (SO4-2)	mg/l	< 0.5	2.6	1.6	1.5	15.9	3.7	2.5	1.7	2.7	4.3	4.1
Total Alkalinity	meq/l	< 0.1	0.70	1.27	1.48	2.08	0.79	1.19	0.94	0.99	0.90	0.90
Total Alkalinity as HC(	mg/l		43	77.6	90.3	127	48.3	72.7	57.4	60.5	54.8	54.7
PARAMETERS CALCULATED FROM ANALYTICAL DATA												
Sum of Analysed Constituents	mg/l	0.8	66	123	136	201	79	116	101	139	176	193
Charge Balance:		0.80%	-0.94%	0.17%	0.70%	0.79%	-0.94%	-0.68%	0.22%	-0.24%	0.50%	2.48%
ION-ION RATIOS												
Br*1000/Cl weight	mg/mg			8.8	22.9				14.5	45.9	17.3	21.2
Br*1000/Cl molal	mol/mol			3.9	10.1				6.5	20.4	7.7	9.4
Na/Cl molal	mol/mol		24.674	6.078	13.306	88.099	6.357	6.326	3.014	1.375	0.841	0.646
K/Na molal	mol/mol		0.051	0.064	0.049	0.009	0.070	0.079	0.063	0.095	0.073	0.151
SO4/Cl molal	mol/mol		0.960	0.087	0.158	6.243	0.333	0.188	0.057	0.033	0.029	0.023
Na/(Cl+SO4)	mol/mol		12.591	5.592	11.489	12.163	4.768	5.323	2.852	1.332	0.818	0.631
ISOTOPE RATIOS												
δ37Cl	pm SMOC	Cl too low	Cl too low	0.06	-0.43	Cl too low	-0.37	0.33	-0.22	0.44	0.65	0.64
error δ37Cl	pm SMOC	/	/	0.20	0.48	/	0.69	0.20	0.01	0.03	0.01	0.09
87Sr/86Sr		Sr too low	0.723735	0.740887	0.725791	0.717172	0.727197	0.731922	0.723022	0.739180	0.730733	0.729768
error 87Sr/86Sr			0.00005	0.00005	0.00005	0.00005	0.00005	0.00005	0.00005	0.00005	0.00005	0.00005

Table 5-2: Continued

Sample		IG_BH05_PW011	IG_BH05_PW012	IG_BH05_PW013	IG_BH05_PW014	IG_BH05_PW015	IG_BH05_PW016	IG_BH05_PW017	IG_BH05_PW018	IG_BH05_PW019	IG_BH05_PW020	IG_BH05_PW021
Hydroisotop Nr.		375614	375615	375616	375617	375618	375619	378360	378361	378362	378363	378364
Interval	mbgs	506.5	525.1	560.1	587.1	612.1	637.5	665.3	692.4	722.2	749.6	774.5
Ratio TW:PW		72.1	65.9	62.3	72.7	61.4	67.9	69.0	59.9	55.5	80.7	74.2
MISCELLANEOUS PROPERTIES												
pH (lab)	-log(H+)	7.4	7.2	7.4	7.7	7.5	7.6	8	7.6	7.5	7.7	7.6
sp. el. Conductivity	µS/cm	351	364	447	294	197	250	250	275	237	285	295
Acid Capacity (4.3)	mmol	0.96	0.98	0.89	1.12	0.98	1.23	1.27	0.87	0.78	0.93	0.83
Base Capacity (8.2)	mmol	-	-	-	-	-	-	-	-	-	-	-
Sample Temperature	ºC	24.6	24.6	24.6	24.6	24.6	24.6	24.6	24.6	24.6	24.6	24.6
DOC	mg/l	6	5.5	7.6	5.6	5	5.3	6.1	7.7	7.6	5.4	4.2
TIC	mg/l	9.9	9.9	8	11.9	11.1	13.8	14.3	10.4	9.3	10.3	9.9
DISSOLVED CONSTITUENTS												
CATIONS	mg/l											
Sodium (Na+)	mg/l	25.1	33.5	33	26.2	21.3	17.5	20.4	26.3	20.9	16	20.1
Potassium (K+)	mg/l	8.2	8.3	6.5	6.3	3	4.4	3	3.2	2.9	4.9	4.3
Calcium (Ca+2)	mg/l	31.9	32.3	43.6	26.6	14.5	27.9	24.1	20.8	21	31.6	30.3
Magnesium (Mg+2)	mg/l	< 0.2	< 0.2	0.22	< 0.2	< 0.2	0.2	< 0.2	< 0.2	0.29	0.26	< 0.2
Strontium (Sr+2)	mg/l	0.328	0.318	0.361	0.215	0.091	0.183	0.213	0.167	0.094	0.279	0.234
Aluminium (Al+3)	mg/l	0.077	0.102	0.033	0.103	0.02	0.047	0.119	0.087	0.048	0.076	0.096
Silicon (Si+4)	mg/l	8.79	9.21	7.29	6.62	7.48	6.58	6.5	7.78	10.29	6.28	7.93
Boron (B)	mg/l	0.01	0.01	0.048	0.035	0.077	0.096	0.114	0.146	0.124	0.068	0.088
ANIONS												
Fluoride (F-)	mg/l	< 0.1	< 0.1	0.18	< 0.1	< 0.1	0.88	0.7	2.5	0.64	0.2	0.76
Chloride (Cl-)	mg/l	66.6	75.9	102	50.1	27	34.8	34.7	43.9	40.2	50.0	53.4
Bromide (Br-)	mg/l	1.3	1.4	2.2	0.95	0.66	0.72	0.71	1.2	0.69	0.94	1.2
Nitrate (NO3-)	mg/l	< 0.2	< 0.2	< 0.2	< 0.2	< 0.2	< 0.2	< 0.2	< 0.2	< 0.2	0.54	< 0.2
Sulphate (SO4-2)	mg/l	3.8	3.4	3.9	3	2.6	3.5	2.5	2.8	4.6	3.3	2.7
Total Alkalinity	meq/l	0.96	0.98	0.89	1.12	0.98	1.23	1.27	0.87	0.78	0.93	0.82
Total Alkalinity as HC(	mg/l	58.6	59.9	54.2	68.6	60	75.2	77.6	52.8	47.3	56.6	50.3
PARAMETERS CALCULATED FROM ANALYTICAL DATA												
Sum of Analysed Constituents	mg/l	196	215	246	182	129	165	164	154	139	164	163
Charge Balance:		-0.71%	1.08%	-1.15%	0.31%	-2.29%	-1.30%	-4.03%	-0.98%	0.19%	-0.38%	1.10%
ION-ION RATIOS												
Br*1000/Cl weight	mg/mg	19.5	18.4	21.6	19.0	24.4	20.7	20.5	27.3	17.2	18.8	22.5
Br*1000/Cl molal	mol/mol	8.7	8.2	9.6	8.4	10.8	9.2	9.1	12.1	7.6	8.3	10.0
Na/Cl molal	mol/mol	0.581	0.681	0.499	0.806	1.217	0.776	0.907	0.924	0.802	0.493	0.580
K/Na molal	mol/mol	0.192	0.146	0.116	0.141	0.083	0.148	0.086	0.072	0.082	0.180	0.126
SO4/Cl molal	mol/mol	0.021	0.017	0.014	0.022	0.036	0.037	0.027	0.024	0.042	0.024	0.019
Na/(Cl+SO4)	mol/mol	0.569	0.670	0.492	0.789	1.175	0.748	0.883	0.903	0.769	0.482	0.570
ISOTOPE RATIOS												
d37Cl	pm SMOC	0.74	0.69	0.82	0.64	0.18	0.05	-1.02	-0.53	0.84	0.00	-0.04
error d37Cl	pm SMOC	0.04	0.04	0.08	0.04	0.05	0.05	0.20	0.21	0.20	0.02	0.20
87Sr/86Sr		0.729899	0.728558	0.728653	0.727002	0.726820	0.733209	0.728166	0.730445	0.720305	0.728717	0.724518
error 87Sr/86Sr		0.00005	0.00005	0.00005	0.00005	0.00005	0.00005	0.00005	0.00005	0.00005	0.00005	0.00005

Table 5-2: Continued

Sample		IG_BH05_PW022	IG_BH05_PW023	IG_BH05_PW024	IG_BH05_PW025	IG_BH05_PW026	IG_BH05_PW027	IG_BH05_PW028	IG_BH05_PW029	IG_BH05_AR033	IG_BH05_AR052	IG_BH05_AR059
Hydroisotop Nr.		378365	378366	378367	378368	379222	379223	379224	379225	392236	392237	392238
Interval	mbgs	801.8	827.2	848.7	881.5	906.1	936.8	963.0	986.5	717.4	856.1	979.0
Ratio Exp.Water : Rock	g/g	0.099	0.098	0.095	0.097	0.096	0.107	0.096	0.095	0.114	0.087	0.122
Ratio TW:PW	g/g	39	62	64	105	93	120	66	49	54	249	218
MISCELLANEOUS PROPERTIES												
pH (lab)	-log(H+)	7.5	7.7	7.7	7.5	7.5	7.4	7.4	7.4	7.6	7.7	7.8
Spec. electr. conductivity	µS/cm	497	314	206	381	290	375	443	1026	528	302	308
Acid Capacity (4.3)	mmol	1.43	0.81	0.85	0.96	0.79	0.79	0.74	0.65	1.40	1.73	1.85
Base Capacity (8.2)	mmol	-	-	-	-	-	-	-	-	-	-	-
Sample Temperature	ºC	24.6	24.6	24.6	24.6	24.6	24.6	24.6	24.6	23.3	23.9	23.1
DOC	mg/l	10.1	6.3	7.2	14.2	5.9	8.9	13.0	7.4	8.2	11.0	9.0
TIC	mg/l	17.2	9.7	10.2	8.4	9.0	9.3	8.1	8.0	18.6	23.4	25.7
DISSOLVED CONSTITUENTS												
CATIONS												
Sodium (Na+)	mg/l	32.3	21.2	16.2	21.3	22.4	19.9	30.3	45.4	34.8	19.9	24.6
Potassium (K+)	mg/l	2.9	3.6	5.7	7.5	5.6	7.2	6.5	10.4	3.08	8.4	5.4
Calcium (Ca+2)	mg/l	52.9	32.5	22.8	43.1	25.5	37.2	42.1	121	65.5	37.2	32.1
Magnesium (Mg+2)	mg/l	0.53	0.47	< 0.2	0.38	0.34	0.61	0.53	0.47	1.19	0.99	1.29
Strontium (Sr+2)	mg/l	0.417	0.26	0.134	0.286	0.28	0.403	0.497	1.47	0.75	0.382	0.401
Aluminium (Al+3)	mg/l	0.021	0.084	0.094	0.04	0.03	< 0,02	< 0,02	< 0,02	0.02	0.06	0.058
Silicon (Si+4)	mg/l	8	7.4	7.52	7.55	8.23	6.84	8.72	6.95	8.19	7.55	4.66
Boron (B)	mg/l	0.179	0.125	0.16	0.12	0.163	0.18	0.315	0.223	0.277	0.155	0.229
ANIONS												
Fluoride (F-)	mg/l	1.9	2.4	0.3	0.17	0.19	< 0.1	0.42	1	1.61	0.6	0.44
Chloride (Cl-)	mg/l	88.3	56.2	44.7	76.6	55.7	76.7	98	269	109	18.4	25.4
Bromide (Br-)	mg/l	4.1	1.3	0.81	2.1	2.3	2.3	1.5	9.6	1.69	0.4	0.41
Nitrate (NO3-)	mg/l	< 0.2	< 0.2	< 0.2	< 0.2	< 0.2	< 0.2	< 0.2	< 0.2	5.08	< 0,2	< 0,2
Sulphate (SO4-2)	mg/l	6.5	4.9	2	3.7	3.4	4	3.7	5.7	19	27.4	10.5
Total Alkalinity	meq/l	1.43	0.81	0.85	0.96	0.79	0.79	0.74	0.65	1.40	1.73	1.85
Total Alkalinity as HCO3	mg/l	87.4	49.3	51.9	58.6	48.3	48.3	45.3	39.5	85.42	105.7	113
PARAMETERS CALCULATED FROM ANALYTICAL DA												
Sum of Analysed Constituents	mg/l	277	172	144	213	164	196	228	502	322	219	214
Charge balance		-0.95%	0.69%	-4.58%	1.02%	-1.11%	-1.84%	0.05%	-1.24%	0.00%	2.86%	1.91%
WATER TYPE		Na-Ca-Cl-HCO3	Na-Ca-Cl-HCO3	Na-Ca-(K)-Cl-HCO3	Ca-Na-Cl-HCO3	Na-Ca-Cl-HCO3	Ca-Na-Cl-HCO3	Na-Ca-Cl-HCO3	Ca-Na-Cl	Ca-Na-Cl-HCO3	Ca-Na-HCO3-(Cl)	Na-Ca-HCO3-Cl
ION-ION RATIOS												
Br*1000/Cl weight		46.4	23.1	18.1	27.4	41.3	30.0	15.3	35.7	15.5	21.7	16.1
Br*1000/Cl molal	mol/mol	20.6	10.3	8.0	12.2	18.3	13.3	6.8	15.8	6.9	9.6	7.2
Na/Cl molal	mol/mol	0.6	0.6	0.6	0.4	0.6	0.4	0.5	0.3	0.5	1.7	1.5
K/Na molal	mol/mol	0.0	0.0	0.0	0.0	0.0	0.0	0.0	0.0	0.0	0.0	0.0
SO4/Cl molal	mol/mol	0.1	0.1	0.2	0.2	0.1	0.2	0.1	0.1	0.1	0.2	0.1
Na/(Cl+SO4)	mol/mol	0.0	0.0	0.0	0.0	0.0	0.0	0.0	0.0	0.1	0.5	0.2
ISOTOPE RATIOS												
δ37Cl	pm SMOC	-0.04	-0.38	-0.43	0.10	-0.01	0.55	-0.69	0.18	0.43	-0.39	-0.43
error δ37Cl	pm SMOC	0.20	0.20	0.26	0.22	0.40	0.20	0.32	0.20	0.10	0.10	0.10
87Sr/86Sr		0.72	0.73	0.72	0.72	0.72	0.72	0.72	0.72	0.71	0.72	0.72
error 87Sr/86Sr		0.00005	0.00005	0.00005	0.00005	0.00005	0.00005	0.00005	0.00005	0.00003	0.00003	0.00003

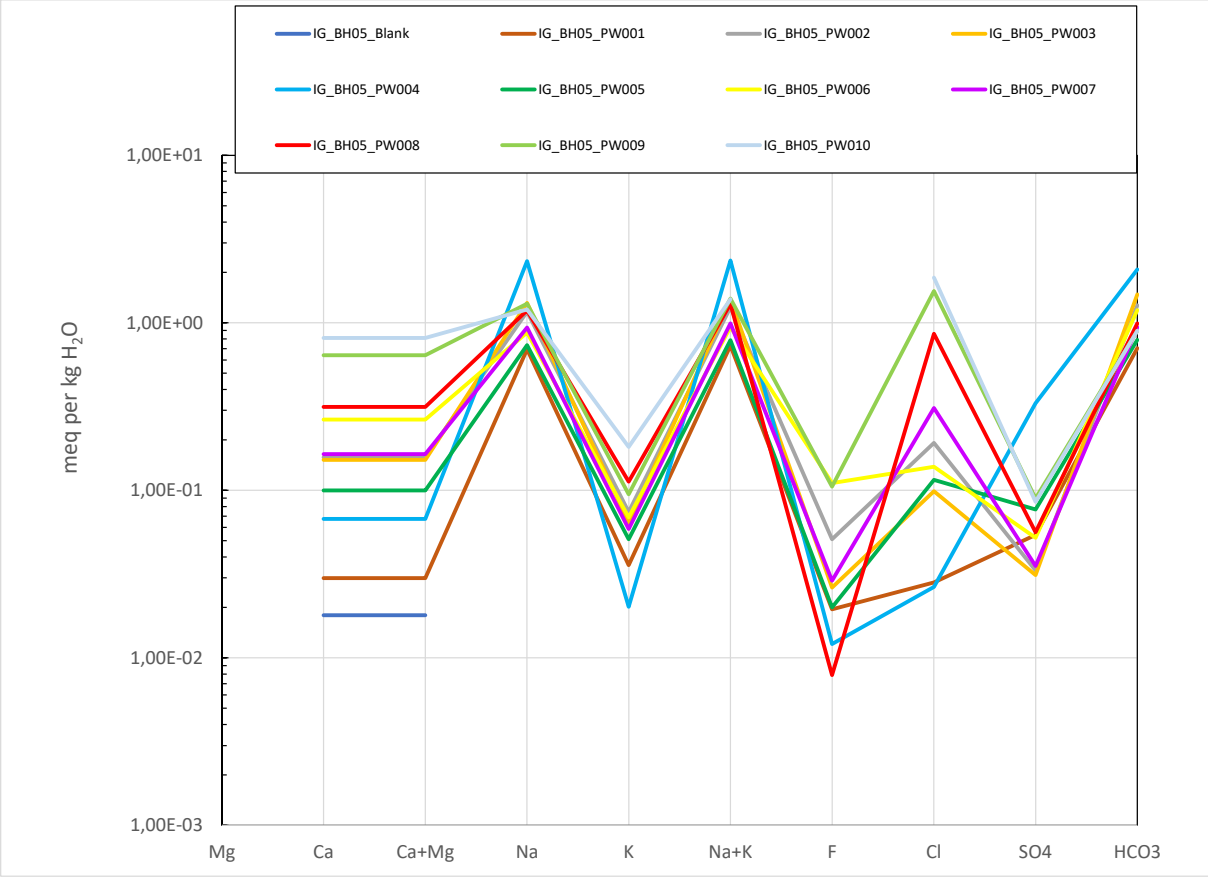


Figure 5-2: Schoeller diagram of experiment solutions from out-diffusion experiments.

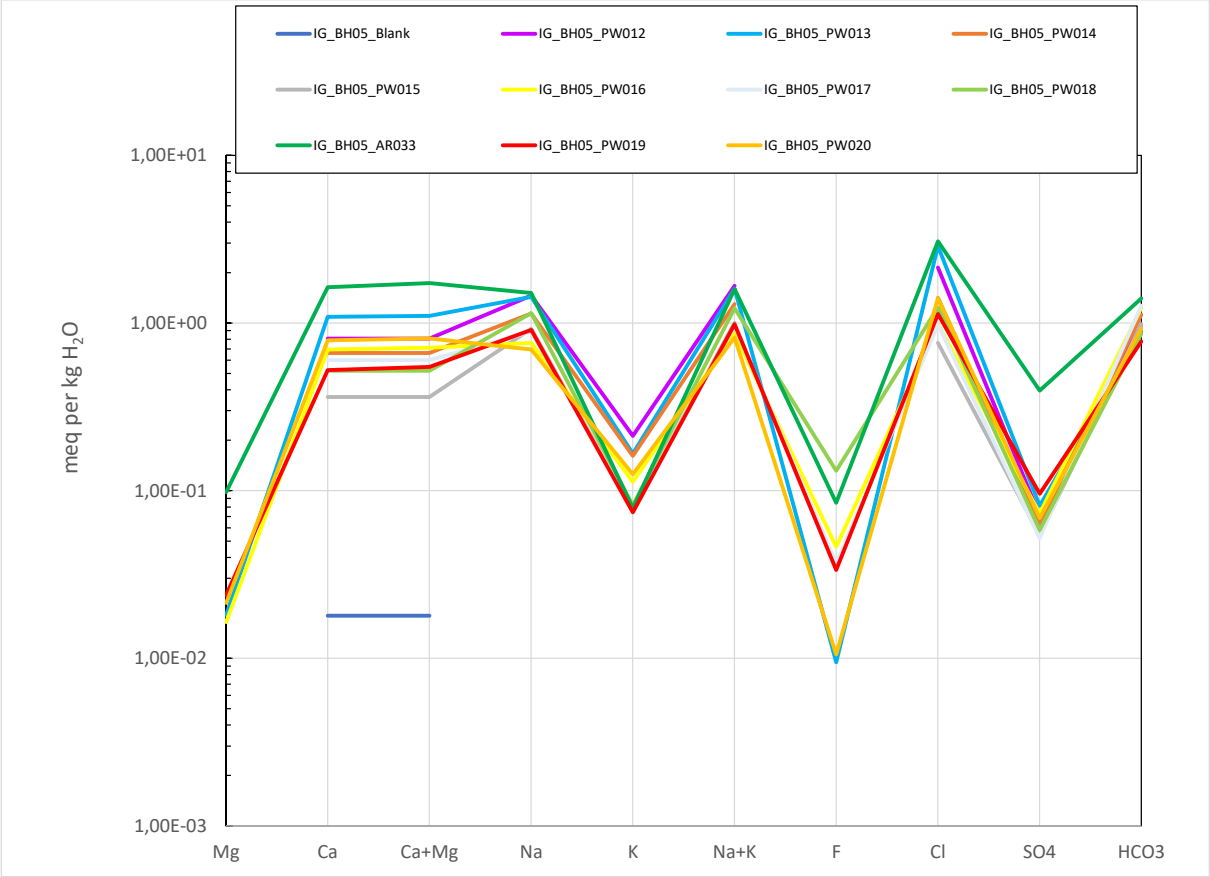


Figure 5-2 continued

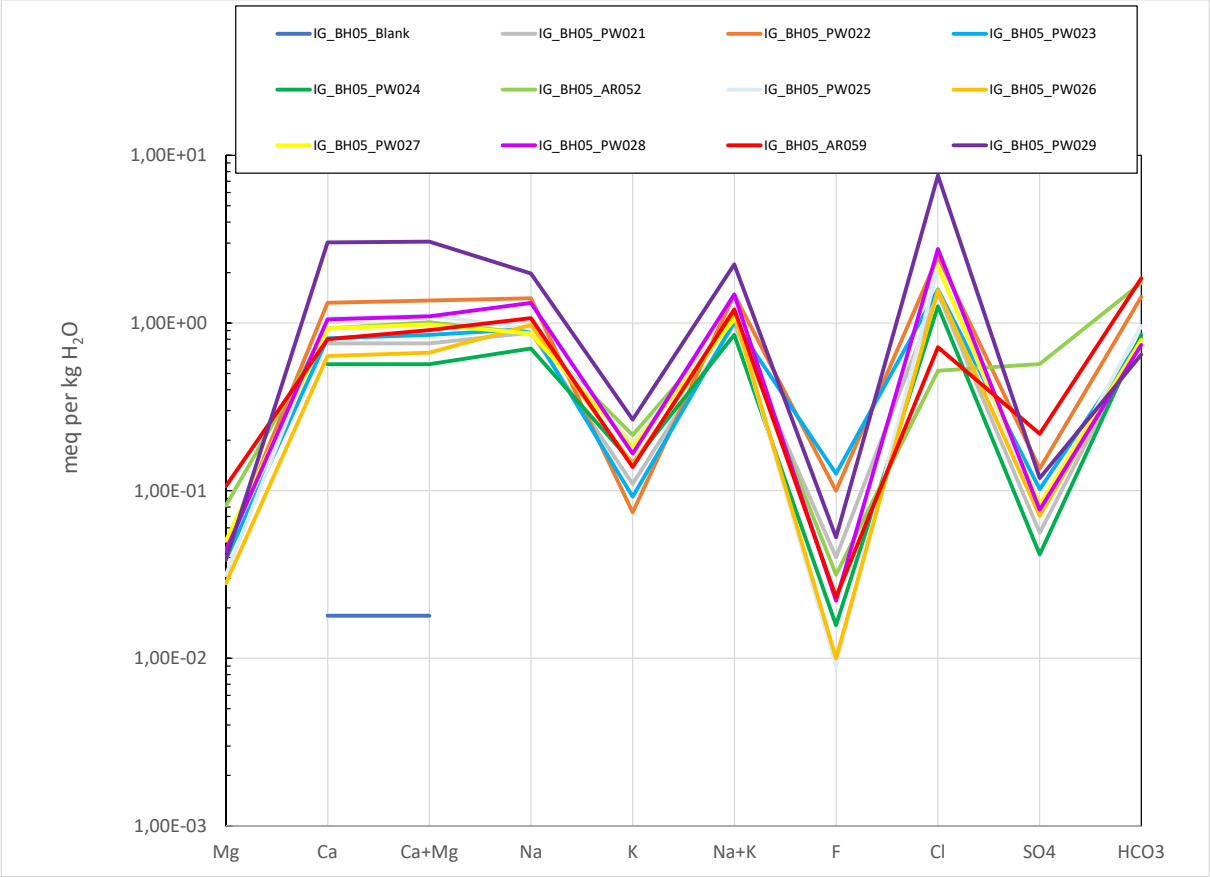


Figure 5-2 continued

6.0 RESULTS FROM ELEMENTAL TIME SERIES AND PORE DIFFUSION COEFFICIENT OF CHLORIDE

6.1 Elemental Elution Curves

Non-destructive out-diffusion experiments are performed based on the concept of chemical exchange between porewater residing in the rock matrix and a test solution of known composition surrounding the rock sample. The experimental setup is maintained until well-defined conditions between the two solution reservoirs are attained. Because of the closed system character of out-diffusion experiments, the target conditions to be achieved between the two solution reservoirs are equilibrium for any solutes for which the porewater is the only source, and which are only subjected to transport processes.

For the present study, improved analytical techniques allowed continuous monitoring of all major solute concentrations in the eluate solutions during out-diffusion. This allows definition of mineral reactions and – at a later stage – possible determination of solute-specific transport (e.g., ion-specific accessible porosity) in the matrix of crystalline rocks.

Porewater chloride and bromide concentrations are calculated based on the final concentrations in the out-diffusion test solutions and the water content of the individual core samples (Section 3). The approach to

equilibrium was monitored by periodically taking sub-samples and analysing them for their Cl and Br concentrations. The criterion for attainment of equilibrium conditions is defined by a difference of less than 5 % in Cl and Br concentrations between the last sub-sample and the final test solution at the end of the experiment. This corresponds to the analytical uncertainty of the Cl and Br measurements. Sub-samples were collected as a function of time during all conducted out-diffusion experiments.

Out-diffusion experiments were run for 113 to 156 days. In order to verify the equilibrium conditions after a longer experiment time, the out-diffusion experiments of core samples IG_BH05_AR033, IG_BH05_AR052 and IG_BH05_AR059 were run for 253 days. Equilibrium with respect to Cl and Br was attained for all samples with respect to the above-mentioned criteria after 29 – 78 days and 13 – 76 days, respectively. For core samples IG_BH05_PW001 and IG_BH05_PW004 the Br concentration of the sub-samples and the final test solution were below the detection limit of 0.05 mg/l (Figure 6-1).

The calculated Br*1000/Cl mass ratios (further expressed as Br/Cl ratio) of the individual out-diffusion experiments either increase within the first days or weeks of elution and are subsequently constant or are constant over the entire period of elution (Figure 6-1). This indicates that there is no significant influence of a diffusional fractionation between bromide and chloride. For core samples IG_BH05_PW001 and IG_BH05_PW004 the Br concentration of the sub-samples and the final test solution are below the detection limit of 0.05 mg/l and therefore no time series elution curve for Br*1000/Cl is available.

Sodium shows a heterogeneous elution behaviour. For most samples, the Na-concentration in the individual test waters shows a steep increase in the first 7-14 days, followed by a flattening of the curve and a continuous increase, which becomes less with ongoing experimental time (Figure 6-1), not reaching a full equilibrium after the experimental time. Only the Na elution curve of samples IG_BH05_PW028 and IG_BH05_PW029 show a diffusion like shape and equilibrium after 57 and 120 days.

Potassium, in contrast, reaches equilibrium in all conducted out-diffusion experiments, although the elution curves are different. The K concentrations in the test solutions of the samples IG_BH05_PW001 and PW006 show a sharp increase within the first 12 to 16 days followed by a flattening of the curve, a continuous increase, which becomes less with ongoing experimental time and achievement of equilibrium for the last subsample and the final sample after 113 to 119 days. All the other samples except samples IG_BH05_PW024 and PW027 also show a sharp increase within the first 7 to 16 days of the experiments, followed by flattening and achievement of equilibrium after approximately 21 to 92 days (Figure 6-1).

Calcium shows heterogeneous elution behaviour in the individual out-diffusion experiments. Some samples reach equilibrium between 61 to 91 days and some samples show equilibrium for the last subsample and final sample after 113 to 121 days. The Ca elution curves of some samples show an increase in Ca concentration during the entire period of elution (Figure 6-1).

For most of the samples, the sulphate concentrations display a steady increase during the elution period and achievement of equilibrium for the last two or three subsamples after 90 to 113 days (Figure 6-1). For samples IG_BH05_PW003, PW017, PW022, PW023, PW024, PW026 and AR052 a steady increase during the entire elution period is observed. This is reasoned to be caused by the oxidation and elution of sulphide minerals, which are probably present in the rock as accessories. Only samples IG_BH05_PW027, PW028 and PW029 show a diffusion like shape and equilibrium after approximately 74 to 75 days.

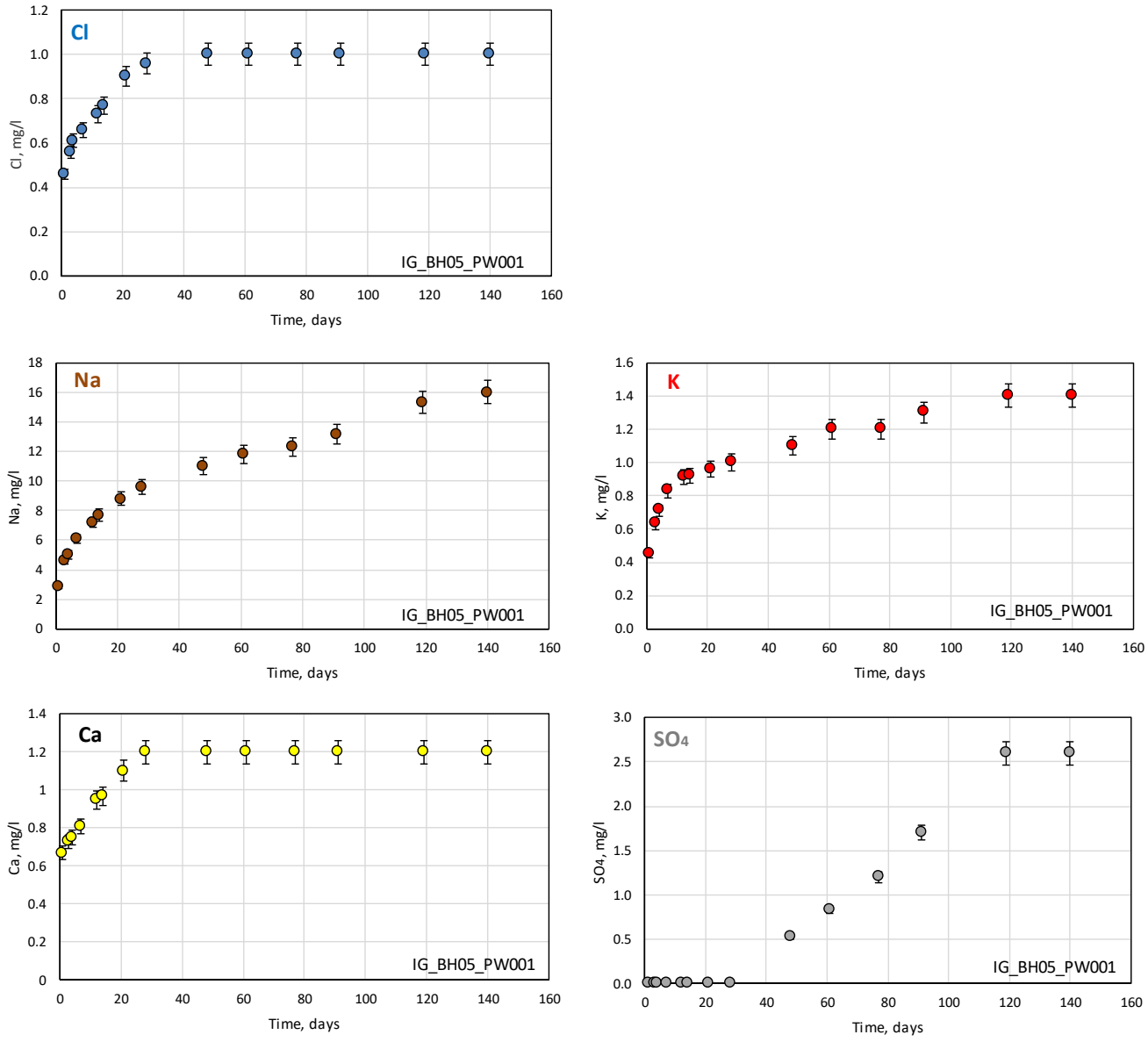


Figure 6-1: Elution curves of anions and cations set-up by the periodic sampling of the test solutions from out-diffusion experiments using core samples from borehole IG_BH05; the errors are the analytical uncertainty of ± 5%.

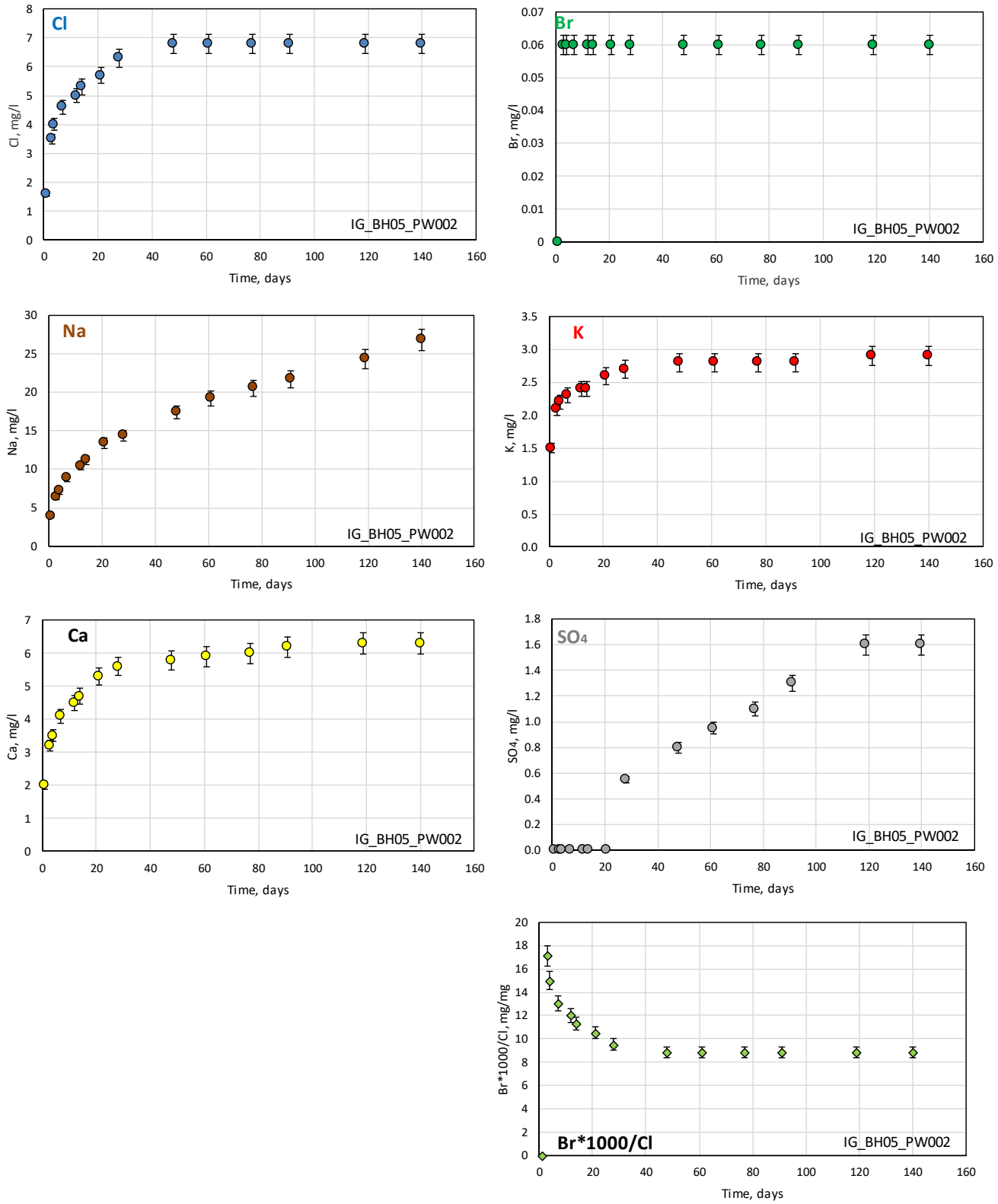


Figure 6-1 continued

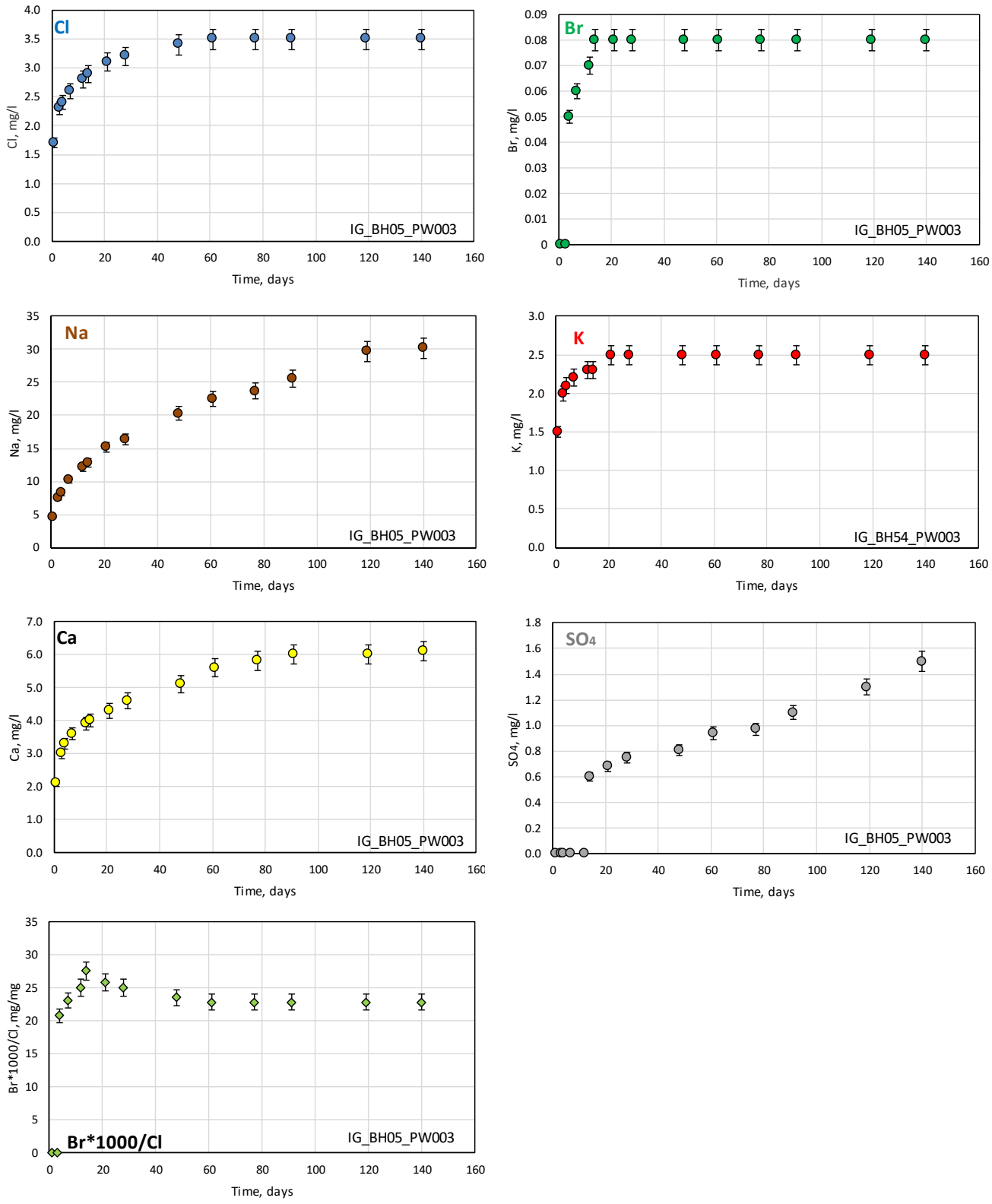


Figure 6-1 continued

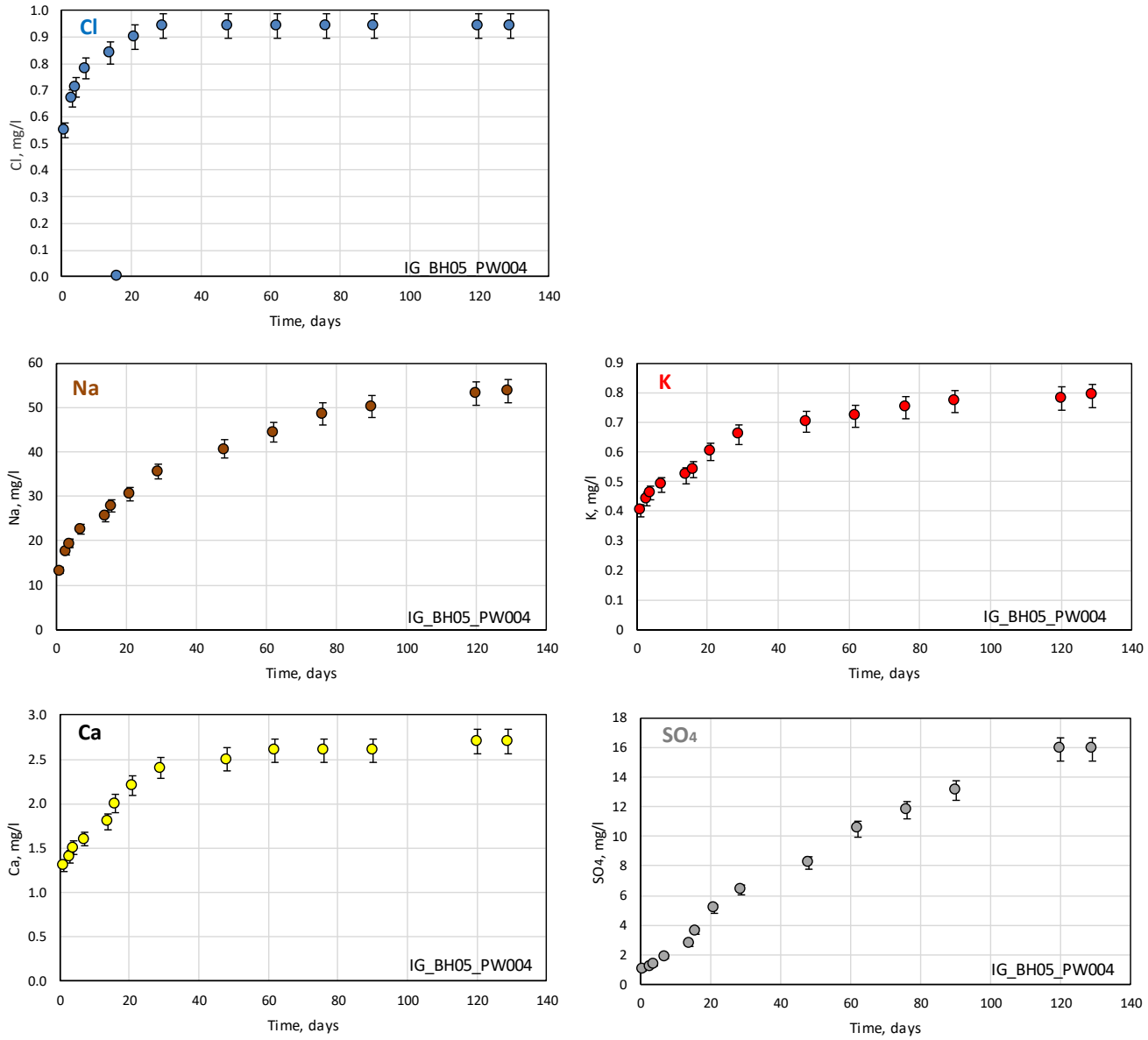
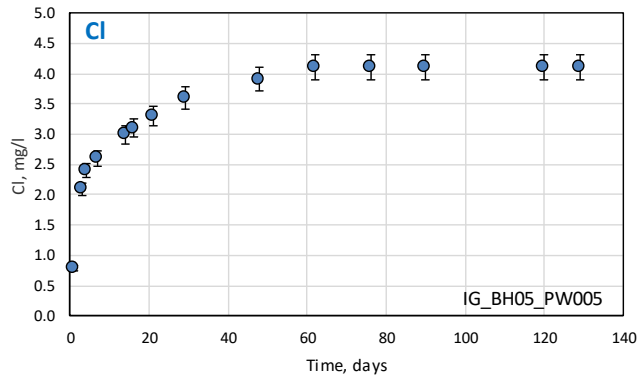
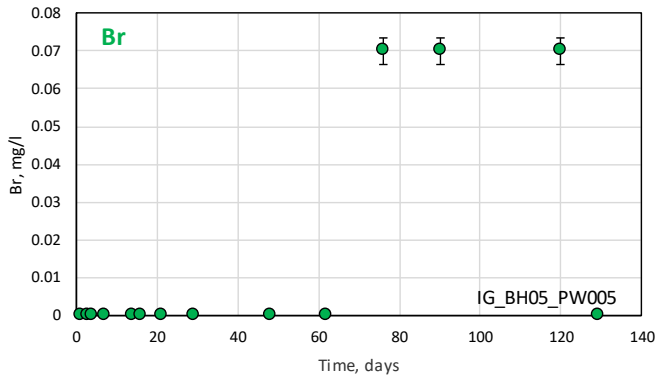
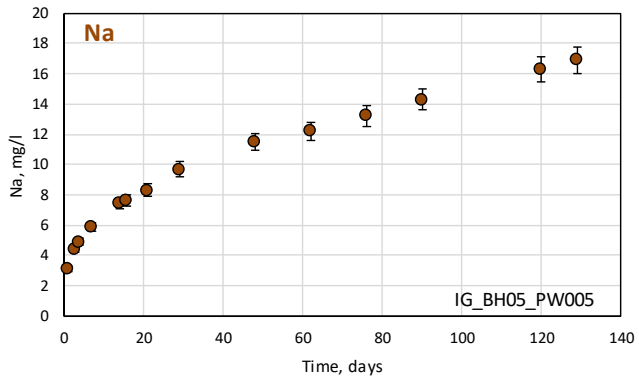
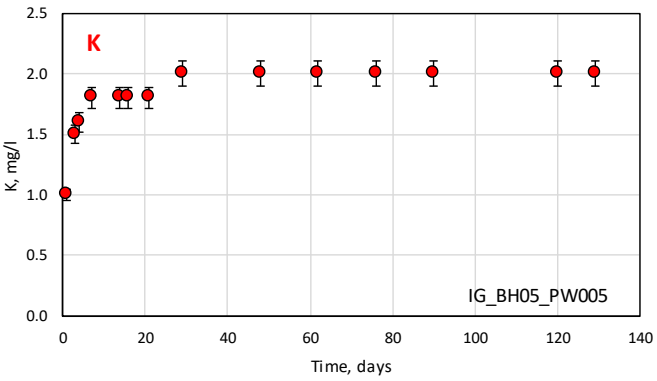


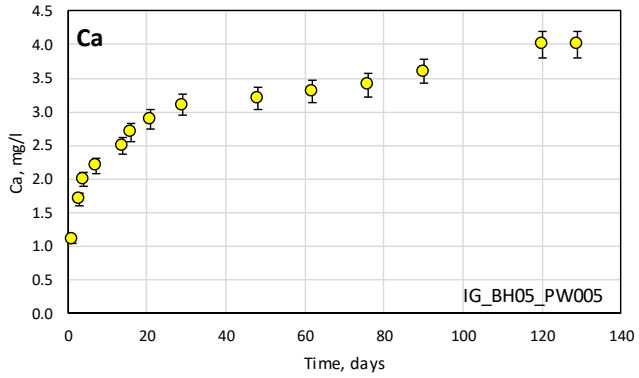
Figure 6-1 continued

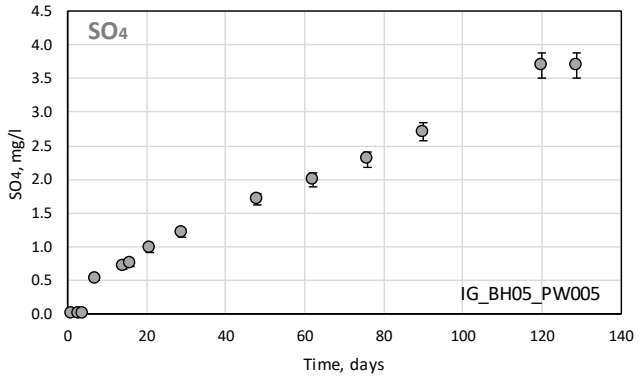












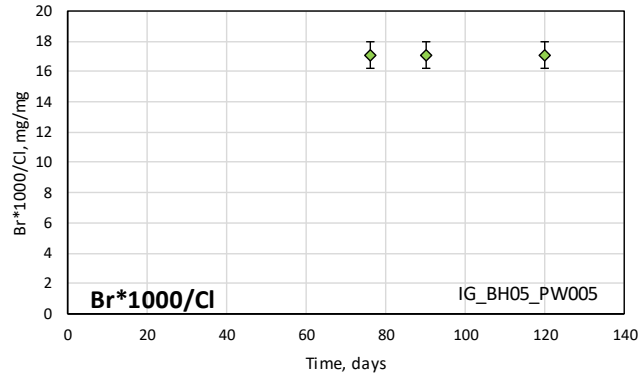


Figure 6-1 continued

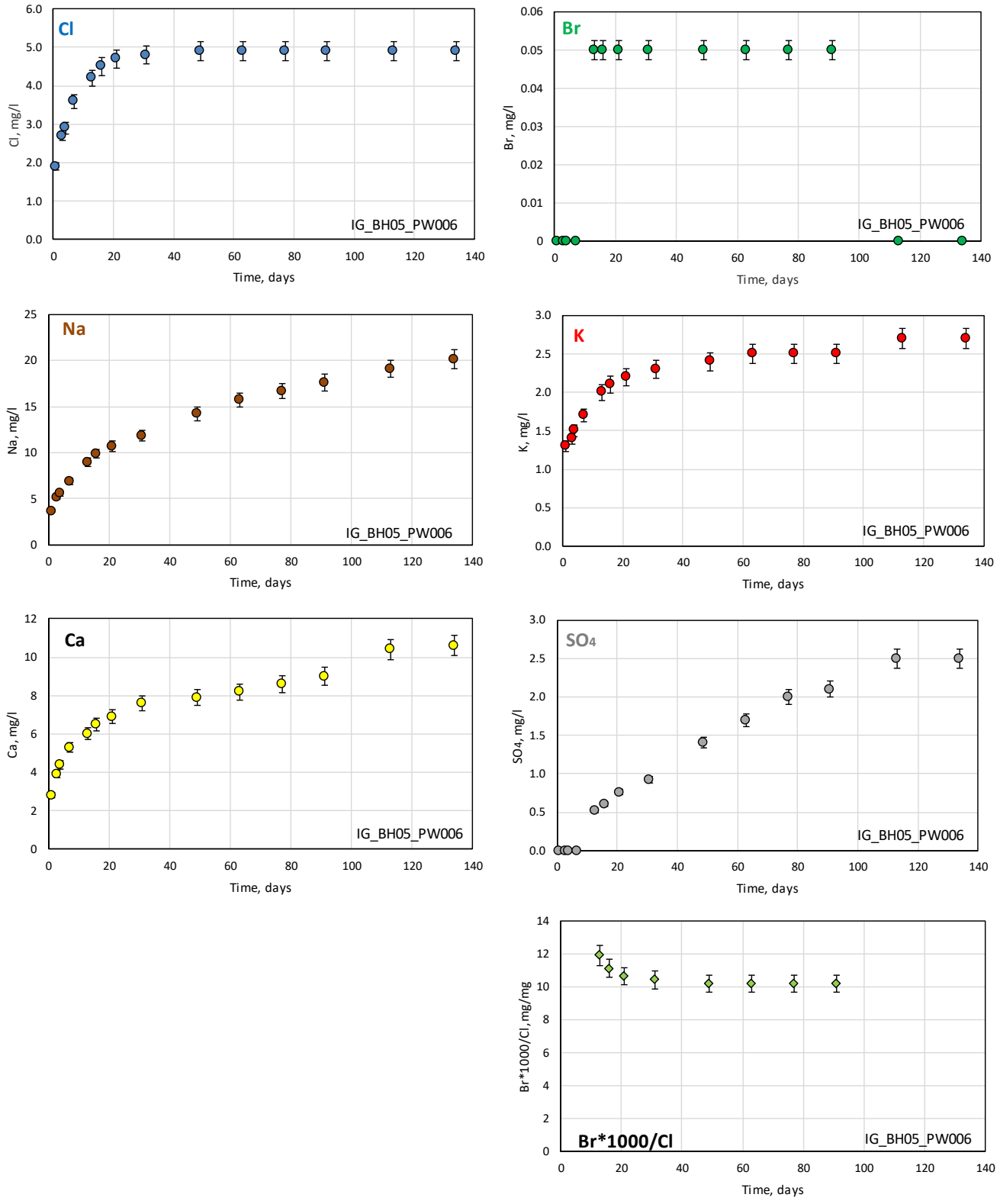


Figure 6-1 continued

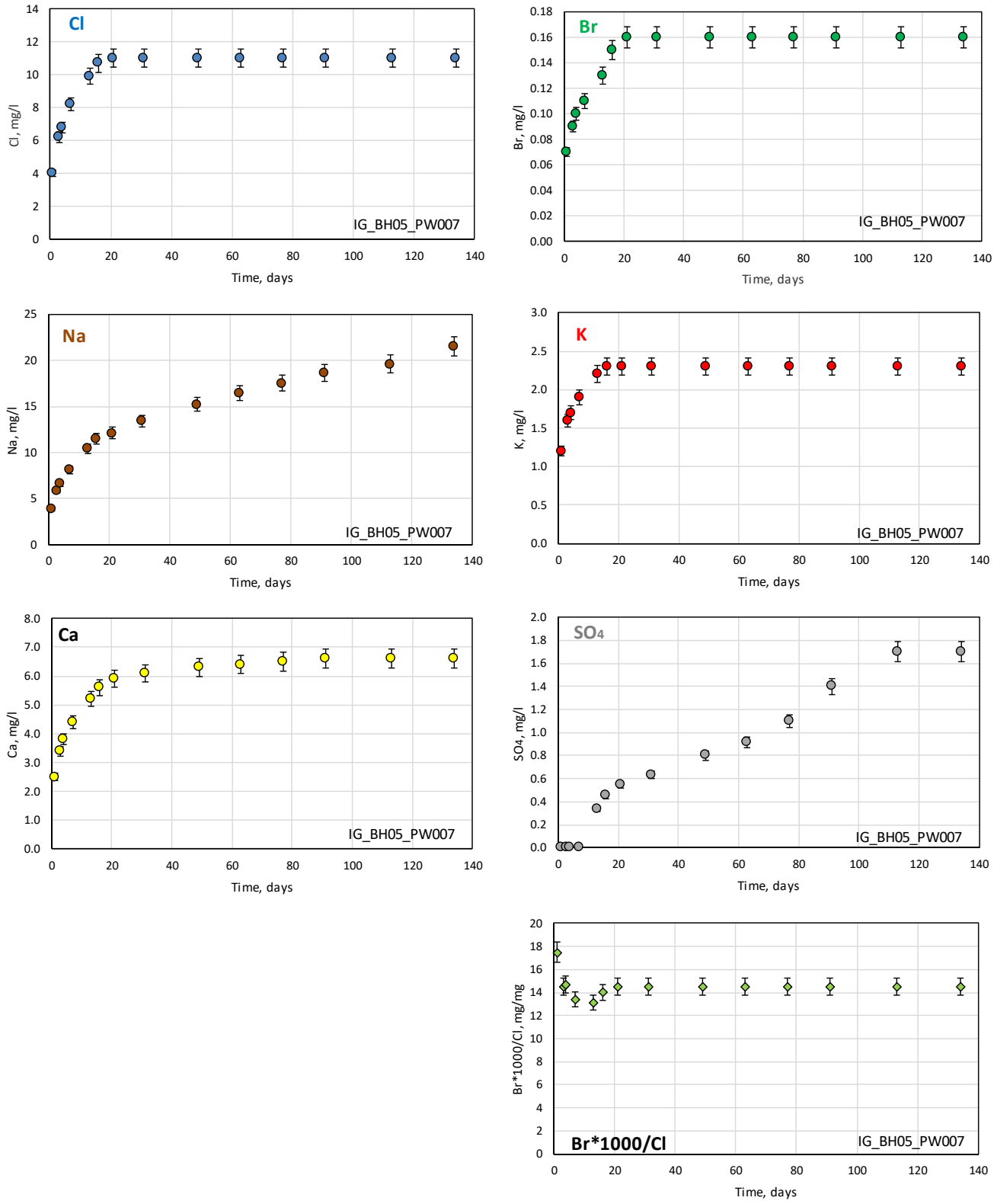


Figure 6-1 continued

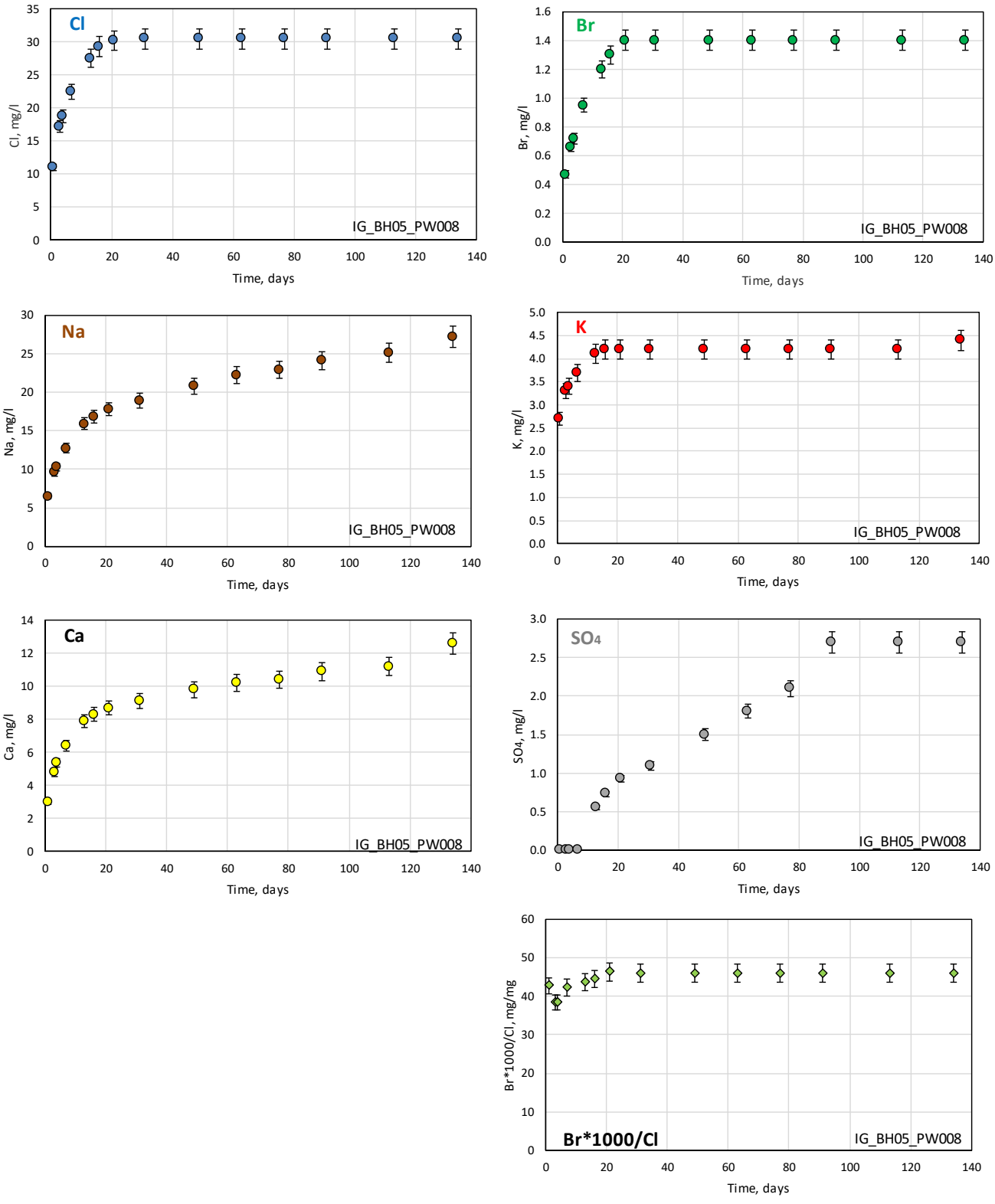


Figure 6-1 continued

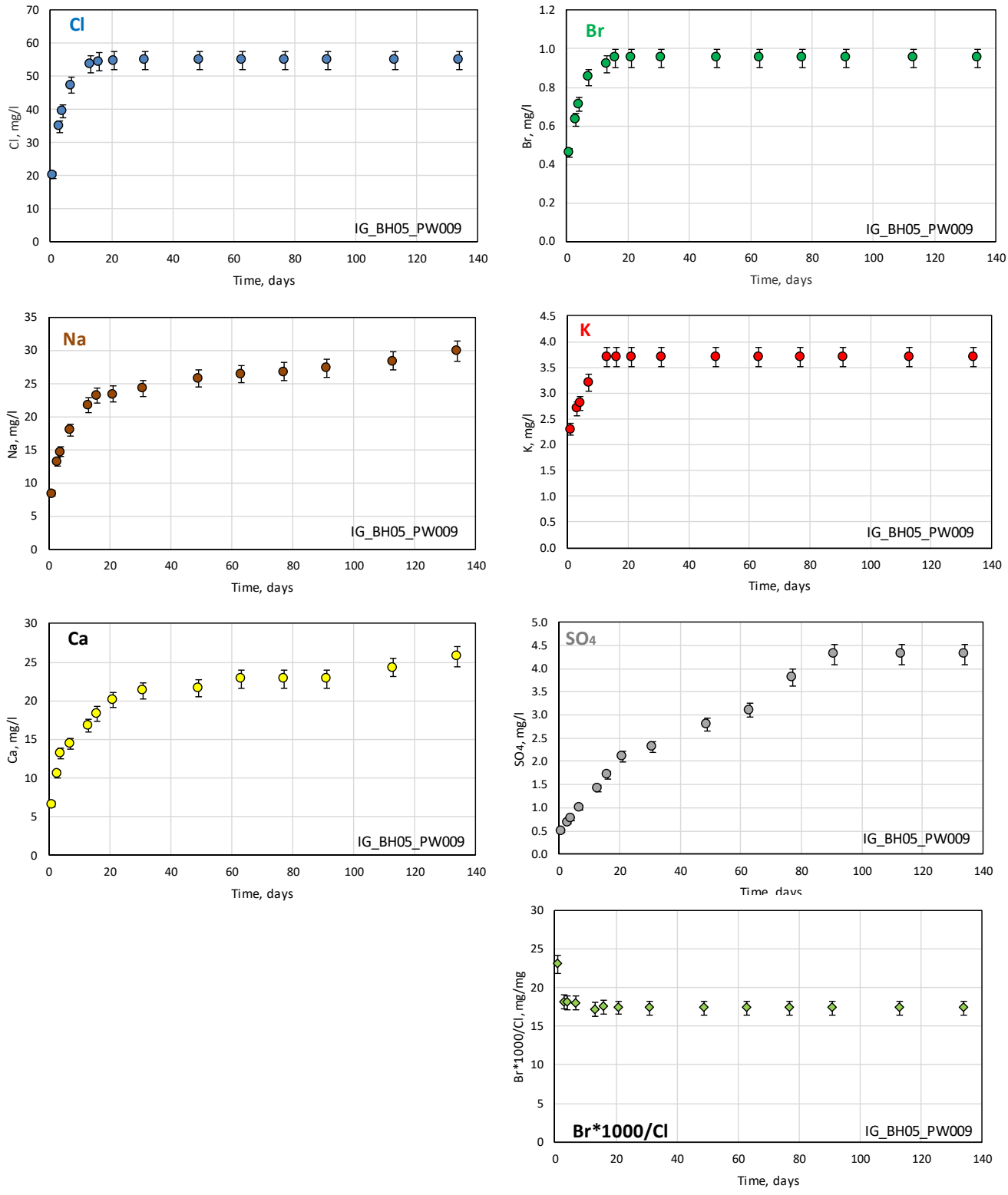


Figure 6-1 continued

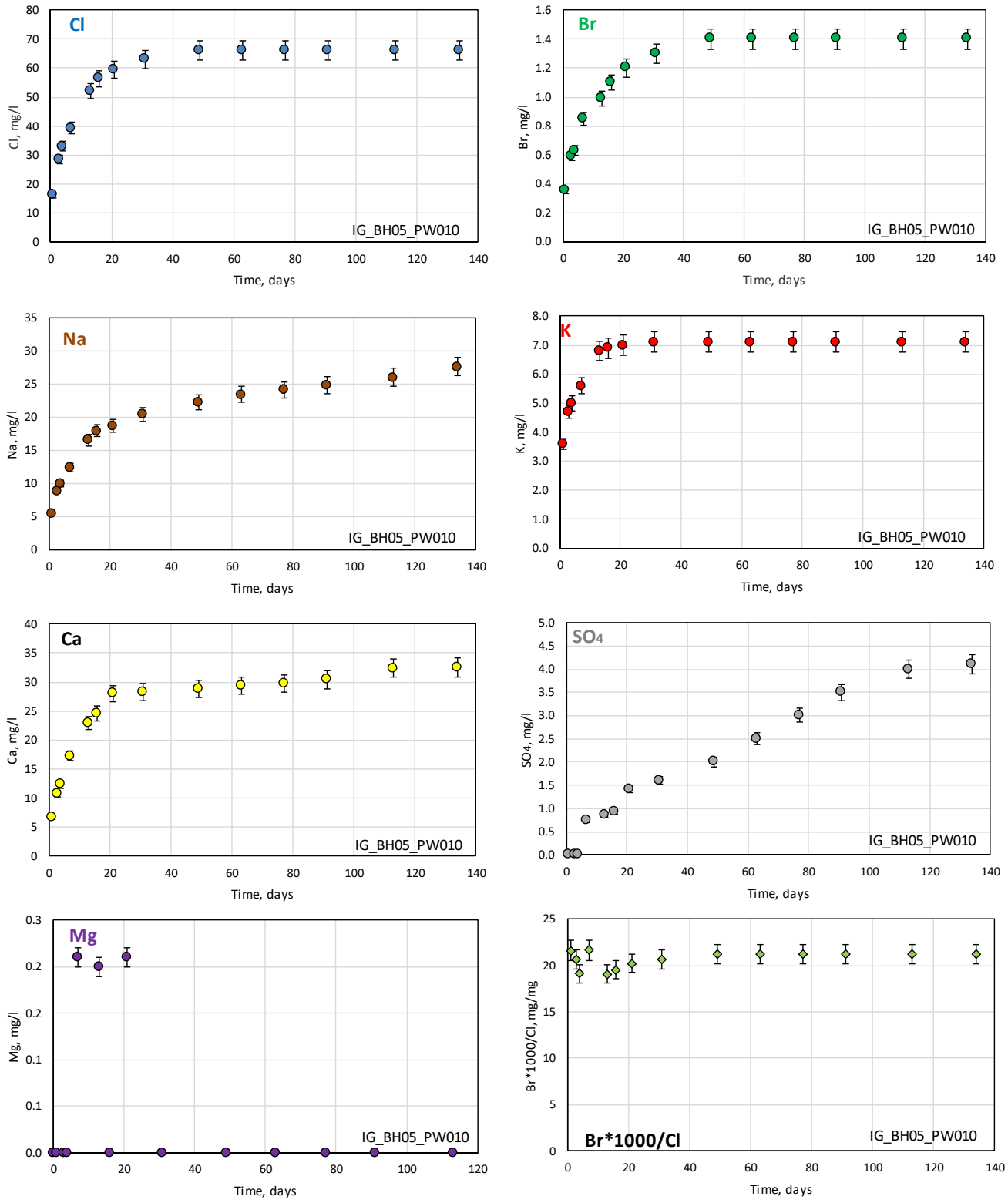


Figure 6-1 continued

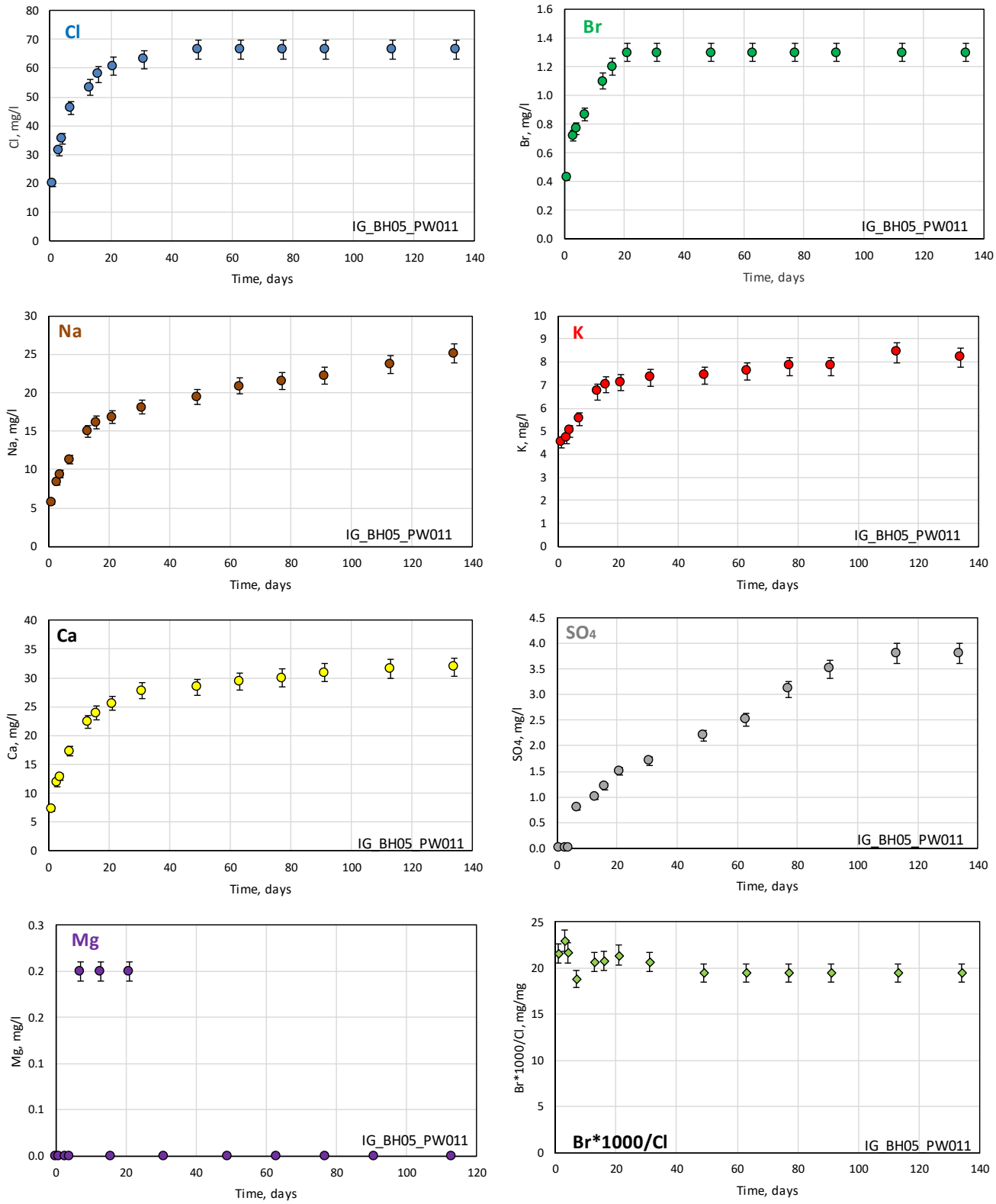


Figure 6-1 continued

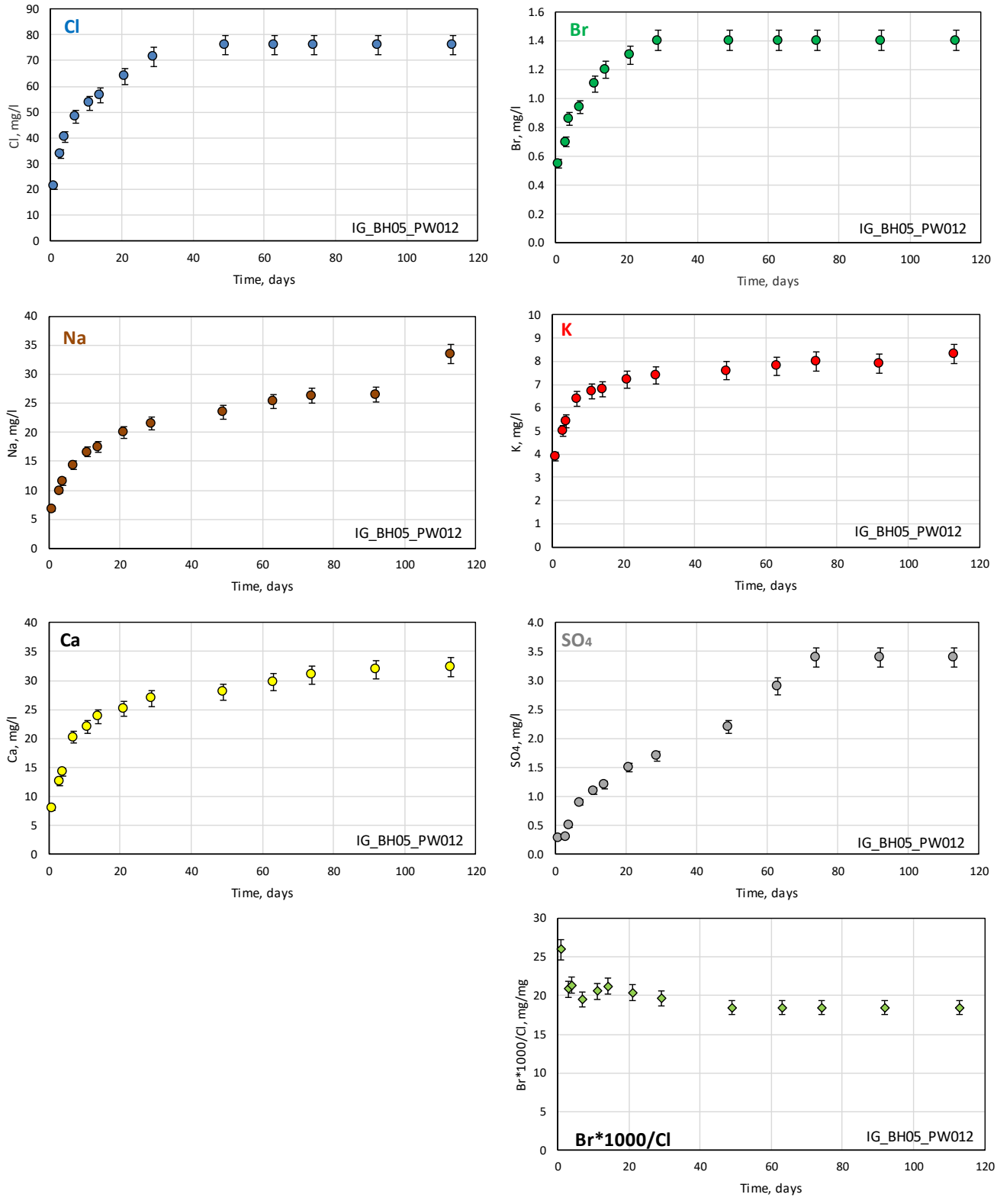


Figure 6-1 continued

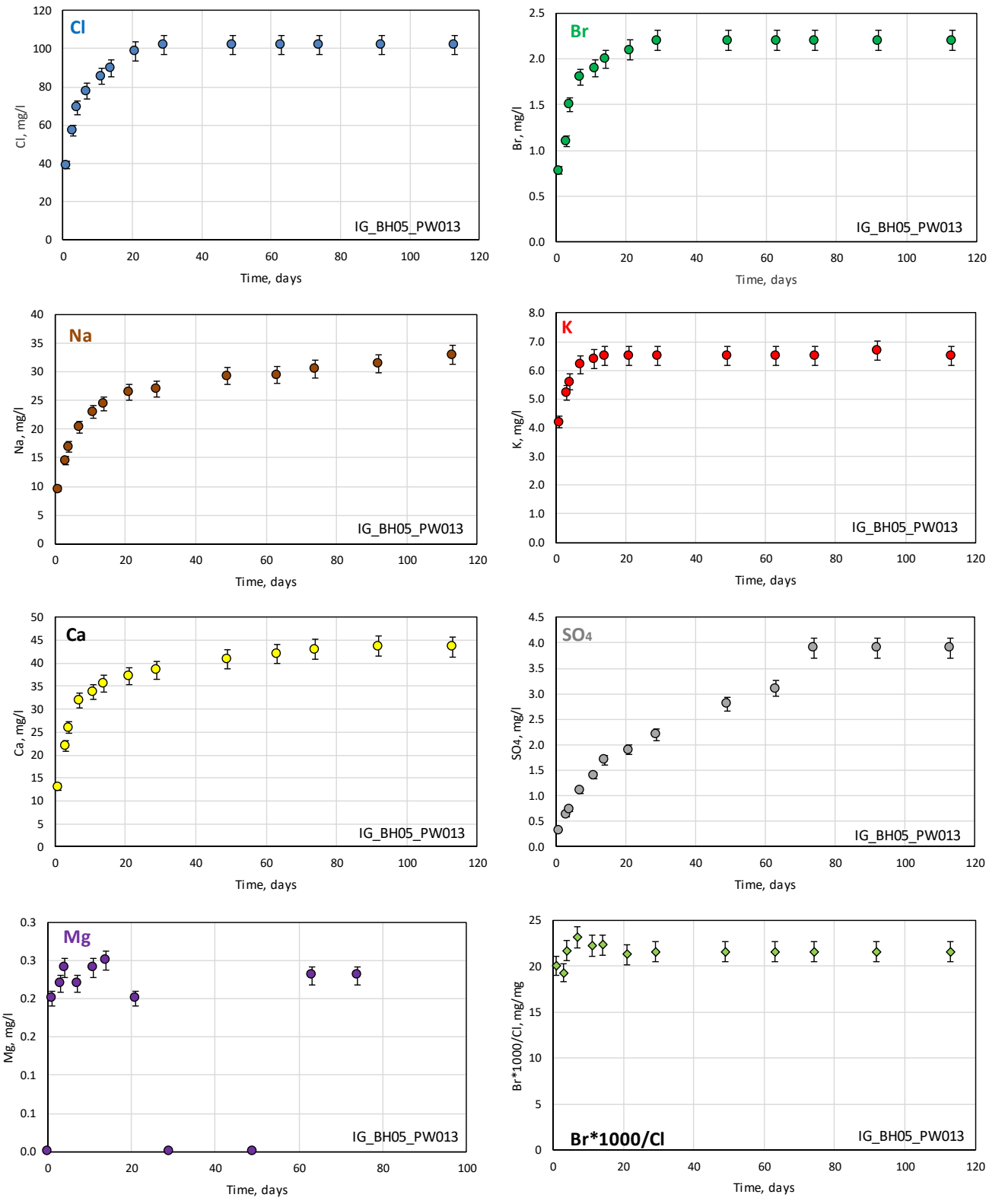


Figure 6-1 continued

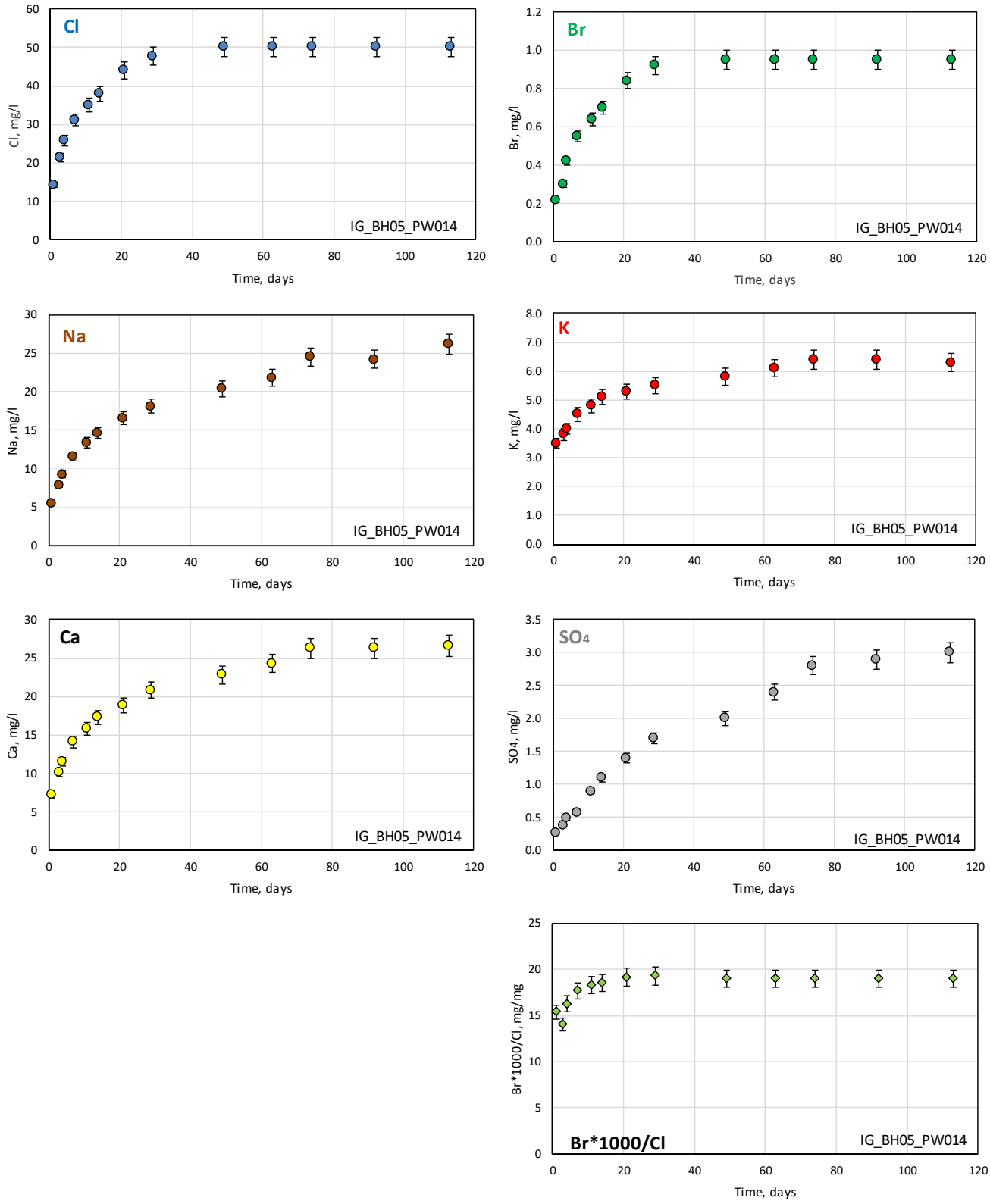


Figure 6-1 continued

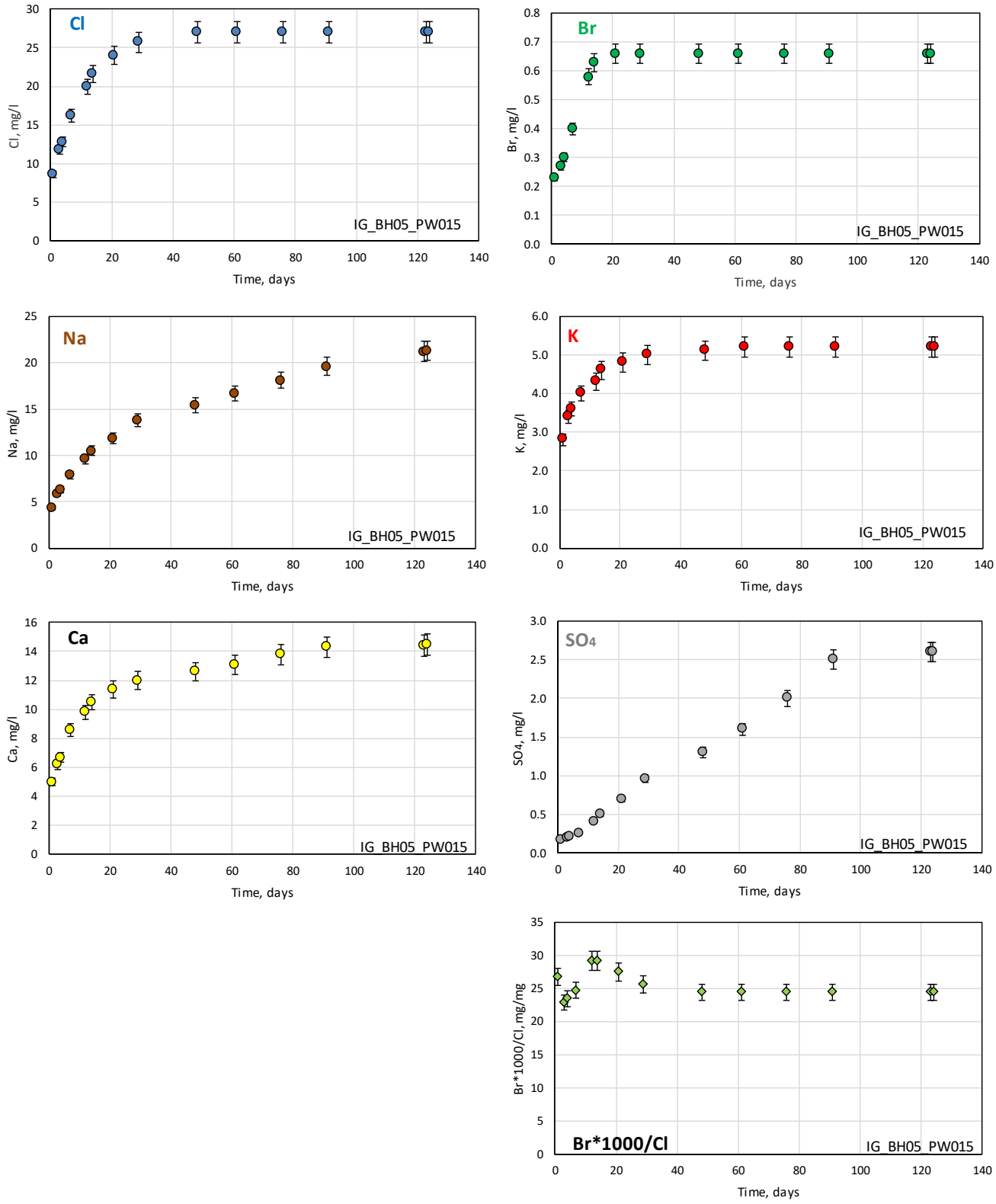


Figure 6-1 continued

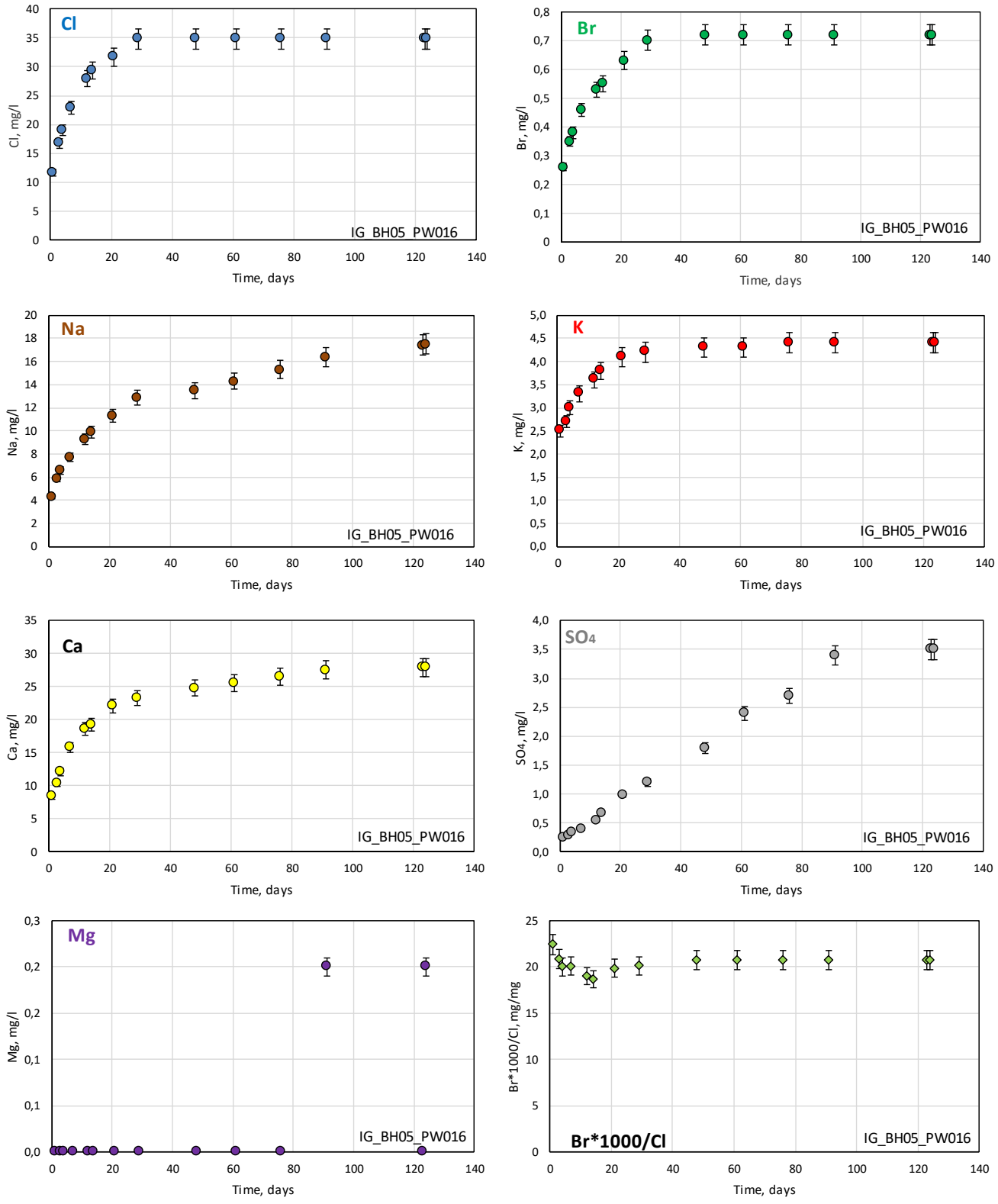


Figure 6-1 continued

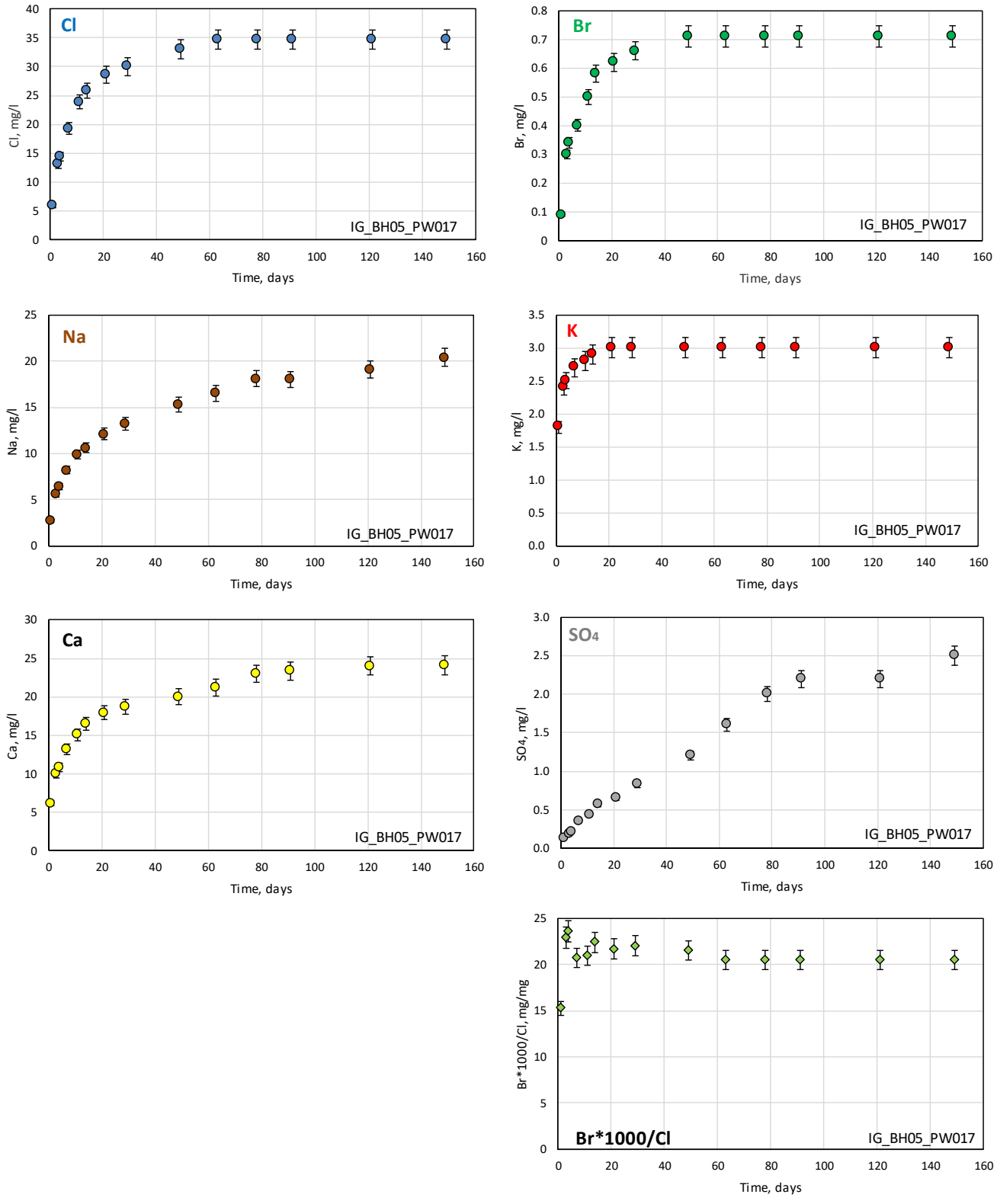


Figure 6-1 continued

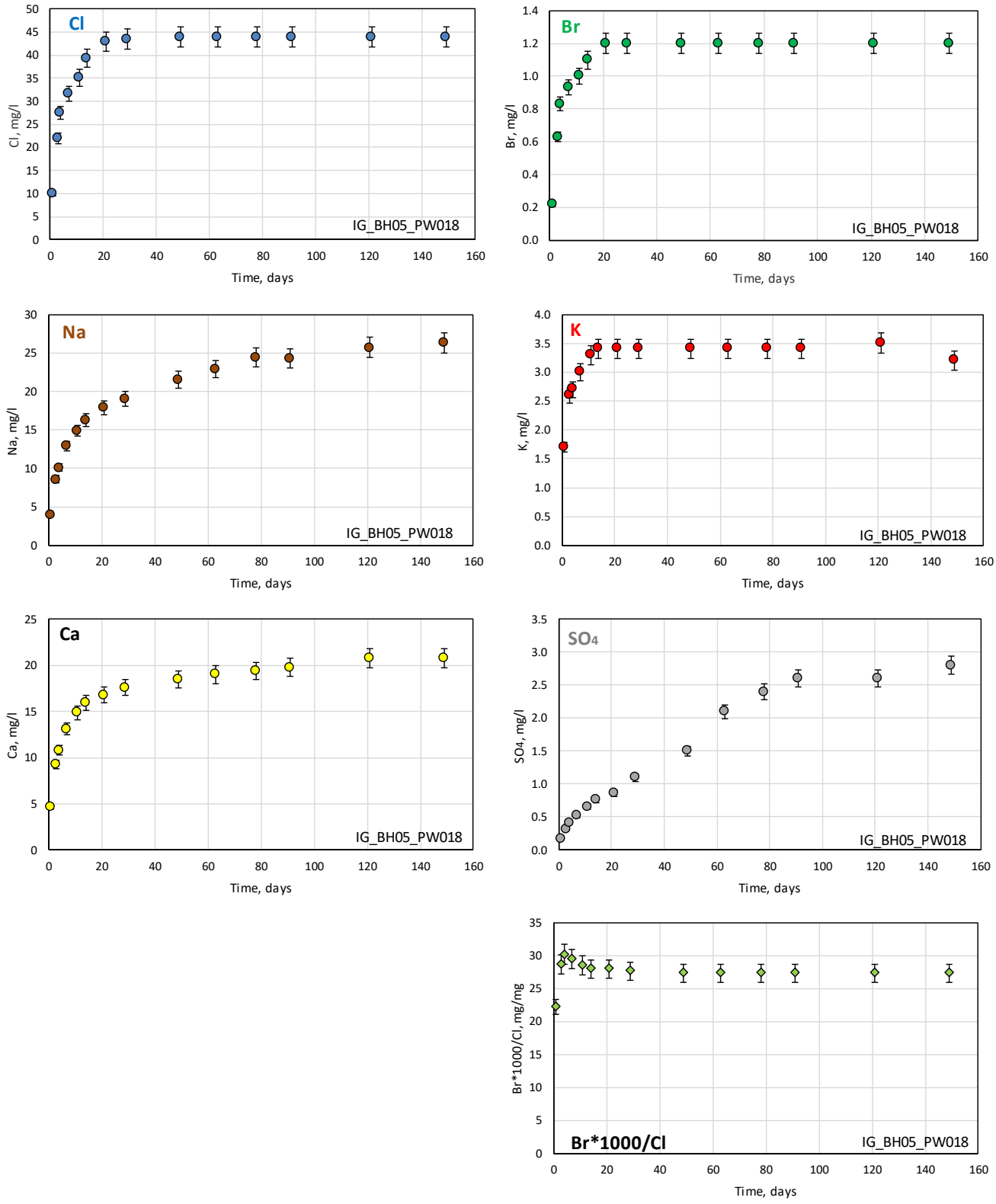


Figure 6-1 continued

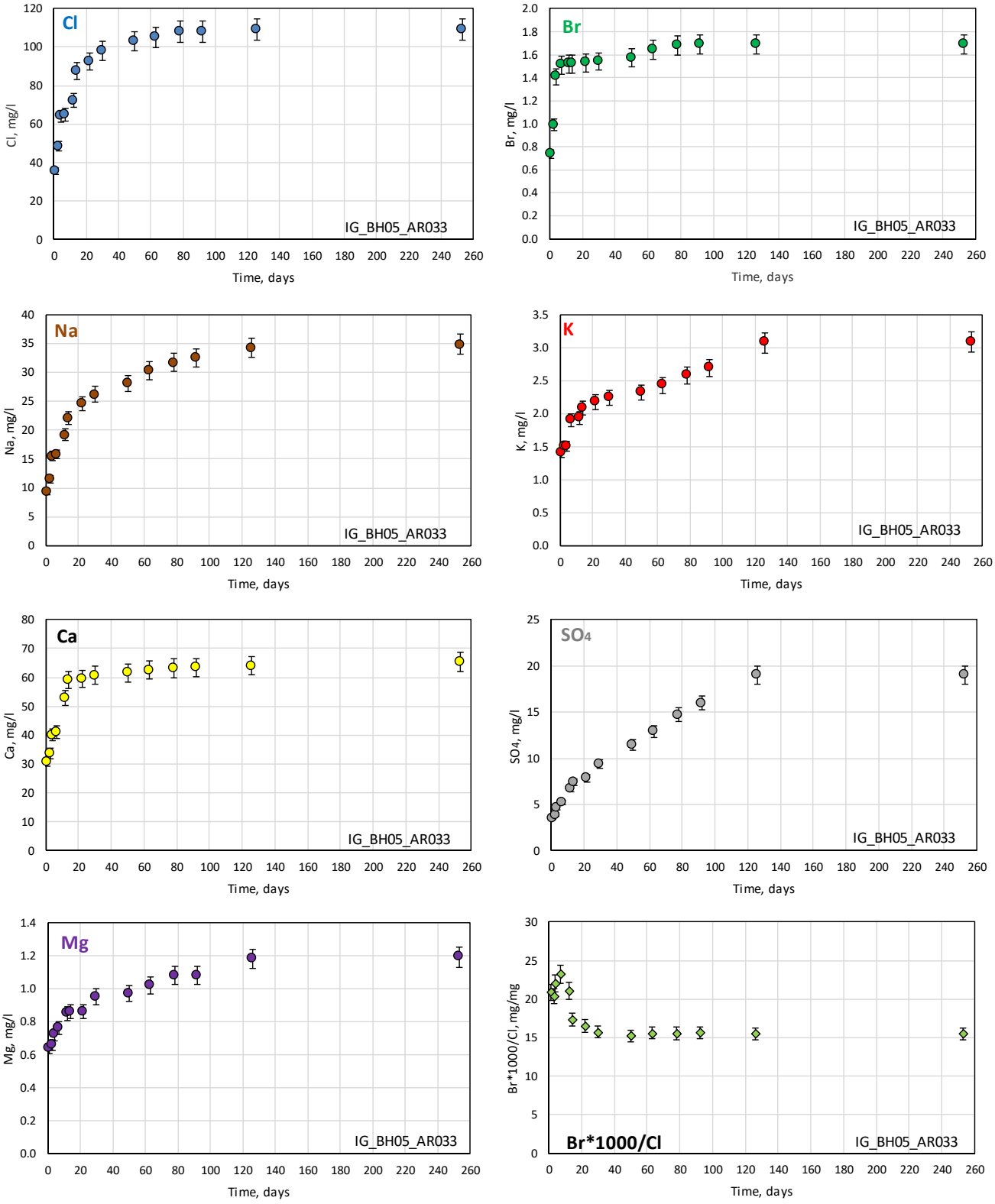


Figure 6-1 continued

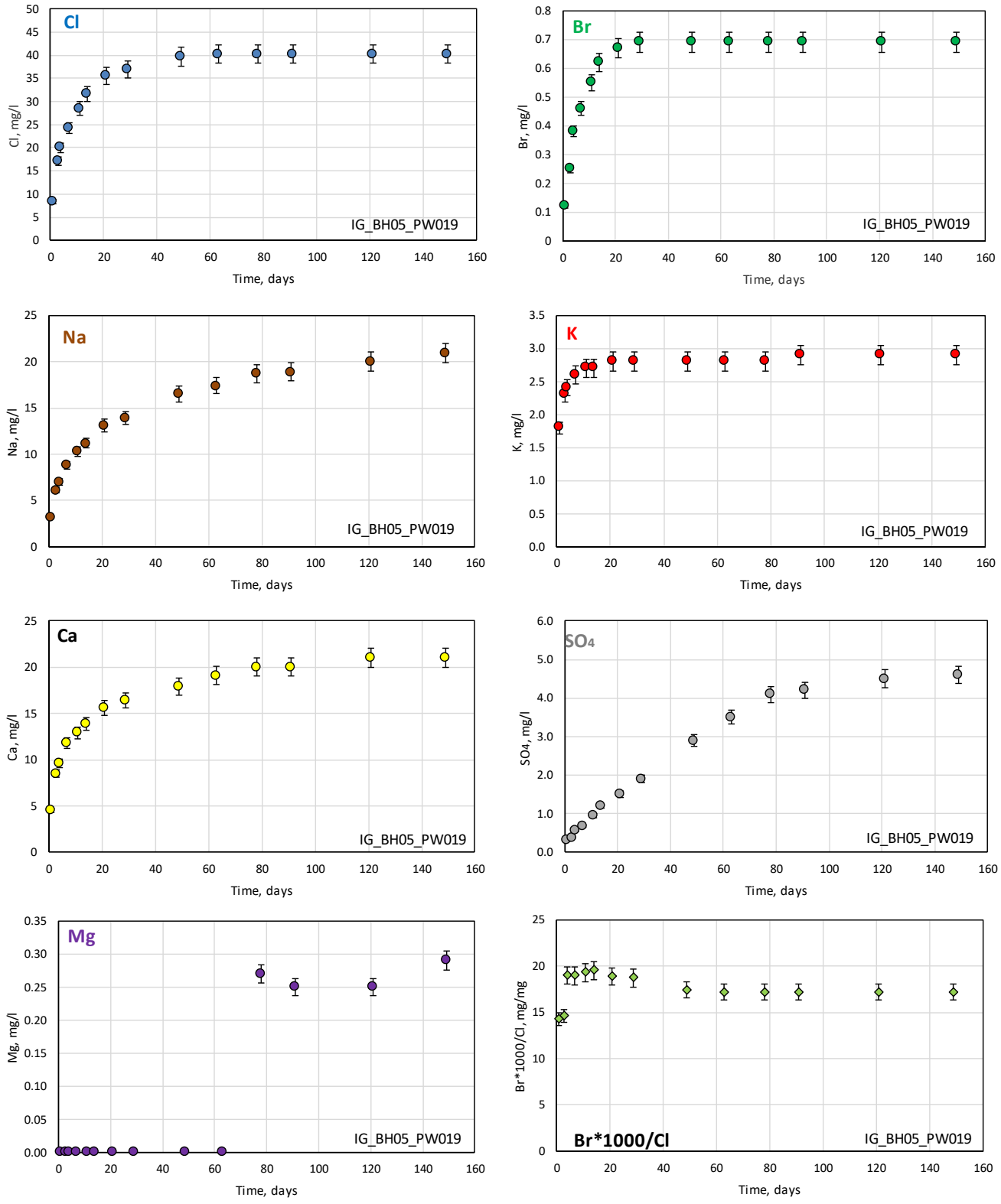


Figure 6-1 continued

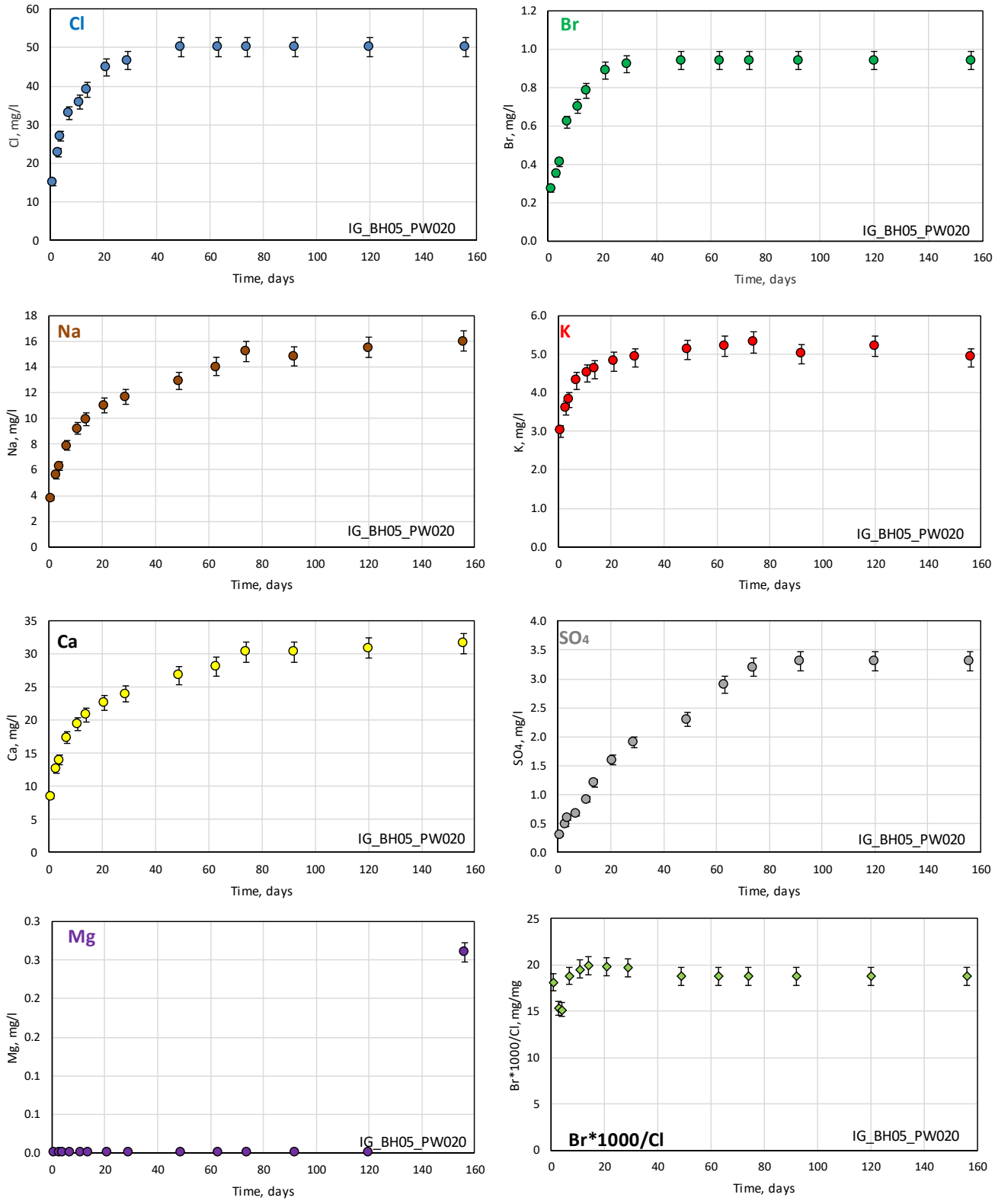


Figure 6-1 continued

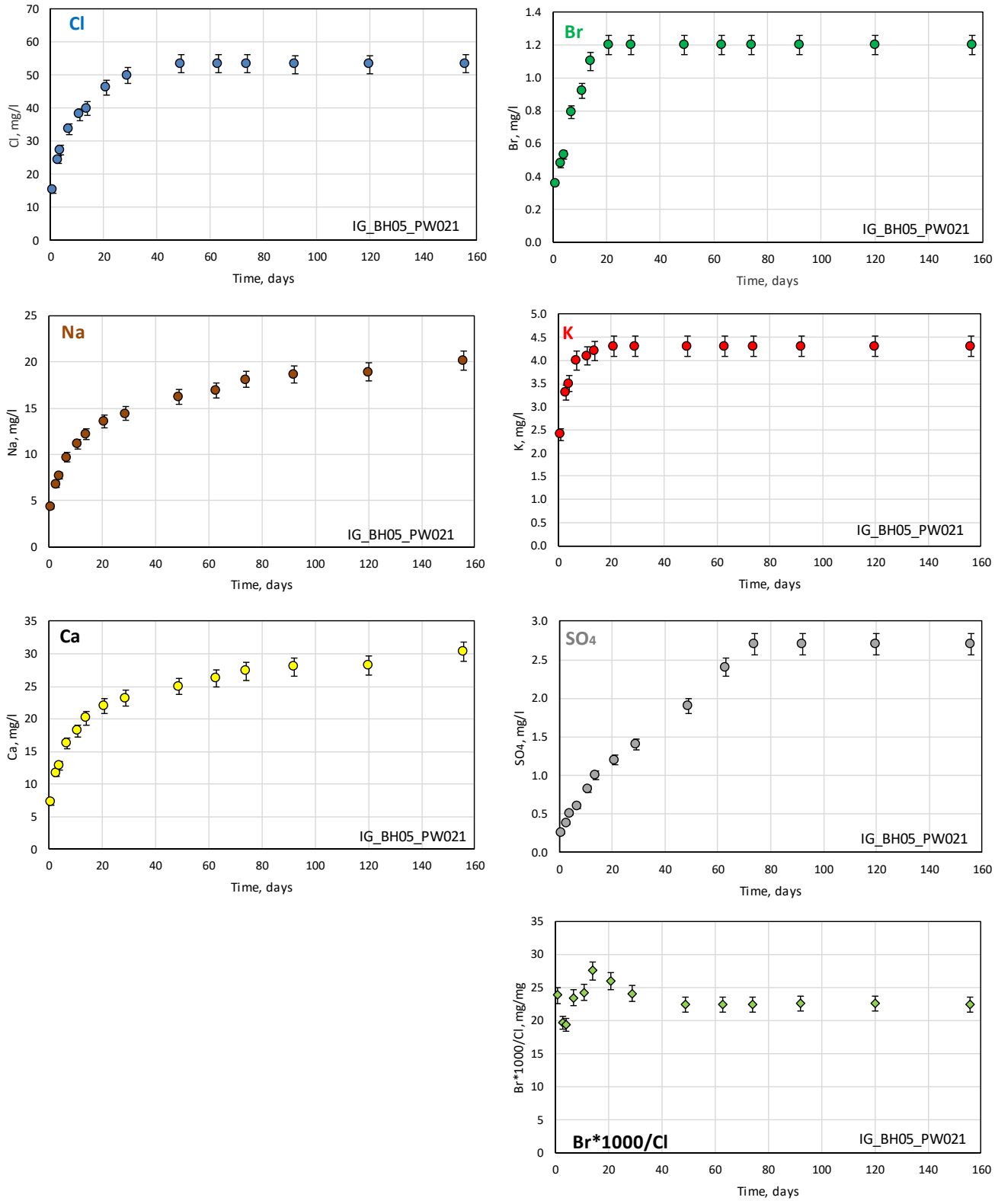


Figure 6-1 continued

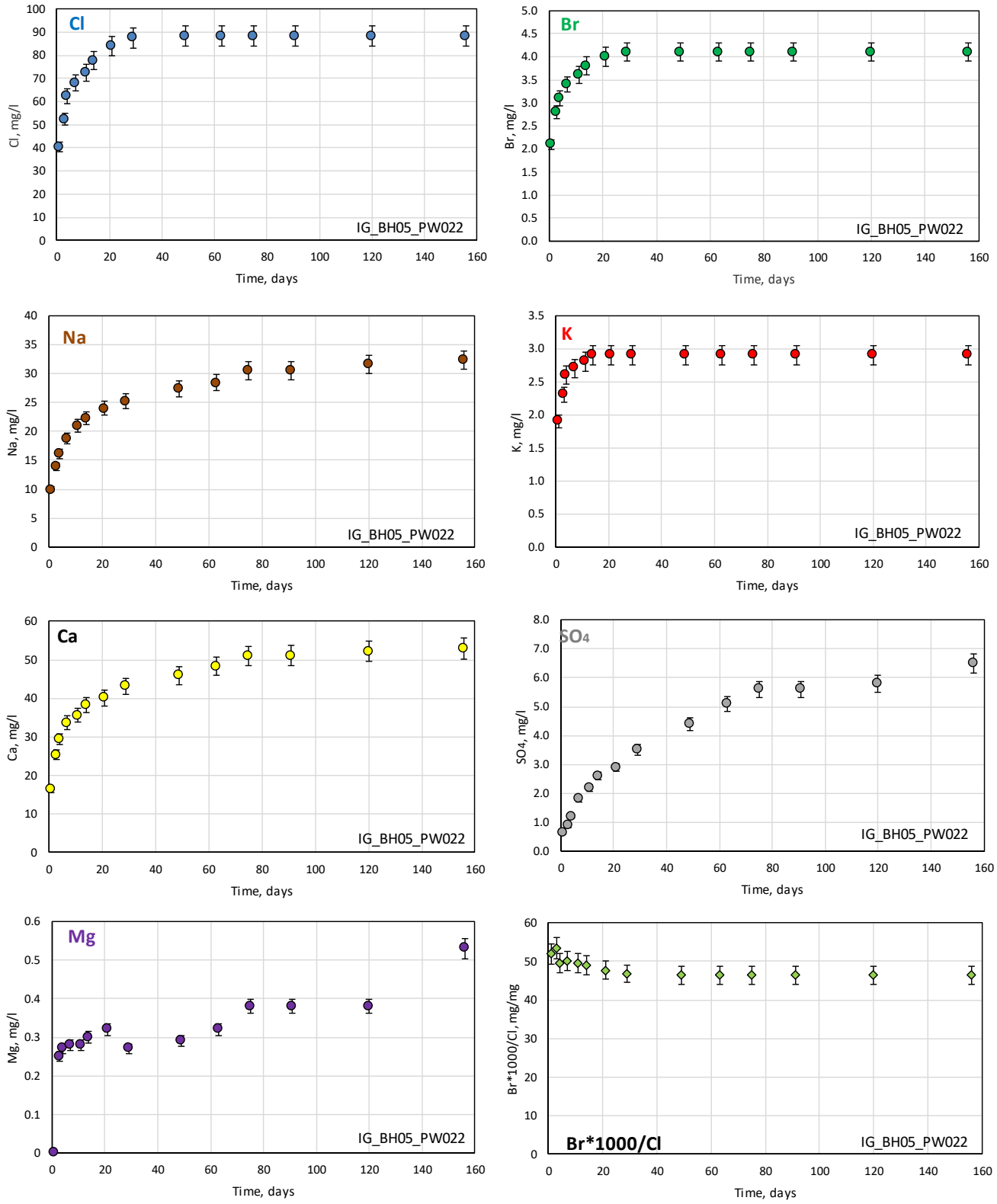


Figure 6-1 continued

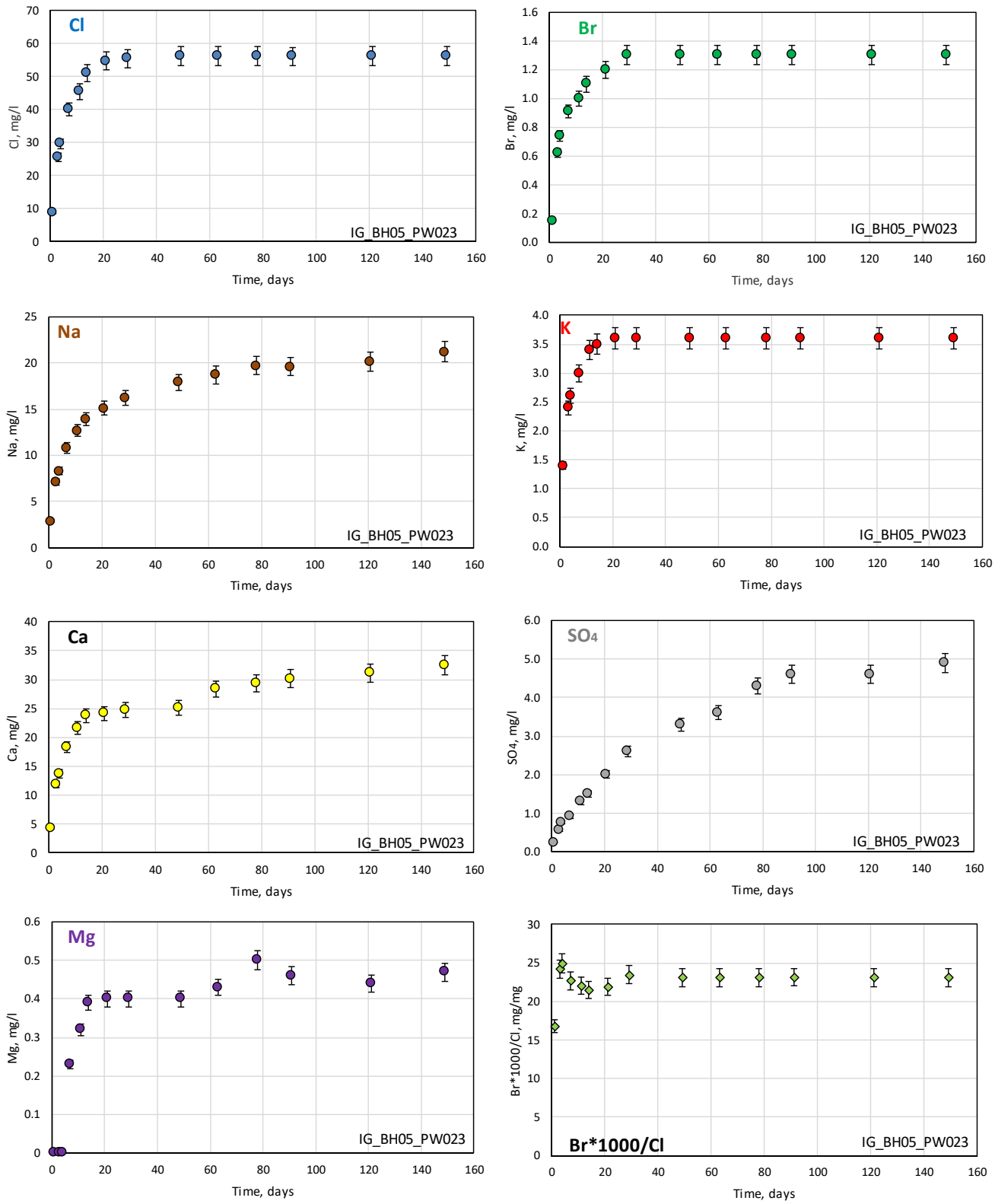


Figure 6-1 continued

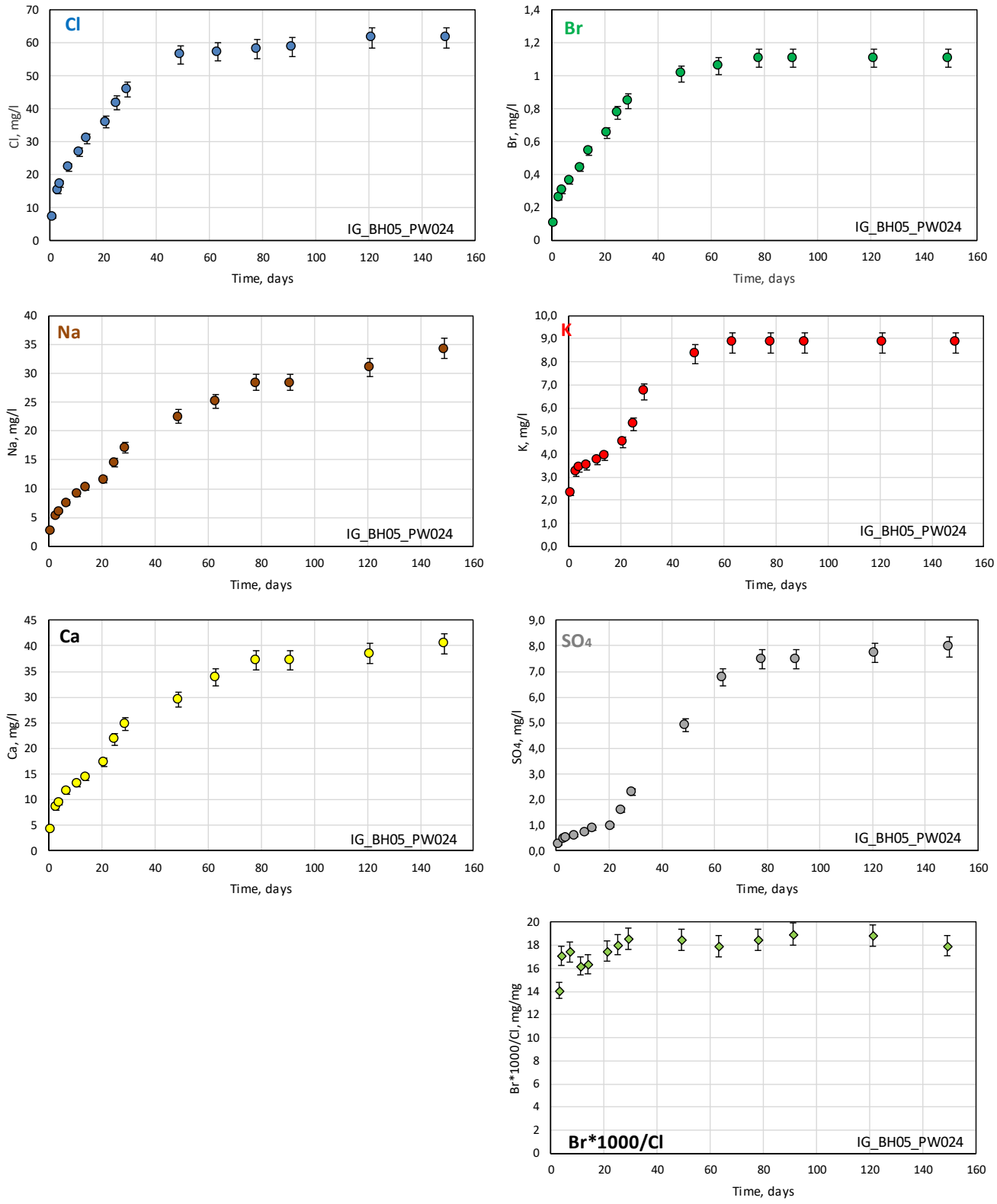


Figure 6-1 continued

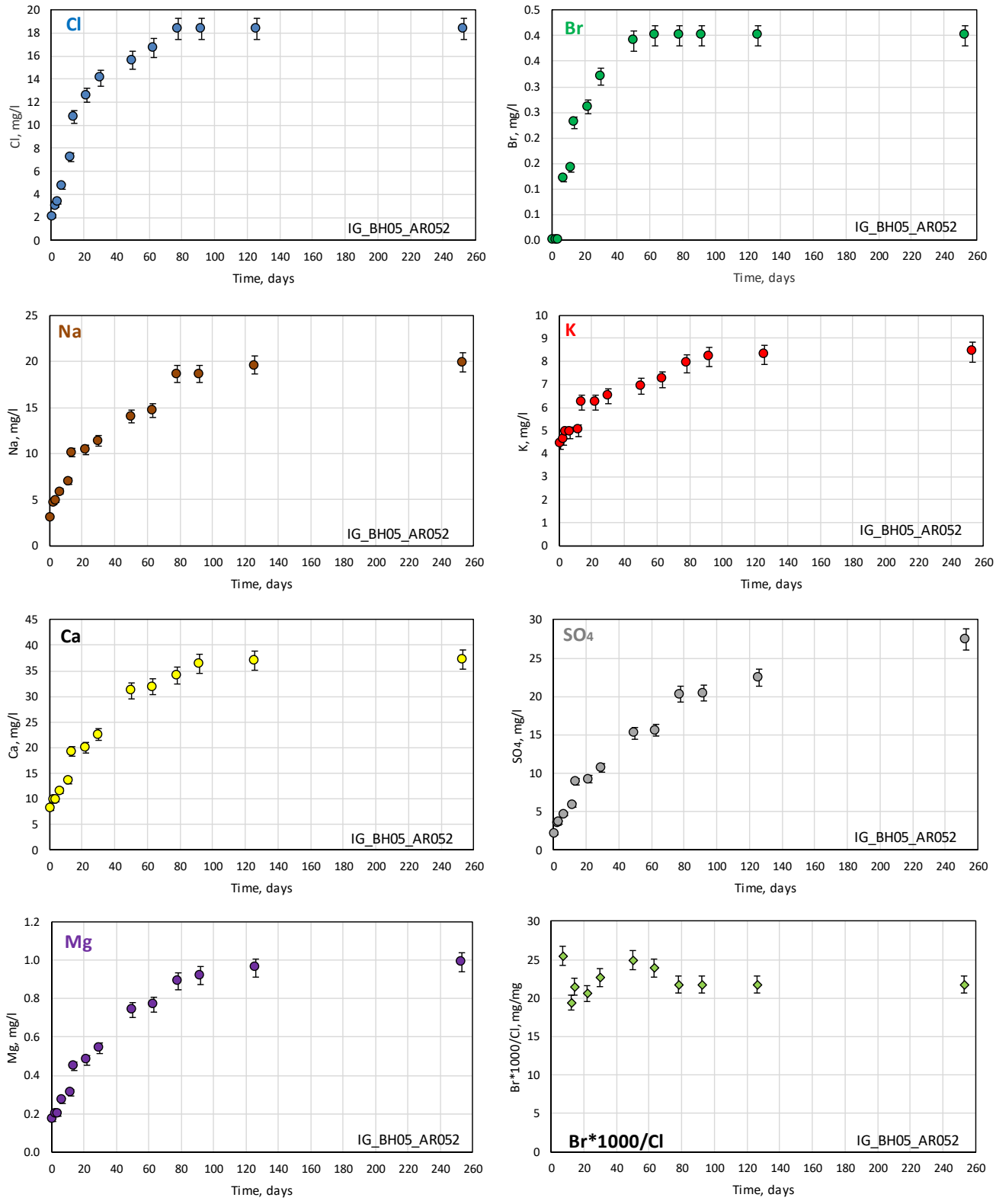


Figure 6-1 continued

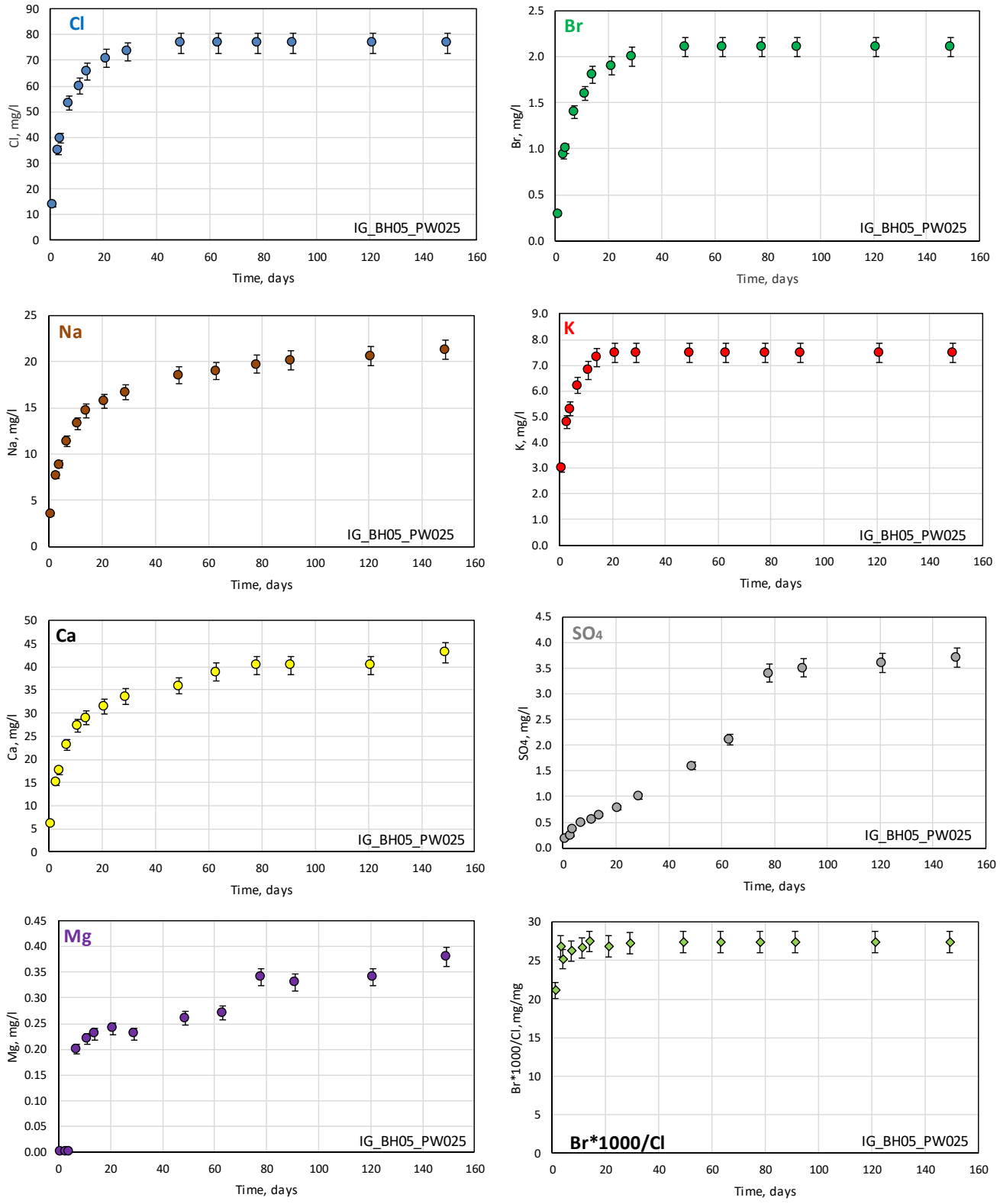


Figure 6-1 continued

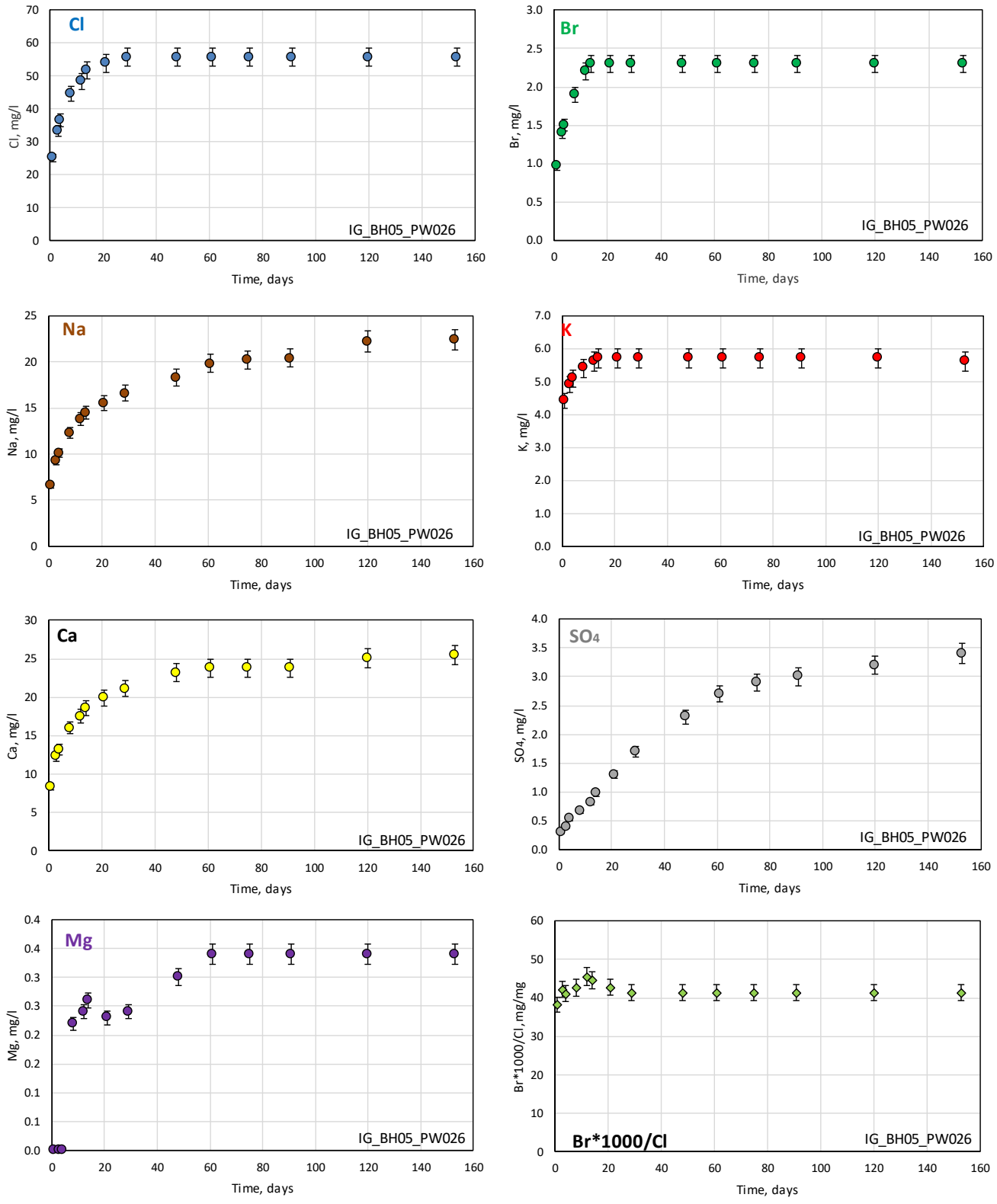


Figure 6-1 continued

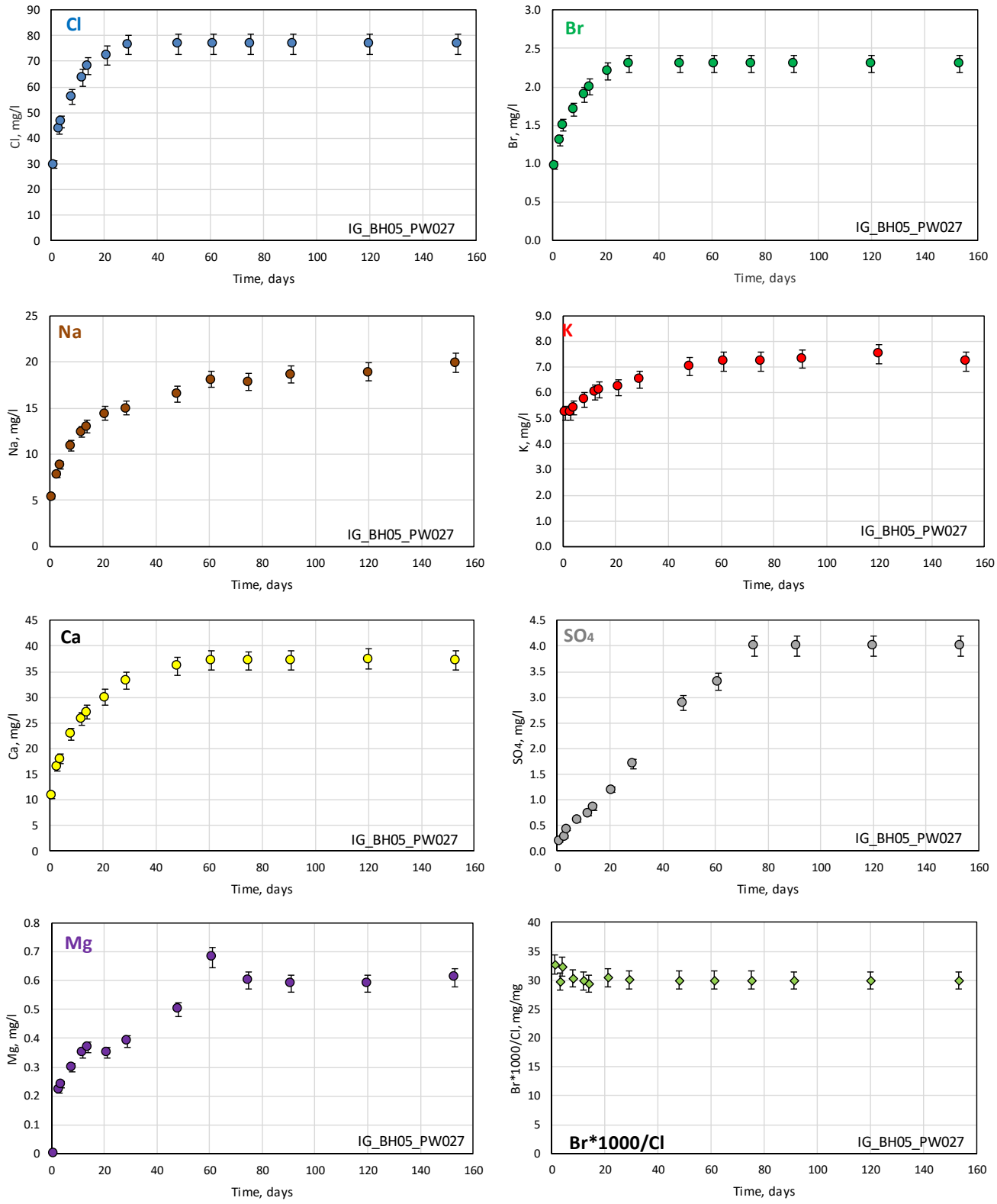


Figure 6-1 continued

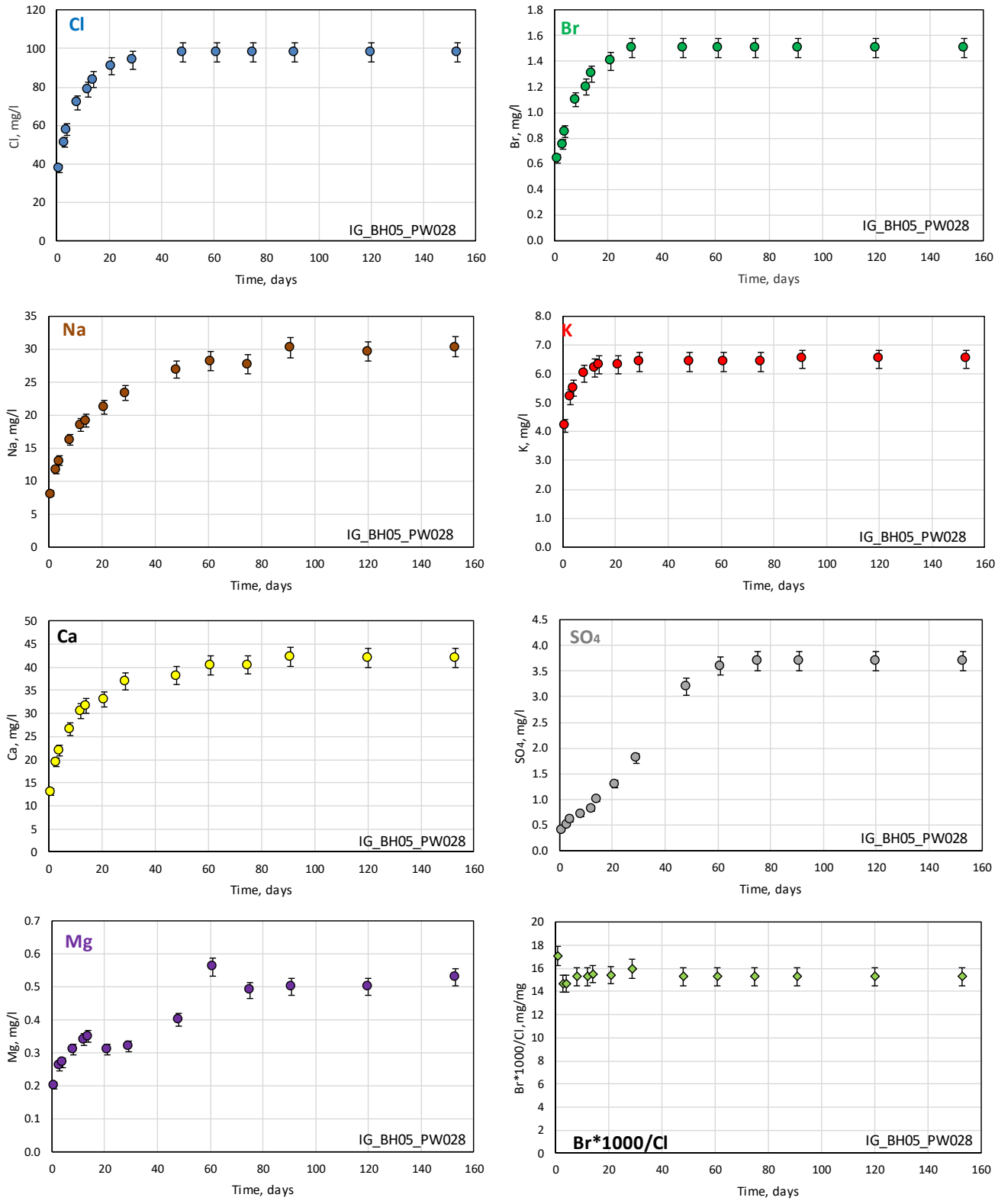


Figure 6-1 continued

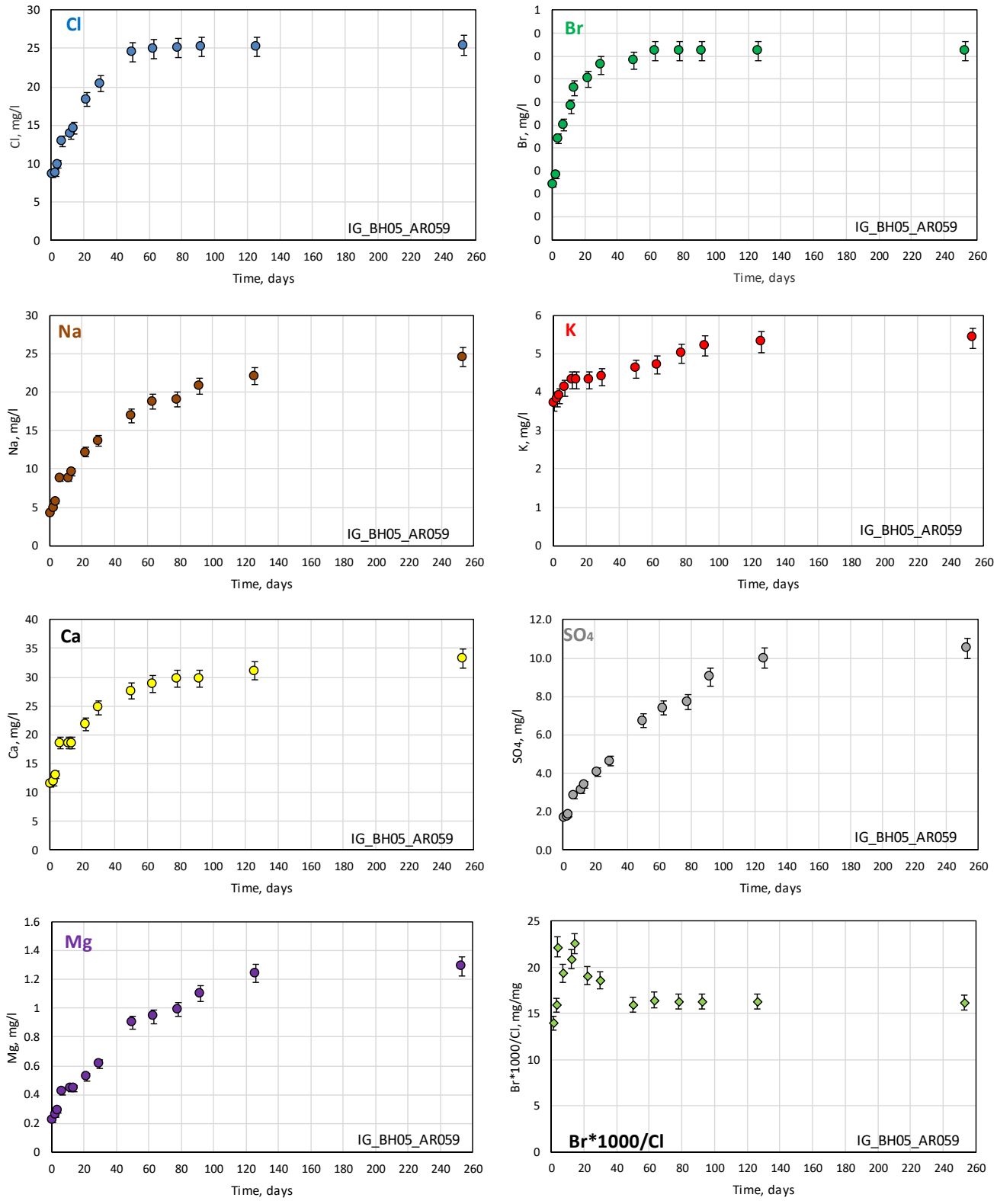


Figure 6-1 continued

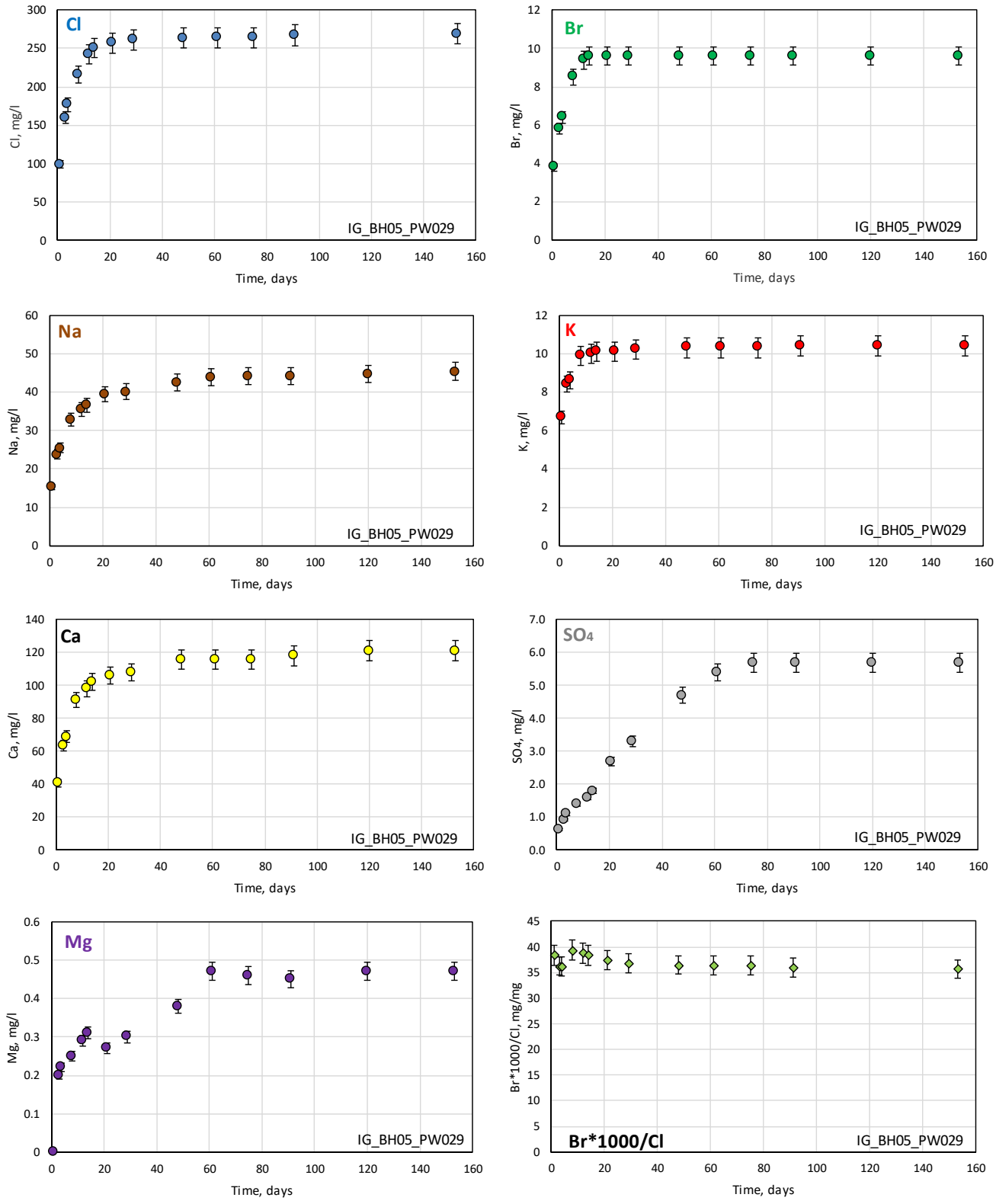


Figure 6-1 continued

6.2 Modelling of Pore Diffusion Coefficients

Chloride pore diffusion coefficients were derived by modelling the chloride breakthrough curves obtained from the out-diffusion experiments of all 32 samples from borehole IG_BH05. The chloride breakthrough curves are deduced from the Cl contents in the small-sized sub-samples that were collected periodically during the out-diffusion experiments (Section 3.3.2, 6.1). The pore diffusion coefficient is obtained by fitting the observed data with an analytical solution for one-dimensional radial diffusion out of the cylinder into a well-mixed solution reservoir (Crank 1975). The applied model (T. Gimmi, RWI, University of Bern) is restricted to homogeneous hydraulic properties (porosity, diffusion coefficient) across the core cylinder, and cannot consider heterogeneous properties due to rock anisotropy or induced effects, such as a drilling disturbed zone and/or stress release (Meier et al. 2015).

The pore diffusion coefficient, D_p, of a solute in a geological media mainly depends on the shape and size of water conducting pores (constrictivity) and on the pathways given by the connected pore network (tortuosity, e.g., Ohlsson and Neretnieks 1995). It can be defined as

$$D_p = D_w \frac{\delta_D}{\tau^2} \qquad (14)$$

where D_P = pore-diffusion coefficient in m^2/s, D_W = diffusion coefficient in pure water in m^2/s, δ_D = constrictivity, τ = tortuosity, and the term δ_D/τ^2 is called the geometry factor.

In a first assumption the pore diffusion coefficient of a given species, D_P, can be converted to the effective diffusion coefficient of this species, D_e, according to:

$$D_e = D_p \Phi_{WC} \qquad (15)$$

where D_e is the effective diffusion coefficient in m^2/s and Φ_{WC} the species-accessible porosity.

The shape of the Cl elution curves obtained for all core samples from borehole IG_BH05 suggests a heterogeneous transport system from the rim to the centre of the core (Figure 6-2). The initial slopes are steeper (in the transient state) during the first five to ten days of out-diffusion than the more moderate slopes observed later in the experiments.

The quality of the D_P fits is controlled by the difference ($\Delta_{meas\text{-}mod}$) of the measured and modelled Cl concentration at equal time and shown graphically by logarithmic plots (Figure 6-2). To determine the lowest $\Delta_{meas\text{-}mod}$ values, a stepwise adjustment ($\pm 0.5 * 10^{-10} m^2/s$) of the single points was conducted and the $\Delta_{meas\text{-}mod}$ values were calculated for every measured point. The determination of the best fits per sampling point indicates a gradual decrease of the modelled pore diffusion coefficients as diffusion progresses deeper into the cores.

The modelled D_P values, which were determined at 45 °C, are additionally converted to 10 and 25 °C by the Stoke-Einstein equation (Lide 1994). For the investigated core samples, the influence of the disturbed zone results in a pore diffusion coefficient that is a factor 2.0 to 5.0 higher than that of the inner core (Table 6-1, Figure 6-2).

The average pore diffusion coefficients (D_P) of the 32 crystalline core samples vary between 0.3 and $2.0 * 10^{-10}$ m^2/s (10 °C), resulting in effective diffusion coefficients (D_e) between 0.1 and $1.4 * 10^{-12}$ m^2/s (10 °C) (Table 6-1, Figure 6-2).

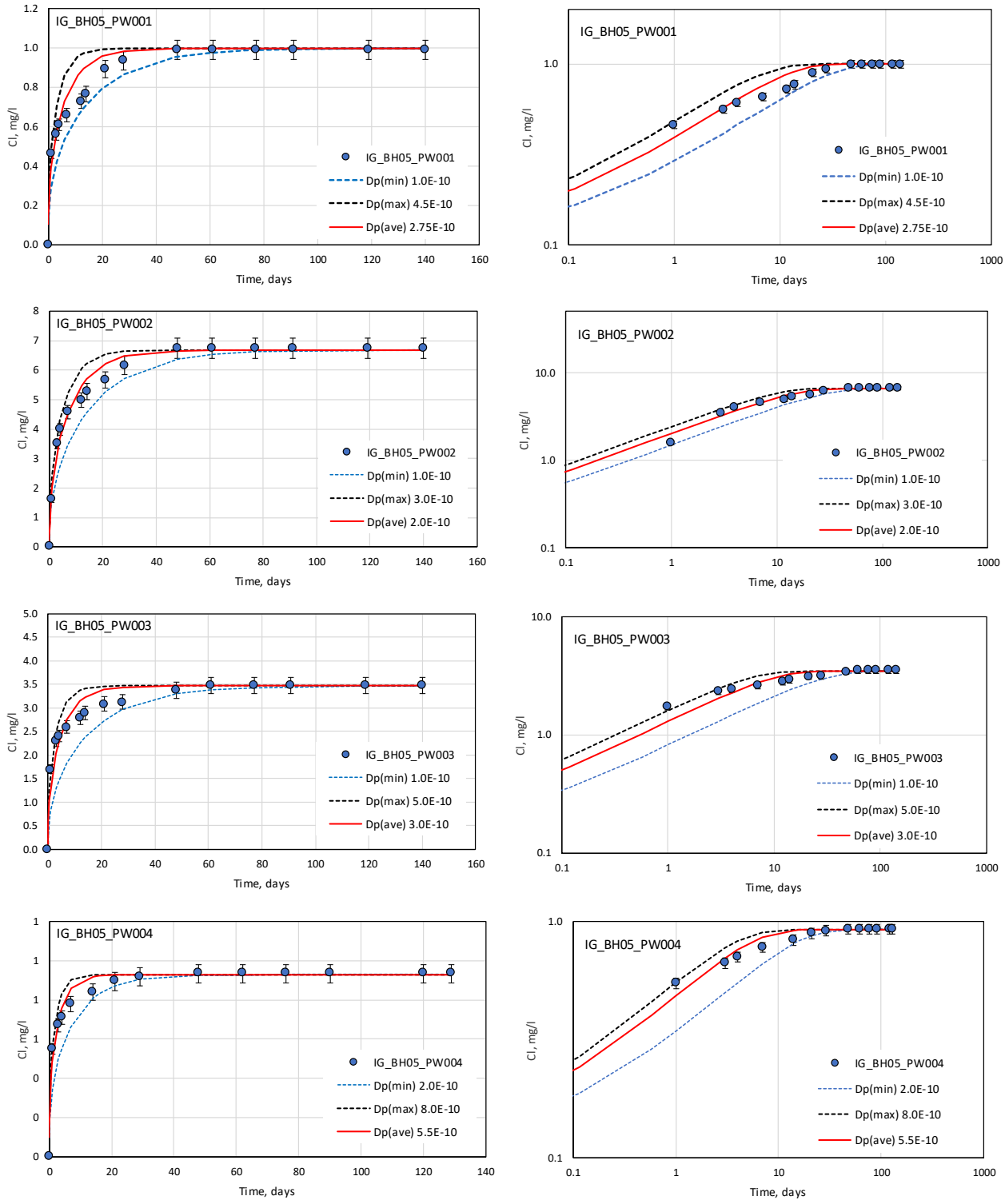


Figure 6-2: Maximum (Dp(max)) and minimum (Dp(min)) pore diffusion coefficients (45 °C) determined ba a best fit of Cl elution curves in linear and logarithmic time and concentration scale; the solid lines mark the average diffusion coefficients (45 °C, Dp (avg)).

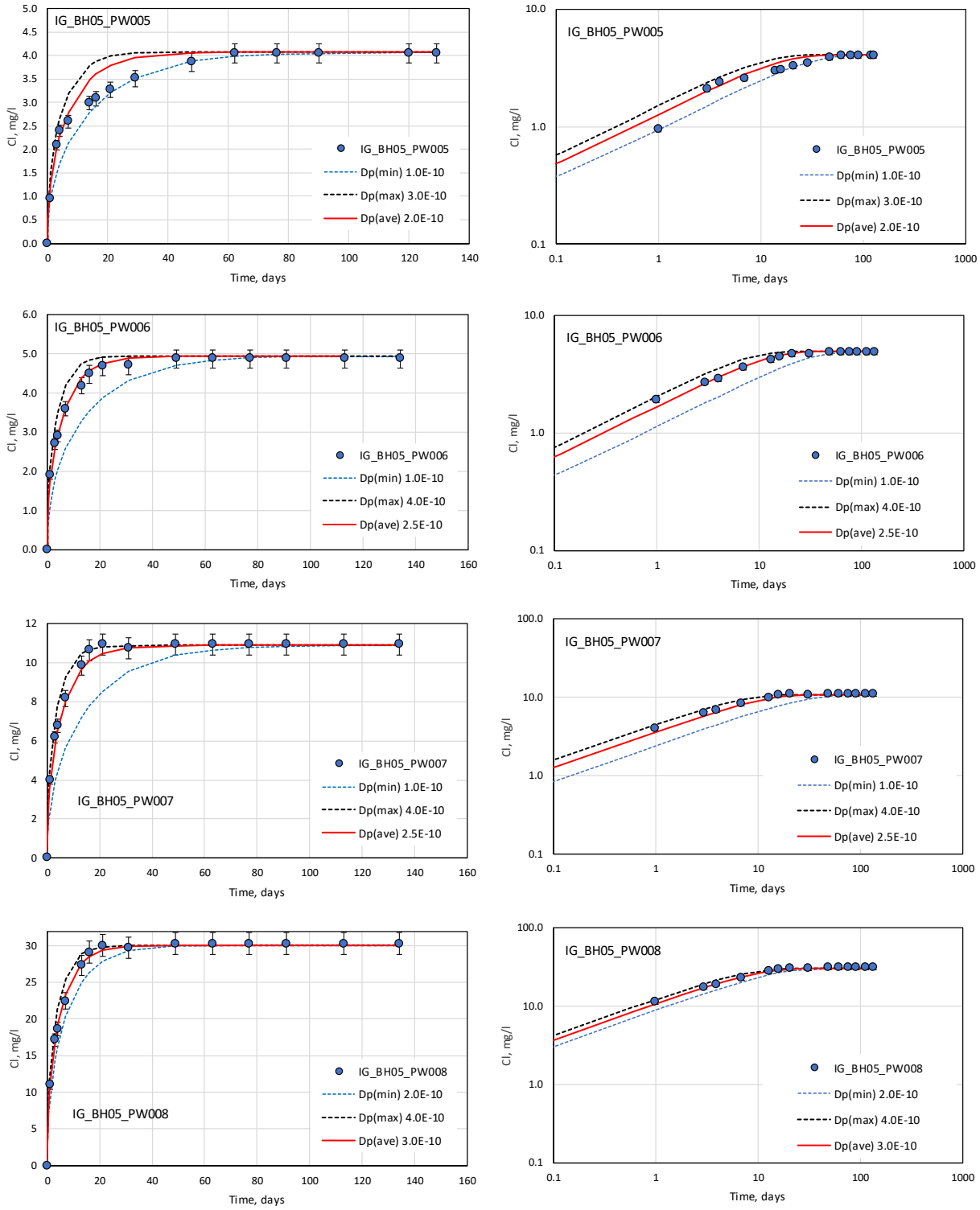


Figure 6-2 continued

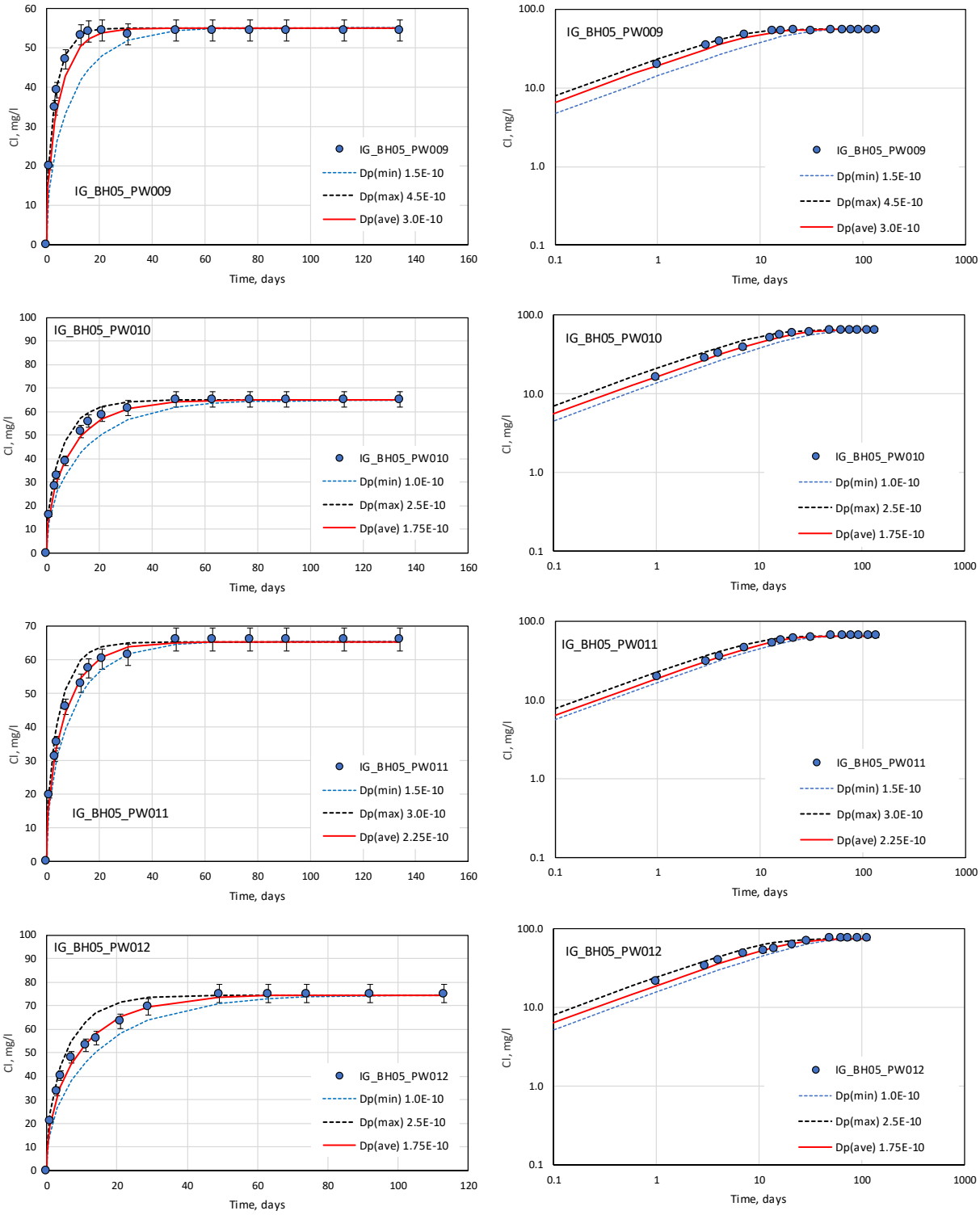


Figure 6-2 continued

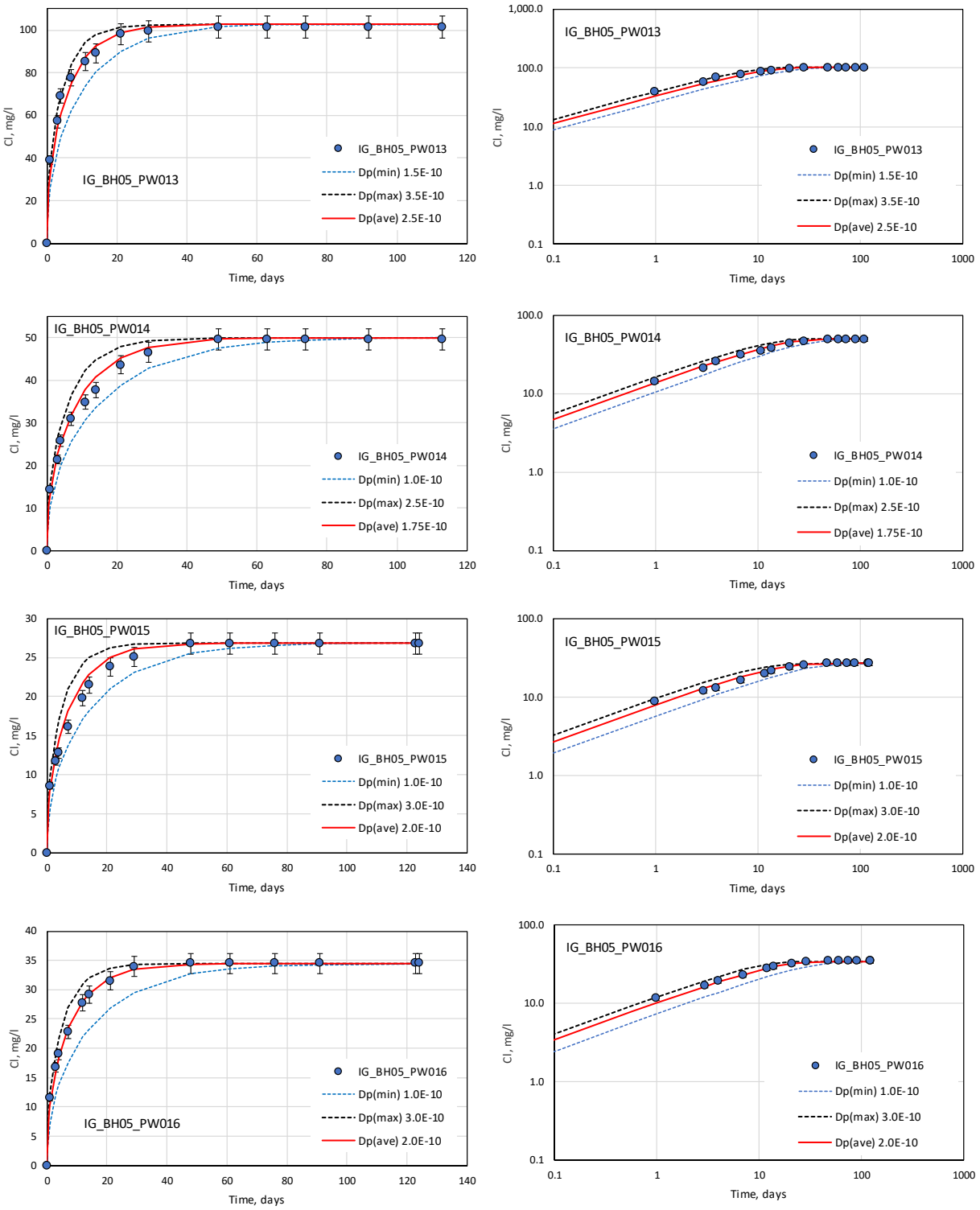


Figure 6-2 continued

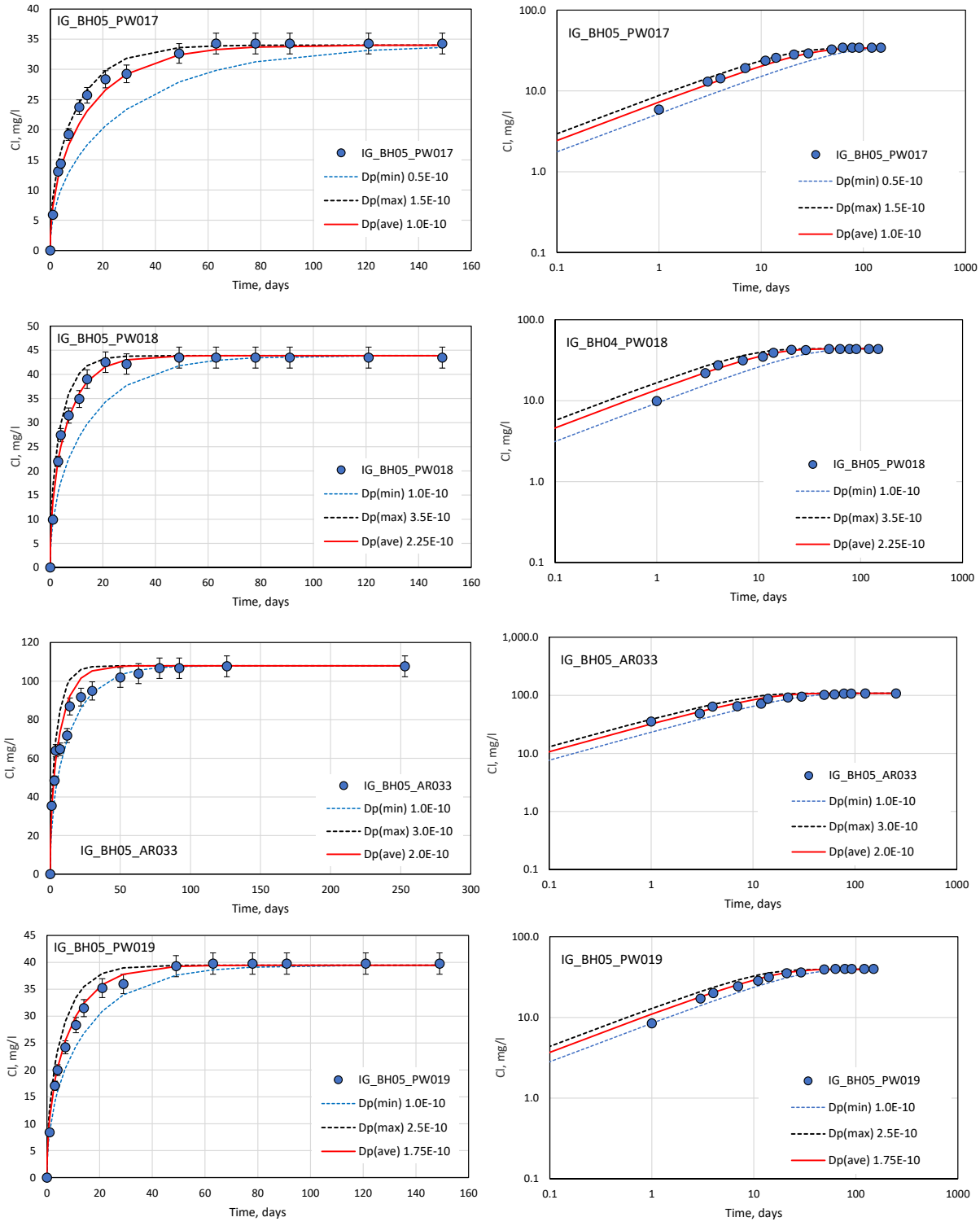


Figure 6-2 continued

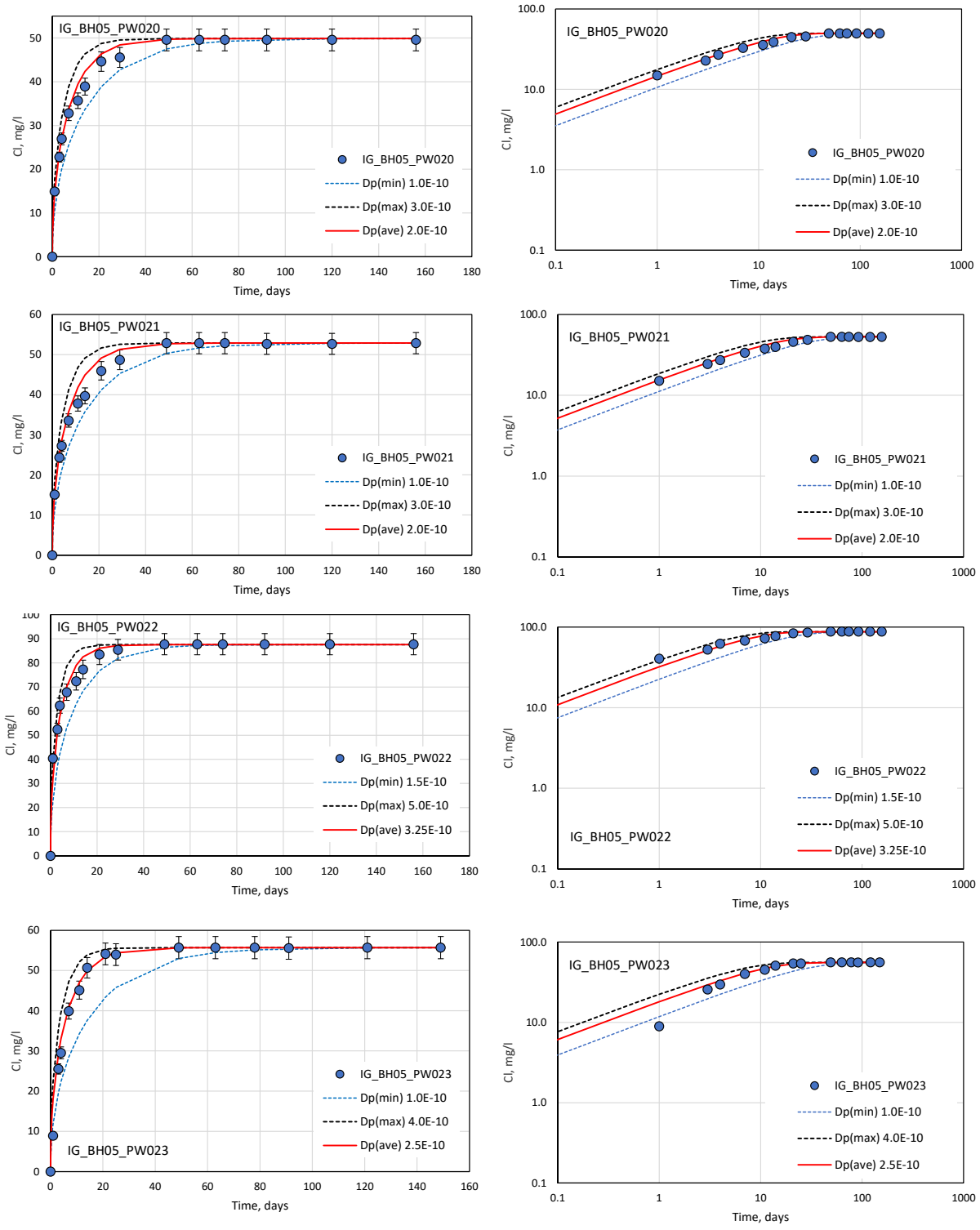


Figure 6-2 continued

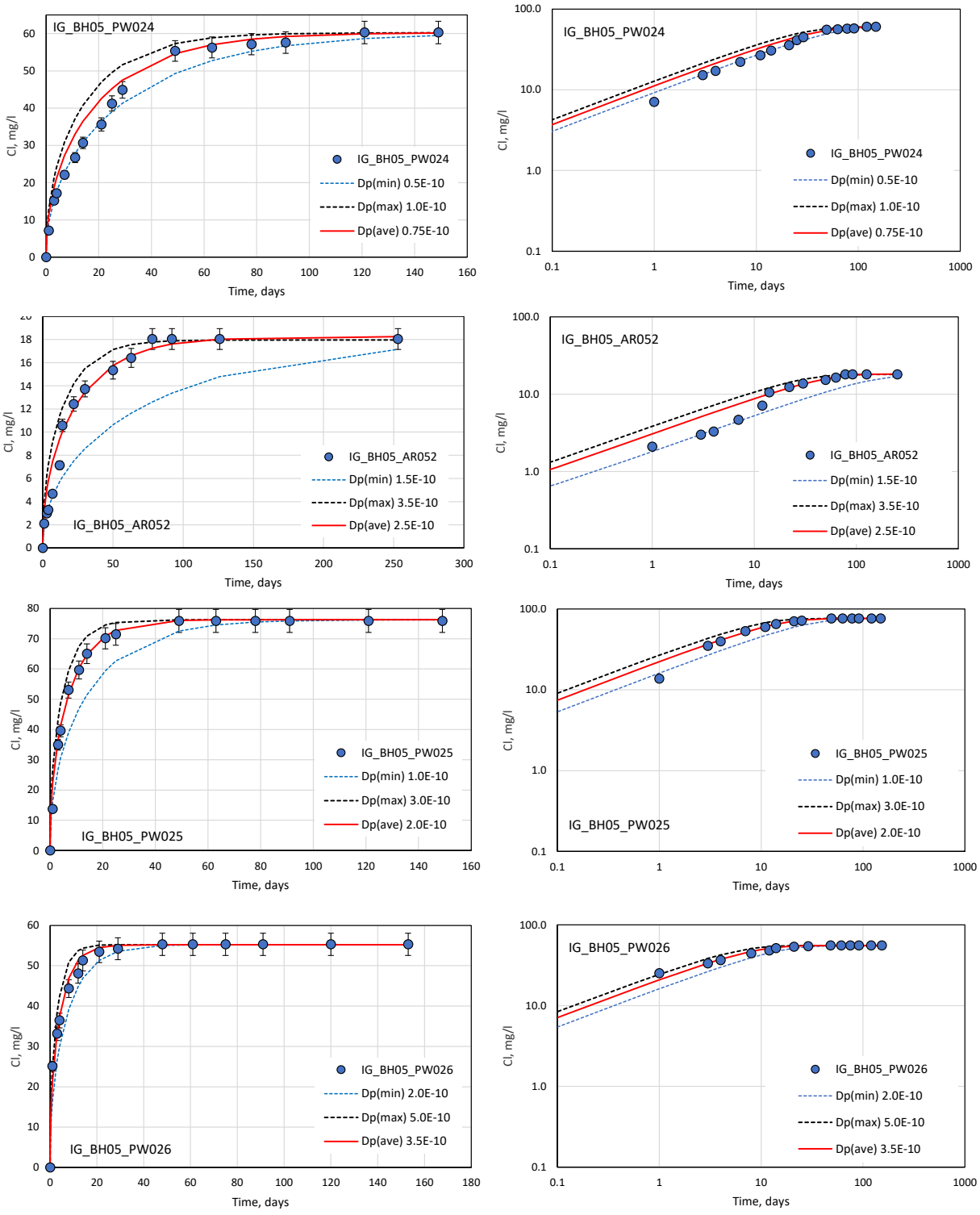


Figure 6-2 continued

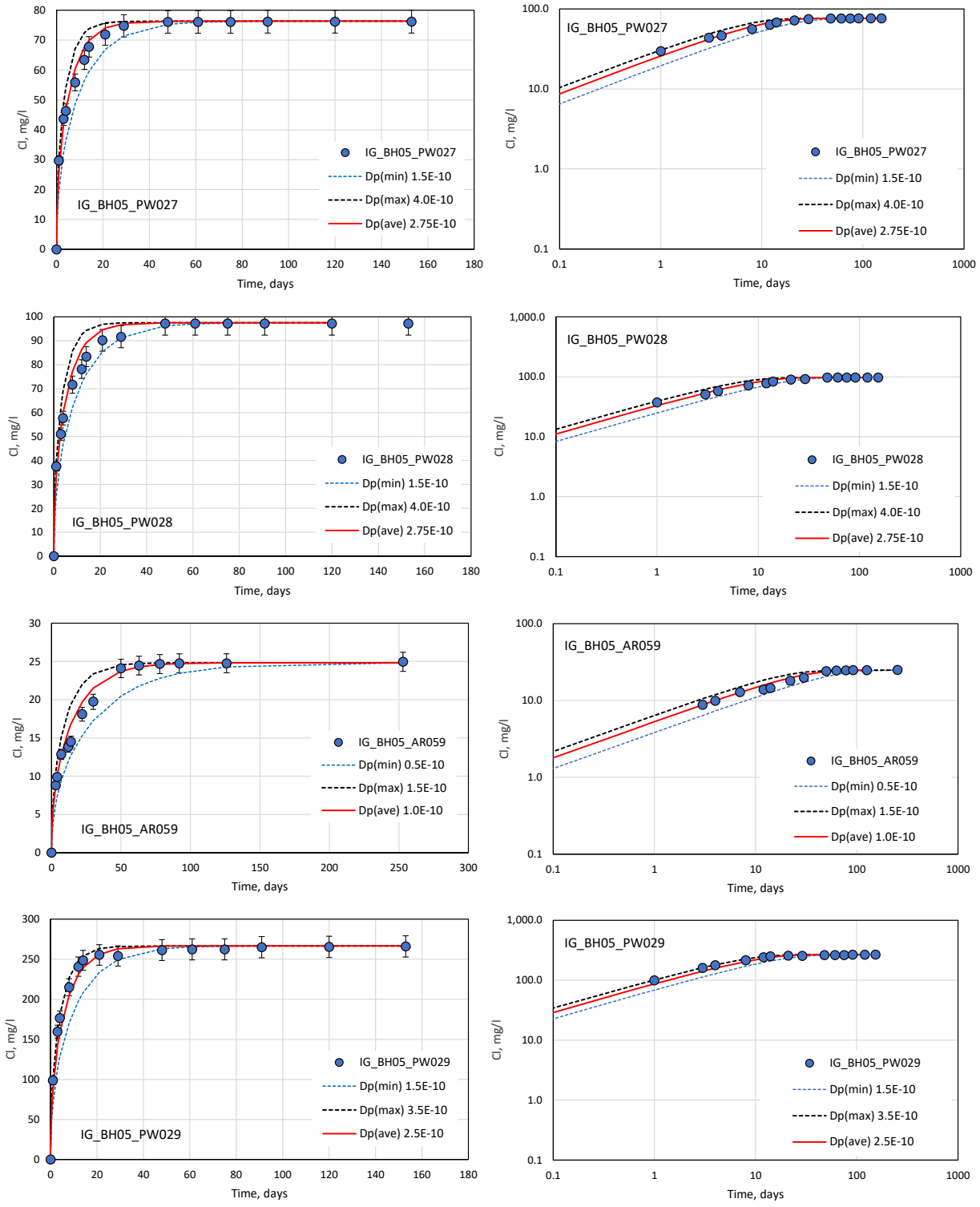


Figure 6-2 continued

Table 6-1: Minimum (min), maximum (max) and average (avg) pore and effective diffusion coefficients determined by 1-dimensional modelling of Cl elution curves of out-diffusion experiments on core samples from IG_BH05 at 45 °C and calculated by the Stoke-Einstein-equation for 10 °C and 25 °C; (G / T: granodiorite / tonalite, D: diabase, A: amphibolite).

Sample	Depth	Lithology	WL-Porosity	D(P) 45°C*E-10			D(P) 10°C*E-10			D(e)*E-12 (10°C)			D(P) 25°C*E-10			D(e)*E-12 (25°C)		
				max	min	ave	max	min	ave	max	min	ave	max	min	ave	max	min	ave
	mbgs		Vol.%	m^2/s	m^2/s	m^2/s	m^2/s	m^2/s	m^2/s	m^2/s	m^2/s	m^2/s	m^2/s	m^2/s	m^2/s	m^2/s	m^2/s	m^2/s
IG_BH05_PW001	171.4	G / T	0.51	1.0	4.5	2.8	0.4	1.8	1.1	0.2	0.9	0.6	0.6	2.8	1.7	0.3	1.4	0.9
IG_BH05_PW002	219.1	G / T	0.46	1.0	3.0	2.0	0.4	1.2	0.8	0.2	0.6	0.4	0.6	1.9	1.3	0.3	0.9	0.6
IG_BH05_PW003	253.5	G / T	0.54	1.0	5.0	3.0	0.4	2.0	1.2	0.2	1.1	0.7	0.6	3.1	1.9	0.3	1.7	1.0
IG_BH05_PW004	290.2	D	0.68	2.0	8.0	5.0	0.8	3.2	2.0	0.6	2.2	1.4	1.3	5.0	3.1	0.9	3.4	2.1
IG_BH05_PW005	341.7	G / T	0.43	1.0	3.0	2.0	0.4	1.2	0.8	0.2	0.5	0.3	0.6	1.9	1.3	0.3	0.8	0.5
IG_BH05_PW006	386.7	G / T	0.51	1.0	4.0	2.5	0.4	1.6	1.0	0.2	0.8	0.5	0.6	2.5	1.6	0.3	1.3	0.8
IG_BH05_PW007	398.5	G / T	0.43	1.0	4.0	2.5	0.4	1.6	1.0	0.2	0.7	0.4	0.6	2.5	1.6	0.3	1.1	0.7
IG_BH05_PW008	426.3	G / T	0.33	2.0	4.0	3.0	0.8	1.6	1.2	0.3	0.5	0.4	1.3	2.5	1.9	0.4	0.8	0.6
IG_BH05_PW009	454.3	G / T	0.50	1.5	4.5	3.0	0.6	1.8	1.2	0.3	0.9	0.6	0.9	2.8	1.9	0.5	1.4	0.9
IG_BH05_PW010	479.4	G / T	0.37	1.0	2.5	1.8	0.4	1.0	0.7	0.1	0.4	0.3	0.6	1.6	1.1	0.2	0.6	0.4
IG_BH05_PW011	506.4	G / T	0.37	1.5	3.0	2.3	0.6	1.2	0.9	0.2	0.5	0.3	0.9	1.9	1.4	0.4	0.7	0.5
IG_BH05_PW012	525.1	G / T	0.36	1.0	2.5	1.8	0.4	1.0	0.7	0.1	0.4	0.3	0.6	1.6	1.1	0.2	0.6	0.4
IG_BH05_PW013	560.1	G / T	0.42	1.5	3.5	2.5	0.6	1.4	1.0	0.3	0.6	0.4	0.9	2.2	1.6	0.4	0.9	0.7
IG_BH05_PW014	587.1	G / T	0.34	1.0	2.5	1.8	0.4	1.0	0.7	0.1	0.3	0.2	0.6	1.6	1.1	0.2	0.5	0.4
IG_BH05_PW015	612.1	G / T	0.42	1.0	3.0	2.0	0.4	1.2	0.8	0.2	0.5	0.3	0.6	1.9	1.3	0.3	0.8	0.5
IG_BH05_PW016	637.4	G / T	0.39	1.0	3.0	2.0	0.4	1.2	0.8	0.2	0.5	0.3	0.6	1.9	1.3	0.2	0.7	0.5
IG_BH05_PW017	665.3	G / T	0.37	0.5	1.5	1.0	0.2	0.6	0.4	0.1	0.2	0.2	0.3	0.9	0.6	0.1	0.4	0.2
IG_BH05_PW018	692.4	G / T	0.45	1.0	3.5	2.3	0.4	1.4	0.9	0.2	0.6	0.4	0.6	2.2	1.4	0.3	1.0	0.6
IG_BH05_AR033	717.4	A	0.57	1.0	3.0	2.0	0.4	1.2	0.8	0.2	0.7	0.5	0.6	1.9	1.3	0.4	1.1	0.7
IG_BH05_PW019	722.2	G / T	0.46	1.0	2.5	1.8	0.4	1.0	0.7	0.2	0.5	0.3	0.6	1.6	1.1	0.3	0.7	0.5
IG_BH05_PW020	749.6	G / T	0.37	1.0	3.0	2.0	0.4	1.2	0.8	0.1	0.4	0.3	0.6	1.9	1.3	0.2	0.7	0.5
IG_BH05_PW021	774.5	G / T	0.37	1.0	3.0	2.0	0.4	1.2	0.8	0.2	0.5	0.3	0.6	1.9	1.3	0.2	0.7	0.5
IG_BH05_PW022	801.8	G / T	0.68	1.5	5.0	3.3	0.6	2.0	1.3	0.4	1.4	0.9	0.9	3.1	2.0	0.6	2.1	1.4
IG_BH05_PW023	827.2	G / T	0.42	1.0	4.0	2.5	0.4	1.6	1.0	0.2	0.7	0.4	0.6	2.5	1.6	0.3	1.1	0.7
IG_BH05_PW024	848.7	G / T	0.39	0.5	1.0	0.8	0.2	0.4	0.3	0.1	0.2	0.1	0.3	0.6	0.5	0.1	0.2	0.2
IG_BH05_AR052	856.0	A	0.10	0.2	1.0	0.6	0.1	0.4	0.2	0.01	0.04	0.02	0.1	0.6	0.4	0.01	0.06	0.04
IG_BH05_PW025	881.5	G / T	0.25	1.0	3.0	2.0	0.4	1.2	0.8	0.1	0.3	0.2	0.6	1.9	1.3	0.2	0.5	0.3
IG_BH05_PW026	906.1	G / T	0.28	2.0	5.0	3.5	0.8	2.0	1.4	0.2	0.6	0.4	1.3	3.1	2.2	0.3	0.9	0.6
IG_BH05_PW027	936.8	G / T	0.23	1.5	4.0	2.8	0.6	1.6	1.1	0.1	0.4	0.3	0.9	2.5	1.7	0.2	0.6	0.4
IG_BH05_PW028	963.0	G / T	0.39	1.5	4.0	2.8	0.6	1.6	1.1	0.2	0.6	0.4	0.9	2.5	1.7	0.4	1.0	0.7
IG_BH05_AR059	979.0	A	0.16	0.5	1.5	1.0	0.2	0.6	0.4	0.03	0.10	0.06	0.3	0.9	0.6	0.05	0.15	0.10
IG_BH05_PW029	986.5	G / T	0.52	1.5	3.5	2.5	0.6	1.4	1.0	0.3	0.7	0.5	0.9	2.2	1.6	0.5	1.1	0.8

7.0 RESULTS FROM CHLORIDE, BROMIDE AND CHLORIDE ISOTOPES IN POREWATER OF CORE SAMPLES FROM BOREHOLE IG_BH05

Chloride and bromide concentrations of porewater were determined by aqueous extraction experiments (Section 3.2.1) and out-diffusion experiments (Section 3.2.2). Aqueous extraction experiments were conducted prior to the other longer-term experiments to obtain preliminary information about porewater salinities.

7.1 Porewater Chloride Concentrations Estimated by Aqueous Extraction Experiments

Aqueous extraction experiments were conducted on 29 core samples from each of the sampled depth intervals. Approximate estimates of porewater Cl concentrations were calculated according to Equation 3 (Section 3.2.1). During crushing of the rock samples, saline fluids from fluid inclusions in quartz and feldspar are released, which contribute to the Cl and Br inventory of the samples. This means that the chloride concentrations determined by aqueous extraction overestimate the actual porewater Cl concentrations.

Estimated porewater Cl concentrations for core samples from borehole IG_BH05 determined by aqueous extractions vary between 1,720 and 20,594 mg/kg H_2O (Table 7-1).

Based on the Cl-concentration range of porewater in core samples taken from borehole IG_BH05 (1,720 – 20,594 mg/kg H_2O = 0.05 - 0.61 mol), the salinity of isotope diffusive exchange experiment solutions was defined at 0.3 mol NaCl (see Section 8.0).

Table 7-1: Porewater Cl and Br concentrations and Br*1000/Cl mass ratios estimated using aqueous extraction experiments; the errors of porewater Cl and Br concentrations and Br*1000/Cl mass ratios are calculated by Gaussian error propagation (Appendix C).

Sample	Depth mbgs*	Estimated Cl_{PW}(aq.ex.) mg/kgH_2O	Br_{PW} mg/kgH_2O	Br*1000/Cl mg/mg
IG_BH05_AQ001	166.4	1767	174	98
IG_BH05_AQ002	221.1	4798	86	18
IG_BH05_AQ003	253.2	4514	202	45
IG_BH05_AQ004	290.0	3785	43	11
IG_BH05_AQ005	343.2	3446	70	20
IG_BH05_AQ006	387.4	2216	54	24
IG_BH05_AQ007	399.9	1720	37	21
IG_BH05_AQ008	427.0	5094	686	135
IG_BH05_AQ009	453.6	4138	81	20
IG_BH05_AQ010	480.1	6931	153	22
IG_BH05_AQ011	507.1	6885	162	24
IG_BH05_AQ012	525.7	7209	169	23
IG_BH05_AQ013	560.7	7141	165	23
IG_BH05_AQ014	588.2	6718	145	22
IG_BH05_AQ015	612.8	7796	513	66
IG_BH05_AQ016	640.4	3107	248	80

Sample	Depth mbgs*	Estimated Cl_{PW}(aq.ex.) mg/kgH_2O	Br_{PW} mg/kgH_2O	Br*1000/Cl mg/mg
IG_BH05_AQ017	664.6	5171	497	96
IG_BH05_AQ018	694.2	6458	665	103
IG_BH05_AQ019	720.7	6719	431	64
IG_BH05_AQ020	750.3	7336	237	32
IG_BH05_AQ021	773.3	7601	255	34
IG_BH05_AQ022	797.6	7755	433	56
IG_BH05_AQ023	827.9	6577	308	47
IG_BH05_AQ024	849.3	10350	397	38
IG_BH05_AQ025	881.8	10954	535	49
IG_BH05_AQ026	906.7	8855	774	87
IG_BH05_AQ027	937.0	9927	365	37
IG_BH05_AQ028	963.1	11850	214	18
IG_BH05_AQ029	982.3	20594	602	29

* mbgs (downhole)

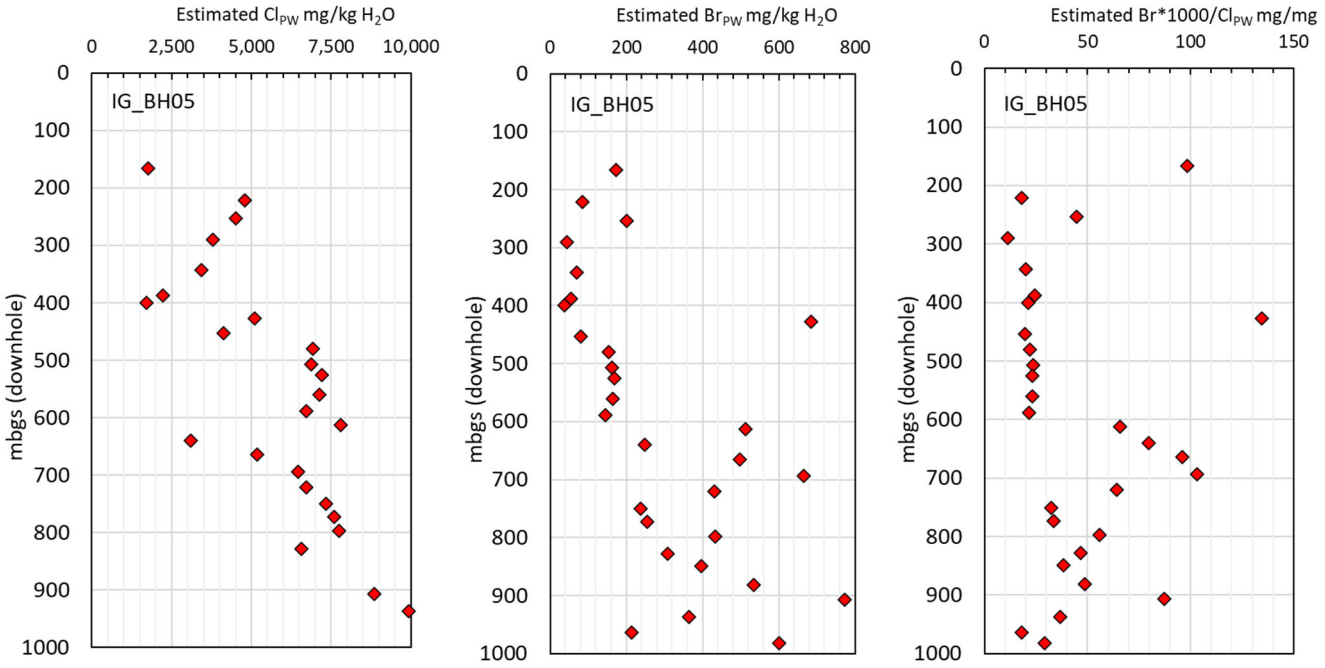


Figure 7-1: Borehole IG_BH05: Estimated porewater Cl and Br concentrations and Br*1000/Cl mass ratios versus depth by aqueous extraction experiments.

7.2 Porewater Chloride Concentrations and Bromide Concentrations and $\delta^{37}Cl$ Isotope Ratios Determined by Out-Diffusion Experiments

The conservative behaviour of chloride and bromide, the absence of Cl- and Br-bearing minerals in the rock, and the non-destructive character of the out-diffusion method, make the porewater the only source for dissolved Cl and Br in the experimental solutions. This allows calculation of the Cl and Br concentration in the porewaters by mass balance according to Equation 4 (Section 3.3.2), given that equilibrium in the out-diffusion experiments is achieved. As shown by their chloride and bromide elution curves, this latter condition is fulfilled for all samples (Section 6.1).

The mass ratio of the two conservative elements, Cl and Br, can serve as a tracer of the origin of Cl and Br in porewater and fracture groundwater. The $\delta^{37}Cl$ ratio measured for the experiment solutions directly corresponds to the porewater Cl isotope signature. This is because the attained equilibrium in the out-diffusion experiment with respect to total Cl is also expected to result in equilibrium with respect to the Cl isotopes (Gimmi and Waber 2004).

Chloride concentrations of porewater taken between 171 and 987 mbgs (downhole) from borehole IG_BH05 vary between 32 and 13,273 mg/kg H_2O (Table 7-2). Porewater bromide concentrations of the same respective samples from borehole IG_BH05 vary between 3.5 and 474 mg/kg H_2O (Table 7-2). The Br*1000/Cl mass ratios (=Br/Cl ratio) of porewater from borehole IG_BH05 vary between 15 and 46 (Table 7-2). In the bromide versus chloride diagram, porewaters extracted from borehole IG_BH05 cores plot significantly above the seawater dilution line (Br*1000/Cl mass ratio of seawater = 3.4, Figure 7-3).

The errors are calculated based on Gaussian error propagation (cf. Appdendix C). In these calculations the mass and water content differences determined before and after the out-diffusion experiments are taken into account. For several core samples, especially for those with low water contents, the high mass differences (cf. Table 4-3, Figure 4-2) lead to high errors of the porewater chloride concentrations

Porewater $\delta^{37}Cl$ isotope signatures vary between -1.02 $\pm$ 0.20 ‰ and 0.84 $\pm$ 0.20 ‰ SMOC along the depth profile between 171 and 987 mbgs (downhole) (Table 7-2). Porewater stable chlorine isotope signatures do not show a trend that correlates with porewater Cl concentrations (Table 7-2 and Figure 7-4).

Some of the porewater $\delta^{37}Cl$ results show large (> 0.40 ‰) errors (Table 7-2). The errors are determined by the standard deviation of a triplicate measurement of the single samples and are high especially for the samples with low Cl-concentrations in the out-diffusion solutions (Table 5-2).

Table 7-2: Porewater Cl and Br concentrations, Br*1000/Cl mass ratios and $\delta^{37}Cl$ isotope signatures. Cl concentrations are determined by out-diffusion experiments; the errors of porewater Cl and Br concentrations and Br*1000/Cl mass ratios are calculated by Gaussian error propagation (Appendix C); the errors of $\delta^{37}Cl$ values are the standard deviation of triplicate analyses; (G / T: granodiorite / tonalite, D: diabase).

Sample	Depth mbgs*	Lithology	Cl_{PW} (o.d.) mg/kgH_2O	Br_{PW} mg/kgH_2O	Br*1000/Cl mg/mg	$\delta^{37}Cl$ ‰ SMOC
IG_BH05_PW001	171.4	G / T	48±3	**		Cl too low
IG_BH05_PW002	219.1	G / T	394±24	3.5±0.2	9±1	0.06±0.20
IG_BH05_PW003	253.5	G / T	173±10	4.0±0.2	23±2	-0.43±0.48
IG_BH05_PW004	290.2	D	32±3	**		Cl too low
IG_BH05_PW005	341.7	G / T	247±15	**		-0.37±0.69
IG_BH05_PW006	386.7	G / T	289±20	**		0.33±0.20
IG_BH05_PW007	398.5	G / T	727±40	10.6±0.6	15±1	-0.22±0.10
IG_BH05_PW008	426.3	G / T	2285±118	105±5.4	46±3	0.44±0.10
IG_BH05_PW009	454.3	G / T	3034±268	52.6±4.6	17±2	0.65±0.10
IG_BH05_PW010	479.4	G / T	4941±488	105±10.4	21±3	0.64±0.10
IG_BH05_PW011	506.4	G / T	4820±336	94.1±6.6	20±2	0.74±0.10
IG_BH05_PW012	525.1	G / T	5014±387	92.5±7.1	18±2	0.69±0.10
IG_BH05_PW013	560.1	G / T	6402±758	138±16.3	22±4	0.82±0.10
IG_BH05_PW014	587.1	G / T	3644±360	69.1±6.8	19±3	0.64±0.10
IG_BH05_PW015	612.1	G / T	1661±92	40.6±2.2	24±2	0.18±0.10
IG_BH05_PW016	637.4	G / T	2369±123	49.0±2.6	21±2	0.05±0.10
IG_BH05_PW017	665.3	G / T	2391±134	48.9±2.7	20±2	-1.02±0.20
IG_BH05_PW018	692.4	G / T	2642±188	72.2±5.1	27±3	-0.53±0.21
IG_BH05_AR033	717.4	D	5615±315	87.1±4.9	16±1	0.43±0.10
IG_BH05_PW019	722.2	G / T	2243±146	38.5±2.5	17±2	0.84±0.20
IG_BH05_PW020	749.6	G / T	4043±347	76.0±6.5	19±2	0.00±0.02
IG_BH05_PW021	774.5	G / T	3972±338	89.2±7.6	22±3	-0.04±0.20
IG_BH05_PW022	801.8	G / T	3504±187	163±8.7	46±4	-0.04±0.20
IG_BH05_PW023	827.2	G / T	3480±274	80.5±6.3	23±3	-0.38±0.20
IG_BH05_PW024	848.7	G / T	2856±181	51.7±3.3	18±2	-0.43±0.26
IG_BH05_AR052	856.0	D	4353±1139	94.6±24.8	22±3	-0.39±0.10
IG_BH05_PW025	881.5	G / T	8028±425	220±11.7	27±2	0.10±0.22
IG_BH05_PW026	906.1	G / T	5171±736	214±30.4	41±8	-0.01±0.40
IG_BH05_PW027	936.3	G / T	9174±666	275±20.0	30±3	0.55±0.20
IG_BH05_PW028	962.9	G / T	6531±338	100±5.2	15±1	-0.69±0.32
IG_BH05_AR059	979.0	D	5250±1222	84.7±19.7	16±1	-0.43±0.10
IG_BH05_PW029	986.5	G / T	13273±1407	474±50.2	36±5	0.18±0.20

* mbgs (downhole)

** below detection limit

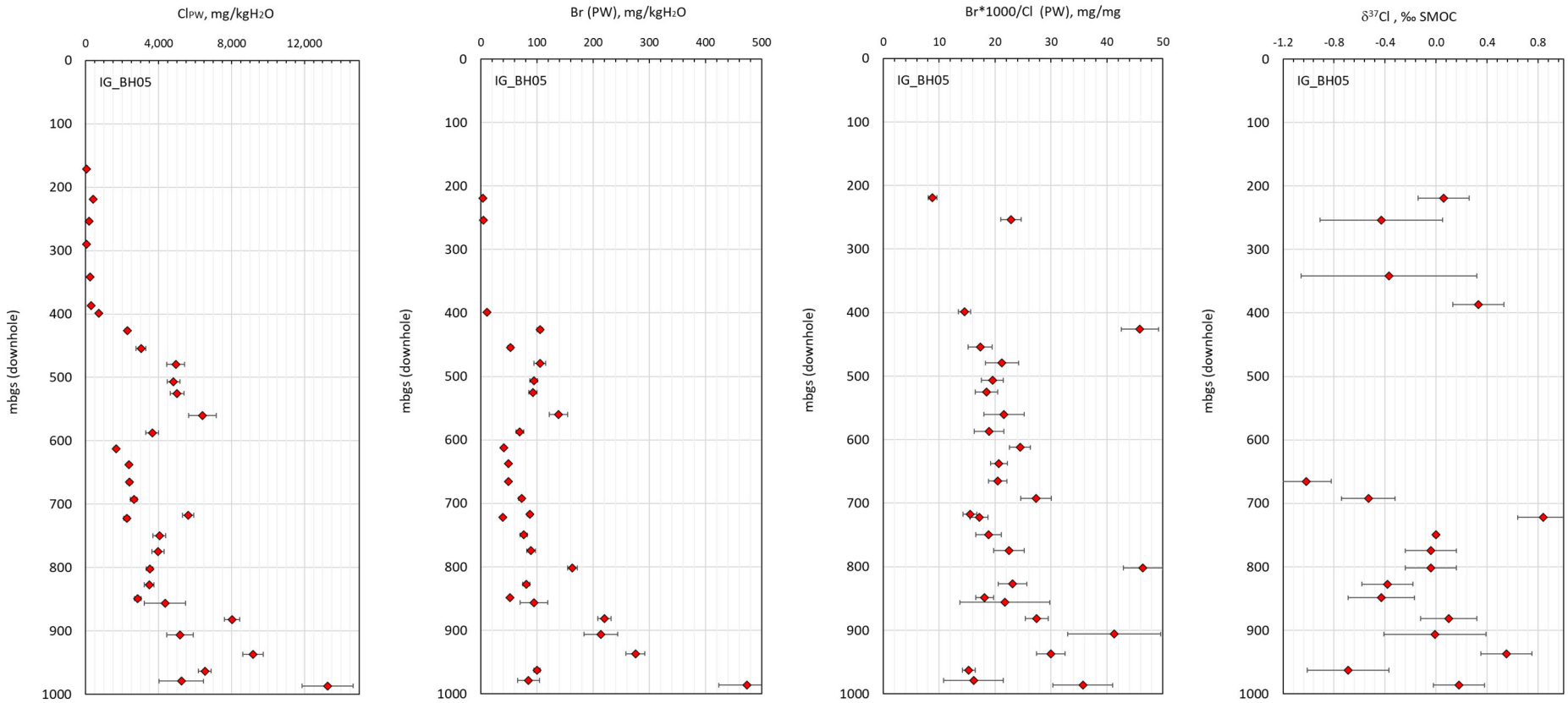


Figure 7-2: Porewater chloride, bromide, Br*1000/Cl mass ratios and $\delta^{37}Cl$ isotope signatures from cores from borehole IG_BH05 as function of depth.

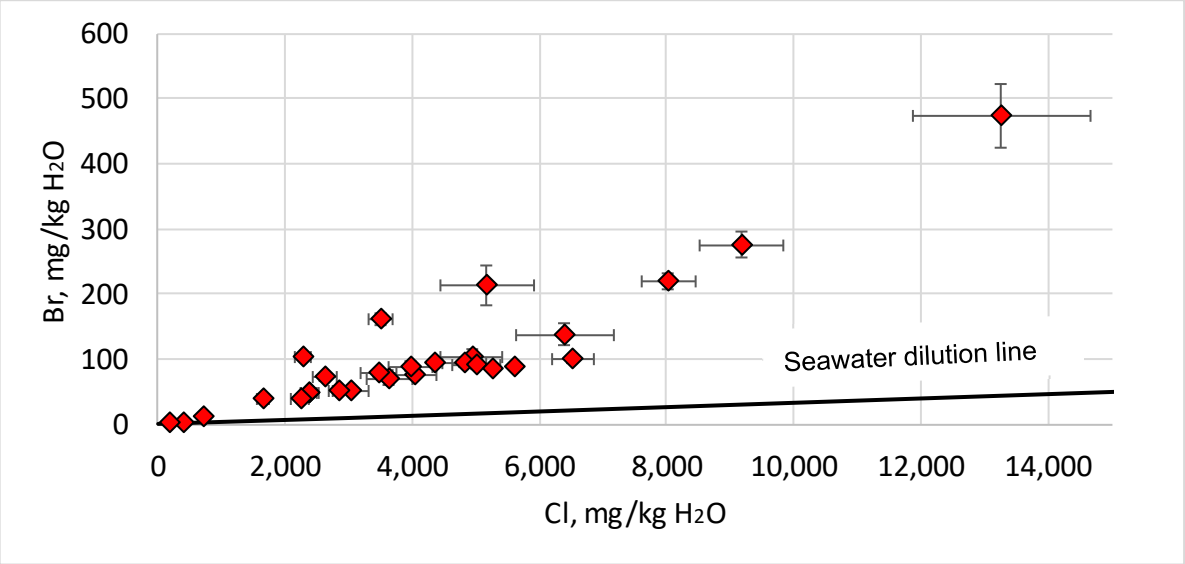


Figure 7-3: Porewater Cl versus Br concentrations determined by out-diffusion experiments on core samples from IG_BH05.

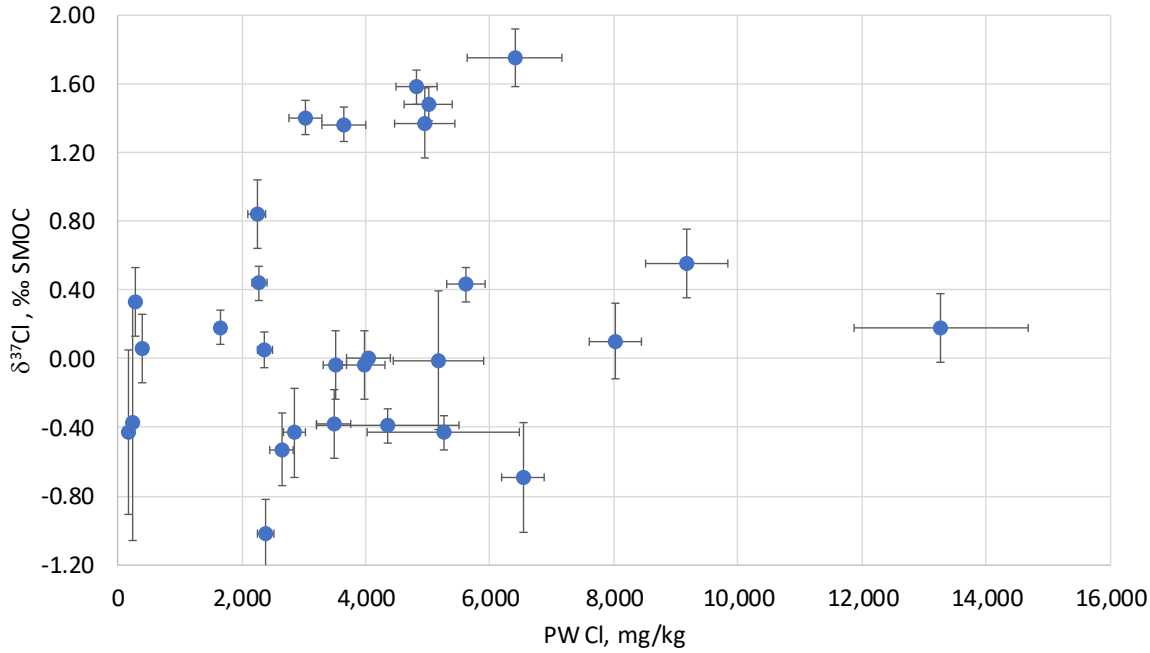


Figure 7-4: Porewater δ^{37}Cl isotope signatures versus porewater Cl concentrations

8.0 RESULTS FROM $\delta^{18}O$ AND $\delta^{2}H$ OF POREWATER OF CORE SAMPLES FROM IG_BH05

Isotope diffusive exchange experiments have been carried out on 30 core samples (60 individual experiments) from borehole IG_BH05. The $\delta^{18}O$ and $\delta^{2}H$ values of porewater are calculated according to Equation 7 (Section 3.3.3), expressed relative to the standard V-SMOW, and are listed in Table 8-1 and graphically shown in Figure 8-1 and Figure 8-2.

The calculated porewater isotope signatures, which are based on the isotope analyses of the test waters, are carefully evaluated for potential artefacts (mainly due to evaporation of test water during the experiment, test water storage and handling). Evaporation of porewater during storage and handling was minimized by careful handling of the core samples (Section 3.2.3). These processes might result in large discrepancies between the gravimetric water content and that calculated from isotope mass balance and errors in the resulting (calculated) porewater isotopic signatures. Such differences were not observed in this study (Section 4.1.2). Some samples showed a higher (>0.5 wt.%) water content determined by isotope diffusive exchange than determined gravimetrically (cf. Section 4.1.2).

According to the quality check of the raw data it was decided to qualify those data as reliable, also if the water contents differ for >0.5 wt%. Evaporation within the experiment was monitored by keeping track of all individual weights before and after the experiments. None of the experiments (except experiment with ICE test water from sample IG_BH05_PW025 (evaporation of 2.4 %)) suffered evaporation > 2 % of the total water mass in the experiments (= mass of porewater determined gravimetrically + mass of test water) during the time of equilibration.

The maximum Cl concentration determined by aqueous extraction prior to the set-up of the isotope diffusive exchange experiments is 20.6 g/kg H_2O, which relates to 0.64 mol $NaCl_{eq}$. However, only sample IG_BH05_AQ029 showed such a high Cl-concentration. The other samples showed a maximum Cl-concentration of 11.9 g/kg H_2O, which relates to 0.37 mol $NaCl_{eq}$. Out-diffusion experiments showed an actual maximum Cl concentration of 13.3 g/kg H_2O, which relates to 0.39 mol $NaCl_{eq}$. Based on the aqueous extraction results, it was decided to adjust the salinity of the test solutions to 0.3 mol NaCl to prevent mass transfer from the test water reservoir to the rocks.

Stable oxygen and hydrogen isotope signatures of porewater extracted from core samples from borehole IG_BH05 vary between -13.49 and -4.39 ‰ for $\delta^{18}O$ and -102.2 and -17.1 ‰ for $\delta^{2}H$ (Table 8-1, Figure 8-1).

Porewaters from borehole IG_BH05 of core samples taken between 171 and 987 mbgs (downhole) plot slightly to the right of the global meteoric water line (GMWL) on the $\delta^{18}O$-$\delta^{2}H$ diagram (Figure 8-2).

The errors, which are calculated by Gaussian error propagation (cf. Appendix C) depend, inter alia, on the porewater to test water mass ratio (R(tw/pw)), which depends on the water content and mass of rocks in the experiments. The correlation of the R(tw/pw) with the porewater $\delta^{18}O$ and $\delta^{2}H$ errors shows that the higher the ratio, the higher the determined error (Figure 8-3). This is the case for the low porosity diabase sample, IG_BH05_AR059 ($WC_{lsox,grav}$ = 0.08 wt.%), for which only ~300 g of rock (compared to > 350 g for other experiments) were available per experiment (Table 4-4).

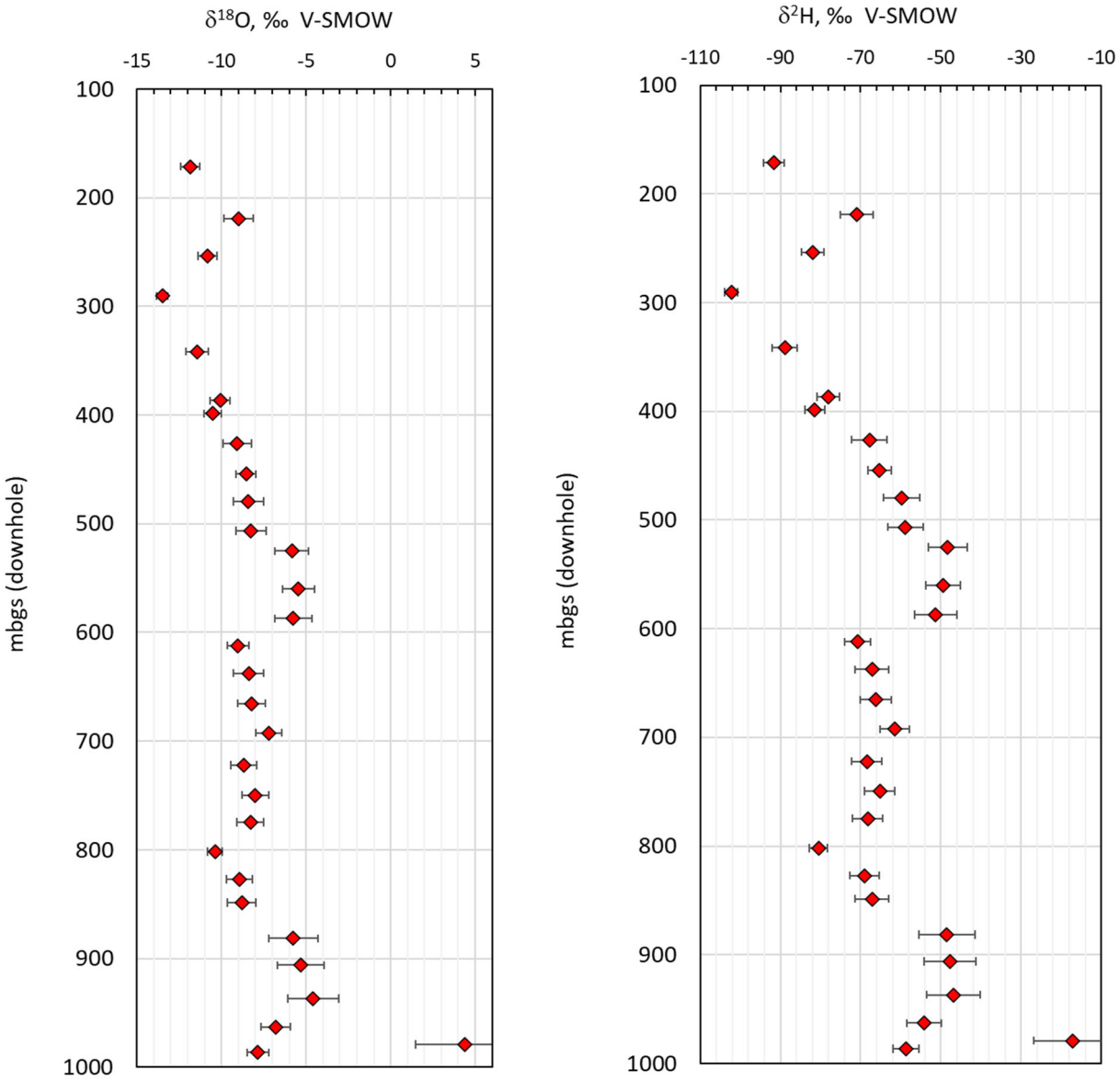


Figure 8-1: $\delta^{18}O$ and $\delta^{2}H$ porewater signatures as function of depth along borehole IG_BH05; errors are calculated by Gaussian error propagation (depth in mbgs (downhole)).

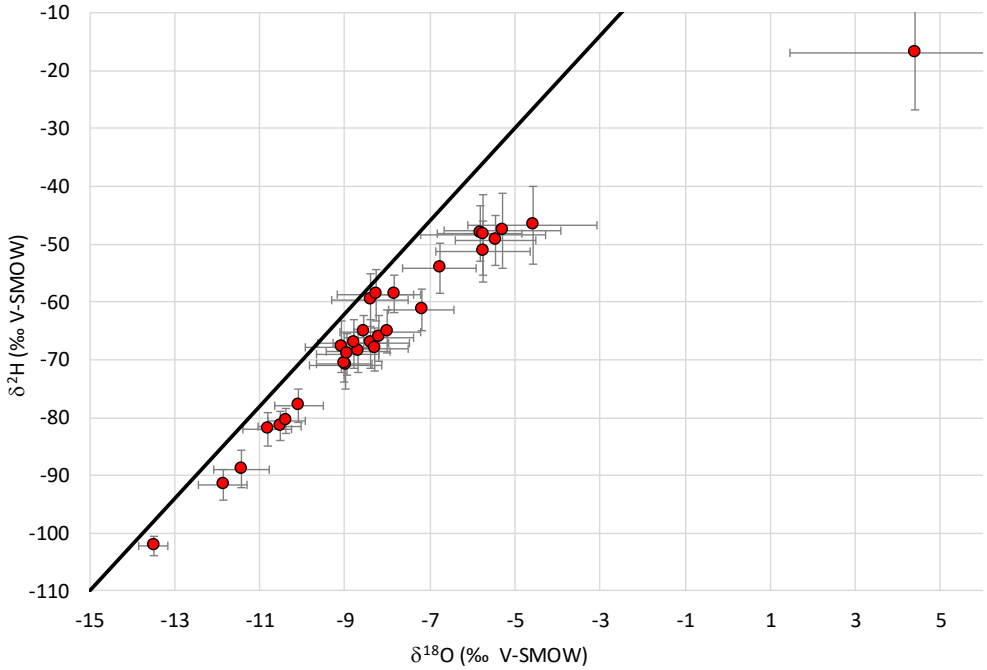


Figure 8-2: $\delta^{18}O$ versus $\delta^{2}H$ values of porewater; the blue line marks the global meteoric water line; the errors of the stable isotope ratios are calculated by Gaussian error propagation.

Table 8-1: $\delta^{18}O$ and $\delta^{2}H$ values of porewater of core samples from borehole IG_BH05; the errors are calculated by Gaussian error propagation; (G / T: granodiorite / tonalite, D: diabase, A: amphibolite).

Sample	Depth mbgs*	Lithology	$\delta^{18}O$ ‰ V-SMOW	Error $\delta^{18}O$ ‰ V-SMOW	$\delta^{2}H$ ‰ V-SMOW	Error $\delta^{2}H$ ‰ V-SMOW
IG_BH05_PW001	171.4	G / T	-11.87	0.56	-91.7	2.6
IG_BH05_PW002	219.1	G / T	-8.98	0.86	-71.0	4.1
IG_BH05_PW003	253.5	G / T	-10.82	0.57	-82.0	2.8
IG_BH05_PW004	290.2	D	-13.49	0.34	-102.2	1.7
IG_BH05_PW005	341.7	G / T	-11.42	0.66	-88.9	3.2
IG_BH05_PW006	386.7	G / T	-10.08	0.57	-78.0	2.9
IG_BH05_PW007	398.5	G / T	-10.53	0.51	-81.4	2.5
IG_BH05_PW008	426.3	G / T	-9.07	0.85	-67.8	4.4
IG_BH05_PW009	454.3	G / T	-8.54	0.58	-65.3	2.9
IG_BH05_PW010	479.4	G / T	-8.41	0.90	-59.8	4.6
IG_BH05_PW011	506.4	G / T	-8.27	0.89	-58.9	4.4
IG_BH05_PW012	525.1	G / T	-5.83	1.00	-48.3	4.8
IG_BH05_PW013	560.1	G / T	-5.45	0.94	-49.4	4.4
IG_BH05_PW014	587.1	G / T	-5.75	1.12	-51.3	5.3
IG_BH05_PW015	612.1	G / T	-9.02	0.65	-70.8	3.1

Sample	Depth mbgs*	Lithology	$\delta^{18}O$ ‰ V-SMOW	Error $\delta^{18}O$ ‰ V-SMOW	$\delta^{2}H$ ‰ V-SMOW	Error $\delta^{2}H$ ‰ V-SMOW
IG_BH05_PW016	637.4	G / T	-8.38	0.89	-67.2	4.2
IG_BH05_PW017	665.3	G / T	-8.21	0.82	-66.3	4.0
IG_BH05_PW018	692.4	G / T	-7.19	0.77	-61.4	3.7
IG_BH05_PW019	722.2	G / T	-8.69	0.77	-68.5	3.7
IG_BH05_PW020	749.6	G / T	-8.00	0.77	-65.2	3.8
IG_BH05_PW021	774.5	G / T	-8.30	0.78	-68.2	3.8
IG_BH05_PW022	801.8	G / T	-10.38	0.44	-80.5	2.2
IG_BH05_PW023	827.2	G / T	-8.94	0.74	-69.1	3.7
IG_BH05_PW024	848.7	G / T	-8.80	0.84	-67.2	4.2
IG_BH05_PW025	881.5	G / T	-5.76	1.46	-48.5	7.0
IG_BH05_PW026	906.1	G / T	-5.30	1.37	-47.7	6.4
IG_BH05_PW027	936.3	G / T	-4.59	1.51	-46.8	6.7
IG_BH05_PW028	962.9	G / T	-6.78	0.87	-54.2	4.3
IG_BH05_AR059	979.0	A	4.39	2.93	-17.1	9.8
IG_BH05_PW029	986.5	G / T	-7.85	0.64	-58.7	3.2

*mbgs (downhole)

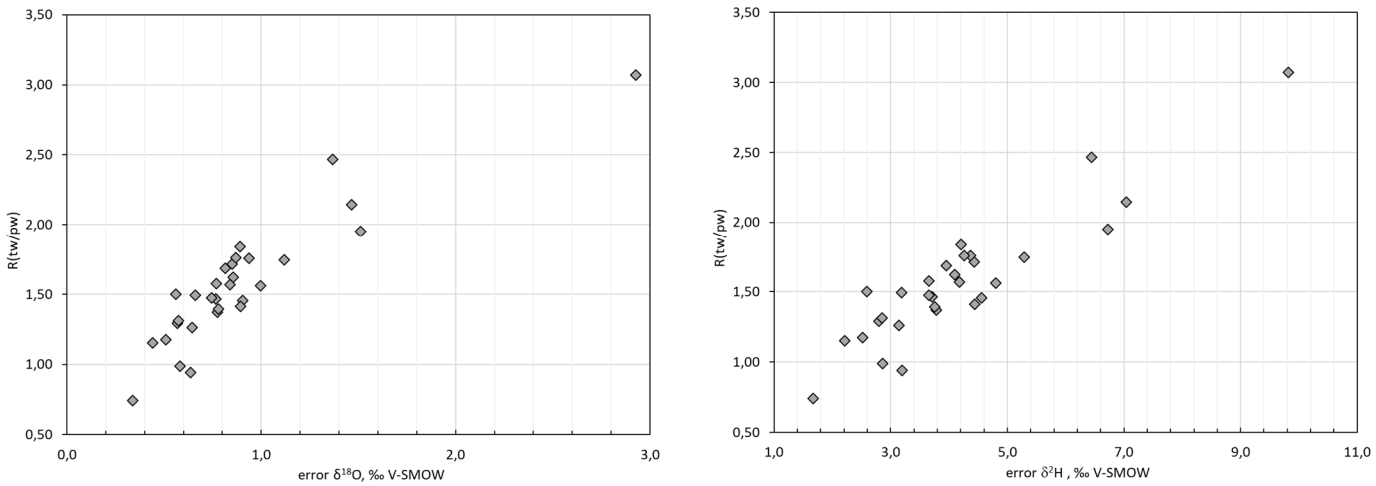


Figure 8-3: Errors of the determination of the $\delta^{18}O$ (left) and $\delta^{2}H$ (right) porewater isotope signatures versus the mass ratio of test water and porewater (R(tw/pw)).

9.0 RESULTS FROM DISSOLVED GASES IN MATRIX POREWATER OF CORE SAMPLES FROM IG_BH05

Gases dissolved in porewater were extracted, chemically and isotopically characterised, and quantified on ten core samples, where five were used for the analyses of noble gases and five for the analyses of non-inert gases. The experiments were conducted using intact core pieces of 20 – 23 cm length with masses between 1,547 and 1,794 g.

A detailed description of the sampling and analytical procedures and the derivation of the porewater gas concentrations is given in Section 2.2 and 3.3. The raw data of the gas-chromatographic and mass-spectrometric measurements, and the corresponding determination of the water contents, are given in Appendix B.

In the experimental set-up, gases dissolved in porewater migrate from the rock to the void volume. The closed system is set under vacuum, allowing an almost complete degassing of the porewater. Based on scoping calculations, using diffusion as the transport mechanism, dissolved hydrocarbon gases and noble gases are estimated to be in equilibrium in the system porewater – void volume in time periods between 45 days (helium) and 230 days (butane, Figure 9-1). The model calculations were performed using a code by T. Gimmi (RWI, University of Bern) with an analytical solution for radial diffusion out of the cylinder into a defined reservoir (Crank 1975). These approaches take only diffusive transport, driven by the concentration gradient between pore water and void volume, into account and, therefore, describe a maximal equilibration time. A faster degassing due to possible suction effects is not taken into account in these scoping calculations.

The core samples were allowed to equilibrate with the surrounding low-pressure atmosphere in the cylinders for 415 to 441 days (DG samples) and for 734 to 759 days (NG samples), respectively.

After the complete diffusive equilibration, the gas present in the void space of the cylinder is in equilibrium with the gas dissolved in matrix pore water. The efficiency of the diffusive release of gases from matrix pore water is given by the ratio of the connected pore volume, to the void space in the cylinder, which varies between 0.0082 and 0.0160 for the experiments (Appendix B). The proportion of the water volume to the sum of pore volume and void volume is < 2 %. The remaining volume of gas in the porewater is thus << 2 % of the total gas volume. Hence, the release of gases from the rock pore space to the void volume of the sampling cell can be considered as quantitative.

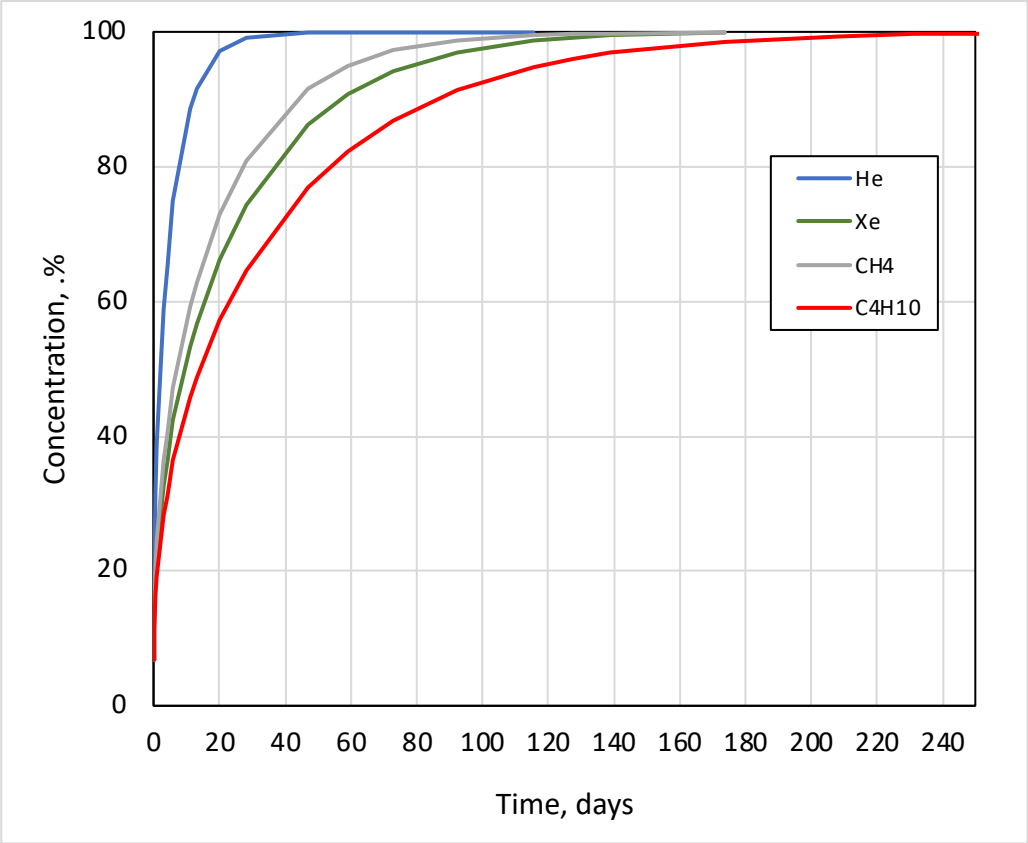


Figure 9-1: Diffusive equilibration of gases dissolved in porewater. The model calculations show that the equilibration time in days is sufficient to achieve equilibrium with respect to the analysed gases. The diffusive exchange in the experiments of the non-inert gases and noble gases with the lowest (Butane, Xenon) and the highest diffusion coefficient in free water (Methane, Helium) were modelled ($D_{(He)}$ = 7.2*10^{-9} m^2/s, $D_{(Xe)}$ = 1.5*10^{-9} m^2/s, $D_{(CH_4)}$ = 1.9*10^{-9} m^2/s, $D_{(C_4H_{10})}$ = 9.6*10^{-10} m^2/s at 20°C, Jähne et al. 1987). The conversion of these diffusion coefficients in free water to pore diffusion coefficients of the single gases in the rock samples was done according to Equation 14 using an average geometry factor of 0.04 as estimated for chloride (cf. Section 6.2).

As for dissolved chemical compounds, the concentration of a dissolved gas in the porewater might be subjected to contamination during drilling and sampling. Such possible artefacts need to be explored before the interpretation of the gas data.

In situ gas concentrations of matrix porewater can be changed by the penetration of drilling fluid in the core triggered by stress release and by the drilling process (drilling disturbed zone). The evaluation of the influence of these disturbing processes done in different studies working with crystalline rocks show only a minor influence on the porewater characteristics (Eichinger et al., 2013, Meier et al., 2015, Eichinger & Iannotta, 2022).

For gases dissolved in pore water, exchange with the surrounding drilling fluid, and/or atmospheric air, might occur in the time period between the release of the core samples from the bedrock and the set-up of the experiments (closing of the gas tight cylinders). The time periods between drilling and recovery of the cores and experimental set-up were below 15 minutes. Modelling of the diffusive loss of He and CH_4 from the cores during the sampling done by Eichinger et al. (2013) show that within two hours only gas dissolved in matrix porewater

that occurs in the rim (~2.5 mm) of the cores is affected. It thus appears that the diffusive loss of gases during sampling is within the error of the gas analyses and can be neglected.

9.1 Non-Inert Gases

Non-inert gases were extracted and evaluated from five core samples taken between 431 and 879 mbgs (downhole).

9.1.1 Concentrations of Non-Inert Gases Dissolved in Porewater

The raw data of the non-inert gas analyses are given in Appendix B and the porewater gas concentrations corrected for air contamination are given in Table 9-1.

The final pressures of the cylinders after equilibration varied between 31 and 35 mbars at 21 °C. Due to the fact that the cores are naturally saturated, the partial pressure of water vapour was calculated according to Equation 10. The subtraction of the water vapour partial pressure, and the correlation to standard conditions, yields total gas pressures between 5.5 and 8.8 mbar STP, corresponding to 1.3 to 1.9 NmL of gas extracted from the porewater.

Oxygen was used as tracer for air contamination in the cylinders, based on the assumption that in situ porewater is oxygen free. The proportion of air contamination was calculated according to Equation 9. Oxygen concentrations vary between 0.6 and 1.4 Vol.%, corresponding to an air contamination between 2.9 and 6.7 % of the total gas volume. The concentrations of the gas species were corrected using the general air composition (Appendix B). These contaminations mainly concern the normal gases, N_2 and CO_2. The calculations show that, for N_2, 94 – 98 % of the detected nitrogen comes from the degassed porewater. Concentrations of hydrocarbons in air are low and air contamination has less effect on such concentrations.

The extracted and corrected volumes of the individual gas species are converted to milliliters gas per liter porewater STP (NmL/L_{PW}, 0°C = 273 K, 1013 hPa) using the volume of porewater according to Equation 11.

9.1.1.1 Porewater Nitrogen-, Hydrogen- and Carbon Dioxide Concentrations

Nitrogen and hydrogen are the most abundant gas species dissolved in porewater of core samples taken between 431 and 879 mbgs downhole from borehole IG_BH05. The concentrations of nitrogen (N_2) vary between 321 NmL/L_{PW} and 495 NmL/L_{PW} and show a general increase with depth (Table 9-1,Figure 9-2). Hydrogen (H_2) concentrations vary between 31 and 64 NmL/L_{PW} and vary along the depth profile (Table 9-1, Figure 9-2). Carbon dioxide (CO_2) could only be detected with concentrations of 0.79 NmL/L_{PW} and 0.09 NmL/L_{PW} in the samples taken at 431 and 536 mbgs downhole, respectively (Table 9-1. In the samples below, CO_2 was below detection.

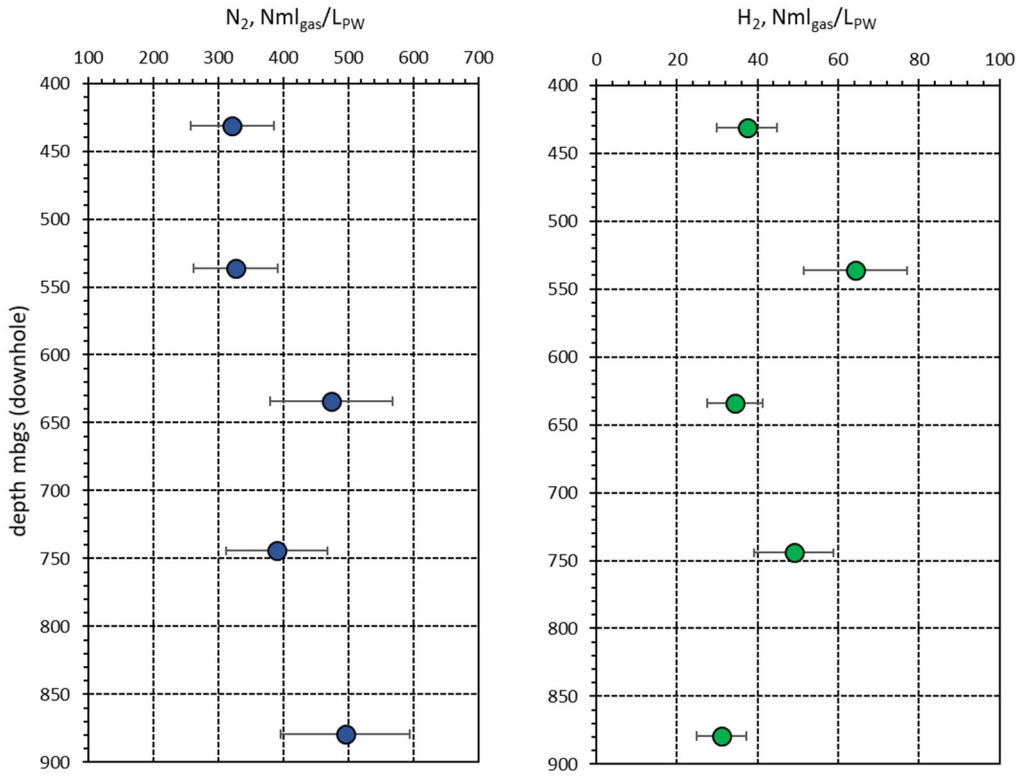


Figure 9-2: Porewater nitrogen (N_2, left) and hydrogen (H_2, right) concentrations as function of depth along borehole IG_BH05; errors are ± 20% (depth in mbgs (downhole)).

9.1.1.2 Porewater Hydrocarbon Gas Concentrations

Methane concentrations dissolved in porewater of cores taken between 431 and 879 mbgs (downhole) from IG_BH05 vary between 0.26 NmL/L_{PW} and 2.43 NmL/L_{PW} and appear to show a decreasing trend with increasing depth, with the exception of sample IG_BH05_DG004, taken at 744 mbgs (downhole) (Figure 9-3,Table 9-1).

In all samples, higher saturated hydrocarbons, up to pentane, could be detected. The concentrations of the individual hydrocarbon species vary between < 0.001 NmL/L_{PW} and 0.07 NmL/L_{PW}, where ethane (C_2H_6) is the most abundant species in almost all samples (Table 9-1). The sum of the detected higher hydrocarbons varies between 0.028 NmL/L_{PW} and 0.127 NmL/L_{PW}. Considering the depth profile, the sum of the gaseous higher hydrocarbons dissolved in porewater is constant (0.053 to 0.055 NmL/L_{PW}) in the zone between 431 and 634 mbgs (downhole) and varies in the deeper samples, 0.127 NmL/L_{PW} (744 mbgs (downhole)) and 0.028 NmL/L_{PW} (879 mbgs (downhole), Table 9-1,Figure 9-3).

In all five samples, unsaturated hydrocarbons up to butene, with concentrations between <0.001 NmL/L_{PW} and 0.008 NmL/L_{PW}, were detected (Table 9-1). The sum of gaseous unsaturated hydrocarbons dissolved in porewater varies between 0.008 NmL/L_{PW} and 0.020 NmL/L_{PW}. The unsaturated higher hydrocarbon concentrations of porewater for core samples taken at 431 and 536 mbgs (downhole) are constant (0.0133 NmL/L_{PW}) and vary in the following depth sections between 0.008 NmL/L_{PW} and 0.020 NmL/L_{PW} (Figure 9-3,Table 9-1).

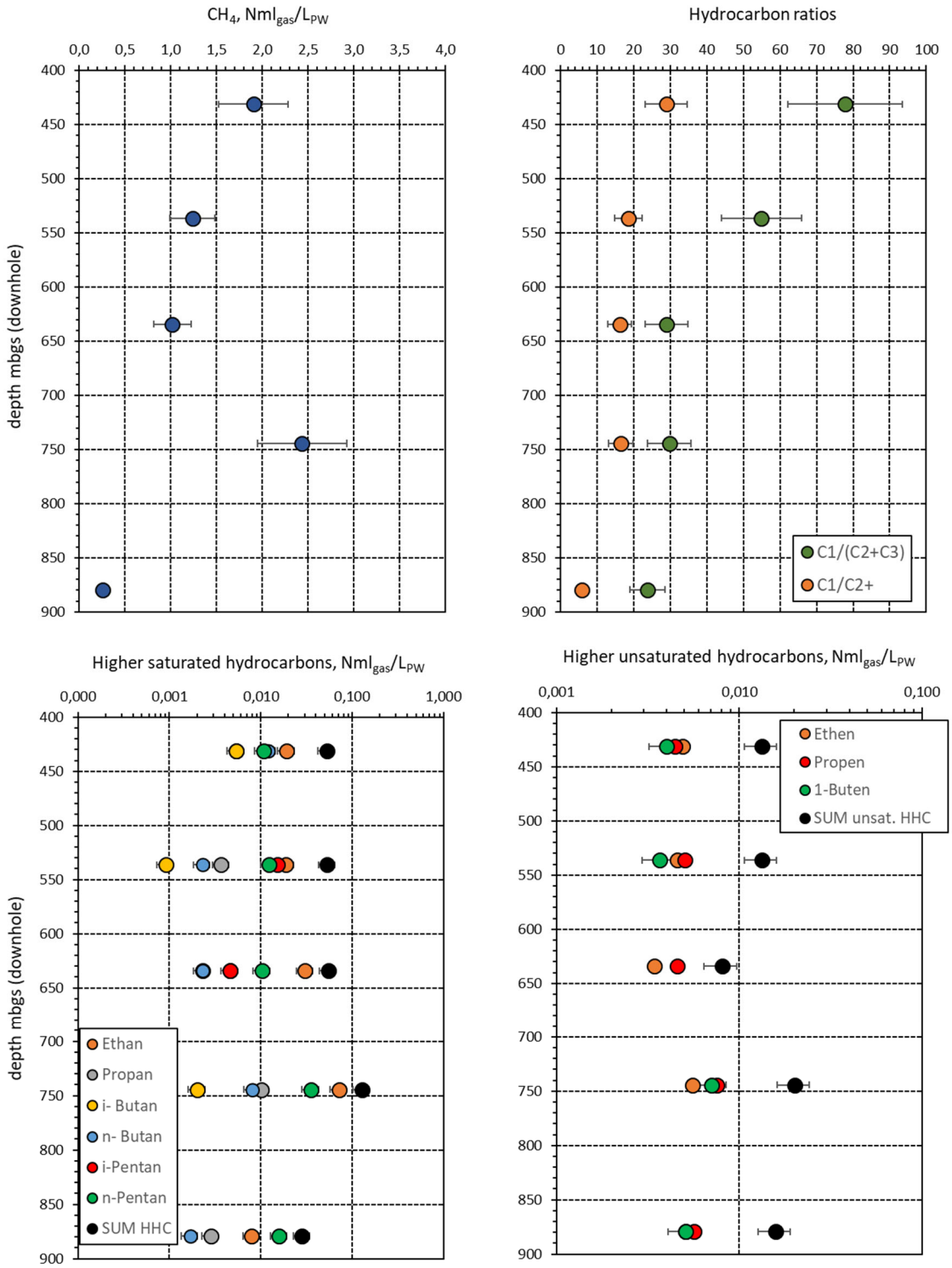


Figure 9-3: Porewater methane (CH_4, top, left), saturated (C_2-C_5, bottom left) and unsaturated (C_2-C_4, bottom right) higher hydrocarbon concentrations and hydrocarbon ratios (top, right) as function of depth along borehole IG_BH05; errors are ± 20%.

The volume ratios of methane over ethane plus propane ($C_1/(C_2+C_3)$) of hydrocarbons dissolved in porewater vary between 24 and 79 and show a decreasing trend between 431 and 634 mbgs (downhole). In the lower zone, between 634 and 879 mbgs (downhole), the $C_1/(C_2+C_3)$ ratios are almost constant between 24 and 30 (Table 9-1, Figure 9-3). The volume ratios of methane over the sum of all gaseous saturated hydrocarbons (C_1/C_{2+}) vary between 6 and 29 and show the same trends with depth as observed for the $C_1/(C_2+C_3)$ ratios.

Table 9-1: Concentrations of gases dissolved in porewater of core samples from borehole IG_BH05; the volumes in NmL/L_{PW} are given normalised to standard conditions (273 K = 0°C, 1 bar); the errors are estimated to be ±20%.

Sample		IG_BH05_DG001	IG_BH05_DG002	IG_BH05_DG003	IG_BH05_DG04	IG_BH05_DG05
Depth a.b.	mbgs*	431	536	634	744	879
Water Content**	wt.%	0.19	0.19	0.18	0.17	0.13
Mass of PW	G	3.11	3.31	3.24	2.78	2.32
Hydrocarbons						
Methane (CH_4)	NmL/L_{PW}	1.90	1.24	1.02	2.43	0.26
Ethane (C_2H_6)	NmL/L_{PW}	0.019	0.019	0.030	0.072	0.008
Propane (C_3H_8)	NmL/L_{PW}	0.005	0.004	0.005	0.010	0.003
i- Butane (i-C_4H_{10})	NmL/L_{PW}	0.005	0.001	0.002	0.002	<0.001
n- Butane (n-C_4H_{10})	NmL/L_{PW}	0.012	0.002	0.002	0.008	0.002
i-Pentane (i-C_5H_{12})	NmL/L_{PW}	<0.001	0.015	0.005	<0.001	<0.001
n-Pentane (n-C_5H_{12})	NmL/L_{PW}	0.011	0.012	0.010	0.035	0.016
Ethene (C_2H_4)	NmL/L_{PW}	0.005	0.005	0.003	0.006	0.005
Propene (C_3H_6)	NmL/L_{PW}	0.004	0.005	0.005	0.008	0.006
1-Butene (1-C_4H_8)	NmL/L_{PW}	0.004	0.004	<0.001	0.007	0.005
Normal gases	NmL/L_{PW}					
Nitrogen (N_2)	NmL/L_{PW}	321	327	474	390	495
Carbon dioxide (CO_2)	NmL/L_{PW}	0.79	0.09	<0.10	<0.10	<0.10
Hydrogen (H_2)	NmL/L_{PW}	37	64	35	49	31
Ratios						
$C_1/(C_2+C_3)$	ml/ml	78	55	29	30	24
C_1/C_{2+}	ml/ml	29	19	16	17	6

* mbgs (downhole)

** mass of porewater determined on gas samples from weight measurements before out-gassing

9.1.2 Stable Isotope Signatures of Non-Inert Gases Dissolved in Porewater

Despite of the low hydrocarbon concentrations dissolved and extracted from porewater of cores taken between 431 and 879 mbgs (downhole) stable carbon isotope signatures could be analysed for the gaseous hydrocarbons (C_1-C_4) for all samples. Hydrogen isotopes of methane could be analysed on only three of the five DG samples due to low concentrations. To warrant a full parameter-set, the stable hydrogen isotopes of methane, and additionally the carbon isotopes of the gaseous hydrocarbons, were analysed on the NG samples after the analyses of noble gases.

Stable nitrogen isotopes ($\delta^{15}N\text{-}N_2$) of nitrogen dissolved in porewater of core samples from IG_BH05 vary between -0.5 ‰ and -0.3 ‰-Air and are almost similar within the analytical error of ± 0.1 ‰ (Table 9-2, Figure 9-4).

Stable isotope signatures of methane dissolved in porewater vary between -44.6 ‰ and – 33.6 ‰ V-PDB for $\delta^{13}C$ and between -334 ‰ and -282 ‰ V-SMOW for $\delta^{2}H$ and show no general trend with depth (Table 9-2, Figure 9-4).

Stable carbon isotope signatures ($\delta^{13}C\text{-}C_2H_6$, $\text{-}C_3H_8$,$\text{-i-}C_4H_{10}$, $\text{n-}C_4H_{10}$) of higher hydrocarbons dissolved in porewater vary between –36.5 ‰ and -16.2 ‰ V-PDB and show no general trends with depth (Table 9-2, Figure 9-5

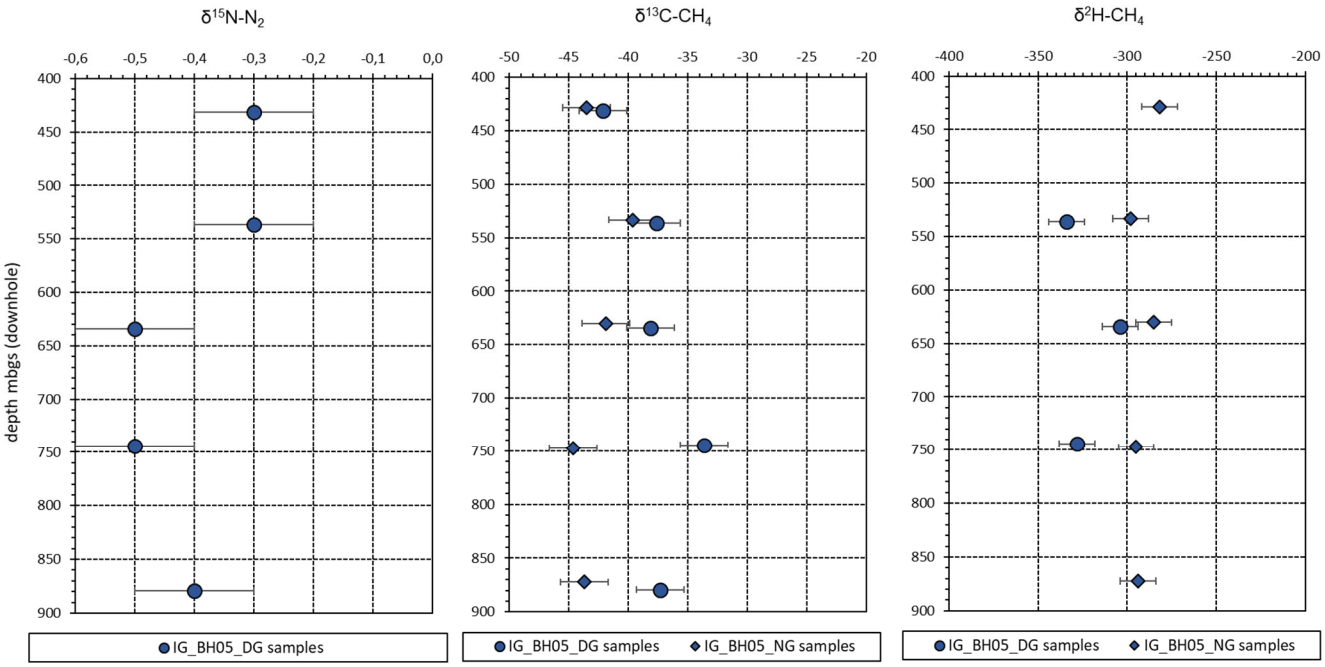


Figure 9-4: Stable isotope signatures of nitrogen ($\delta^{15}N\text{-}N_2$, left) and methane ($\delta^{13}C\text{-}CH_4$, center, $\delta^{2}H\text{-}CH_4$, right) dissolved in porewater as function of depth along borehole IG_BH05; errors are ± 0.1 ‰ for $\delta^{15}N\text{-}N_2$, ± 2.0 ‰ for $\delta^{13}C\text{-}CH_4$ and ± 10.0 ‰ for $\delta^{2}H\text{-}CH_4$.

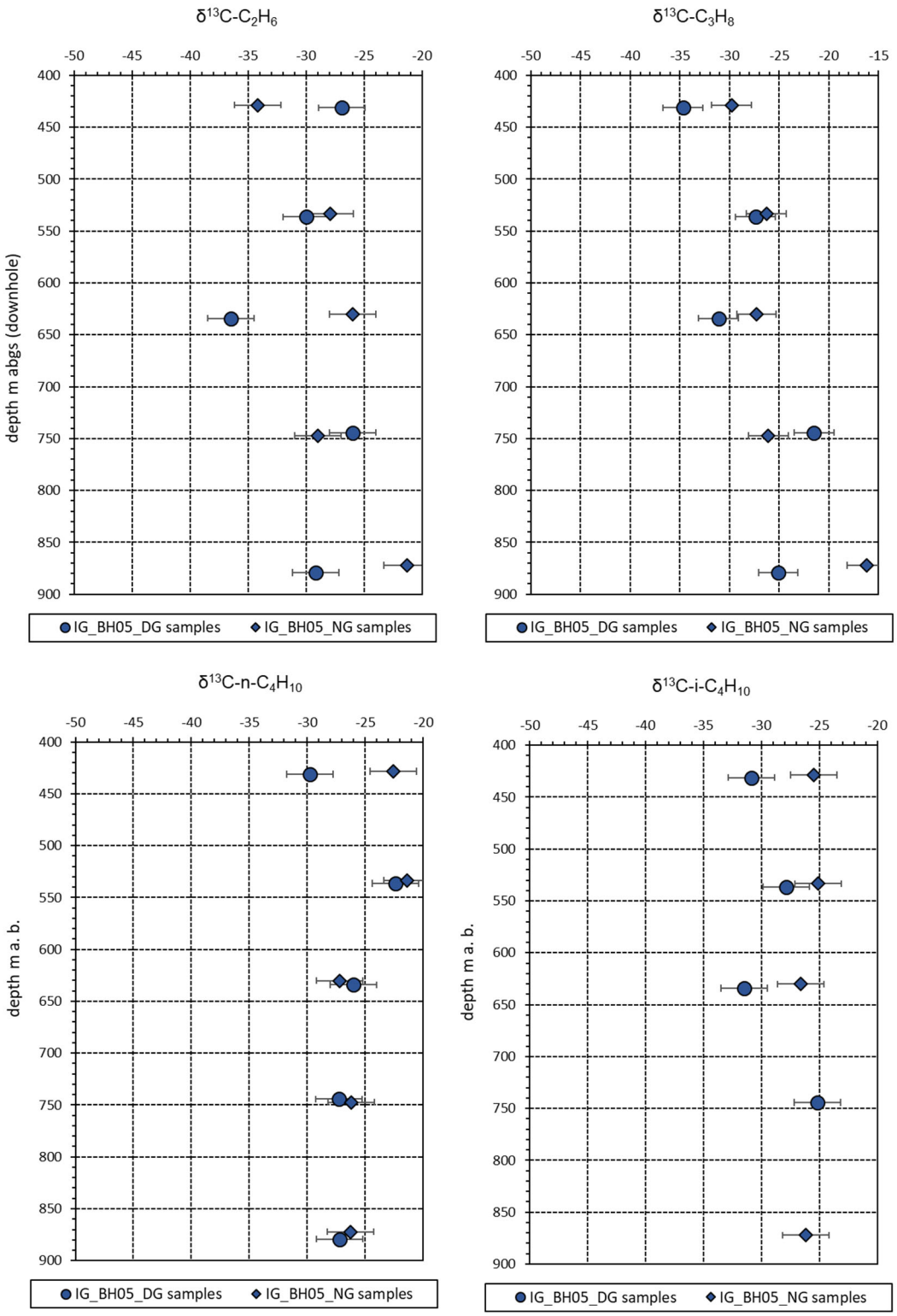


Figure 9-5: Stable carbon isotope signatures of higher hydrocarbons dissolved in porewater as function of depth along borehole IG_BH05; errors are ± 2.0‰.

Stable isotope signatures of hydrocarbons give valuable information about their genesis and origin in combination with their composition and their volume ratios. Therefore, the hydrocarbon data from the porewaters of core samples from borehole IG_BH05 are correlated to end-member signatures and ratios according to the recent literature. The correlation of $\delta^{13}C$- and $\delta^{2}H$ isotope signatures of methane dissolved in porewater from borehole IG_BH05 indicates, according to Whiticar (2020), for all samples taken between 428 and 872 mbgs (downhole) a hydrothermal (crystalline) origin (Figure 9-6).

The $\delta^{13}C$ pattern of the dissolved hydrocarbons of porewater from borehole IG_BH05 show almost homogeneous patterns, with increasing carbon isotope signatures with increasing carbon numbers (Figure 9-7, Table 9-2). They show a similar pattern to hydrocarbons formed under thermogenic conditions (Sherwood Lollar et al. 1994), but with more enriched isotopic signatures. The enrichment in ^{13}C in almost all hydrocarbons compared to the literature data agrees with the $\delta^{13}C$-, and $\delta^{2}H$-CH_4 isotopic signatures, which are more enriched in ^{2}H and ^{13}C compared to methane from thermogenic organic sources (Figure 9-6).

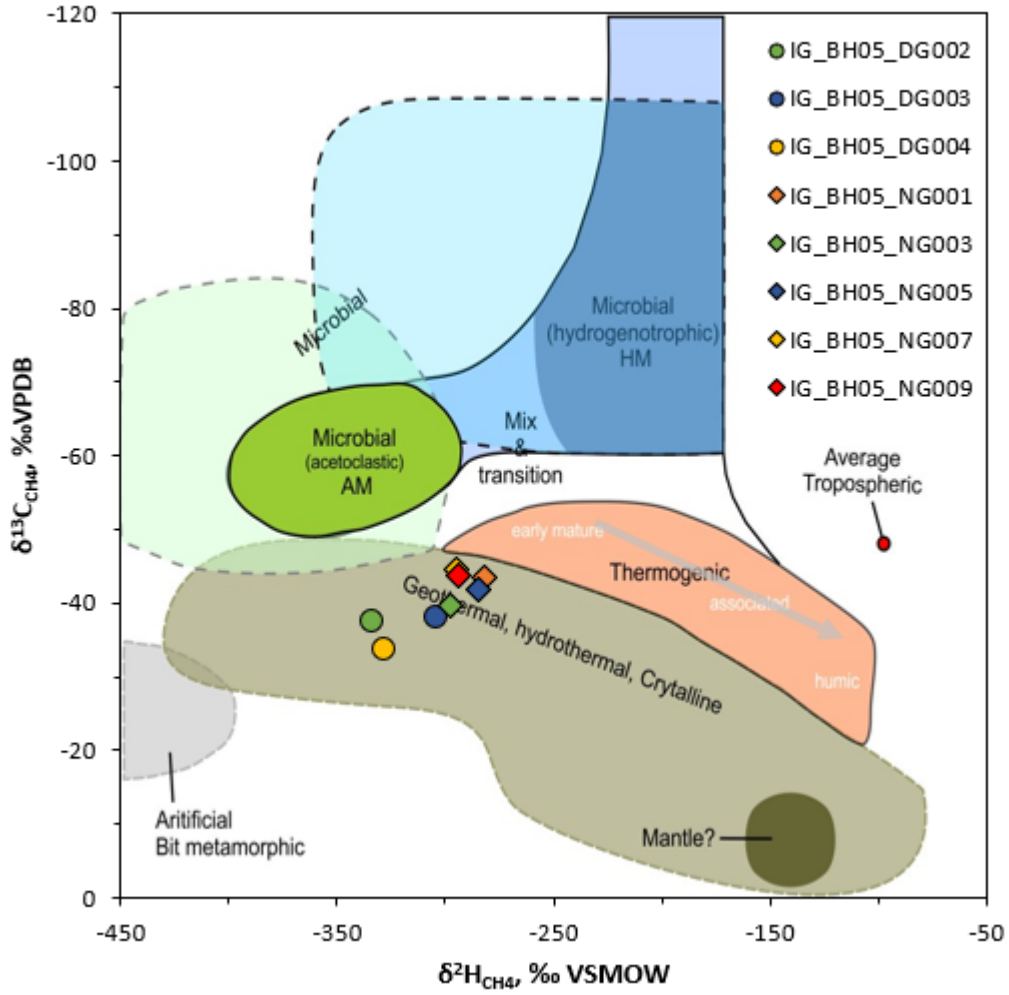


Figure 9-6: Isotopic classification of methane dissolved in porewater from core samples from borehole IG_BH05. The porewater results are compared to end-member signatures according to Whiticar (2020).

In the δ^{13}C-CH_4 versus C_1/C_2+C_3 diagram, the porewater hydrocarbon data plot in the upper area of the thermogenic field according to Kietäväinen et al. (2017), indicating a thermogenic origin of the dissolved hydrocarbons in the porewater of cores from borehole IG_BH05 (Figure 9-8).

In summary, a coherent pattern of porewater methane and higher hydrocarbon concentrations, hydrocarbon ratios and stable isotopes is obtained, suggesting a hydrothermal crystalline origin of the dissolved hydrocarbons over the entire depth profile.

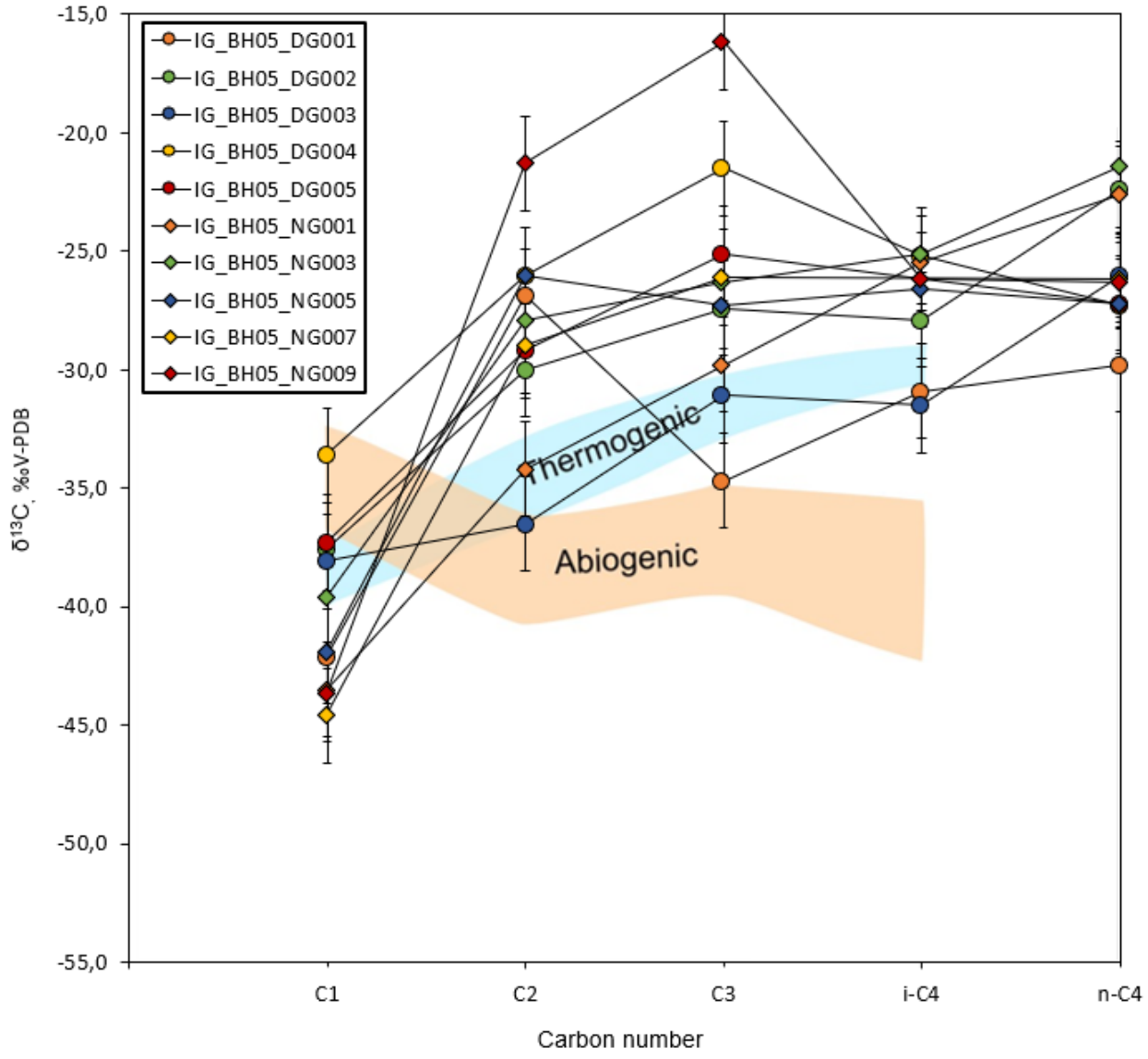


Figure 9-7: Carbon isotope signature patterns of hydrocarbons dissolved in porewater of cores from borehole IG_BH05 versus carbon numbers compared to patters of hydrocarbons produced by abiogenic processes (Sherwood Lollar et al. 2002) and thermogenic processes (Sherwood Lollar et al. 1994).

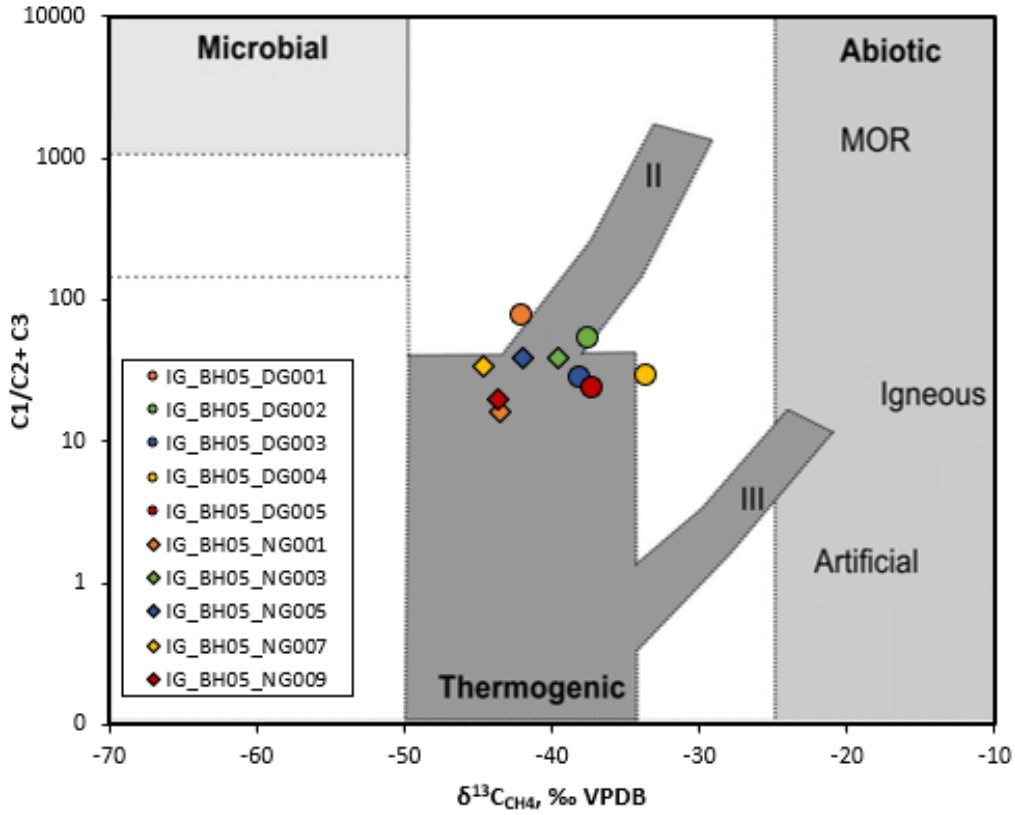


Figure 9-8: Carbon isotope signatures of methane versus the hydrocarbon ratio of methane over ethane plus propane (C1/C2+C3) dissolved in porewater of cores from borehole IG_BH05 compared to end-member fields according to Faber (1987), Whiticar (1999) and Kietäväinen et al. (2017) and references therein.

Table 9-2: Stable isotope signatures of gases dissolved in porewater of core samples from borehole IG_BH05.

Sample Depth	mbgs (downhole)	IG_BH05_ DG001 431.2	IG_BH05_ DG002 536.4	IG_BH05_ DG003 634.2	IG_BH05_ DG004 744.3	IG_BH05_ DG005 879.3
$\delta^{15}N\text{-}N_2$	‰-Air	-0.3	-0.3	-0.5	-0.5	-0.4
$\delta^{13}C\text{-}CH_4$	‰-V-PDB	-42.1	-37.6	-38.1	-33.6	-37.3
$\delta^{2}H\text{-}CH_4$	‰ V-SMOW	n.d.	-334	-304	-328	n.d.
$\delta^{13}C\text{-}C_2H_6$	‰-V-PDB	-26.9	-30	-36.5	-26	-29.2
$\delta^{13}C\text{-}C_3H_8$	‰-V-PDB	-34.7	-27.4	-31.1	-21.5	-25.1
$\delta^{13}C\text{-i-}C_4H_{10}$	‰-V-PDB	-30.9	-27.9	-31.5	-25.2	n.d.
$\delta^{13}C\text{-n-}C_4H_{10}$	‰-V-PDB	-29.8	-22.4	-26	-27.3	-27.2

* n.d. = not determined due to low concentrations.

Table 9-2: continued

Sample		IG_BH05_ NG001	IG_BH05_ NG003	IG_BH05_ NG005	IG_BH05_ NG007	IG_BH05_ NG009
Depth	mbgs (downhole)	428.5	533.3	630.2	747.3	872.2
$\delta^{15}N\text{-}N_2$	‰-Air	n.a.	n.a.	n.a.	n.a.	n.a.
$\delta^{13}C\text{-}CH_4$	‰-V-PDB	-43.5	-39.6	-41.9	-44.6	-43.7
$\delta^{2}H\text{-}CH_4$	‰ V-SMOW	-282	-298	-285	-295	-294
$\delta^{13}C\text{-}C_2H_6$	‰-V-PDB	-34.2	-27.9	-26	-29	-21.3
$\delta^{13}C\text{-}C_3H_8$	‰-V-PDB	-29.8	-26.3	-27.3	-26.1	-16.2
$\delta^{13}C\text{-i-}C_4H_{10}$	‰-V-PDB	-25.5	-25.1	-26.6	n.d.	-26.2
$\delta^{13}C\text{-n-}C_4H_{10}$	‰-V-PDB	-22.6	-21.4	-27.2	-26.2	-26.3

n.a. = not analysed, N_2 was used as flushing gas

9.2 Noble Gases

Noble gases, like helium and argon, are continuously produced by radioactive decay of different elements in rock forming minerals (e.g., Porcelli et al. 2002). Noble gases are differentiated by either radiogenic or nucleogenic origin. Noble gas isotopes, which are directly produced by radioactive decay, such as ^{4}He and ^{40}Ar, are described as radiogenic. Those produced by nuclear reactions of α particles or by thermogenic neutrons, such as ^{3}He and ^{36}Ar, are described as nucleogenic noble gas isotopes. Helium produced in minerals is readily released to the surrounding porewater due to the strong activation energy during the production process (Lehmann et al. 2003; Tolstikhin et al. 2005). In contrast, in situ produced argon tends to remain in the minerals (K-Ar dating, e.g., Ballentine and Burnard 2002, Kelley 2002).

Once released to the porewater, noble gases are transported by diffusion from the rock matrix into adjacent fracture groundwater. The chemically inert character of noble gases as trace dissolved gases, and their continuous in situ production, make them a valuable tracer to investigate solute transport processes. Transport processes can be evaluated by comparing 1) the calculated noble gas production rates, 2) the measured noble gas concentrations in the rock, porewater and groundwater, and 3) the possible external input of noble gases into the system (Ballentine et al. 2002, Ozima & Podosek 2005).

Radiogenic and nucleogenic noble gases dissolved in matrix porewater and fracture groundwater in subsurface bedrock systems can either have a local source (i.e. in situ production in the rock matrix), or can be influenced by the ingress of noble gases produced in external sources (i.e. the mantle or the atmosphere) (Porcelli & Ballentine 2002). The different provenances of noble gases dissolved in porewater and fracture groundwater can be distinguished by comparing noble gas isotope ratios such as $^{3}He/^{4}He$ and $^{40}Ar/^{36}Ar$.

Noble gases (He, Ar) and noble gas isotopes ($^{3,4}He$, $^{20,22}Ne$, $^{36,40}Ar$, ^{84}Kr, ^{132}Xe) were extracted and analysed on five samples taken between 428 and 872 mbgs (downhole) from borehole IG_BH05.

The final pressures of the cylinders, after equilibration, varied between 28.9 and 32.4 mbars at temperatures of 22.5 to 23.2 °C. Due to the fact that the cores are naturally saturated, the partial pressure of water vapour was calculated according to Equation 10. The subtraction of the water vapour partial pressure, and the correlation to standard conditions, yields total gas pressures between 0.9 and 4.7 mbar STP, corresponding to 0.2 to 0.9 NmL of gas extracted from the porewater.

The individual noble gas concentrations were corrected for air contamination by the measurements of the ^{20,22}Ne concentrations. The calculations were carried out according to Equation 13. A correction for the ^{20,22}Ne concentration is feasible, because the geogenic production rate is very low in the crust ($1.5*10^{-21}$ ccSTP/(g_{rock}*a) for ^{20}Ne and $5.2*10^{-22}$ ccSTP/(g_{rock}*a) for ^{22}Ne (Leya and Wieler 1999)).

The extracted ^{20,22}Ne concentrations vary between $7.76*10^{-9}$ and $8.89*10^{-7}$ NmL, which corresponds to an air contamination between 0.38 and 4.2 % of the total gas volume. The concentrations of the gas species were corrected using the general air composition (Appendix B).

The extracted and corrected volumes of the individual gas species are converted to milliliters gas per liter porewater STP (NmL/L_{PW}, 0°C = 273 K, 1013 hPa) using the volume of porewater according to Equation 11.

The concentrations of total helium and total argon dissolved in porewater vary between 0.13 and 2.42 NmL/L_{PW} for He and between 0.19 and 3.54 NmL/L_{PW} for Ar (Table 9-3). The porewater helium concentrations increase with increasing depth from 0.38 NmL/L_{PW} at 428 m to 2.42 NmL/L_{PW} at 630 mbgs (downhole), followed by a sharp decrease to 0.13 NmL/L_{PW} at 747 m and a subsequent increase to 0.88 NmL/L_{PW} at 872 mbsg (downhole) (Figure 9-9). Total argon concentrations show the same trend with an increase from 1.04 NmL/L_{PW} at 428 m to 3.54 NmL/L_{PW} at 630 mbgs (downhole), followed by a decrease to 0.19 NmL/L_{PW} at 747 m and an increase to 2.015 NmL/L_{PW} at 872 mbgs (downhole) (Figure 9-9).

^{84}Kr and ^{132}Xe concentrations were also determined and vary between 0.00005 and 0.00088 NmL/L_{PW} for ^{84}Kr and between 0.00001 and 0.00013 NmL/L_{PW} for ^{132}Xe (Table 9-3).

Porewater ^{40}Ar/^{36}Ar ratios vary between 331 and 372 along the depth profile of borehole IG_BH05 (428 – 872 mbgs (downhole)) and are significantly higher than that of air (296), indicating a radiogenic accumulation over time (Table 9-3). The ^{40}Ar/^{36}Ar increases from 331 at 428 m to 363 at 533 m, remains constant between 363 and 372 to a depth of 747 mbgs (downhole), and decreases to 342 at 872 mbgs (downhole) (Figure 9-10).

Porewater ^{3}He/^{4}He ratios range between $1.02*10^{-8}$ and $3.25*10^{-8}$ (Table 9-3). In the bedrock section between 428 and 747 mbgs (downhole) the values are almost constant, ranging between $2.40*10^{-8}$ and $3.25*10^{-8}$. The lowest sample, taken at 872 m, shows a lower ^{3}He/^{4}He ratio of $1.02*10^{-8}$ (Figure 9-10).

The comparison with end-member ^{3}He/^{4}He ratios suggests that the ^{3}He/^{4}He dissolved in porewater of core samples taken along IG_BH05 are low compared to air and mantle derived helium due to accumulation of radiogenic ^{4}He (Figure 9-10, Figure 9-11). They are in the range of crustal derived helium (Figure 9-11, Osenbrück, 1996). Proportions of mantle derived helium are not indicated.

Table 9-3: Noble gas concentrations and ratios dissolved in porewater of cores taken from borehole IG_BH05.

Sample Depth	mbgs (downhole)	IG_BH05_ NG001 428.5	IG_BH05_ NG003 533.3	IG_BH05_ NG005 630.2	IG_BH05_ NG007 747.3	IG_BH05_ NG009 872.2
Water Content	wt. %	0.18	0.18	0.09	0.22	0.14
Mass of PW	G	2.86	2.87	1.60	3.55	2.44
Helium	NmL/L_{PW}	0.38	0.77	2.42	0.13	0.88
Argon	NmL/L_{PW}	1.04	1.49	3.54	0.19	2.01

Sample Depth	mbgs (downhole)	IG_BH05_ NG001 428.5	IG_BH05_ NG003 533.3	IG_BH05_ NG005 630.2	IG_BH05_ NG007 747.3	IG_BH05_ NG009 872.2
Krypton-84	NmL/L_{PW}	0.00030	0.00041	0.00088	0.00005	0.00054
Xenon-132	NmL/L_{PW}	0.00005	0.00007	0.00013	0.00001	0.00009
$^{40}Ar/^{36}Ar$		331	363	372	370	342
$^{3}He/^{4}He$		3.22E-08	2.53E-08	3.25E-08	2.40E-08	1.02E-08

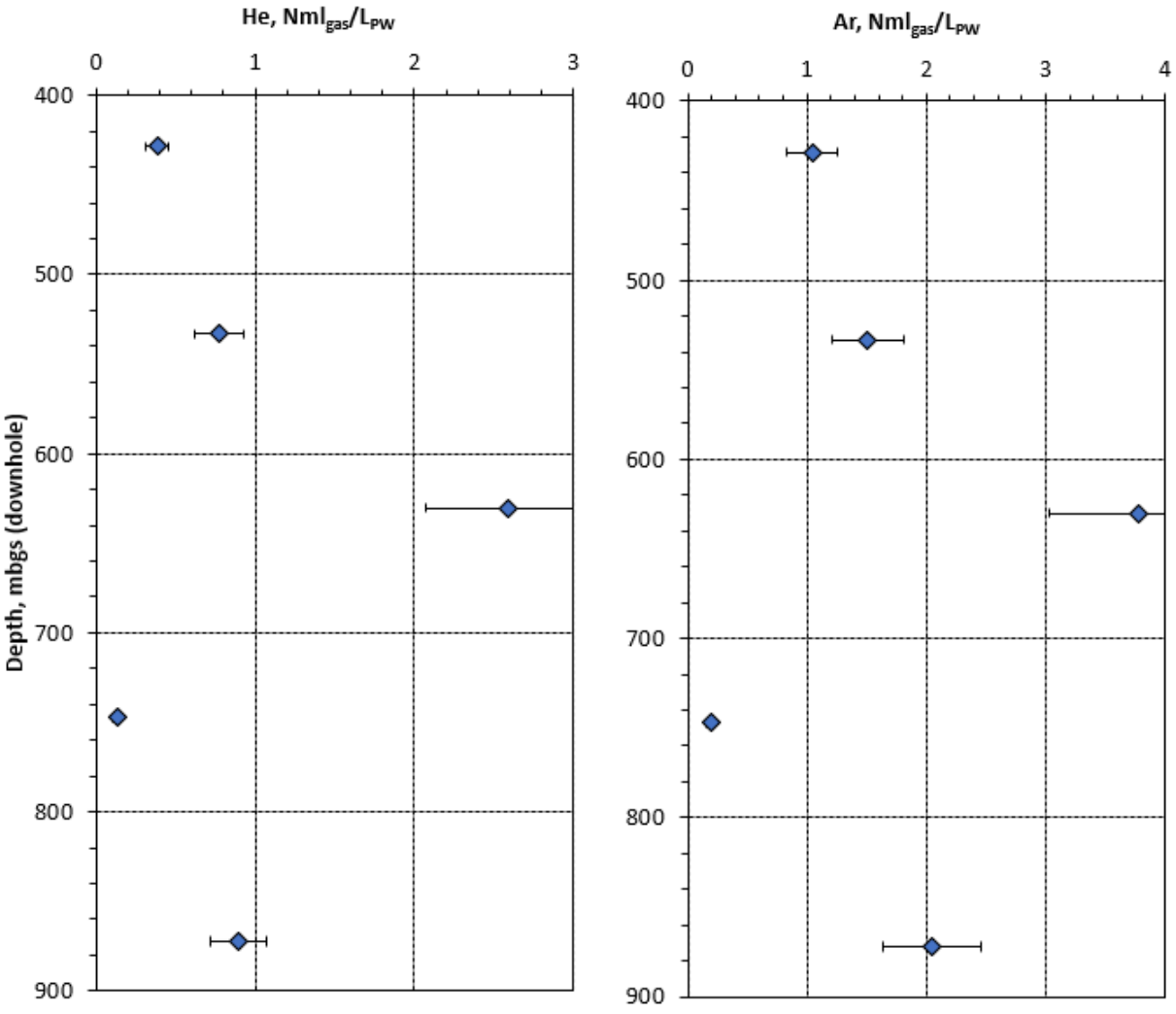


Figure 9-9: Helium (left) and argon concentrations of porewater as function of depth along borehole IG_BH05; errors are ± 20.0%.

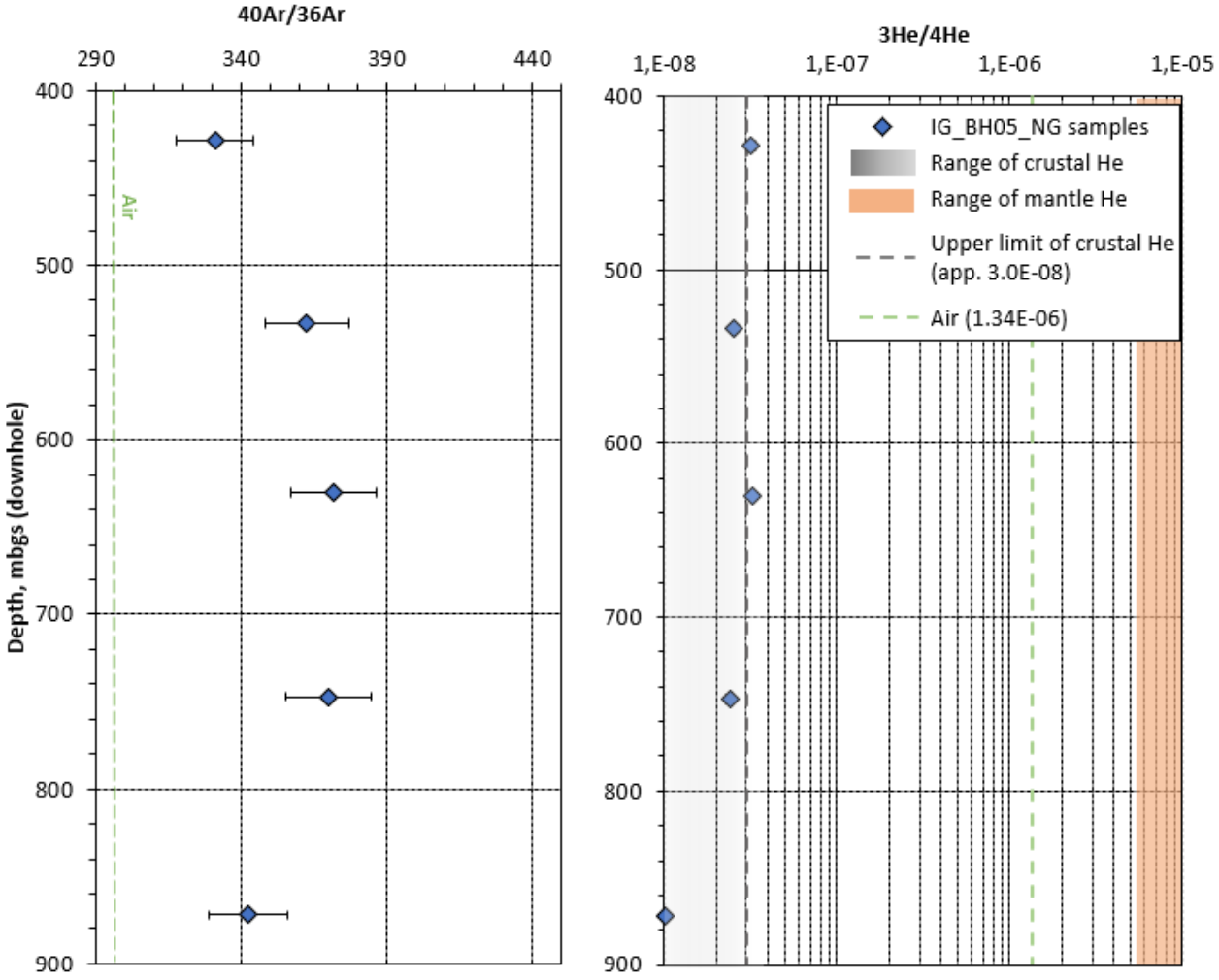


Figure 9-10: $^{40}Ar/^{36}Ar$ and $^{3}He/^{4}He$ isotope ratios dissolved in porewater as function of depth along borehole IG_BH05 compared to end-members of air and crustal and mantle He.

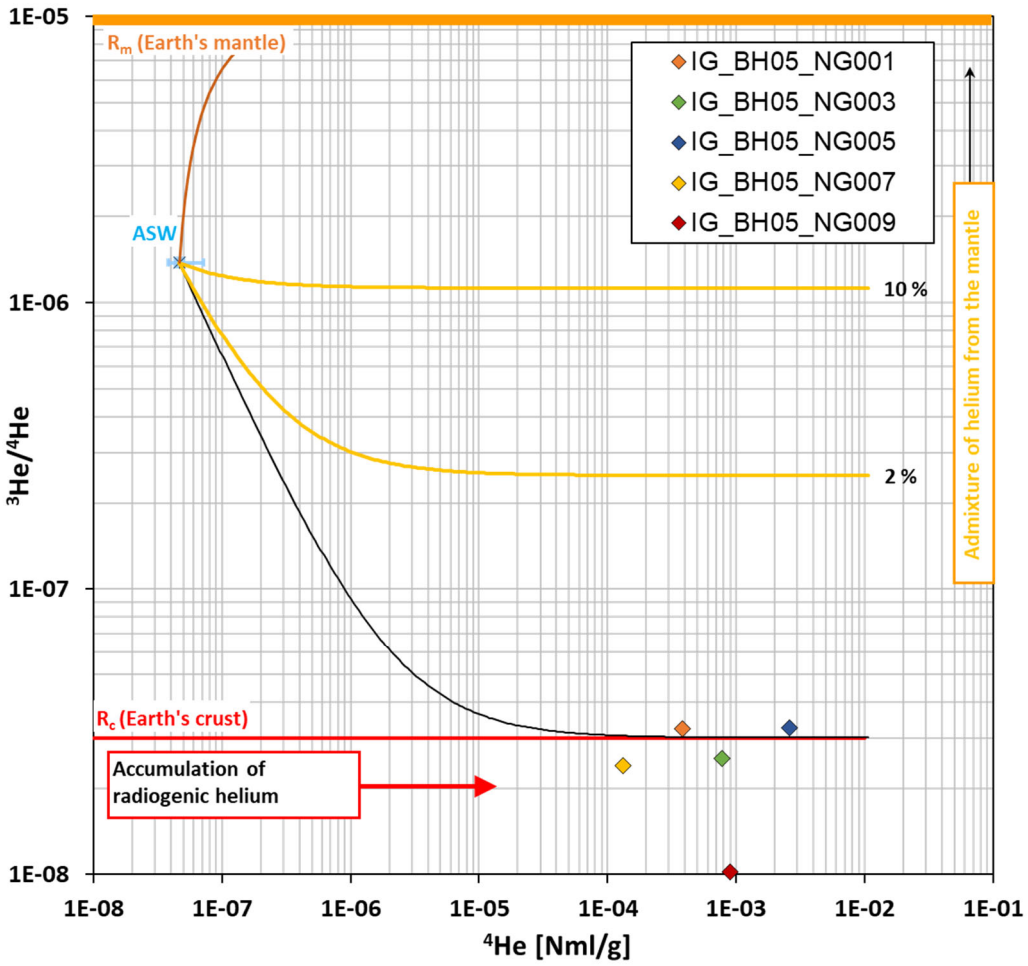


Figure 9-11: ^{3}He/^{4}He isotope ratios versus helium concentrations dissolved in porewater of cores taken from borehole IG_BH05 compared to end-member concentration of air saturated water (ASW), crust and mantle signature and potential mantle mixing paths (Osenbrück 1996).

10.0 REFERENCES

Ballentine, C.J., Burnard, P.G., 2002. Production, Release and Transport of Noble Gases in the Continental Crust. Reviews in Mineralogy & Geochemistry, 47, 481-529.

Ballentine, C.J., Burgess, R., Marty, B., 2002. Tracing Fluid Origin, Transport and Interaction in the crust. Reviews in Mineralogy & Geochemistry, 47, 539-608.

Blackburn, C.E. and Hinz, P., 1996. Gold and base metal potential of the northwest part of the Raleigh Lake greenstone belt, northwestern Ontario-Kenora Resident Geologist's District; in Summary of Field Work and Other Activities 1996, Ontario Geological Survey, Miscellaneous Paper 166, p.113-115.

Crank, J., 1975. The Mathematics of Diffusion; Oxford Science Publications; Oxford.

DesRoches, A., Sykes, M., Parmenter, A. and Sykes, E., 2018. Lineament Interpretation of the Revell Batholith and Surrounding Greenstone Belts (Nuclear Waste Management Organization. No. NWMO-TR-2018-19.

Eichinger, F.L., Waber, H.N., Smellie, J.A.T., 2006. Characterisation of Matrix Porewater at the Olkiluoto Investigation Site, Finland. Posiva Working Report 2006-103, Posiva OY, Olkiluoto Finland.

Eichinger, F., Hämmerli, J., Waber, H.N., Diamond, L.W., Smellie, J.A.T., 2013. Chemistry and Dissolved Gases of Matrix Porewater and Fluid Inclusions in Olkiluoto Bedrock from Drillhole ONK-PH9. Posiva Working Report 2011-63, Posiva Oy, Olkiluoto, Finland.

Eichinger, F., Iannotta, J., 2022. Characterisation of porewater of core samples from borehole KFR 121. SKB Report R-21-21, SKB, Stockholm, Sweden.

Ertl, S., Pichlmaier, J., Voropaev, A., Eichinger, F., 2024. A new method to determine d37Cl values of chloride in aquatic systems. Grundwasser, https://doi.org/10.1007/s00767-023-00564-3

Faber, E., Gerling, P., Dumke, I., 1987. Gaseous hydrocarbons of unknown origin found while drilling. Advances in Organic Geochemistry, 13, 875-879.

Friedrich, R., 2007. Grundwassercharakterisierung mit Umwelttracern: Erkundung des Grundwassers der Odenwald-Region sowie Implementierung eines neuen Edelgas-Massenspektrometersystems. Inaugural-Dissertation, Ruprecht-Karls-Universität, Heidelberg, Germany.

Golder, 2021. Phase 2 Initial Borehole Drilling and Testing at IG_BH04/05/06, Ignace Area – Borehole Characterization Plan for IG_BH05. NWMO Report Number: APM-PLAN-01332-0274

Golder and PGW (Paterson Grant and Watson Ltd.), 2017. Phase 2 Geoscientific Preliminary Assessment, Geological Mapping, Township of Ignace and Area, Ontario. NWMO Report Number: APM-REP-01332-0225.

Gimmi, T. and Waber, H.N., 2004. Modelling of Tracer Profiles in Pore Water of Argillaceous Rocks in the Benken Borehole: Stable Water Isotopes, Chloride, and Chlorine Isotopes; Nagra Tech. Rep. 2004-05, Nagra, Wettingen, Switzerland.

Jäckli, H., 1970. Kriterien zur Klassifikation von Grundwasservorkommen. Ecologae geol. Helv., 63 (2), 389-434.

Jähne, B., Heinz, G., Dietrich, W., 1987. Measurement of the Diffusion Coefficients of Sparingly Soluble Gases in Water. Journal of Geophysical Research, 92, C10, 10,767-10,776.

Kelley, S., 2002. K-Ar and Ar-Ar Dating. Reviews in Mineralogy & Geochemistry, 47, 785-810.

Kietäväinen, R., Ahonen, L., Niinikosi, P., Nykänen, H., Kukkonen, I.T., 2017. Abiotic and biotic controls on methane formation down to 2.5 km depth within the Precambrian Fennoscandian Shield. Geochimica et Cosmochimica Acta 202, 124-145.

Lehmann, B.E., Waber, H.N., Tolstikhin, I., Kamensky, I., Gannibal, M., Kalashnikov, E., Pevzner, B., 2003. Helium in solubility equilibrium with quartz and porefluids in rocks: A new approach in hydrology. Geophysical Research Letters, 30, 3, 28-1 – 28-4.

Leya, I., Wieler, R., 1999. Nucleogenic production of Ne isotopes in Earth's crust and upper mantle induced by alpha particles from the decay of U and Th. Journal of Geophysical Research, 104, 15439-15450.

Lide, D.R., 1994. CRC Handbook of chemistry and physics. 75th ed., CRC Press, Boca Raton, USA.

Meier, D.B., Waber, H.N., Gimmi, T., Eichinger, F., Diamond, L.W., 2015. Reconstruction of in situ porosity and porewater compositions of low-permeability crystalline rocks: Magnitude of artefacts induced by drilling and sample recovery. Journal of Contaminant Hydrology, 183, 55-71.

OGS (Ontario Geological Survey), 2011. 1:250 000 scale bedrock geology of Ontario, Ontario Geological Survey, Miscellaneous Release Data 126 - Revision 1.

Ohlsson, Y. and Neretnieks, I., 1995. Literature survey of matrix diffusion theory and of experiments and data including natural analogues; SKB Tech. Rep. 95-12, Svensk Kärnbränslehantering AB, Stockholm, Sweden.

Osenbrück, K., 1996. Alter und Dynamik tiefer Grundwässer: Eine neue Methode zur Analyse der Edelgase im Porenwasser in Gesteinen. Dissertation Ruprecht-Karls-Universität Heidelberg, Heidelberg, Germany.

Ozima, M., Podosek, F.A., 2005. Noble gas geochemistry. Cambridge University Press, Cambridge, UK.

Parmenter, A., Waffle, L. and DesRoches, A., 2020. An updated bedrock geology map and geological database for the northern portion of the Revell batholith (No. NWMO-TR-2020-08). Nuclear Waste Management Organization.

Porcelli, D., Ballentine, C.J., 2002. Models for the Distribution of Terrestrial Noble Gases and Evolution of the Atmosphere. Reviews in Mineralogy & Geochemistry, 47, 411-469.

Rogge, T., 1997. Eine molekular-diffusive Methode zur Bestimmung des Porenwassergehaltes und der Zusammensetzung von stabilen Isotopen im Porenwasser von Gestein; unveröffentlichte Diplomarbeit; Heidelberg.

Rübel, A.P., Sonntag, Ch., Lippmann, J., Pearson, F.J. and Gautschi, A., 2002. Solute transport in formations of very low permeability: Profiles of stable isotope and dissolved noble gas contents of pore water in the Opalinus Clay. Mont Terri, Switzerland; Geochim. Cosmochim. Acta, 66, 1311-1321.

Schmid, R., Douglas, Fettes D., Harte, B., Davis, E., Desmons, J., 2007. How to Name a Metamorphic Rock. Recommendations by the IUGS Subcomission on the Systematics of Metamorphic Rocks.

SGL (Sander Geophysics Limited), 2015. Phase 2 Geoscientific Preliminary Assessment, Acquisition, Processing and Interpretation of High-Resolution Airborne Geophysical Data, Township of Ignace, Ontario. Prepared for Nuclear Waste Management Organization (NWMO). NWMO Report Number: APM-REP-06145-0002.

Sherwood-Lollar, B. S., Weise, S. M., Frape, S. K., Barker, J. F., 1994. Isotopic constraints on the migration of hydrocarbon and helium gases southwestern Ontario. Bull. Can. Petrol. Geol. 42, 283-295.

Sherwood Lollar, B., Westgate, T.D., Ward, J.A., Slater, G.F., Lacrampe-Couloume, G., 2002. Abiogenic formation of alkanes in the Earth's crust as a minor source for global hydrocarbon reservoirs. Nature, 416, 522-524.

SRK (SRK Consulting, Inc.) and Golder, 2015. Phase 2 Geoscientific Preliminary Assessment, Observation of General Geological Features, Township of Ignace, Ontario. Prepared for Nuclear Waste Management Organization. NWMO Report Number: APM-REP-06145-0004.

Stone, D., 2009. Geology of the Bending Lake Area, Northwestern Ontario; in Summary of Field Work and Other Activities 2009. Ontario Geological Survey. Open File Report 6240.

Stone, D., 2010a. Geology of the Stormy Lake Area, Northwestern Ontario; in Summary of Field Work and Other Activities 2010. Ontario Geological Survey, Open File Report 6260.

Stone, D., 2010b. Precambrian geology of the central Wabigoon Subprovince area, northwestern Ontario. Ontario Geological Survey, Open File Report 5422.

Stone, D., Halle, J. and Chaloux, E., 1998. Geology of the Ignace and Pekagoning Lake Areas, Central Wabigoon Subprovince; in Summary of Field Work and Other Activities 1998, Ontario Geological Survey, Misc. Paper 169.

Stone, D., Davis, D.W., Hamilton, M.A. and Falcon, A., 2010. Interpretation of 2009 Geochronology in the Central Wabigoon Subprovince and Bending Lake Areas, Northwestern Ontario, in Summary of Field Work and Other Activities 2010, Ontario Geological Survey, Open File Report 6260.

Tolstikhin, I.N., Gannibal, M., Tarakanov, S., Pevzner, B., Lehmann, B., Ihly, B., Waber, H.N., 2005. Helium transfer from water into quartz crystals: A new approach for porewater dating. Earth and Planetary Science Letters, 238, 31-41.

Waber, H.N. and Smellie, J.A.T., 2005. SKB Site Investigations Forsmark – Borehole KFM06: Characterisation of porewater. Part I: Diffusion experiments; SKB P-Rep. P-05-196, Svensk Kärnbränslehantering AB, Stockholm, Sweden.

Waber, H.N. and Smellie, J.A.T., 2006. Oskarshamn site investigations. Borehole KLX03: Characterisation of porewater. Part 2: Rock properties and diffusion experiments; SKB P-Report P-06-77. Svensk Kärnbränslehantering AB, Stockholm, Sweden.

Whiticar, M.J., 1999. Carbon and hydrogen isotope systematics of bacterial formation and oxidation of methane. Chemical Geology, 161, 291-314.

Whiticar, M.J., 2020. The Biogeochemical Methane Cycle. In H. Wilkes (ed.), Hydrocarbons, Oils and Lipids: Diversity, Origin, Chemistry and Fate. Handbook of Hydrocarbon and Lipid Microbiology, Springer Nature, Switzerland.

WSP, 2024. Phase 2 Initial Borehole Drilling and Testing at IG_BH04/05/06, Ignace Area – WP04D Mineralogical and Geochemical Analysis of Core for IG_BH05 – (In preparation).

https://wsponlinecan.sharepoint.com/sites/ca-gld-20253946/externalsharing/wp04c shared files/ig_bh05 wp04c/17 final report ig_bh05 wp04c 09dec2024/20253946 ig_bh05 wp04c rpt_dec2024_r9a.docx

APPENDIX A

Core Logging Depth Correction and Photo Documentation

TECHNICAL MEMORANDUM

DATE August 4, 2024 **Reference No.** 20253946-5043-TM-001

TO File
WSP Canada Inc.

CC File

FROM George Schneider **EMAIL george.schneider@wsp.com**

ADDENDUM TO LABORATORY REPORT FROM HYDROISOTOP FOR WORK PACKAGE WP04C - BOREHOLE IG_BH05

This addendum corrects the depths (along borehole) of the samples for porewater extraction and analysis included in this report. The depth adjustment is the result of a correction applied to the core logging depths after reconciliation with the drilling depth records. Refer to the WP03 report for details and to the acQuire database for corrected depths.

Refer to Table 1 for the list of samples containing the original logged depths and the corrected depths after reconciliation between the core logging and drilling depths. This addendum shall always accompany the laboratory report when distributed to other parties.

Table 1: List of samples requiring depth correction

Sample ID	Test / Sample Type	Original Logged Depth (mbgs downhole)		Corrected Depth (mbgs downhole)	
		From	To	From	To
IG_BH05_AQ001	Aqueous Extraction	166.22	166.48	166.11	166.37
IG_BH05_AQ002	Aqueous Extraction	221.06	221.23	220.91	221.08
IG_BH05_AQ003	Aqueous Extraction	253.13	253.31	252.96	253.14
IG_BH05_AQ004	Aqueous Extraction	289.90	290.06	289.71	289.87
IG_BH05_AQ005	Aqueous Extraction	343.14	343.35	342.94	343.15
IG_BH05_AQ006	Aqueous Extraction	387.14	387.56	386.94	387.36
IG_BH05_AQ007	Aqueous Extraction	399.85	400.04	399.65	399.84
IG_BH05_AQ008	Aqueous Extraction	426.89	427.09	426.68	426.88
IG_BH05_AQ009	Aqueous Extraction	453.53	453.72	453.32	453.51
IG_BH05_AQ010	Aqueous Extraction	480.00	480.19	479.78	479.97
IG_BH05_AQ011	Aqueous Extraction	507.04	507.23	506.81	507.00
IG_BH05_AQ012	Aqueous Extraction	525.63	525.82	525.40	525.59
IG_BH05_AQ013	Aqueous Extraction	560.62	561.81	560.38	561.57
IG_BH05_AQ014	Aqueous Extraction	588.12	588.36	587.87	588.11

Sample ID	Test / Sample Type	Original Logged Depth (mbgs downhole)		Corrected Depth (mbgs downhole)	
		From	To	From	To
IG_BH05_AQ015	Aqueous Extraction	612.68	612.85	612.42	612.59
IG_BH05_AQ016	Aqueous Extraction	640.32	640.52	640.05	640.25
IG_BH05_AQ017	Aqueous Extraction	664.49	664.71	664.22	664.44
IG_BH05_AQ018	Aqueous Extraction	694.07	694.30	693.79	694.02
IG_BH05_AQ019	Aqueous Extraction	720.62	720.85	720.33	720.56
IG_BH05_AQ020	Aqueous Extraction	750.19	750.41	749.89	750.11
IG_BH05_AQ021	Aqueous Extraction	773.15	773.47	772.85	773.17
IG_BH05_AQ022	Aqueous Extraction	797.16	797.44	796.85	797.13
IG_BH05_AQ023	Aqueous Extraction	827.74	827.96	827.43	827.65
IG_BH05_AQ024	Aqueous Extraction	849.22	849.39	848.91	849.08
IG_BH05_AQ025	Aqueous Extraction	881.73	881.91	881.42	881.60
IG_BH05_AQ026	Aqueous Extraction	906.66	906.82	906.35	906.51
IG_BH05_AQ027	Aqueous Extraction	936.89	937.09	936.58	936.78
IG_BH05_AQ028	Aqueous Extraction	963.07	963.22	962.76	962.91
IG_BH05_AQ029	Aqueous Extraction	982.24	982.44	981.93	982.13
IG_BH05_AR033	Archive Sample	717.28	717.48	716.99	717.19
IG_BH05_AR052	Archive Sample	855.93	856.16	855.62	855.85
IG_BH05_AR059	Archive Sample	978.81	979.10	978.50	978.79
IG_BH05_DG001	Non-Inert Gas	431.14	431.35	430.93	431.14
IG_BH05_DG002	Non-Inert Gas	536.24	536.47	536.00	536.23
IG_BH05_DG003	Non-Inert Gas	634.11	634.33	633.85	634.07
IG_BH05_DG004	Non-Inert Gas	744.22	744.43	743.93	744.14
IG_BH05_DG005	Non-Inert Gas	879.21	879.44	878.90	879.13
IG_BH05_NG001	Noble Gas	428.43	428.63	428.22	428.42
IG_BH05_NG003	Noble Gas	533.15	533.35	532.91	533.11
IG_BH05_NG005	Noble Gas	630.13	630.35	629.87	630.09
IG_BH05_NG007	Noble Gas	747.15	747.37	746.85	747.07
IG_BH05_NG009	Noble Gas	872.08	872.30	871.77	871.99
IG_BH05_PW001	Porewater	171.18	171.61	171.07	171.50
IG_BH05_PW002	Porewater	218.92	219.29	218.77	219.14
IG_BH05_PW003	Porewater	253.31	253.68	253.14	253.51
IG_BH05_PW004	Porewater	290.06	290.43	289.87	290.24
IG_BH05_PW005	Porewater	341.50	341.87	341.30	341.67

Sample ID	Test / Sample Type	Original Logged Depth (mbgs downhole)		Corrected Depth (mbgs downhole)	
		From	To	From	To
IG_BH05_PW006	Porewater	386.48	386.88	386.28	386.68
IG_BH05_PW007	Porewater	398.29	398.70	398.09	398.50
IG_BH05_PW008	Porewater	426.09	426.51	425.88	426.30
IG_BH05_PW009	Porewater	454.08	454.49	453.87	454.28
IG_BH05_PW010	Porewater	479.25	479.62	479.03	479.40
IG_BH05_PW011	Porewater	506.24	506.65	506.01	506.42
IG_BH05_PW012	Porewater	524.85	525.25	524.62	525.02
IG_BH05_PW013	Porewater	559.89	560.26	559.65	560.02
IG_BH05_PW014	Porewater	586.92	587.30	586.67	587.05
IG_BH05_PW015	Porewater	611.93	612.31	611.67	612.05
IG_BH05_PW016	Porewater	637.26	637.63	636.99	637.36
IG_BH05_PW017	Porewater	665.05	665.49	664.78	665.22
IG_BH05_PW018	Porewater	692.17	692.56	691.89	692.28
IG_BH05_PW019	Porewater	721.98	722.38	721.69	722.09
IG_BH05_PW020	Porewater	749.38	749.79	749.08	749.49
IG_BH05_PW021	Porewater	774.29	774.72	773.99	774.42
IG_BH05_PW022	Porewater	801.55	801.95	801.24	801.64
IG_BH05_PW023	Porewater	827.01	827.38	826.70	827.07
IG_BH05_PW024	Porewater	848.51	848.86	848.20	848.55
IG_BH05_PW025	Porewater	881.36	881.73	881.05	881.42
IG_BH05_PW026	Porewater	905.93	906.27	905.62	905.96
IG_BH05_PW027	Porewater	936.13	936.51	935.82	936.20
IG_BH05_PW028	Porewater	962.72	963.07	962.41	962.76
IG_BH05_PW029	Porewater	986.30	986.68	985.99	986.37

WSP Canada Inc.



George Schneider, M.Sc., P.Geo.

GWS/

Distribution: File

Attachments: N/A

c:\gws-work\1 - active\nwmo bh456\lab samples\ig_bh05 wp04c depth memo 04aug2024.docx

Figure A-1: On site documentation of core samples for porewater characterization sent to Hydroisotop (photos provided by Golder); Core samples are packed in the first evacuated and sealed plastic bag



IG_BH05_AQ001: 166.22-166.48 m



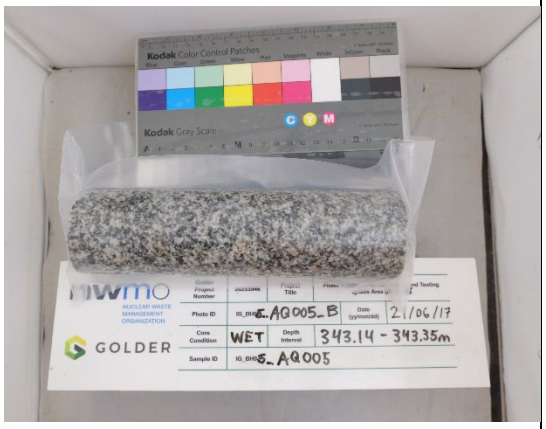
IG_BH05_AQ002: 221.06-221.23 m



IG_BH05_AQ003: 253.13-253.31 m



IG_BH05_AQ004: 289.90-290.06 m



IG_BH05_AQ005: 343.14-343.35 m



IG_BH05_AQ006: 387.14-387.56 m



IG_BH05_AQ007: 399.85-400.04 m



IG_BH05_AQ008: 426.89-427.09 m



IG_BH05_AQ009: 453.53-453.72 m



IG_BH05_AQ010: 480.00-480.19 m



IG_BH05_AQ011: 507.04-507.23 m



IG_BH05_AQ012: 525.63-525.82 m



IG_BH05_AQ013: 560.62-560.81 m



IG_BH05_AQ014: 588.12.588.36 m



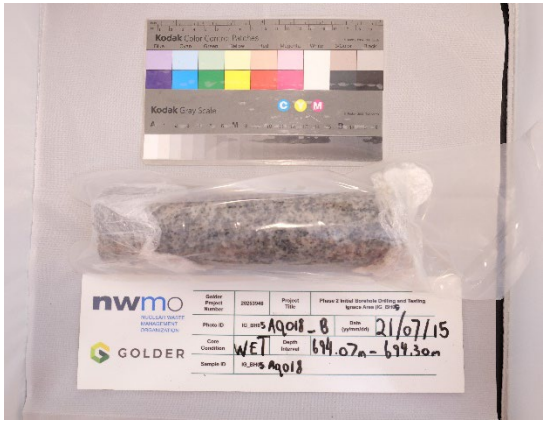
IG_BH05_AQ015: 612.68-612.85 m



IG_BH05_AQ016: 640.32-640.52 m



IG_BH05_AQ017: 644.49-664.71 m



IG_BH05_AQ018: 694.07-694.30 m



IG_BH05_AQ019: 720.62-720.85 m



IG_BH05_AQ020: 750.19-750.41 m



IG_BH05_AQ021: 773.15-773.47 m



IG_BH05_AQ022: 797.16-797.44 m



IG_BH05_AQ023: 827.74-827.96 m



IG_BH05_AQ024: 849.22-849.39 m



IG_BH05_AQ025: 881.73-881.93 m



IG_BH05_AQ026: 906.66-906.82 m



IG_BH05_AQ027: 936.89-937.09 m



IG_BH05_AQ028: 963.07-963.22 m



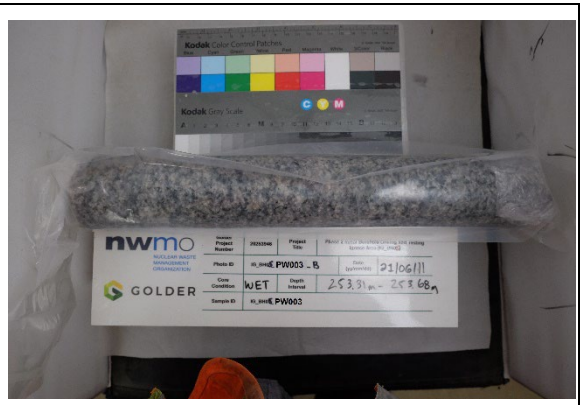
IG_BH05_AQ029: 982.24-982.44 m



IG_BH05_PW001: 171.18-171.61 m



IG_BH05_PW002: 218.92-219.29 m



IG_BH05_PW003: 253.31-253.68 m



IG_BH05_PW004: 290.06-290.43 m



IG_BH05_PW005: 341.50-341.87 m



IG_BH05_PW006: 386.48-348.88 m



IG_BH05_PW007: 398.29-398.70 m



IG_BH05_PW008: 426.09-426.51 m



IG_BH05_PW009: 454.08-454.49 m



IG_BH05_PW010: 479.25-479.62 m



IG_BH05_PW011: 506.24-506.65 m



IG_BH05_PW012: 524.85-525.25 m



IG_BH05_PW013: 559.89-560.26 m



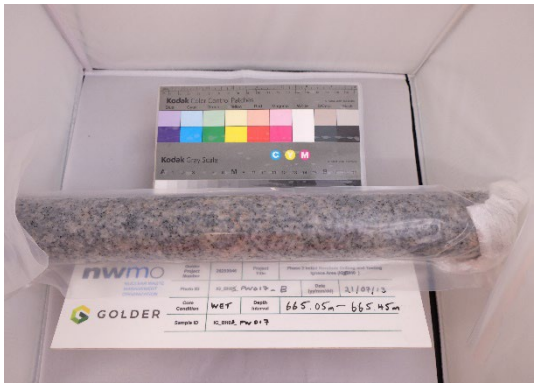
IG_BH05_PW014: 586.92-587.30 m



IG_BH05_PW015: 611.93-612.31 m



IG_BH05_PW016: 637.26-637.63 m



IG_BH05_PW017: 665.05-665.49 m



IG_BH05_PW018: 692.17-692.56 m



IG_BH05_PW019: 721.98-722.38 m



IG_BH05_PW020: 749.38-749.79 m



IG_BH05_PW021: 774.29-774.72 m



IG_BH05_PW022: 801.55-801.95 m



IG_BH05_PW023: 827.01-827.38 m



IG_BH05_PW024: 848.51-848.86 m



IG_BH05_PW025: 881.36-881.73 m



IG_BH05_PW026: 905.93-906.27 m



IG_BH05_PW027: 936.13-936.51 m



IG_BH05_PW028: 962.72-963.07 m



IG_BH05_PW029: 986.30-986.68 m



IG_BH05_AR033: 717.28-717.48 m



IG_BH05_AR052: 855.93-856.16 m



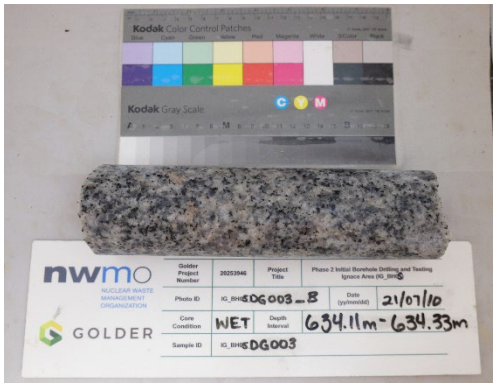
IG_BH05_AR059: 978.81-979.10 m



IG_BH05_DG001: 431.14-431.35 m



IG_BH05_DG002: 536.24-536.47 m



IG_BH05_DG003: 634.11-634.33 m



IG_BH05_DG004: 744.22-744.43 m



IG_BH05_DG005: 879.21-879.44 m



IG_BH05_NG001: 428.43-428.63 m



IG_BH05_NG003: 533.15-533.35 m



IG_BH05_NG005: 630.12-630.35 m



IG_BH05_NG007: 747.15-747.37 m

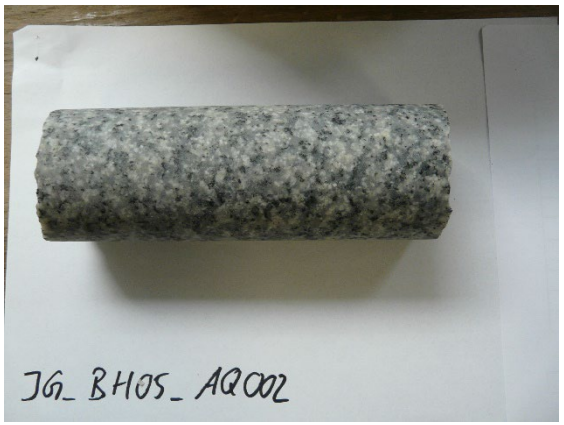


IG_BH05_NG009: 872.08-872.30 m

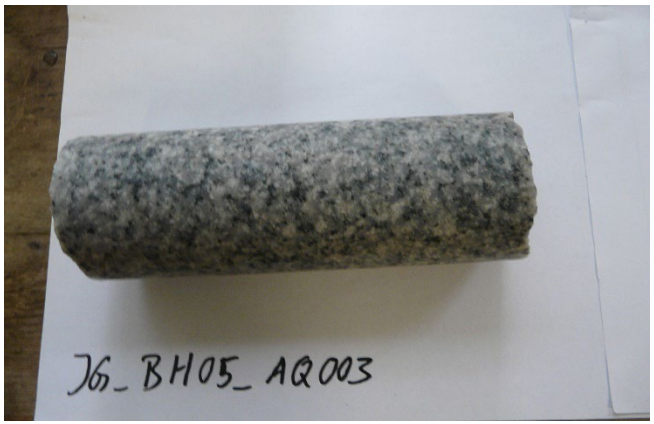
Figure A-2: Laboratory documentation of core samples for porewater characterization sent to Hydroisotop; photos were taken right after unpacking



IG_BH05_AQ001: 166.22-166.48 m



IG_BH05_AQ002: 221.06-221.23 m



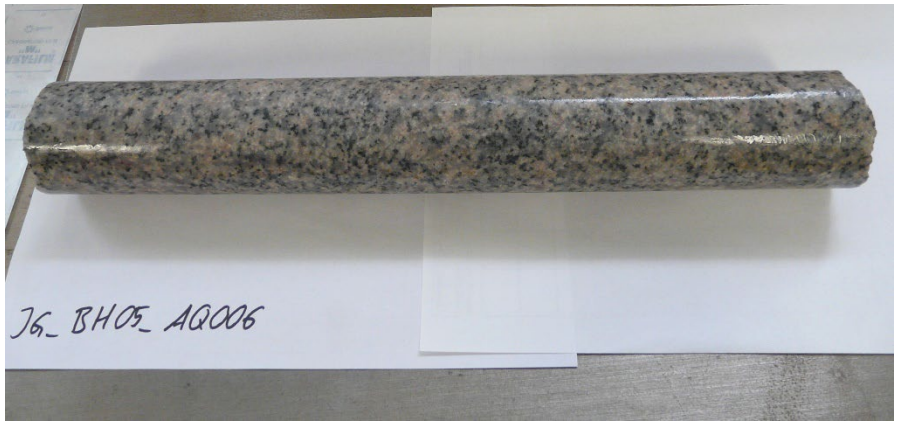
IG_BH05_AQ003: 253.13-253.31 m



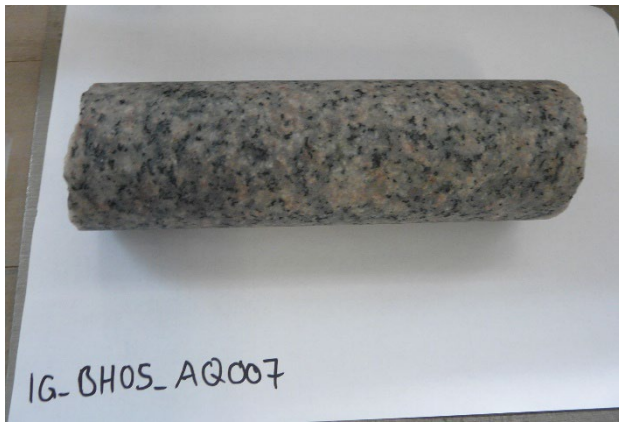
IG_BH05_AQ004: 289.90-290.06 m



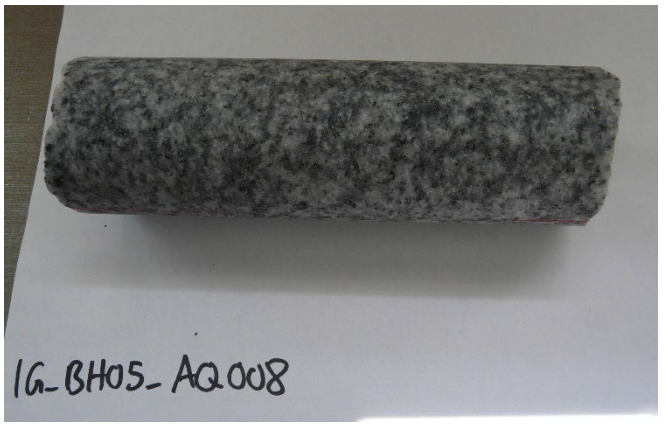
IG_BH05_AQ005: 343.14-343.35 m



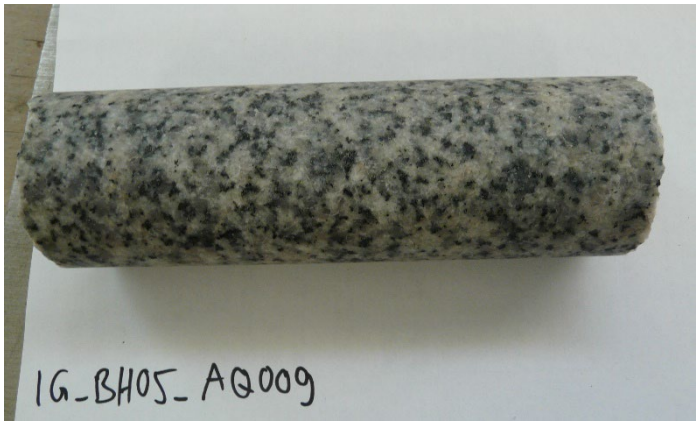
IG_BH05_AQ006: 387.14-387.56 m



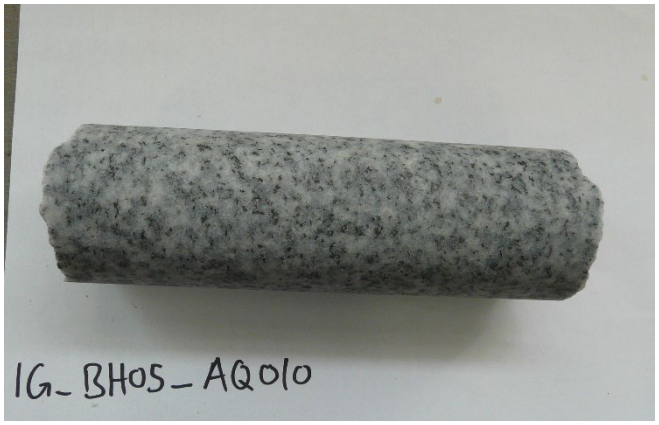
IG_BH05_AQ007: 399.85-400.04 m



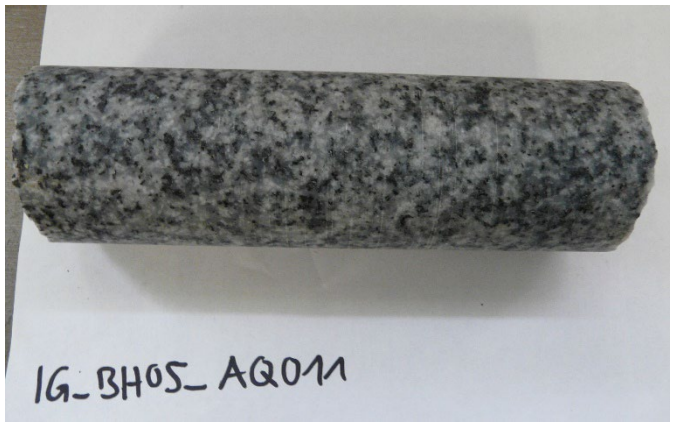
IG_BH05_AQ008: 426.89-427.09 m



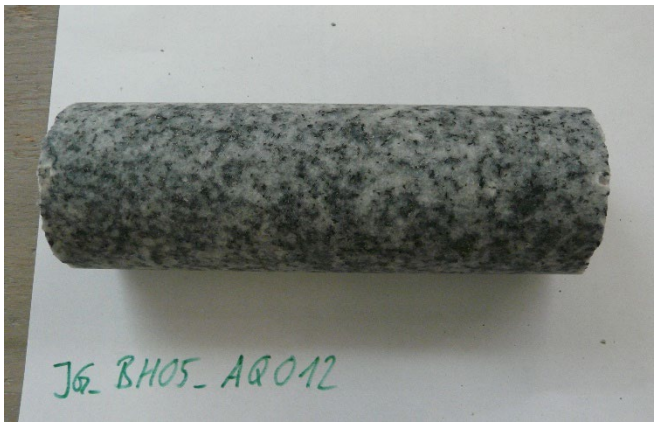
IG_BH05_AQ009: 453.53-453.72 m



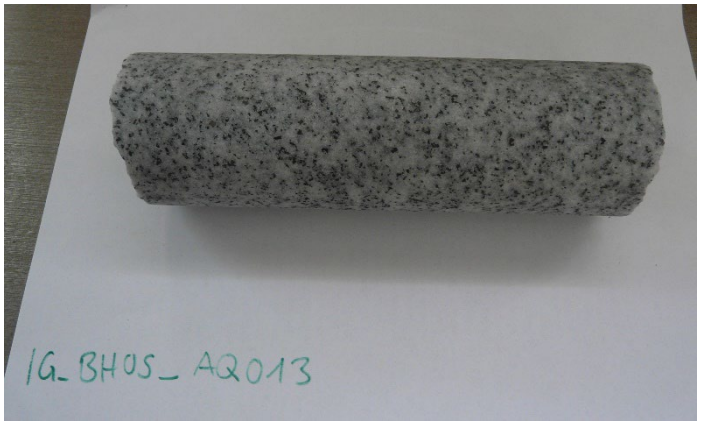
IG_BH05_AQ010: 480.00-480.19 m



IG_BH05_AQ011: 507.04-507.23 m



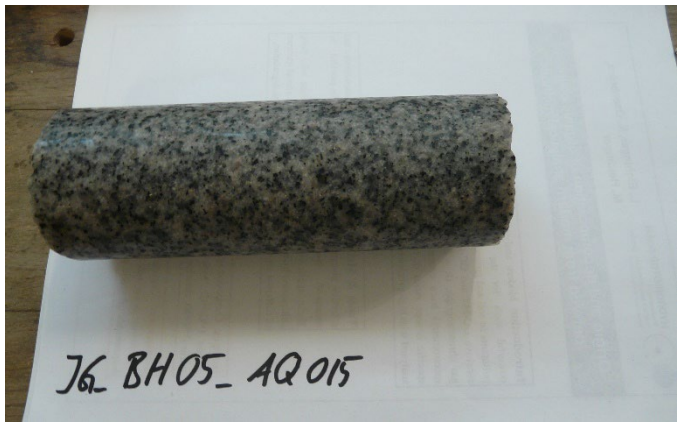
IG_BH05_AQ012: 525.63-525.82 m



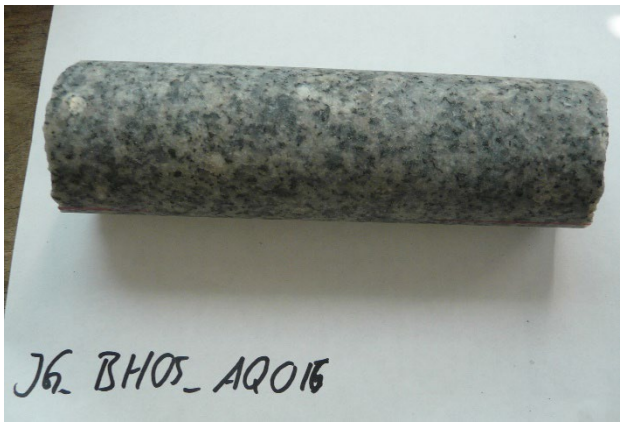
IG_BH05_AQ013: 560.62-560.81 m



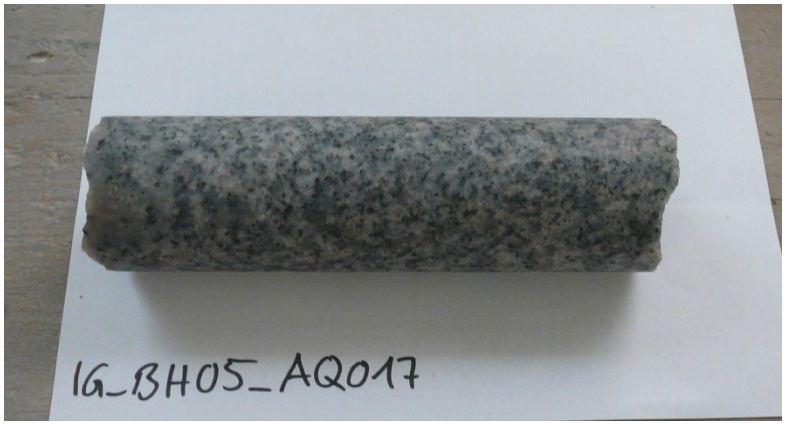
IG_BH05_AQ014: 588.12-588.36 m



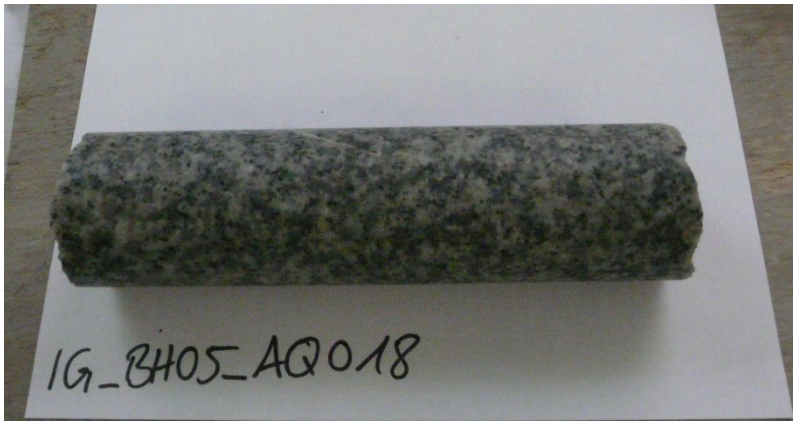
IG_BH05_AQ015: 612.68-612.85 m



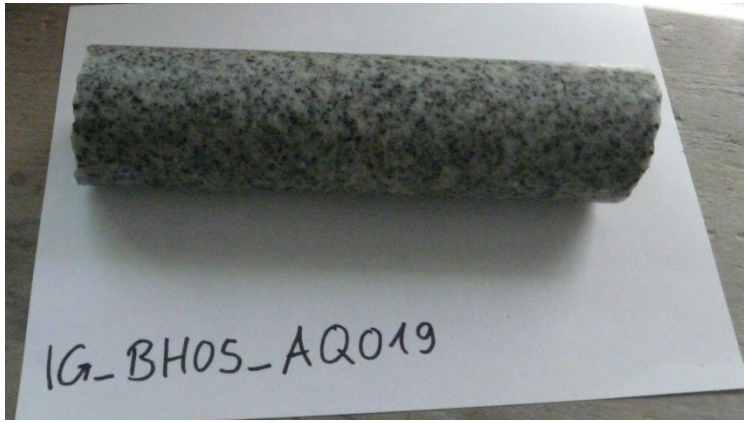
IG_BH05_AQ016: 640.32-640.52 m



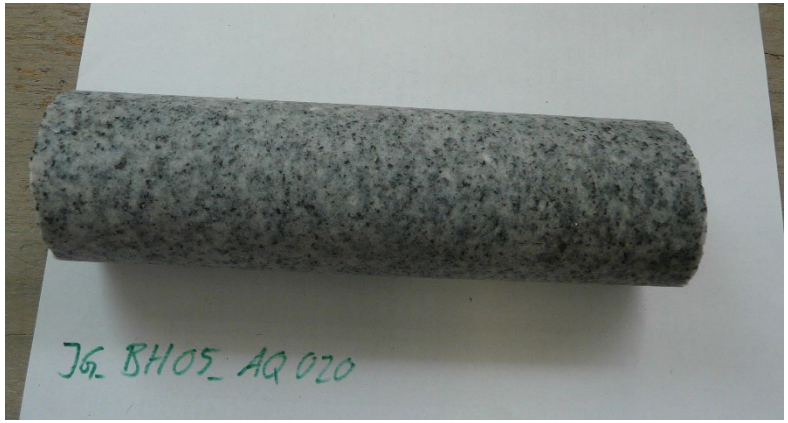
IG_BH05_AQ017: 644.49-664.71 m



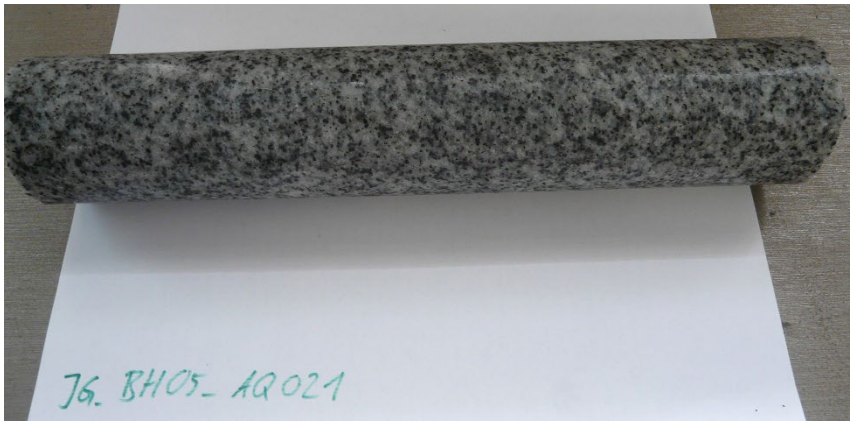
IG_BH05_AQ018: 694.07-694.30 m



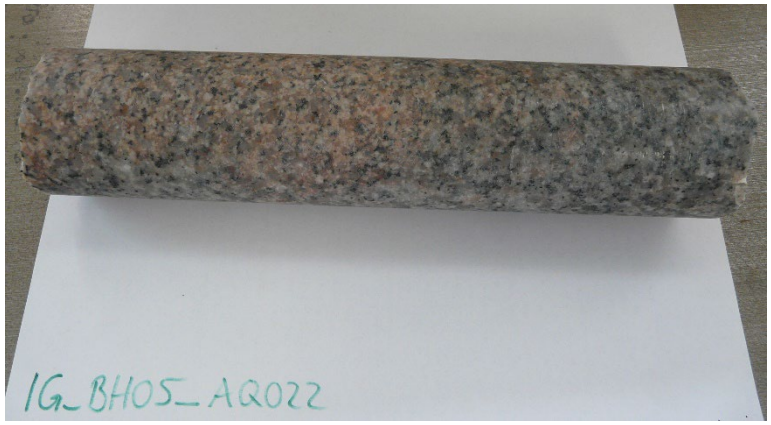
IG_BH05_AQ019: 720.62-720.85 m



IG_BH05_AQ020: 750.19-750.41 m



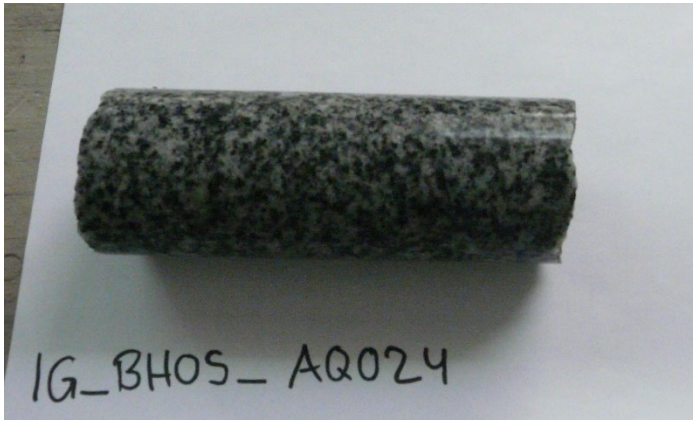
IG_BH05_AQ021: 773.15-773.47 m



IG_BH05_AQ022: 797.16-797.44 m



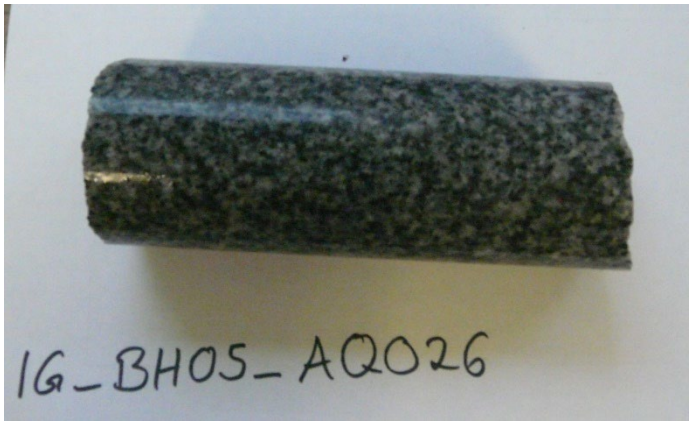
IG_BH05_AQ023: 827.74-827.96 m



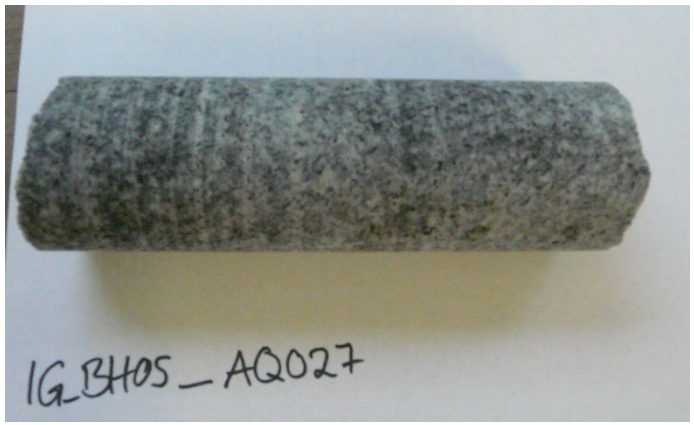
IG_BH05_AQ024: 849.22-849.39 m



IG_BH05_AQ025: 881.73-881.91 m



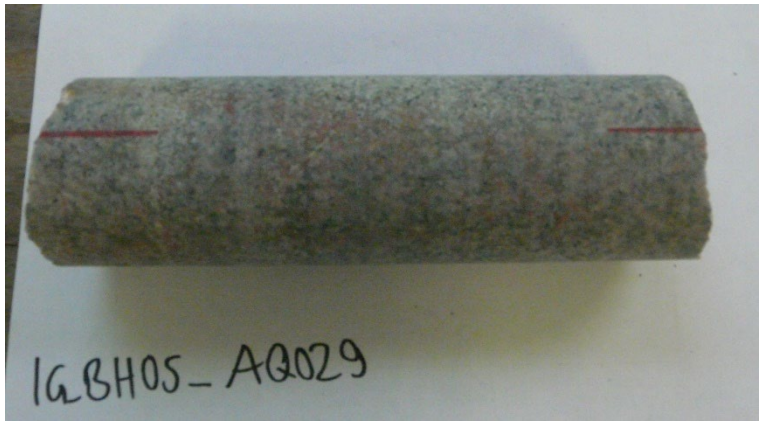
IG_BH05_AQ026: 906.66-906.82 m



IG_BH05_AQ027: 936.89-937.09 m



IG_BH05_AQ028: 963.07-963.22 m



IG_BH05_AQ029: 982.24-982.44 m



IG_BH05_PW001: 171.18-171.61 m



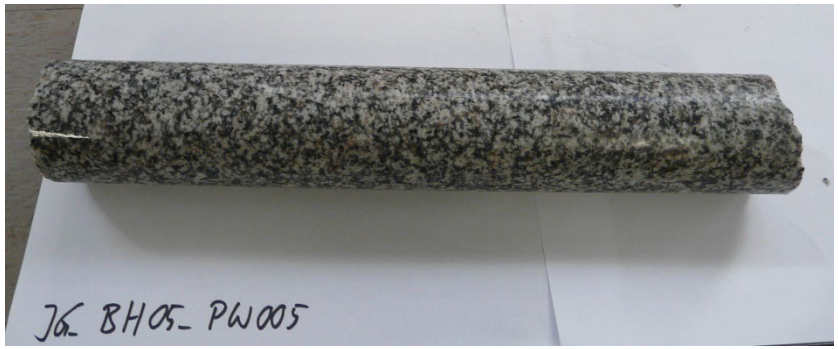
IG_BH05_PW002: 218.92-219.29 m



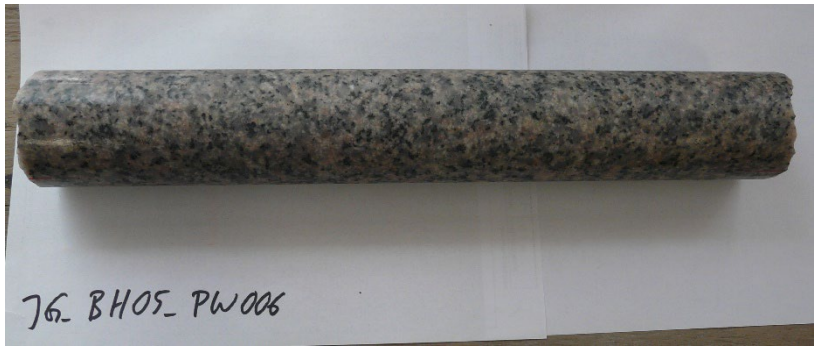
IG_BH05_PW003: 253.31-253.68 m



IG_BH05_PW004: 290.06-290.43 m



IG_BH05_PW005: 341.50-341.87 m



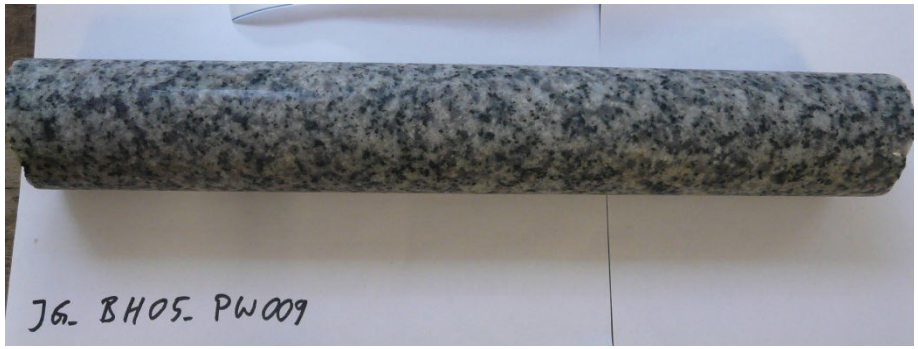
IG_BH05_PW006: 386.48-386.88 m



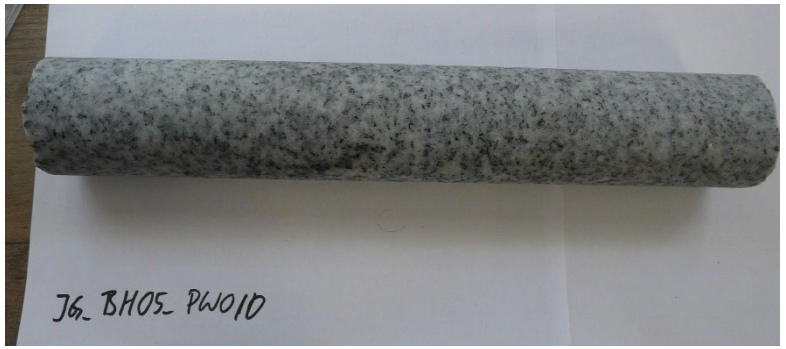
IG_BH05_PW007: 398.29-398.70 m



IG_BH05_PW008: 426.09-426.51 m



IG_BH05_PW009: 454.08-454.49 m



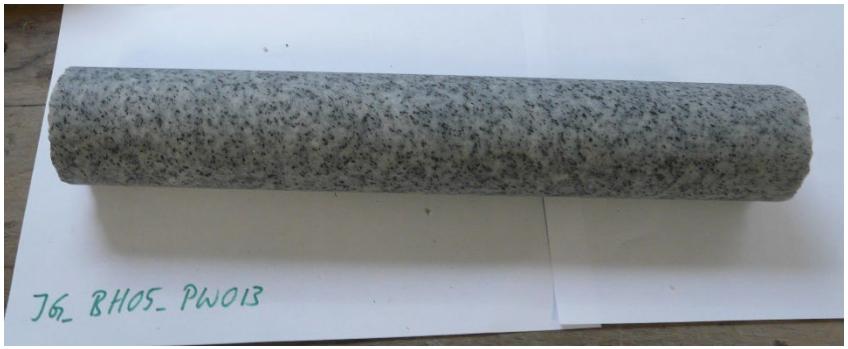
IG_BH05_PW010: 479.25-479.62 m



IG_BH05_PW011: 506.24-506.65 m



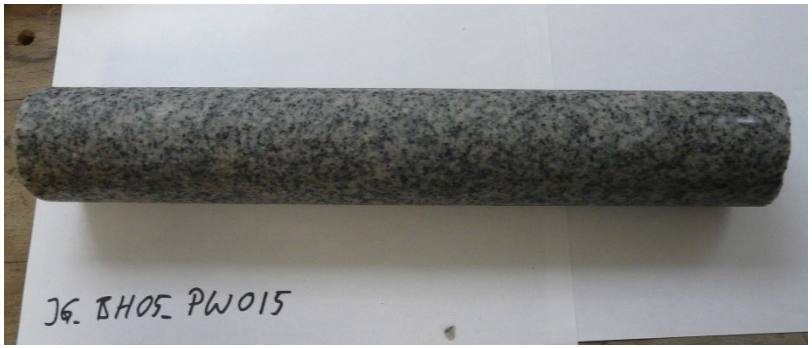
IG_BH05_PW012: 524.85-525.25 m



IG_BH05_PW013: 559.89-560.26 m



IG_BH05_PW014: 586.92-587.30 m



IG_BH05_PW015: 611.93-612.31 m



IG_BH05_PW016: 637.26-637.63 m



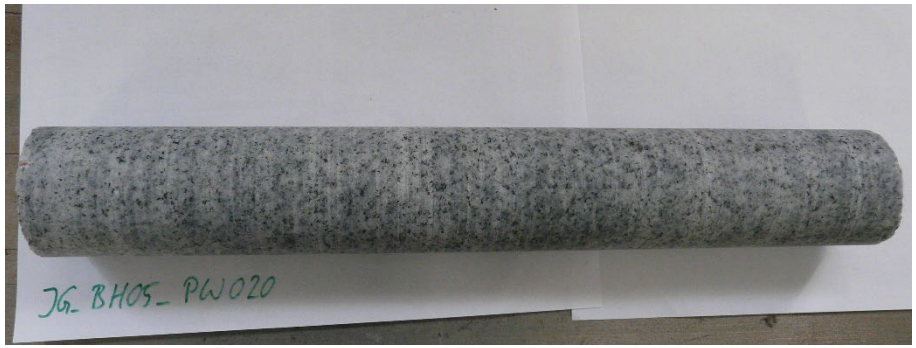
IG_BH05_PW017: 665.05-665.49 m



IG_BH05_PW018: 692.17-692.56 m



IG_BH05_PW019: 721.98-722.38 m



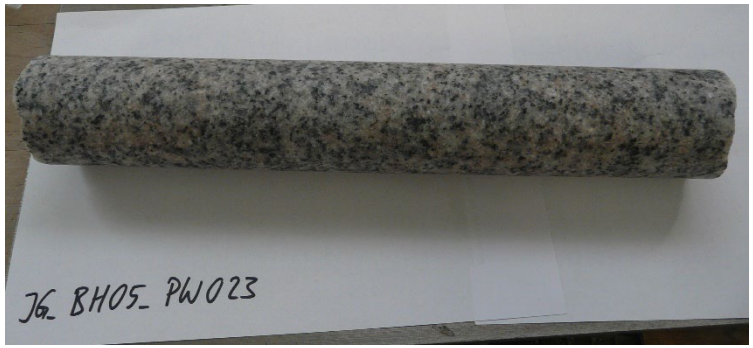
IG_BH05_PW020: 749.38-749.79 m



IG_BH05_PW021: 774.29-774.72 m



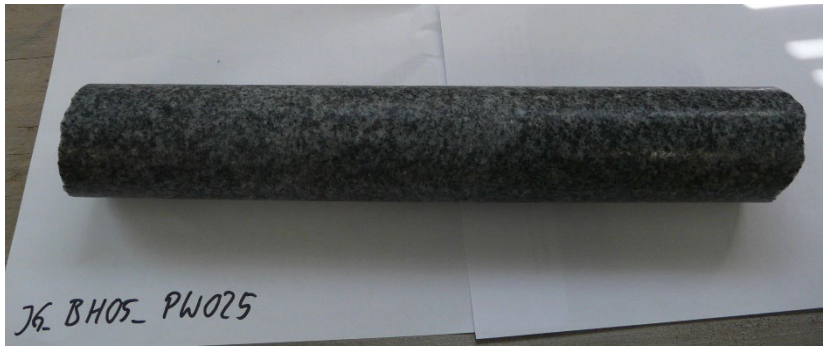
IG_BH05_PW022: 801.55-801.95 m



IG_BH05_PW023: 827.01-827.38 m



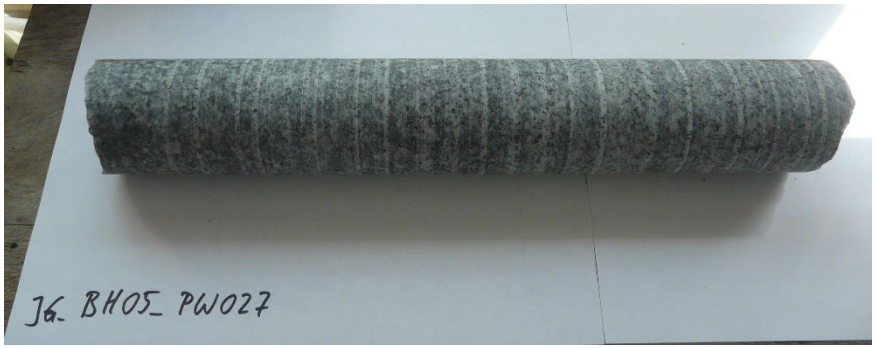
IG_BH05_PW024: 848.51-848.86 m



IG_BH05_PW025: 881.36-881.73 m



IG_BH05_PW026: 905.93-906.27 m



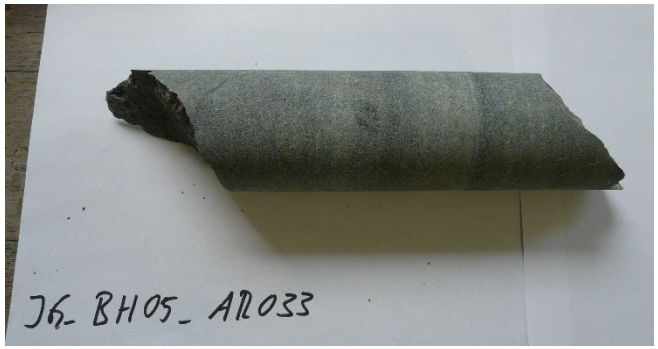
IG_BH05_PW027: 936.13-936.51 m



IG_BH05_PW028: 962.72-963.07 m



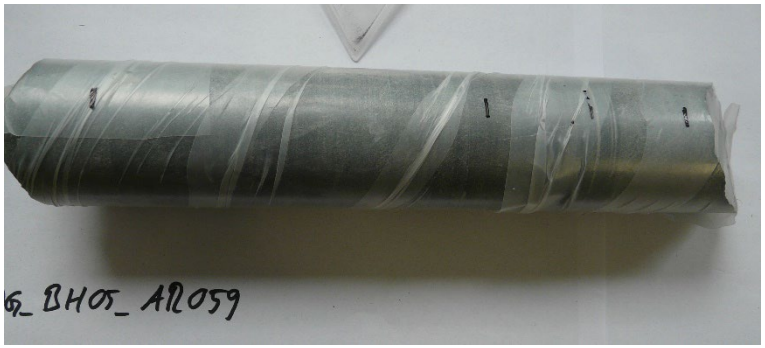
IG_BH05_PW029: 986.30-986.68 m



IG_BH05_AR033: 717.28-717.48 m



IG_BH05_AR052: 855.93-856.16 m



IG_BH05_AR059: 978.81-979.10 m

APPENDIX B

Analytical Raw Data

Table B-1.1: Determination of gravimetric water content; sample weights, drying times and calculated water contents of core pieces used for aqueous extraction experiments

Sample	Date prepared	m (cryst.dish)	m (cryst+ rock)	02.07.2021	16.07.2021	30.07.2021									Sample	m(rock, wet)	m (rock, dry)
Drying times	days			7	21	35										g	g
IG_BH05_AQ001	25.06.2021	89.008	526.261	525.325	525.327										IG_BH05_AQ001	437.253	436.317
IG_BH05_AQ002	25.06.2021	87.505	433.894	433.371	433.358	433.358									IG_BH05_AQ002	346.389	345.853
IG_BH05_AQ003	25.06.2021	87.001	469.416	468.660	468.660										IG_BH05_AQ003	382.415	381.659
Sample	Date prepared	m (cryst.dish)	m (cryst+ rock)	13.07.2021	27.07.2021	10.08.2021	24.08.2021	14.09.2021	28.09.2021	13.10.2021	27.10.2021	11.11.2021	25.11.2021	09.12.2021			
Drying times	days			7	21	35	49	70	84	99	113	128	142	156			
IG_BH05_AQ004	06.07.2021	90.679	526.246	524.713	524.334	524.178	524.110	524.077	524.037	524.003	523.968	523.958	523.974	523.973	IG_BH05_AQ004	435.567	433.279
IG_BH05_AQ005	06.07.2021	92.967	487.798	487.221	487.199	487.192	487.190								IG_BH05_AQ005	394.831	394.223
Sample	Date prepared	m (cryst.dish)	m (cryst+ rock)	05.08.2021	23.08.2021	14.09.2021											
Drying times	days			7	25	47											
IG_BH05_AQ006	29.07.2021	93.406	664.726	663.737	663.731	663.734									IG_BH05_AQ006	571.320	570.325
IG_BH05_AQ007	29.07.2021	87.218	631.823	630.921	630.923										IG_BH05_AQ007	544.605	543.703
IG_BH05_AQ008	29.07.2021	90.029	549.595	549.044	549.025	549.030									IG_BH05_AQ008	459.566	458.996
IG_BH05_AQ009	29.07.2021	87.590	527.295	526.649	526.645	526.648									IG_BH05_AQ009	439.705	439.055
IG_BH05_AQ010	29.07.2021	88.043	575.237	574.577	574.562	574.565									IG_BH05_AQ010	487.194	486.519
IG_BH05_AQ011	29.07.2021	88.439	597.700	597.070	597.057	597.060									IG_BH05_AQ011	509.261	508.618
IG_BH05_AQ015	29.07.2021	88.787	465.838	465.278	465.27	465.273									IG_BH05_AQ015	377.051	376.483
IG_BH05_AQ016	29.07.2021	87.937	522.138	521.610	521.605	521.609									IG_BH05_AQ016	434.201	433.668
Sample	Date prepared	m (cryst.dish)	m (cryst+ rock)	20.08.2021	31.08.2021	14.09.2021											
Drying times	days			11	22	36											
IG_BH05_AQ012	09.08.2021	93.450	573.582	572.964	572.979	572.99									IG_BH05_AQ012	480.132	479.514
IG_BH05_AQ013	09.08.2021	87.839	510.381	509.843	509.844	509.856									IG_BH05_AQ013	422.542	422.004
IG_BH05_AQ014	09.08.2021	84.292	489.437	488.906	488.911	488.923									IG_BH05_AQ014	405.145	404.614
IG_BH05_AQ020	09.08.2021	91.516	523.950	523.338	523.362	523.374									IG_BH05_AQ020	432.434	431.822
IG_BH05_AQ021	09.08.2021	81.087	451.577	450.996	451.039	451.050									IG_BH05_AQ021	370.490	369.909
IG_BH05_AQ022	09.08.2021	86.536	502.510	501.566	501.594	501.600									IG_BH05_AQ022	415.974	415.030
Sample	Date prepared	m (cryst.dish)	m (cryst+ rock)	20.08.2021	10.09.2021	24.09.2021	08.10.2021	22.10.2021	04.11.2021								
Drying times	days			7	28	42	56	70	83								
IG_BH05_AQ017	13.08.2021	92.806	508.555	508.033	508.044	508.038	508.033	508.023	508.030						IG_BH05_AQ017	415.749	415.217
IG_BH05_AQ018	13.08.2021	87.192	561.737	560.942	560.892	560.918	560.915	560.901	560.903						IG_BH05_AQ018	474.545	473.700
IG_BH05_AQ019	13.08.2021	92.883	571.568	570.845	570.821	570.813	570.805	570.793	570.797						IG_BH05_AQ019	478.685	477.910
IG_BH05_AQ023	13.08.2021	88.397	501.339	500.710	500.696	500.686	500.690	500.666	500.670						IG_BH05_AQ023	412.942	412.269
IG_BH05_AQ024	13.08.2021	89.976	554.165	553.704	553.673	553.661	553.652	553.635	553.637						IG_BH05_AQ024	464.189	463.659
IG_BH05_AQ025	13.08.2021	88.333	562.587	562.190	562.168	562.155	562.147	562.128	562.130						IG_BH05_AQ025	474.254	473.795
Sample	Date prepared	m (cryst.dish)	m (cryst+ rock)	13.09.2021	23.09.2021	07.10.2021	21.10.2021	04.11.2021									
Drying times	days			11	21	35	49	63									
IG_BH05_AQ026	02.09.2021	89.923	455.990	455.665	455.651	455.64	455.636	455.634							IG_BH05_AQ026	366.067	365.711
IG_BH05_AQ027	02.09.2021	91.409	527.697	527.376	527.349	527.336	527.326	527.324							IG_BH05_AQ027	436.288	435.915
IG_BH05_AQ028	02.09.2021	88.298	436.494	436.105	436.090	436.081	436.077	436.075							IG_BH05_AQ028	348.196	347.777
IG_BH05_AQ029	02.09.2021	92.999	469.156	468.675	468.656	468.646	468.644								IG_BH05_AQ029	376.157	375.645

Table B-1.1: Continued

			m(dry surf)	02.07.2021	16.07.2021	30.07.2021	13.08.2021	27.08.2021	14.09.2021							Sample	m(rock, wet)	m (rock, dry)
Drying times	**days**			7	21	35	49	63	81								g	g
IG_BH05_AQ001-A	25.06.2021		192.867	192.488	192.481	192.483										IG_BH05_AQ001-A	192.867	192.481
IG_BH05_AQ001-B	25.06.2021		755.701	754.262	754.118	754.109	754.095	754.068	754.098							IG_BH05_AQ001-B	755.701	754.068
IG_BH05_AQ002-A	25.06.2021		276.458	276.030	276.012	276.008	276.000	275.993	276.000							IG_BH05_AQ002-A	276.458	275.993
IG_BH05_AQ002-B	25.06.2021		211.169	210.839	210.826	210.822	210.818	210.813	210.820							IG_BH05_AQ002-B	211.169	210.813
IG_BH05_AQ003-A	25.06.2021		188.290	187.962	187.958	187.960										IG_BH05_AQ003-A	188.290	187.958
IG_BH05_AQ003-B	25.06.2021		199.075	198.643	198.637	198.638										IG_BH05_AQ003-B	199.075	198.637
			m(dry surf)	13.07.2021	27.07.2021	10.08.2021	24.08.2021	14.09.2021	28.09.2021	13.10.2021	28.10.2021	11.11.2021	25.11.2021					
Drying times	**days**			7	21	35	49	70	84	99	114	128	142					
IG_BH05_AQ004-A	06.07.2021		190.654	190.221	190.079	190.016	189.988	189.973	189.957	189.942	189.938	189.924	189.925			IG_BH05_AQ004-A	190.654	189.924
IG_BH05_AQ004-B	06.07.2021		160.908	160.516	160.389	160.342	160.319	160.307	160.295	160.281	160.278	160.265	160.265			IG_BH05_AQ004-B	160.908	160.265
IG_BH05_AQ005-A	06.07.2021		191.464	191.176	191.164	191.160	191.157	191.159								IG_BH05_AQ005-A	191.464	191.157
IG_BH05_AQ005-B	06.07.2021		246.244	245.869	245.854	245.847	245.843	245.849								IG_BH05_AQ005-B	246.244	245.843
			m(dry surf)	05.08.2021	23.08.2021	14.09.2021	28.09.2021											
Drying times	**days**			7	25	47	61											
IG_BH05_AQ006-A	29.07.2021		221.437	221.028	221.024	221.026										IG_BH05_AQ006-A	221.437	221.024
IG_BH05_AQ006-B	29.07.2021		294.755	294.231	294.223	294.223										IG_BH05_AQ006-B	294.755	294.223
IG_BH05_AQ007-A	29.07.2021		210.768	210.379	210.369	210.368										IG_BH05_AQ007-A	210.768	210.368
IG_BH05_AQ007-B	29.07.2021		171.173	170.865	170.866											IG_BH05_AQ007-B	171.173	170.865
IG_BH05_AQ008-A	29.07.2021		217.735	217.471	217.459	217.458										IG_BH05_AQ008-A	217.735	217.458
IG_BH05_AQ008-B	29.07.2021		238.379	238.094	238.082	238.082										IG_BH05_AQ008-B	238.379	238.082
IG_BH05_AQ009-A	29.07.2021		252.625	252.255	252.248	252.250										IG_BH05_AQ009-A	252.625	252.248
IG_BH05_AQ009-B	29.07.2021		221.169	220.844	220.838	220.838										IG_BH05_AQ009-B	221.169	220.838
IG_BH05_AQ010-A	29.07.2021		234.768	234.459	234.450	234.449										IG_BH05_AQ010-A	234.768	234.449
IG_BH05_AQ010-B	29.07.2021		202.477	202.197	202.186	202.184										IG_BH05_AQ010-B	202.477	202.184
IG_BH05_AQ011-A	29.07.2021		263.003	262.653	262.638	262.637										IG_BH05_AQ011-A	263.003	262.637
IG_BH05_AQ011-B	29.07.2021		211.995	211.704	211.693	211.694										IG_BH05_AQ011-B	211.995	211.693
IG_BH05_AQ015-A	29.07.2021		209.513	209.179	209.170	209.169										IG_BH05_AQ015-A	209.513	209.169
IG_BH05_AQ015-B	29.07.2021		196.685	196.365	196.363											IG_BH05_AQ015-B	196.685	196.363
IG_BH05_AQ016-A	29.07.2021		431.100	430.587	430.570	430.571										IG_BH05_AQ016-A	431.100	430.570
IG_BH05_AQ016-B	29.07.2021		204.075	203.833	203.823	203.814	203.812									IG_BH05_AQ016-B	204.075	203.812

Table B-1.1: Continued

			m(dry surf)	20.08.2021	10.09.2021	17.09.2021	01.10.2021	15.10.2021	28.10.2021	11.11.2021						Sample	m(rock, wet)	m (rock, dry)
Drying times	**days**			11	32	39	53	67	80	94							g	g
IG_BH05_AQ012-A	09.08.2021		272.243	271.923	271.915	271.909	271.902	271.898	271.893	271.891						IG_BH05_AQ012-A	272.243	271.891
IG_BH05_AQ012-B	09.08.2021		169.541	169.336	169.323	169.323										IG_BH05_AQ012-B	169.541	169.323
IG_BH05_AQ013-A	09.08.2021		216.002	215.742	215.729	215.729										IG_BH05_AQ013-A	216.002	215.729
IG_BH05_AQ013-B	09.08.2021		325.164	324.775	324.766	324.766										IG_BH05_AQ013-B	325.164	324.766
IG_BH05_AQ014-A	09.08.2021		304.155	303.783	303.764	303.766										IG_BH05_AQ014-A	304.155	303.764
IG_BH05_AQ014-B	09.08.2021		435.790	435.250	435.241	435.235	435.223	435.221								IG_BH05_AQ014-B	435.790	435.221
IG_BH05_AQ020-A	09.08.2021		314.640	314.218	314.211	314.209										IG_BH05_AQ020-A	314.640	314.209
IG_BH05_AQ020-B	09.08.2021		361.441	360.959	360.952	360.948	360.940	360.934	360.925	360.925						IG_BH05_AQ020-B	361.441	360.925
IG_BH05_AQ021-A	09.08.2021		237.389	237.408	237.039	237.040										IG_BH05_AQ021-A	237.389	237.039
IG_BH05_AQ021-B	09.08.2021		324.731	324.258	324.239	324.233	324.222	324.220								IG_BH05_AQ021-B	324.731	324.220
IG_BH05_AQ022-A	09.08.2021		298.931	298.468	298.465	298.463										IG_BH05_AQ022-A	298.931	298.463
IG_BH05_AQ022-B	09.08.2021		304.814	304.235	304.232	304.227	304.216	304.216								IG_BH05_AQ022-B	304.814	304.216
			m(dry surf)	20.08.2021	10.09.2021	17.09.2021	01.10.2021	15.10.2021	28.10.2021	11.11.2021								
Drying times	**days**			7	28	35	49	63	76	90								
IG_BH05_AQ017-A	13.08.2021		409.264	408.755	408.738	408.732	408.722	408.717	408.713	408.712						IG_BH05_AQ017-A	409.264	408.712
IG_BH05_AQ017-B	13.08.2021		292.620	292.245	292.238	292.237										IG_BH05_AQ017-B	292.620	292.237
IG_BH05_AQ018-A	13.08.2021		276.595	276.066	276.050	276.049										IG_BH05_AQ018-A	276.595	276.049
IG_BH05_AQ018-B	13.08.2021		399.162	398.450	398.442	398.442										IG_BH05_AQ018-B	399.162	398.442
IG_BH05_AQ019-A	13.08.2021		332.119	331.500	331.481	331.480										IG_BH05_AQ019-A	332.119	331.480
IG_BH05_AQ019-B	13.08.2021		407.409	406.729	406.713	406.709	406.697	406.691	406.680	406.680						IG_BH05_AQ019-B	407.409	406.680
IG_BH05_AQ023-A	13.08.2021		359.605	358.992	358.973	358.966	358.953	358.948	358.942	358.942						IG_BH05_AQ023-A	359.605	358.942
IG_BH05_AQ023-B	13.08.2021		403.948	403.257	403.240	403.237	403.221	403.219								IG_BH05_AQ023-B	403.948	403.219
IG_BH05_AQ024-A	13.08.2021		175.391	175.165	175.146	175.143	175.134	175.132								IG_BH05_AQ024-A	175.391	175.132
IG_BH05_AQ024-B	13.08.2021		169.773	169.564	169.545	169.543	169.535	169.533								IG_BH05_AQ024-B	169.773	169.533
IG_BH05_AQ025-A	13.08.2021		207.668	207.476	207.460	207.456	207.444	207.411	207.403	207.401						IG_BH05_AQ025-A	207.668	207.401
IG_BH05_AQ025-B	13.08.2021		225.767	225.582	225.566	225.563	225.555	225.553								IG_BH05_AQ025-B	225.767	225.553
			m(dry surf)	13.09.2021	23.09.2021	07.10.2021	21.10.2021	04.11.2021	18.11.2021	02.12.2021								
Drying times	**days**			11	21	35	49	63	77	91								
IG_BH05_AQ026-A	02.09.2021		185.607	185.395	185.382	185.370	185.367	185.358	185.356							IG_BH05_AQ026-A	185.607	185.356
IG_BH05_AQ026-B	02.09.2021		130.056	129.911	129.904	129.898	129.891	129.885	129.884							IG_BH05_AQ026-B	130.056	129.884
IG_BH05_AQ027-A	02.09.2021		243.247	243.068	243.055	243.049	243.044	243.038	243.036							IG_BH05_AQ027-A	243.247	243.036
IG_BH05_AQ027-B	02.09.2021		210.845	210.688	210.676	210.669	210.665	210.662	210.660							IG_BH05_AQ027-B	210.845	210.660
IG_BH05_AQ028-A	02.09.2021		183.373	183.118	183.108	183.103	183.098	183.094	183.093							IG_BH05_AQ028-A	183.373	183.093
IG_BH05_AQ028-B	02.09.2021		215.931	215.633	215.622	215.616	215.611	215.607	215.605							IG_BH05_AQ028-B	215.931	215.605
IG_BH05_AQ029-A	02.09.2021		264.218	263.871	263.838	263.832	263.827	263.822	263.821							IG_BH05_AQ029-A	264.218	263.821
IG_BH05_AQ029-B	02.09.2021		315.790	315.290	315.263	315.245	315.235	315.231	315.227	315.226						IG_BH05_AQ029-B	315.790	315.226

Table B-1.2: Determination of gravimetric water content; sample weights, drying times and calculated water contents of rim core pieces of samples used for out-diffusion experiments

	Set-up date	m(dry surf)		02.07.2021	16.07.2021	30.07.2021	13.08.2021	27.08.2021	14.09.2021							Sample	m wet	m dry
Drying time (days)				7	21	35	49	63	81								g	g
IG_BH05_PW001-A	25.06.2021	266.501		265.906	265.886	265.886										IG_BH05_PW001-A	266.501	265.886
IG_BH05_PW001-B	25.06.2021	615.987		614.686	614.619	614.611	614.597	614.573	614.606							IG_BH05_PW001-B	615.987	614.573
IG_BH05_PW002-A	25.06.2021	178.501		178.227	178.216	178.214										IG_BH05_PW002-A	178.501	178.214
IG_BH05_PW002-B	25.06.2021	151.922		151.67	151.655	151.652	151.648	151.646								IG_BH05_PW002-B	151.922	151.646
IG_BH05_PW003-A	25.06.2021	227.343		226.924	226.914	226.913										IG_BH05_PW003-A	227.343	226.913
IG_BH05_PW003-B	25.06.2021	199.911		199.513	199.505	199.505										IG_BH05_PW003-B	199.911	199.505
	Set-up date	m(dry surf)		13.07.2021	27.07.2021	10.08.2021	24.08.2021	10.09.2021	24.09.2021	08.10.2021	22.10.2021	09.11.2021	18.11.2021	02.12.2021				
Drying time (days)				7	21	35	49	66	80	94	108	126	135	149				
IG_BH05_PW004-A	06.07.2021	153.211		152.916	152.809	152.763	152.741	152.732	152.720	152.711	152.706	152.695	152.694			IG_BH05_PW004-A	153.211	152.694
IG_BH05_PW004-B	06.07.2021	482.521		481.824	481.549	481.405	481.327	481.269	481.226	481.188	481.152	481.122	481.117	481.116		IG_BH05_PW004-B	482.521	481.117
IG_BH05_PW005-A	06.07.2021	224.537		224.184	224.165	224.157	224.154	224.154								IG_BH05_PW005-A	224.537	224.154
IG_BH05_PW005-B	06.07.2021	127.565		127.376	127.371	127.365	127.361	127.363								IG_BH05_PW005-B	127.565	127.361
	Set-up date	m(dry surf)		26.07.2021	10.08.2021	23.08.2021	14.09.2021	28.09.2021										
Drying time (days)				7	22	35	57	71										
IG_BH05_PW006-A	19.07.2021	222.916		222.489	222.472	222.468	222.469									IG_BH05_PW006-A	222.916	222.468
IG_BH05_PW006-B	19.07.2021	199.274		198.899	198.890	198.886	198.884									IG_BH05_PW006-B	199.274	198.884
IG_BH05_PW007-A	19.07.2021	192.601		192.307	192.302	192.302										IG_BH05_PW007-A	192.601	192.302
IG_BH05_PW007-B	19.07.2021	276.321		275.834	275.827	275.823	275.823									IG_BH05_PW007-B	276.321	275.823
IG_BH05_PW008-A	19.07.2021	362.828		362.351	362.331	362.322	362.324									IG_BH05_PW008-A	362.828	362.322
IG_BH05_PW008-B	19.07.2021	258.447		258.142	258.129	258.127										IG_BH05_PW008-B	258.447	258.127
IG_BH05_PW009-A	19.07.2021	136.648		136.429	136.424	136.419	136.417									IG_BH05_PW009-A	136.648	136.417
IG_BH05_PW009-B	19.07.2021	206.091		205.756	205.751	205.746	205.746									IG_BH05_PW009-B	206.091	205.746
IG_BH05_PW010-A	19.07.2021	225.827		225.537	225.527	225.525										IG_BH05_PW010-A	225.827	225.525
IG_BH05_PW010-B	19.07.2021	124.059		123.912	123.906	123.902	123.896	123.894								IG_BH05_PW010-B	124.059	123.894
IG_BH05_PW011-A	19.07.2021	281.167		280.805	280.791	280.788	280.789									IG_BH05_PW011-A	281.167	280.788
IG_BH05_PW011-B	19.07.2021	223.809		223.521	223.511	223.503	223.505									IG_BH05_PW011-B	223.809	223.503
	Set-up date	m(dry surf)		05.08.2021	23.08.2021	10.09.2021	17.09.2021	01.10.2021										
Drying time (days)				7	25	43	50	64										
IG_BH05_PW015-A	29.07.2021	152.786		152.547	152.543	152.539	152.532	152.528								IG_BH05_PW015-A	152.786	152.528
IG_BH05_PW015-B	29.07.2021	105.873		105.714	105.710	105.703	105.700	105.698								IG_BH05_PW015-B	105.873	105.698
IG_BH05_PW016-A	29.07.2021	244.830		244.511	244.502	244.494	244.494									IG_BH05_PW016-A	244.830	244.494
IG_BH05_PW016-B	29.07.2021	146.224		146.036	146.030	146.022	146.024									IG_BH05_PW016-B	146.224	146.022

Table B-1.2: Continued

	Set-up date	m(dry surf)		20.08.2021	31.08.2021	14.09.2021									Sample	m wet	m dry
Drying time (days)				11	22	36										g	g
IG_BH05_PW012-A	09.08.2021	164.244		164.044	164.030	164.031									IG_BH05_PW012-A	164.244	164.03
IG_BH05_PW012-B	09.08.2021	272.632		272.304	272.288	272.290									IG_BH05_PW012-B	272.632	272.288
IG_BH05_PW013-A	09.08.2021	181.586		181.355	181.345	181.347									IG_BH05_PW013-A	181.586	181.345
IG_BH05_PW013-B	09.08.2021	203.490		203.221	203.206	203.208									IG_BH05_PW013-B	203.490	203.206
IG_BH05_PW014-A	09.08.2021	158.536		158.361	158.345	158.345									IG_BH05_PW014-A	158.536	158.345
IG_BH05_PW014-B	09.08.2021	160.103		159.929	159.916	159.916									IG_BH05_PW014-B	160.103	159.916
IG_BH05_PW020-A	09.08.2021	204.604		204.363	204.354	204.356									IG_BH05_PW020-A	204.604	204.354
IG_BH05_PW020-B	09.08.2021	202.287		202.043	202.031	202.032									IG_BH05_PW020-B	202.287	202.031
IG_BH05_PW021-A	09.08.2021	548.149		547.474	547.450	547.452									IG_BH05_PW021-A	548.149	547.45
IG_BH05_PW021-B	09.08.2021	198.738		198.473	198.448	198.450									IG_BH05_PW021-B	198.738	198.448
IG_BH05_PW022-A	09.08.2021	232.210		231.731	231.717	231.719									IG_BH05_PW022-A	232.210	231.717
IG_BH05_PW022-B	09.08.2021	256.689		255.908	255.893	255.892									IG_BH05_PW022-B	256.689	255.892
	Set-up date	**m(dry surf)**		**20.08.2021**	**10.09.2021**	**24.09.2021**	**08.10.2021**	**22.10.2021**	**04.11.2021**								
Drying time (days)				7	28	42	56	70	83								
IG_BH05_PW017-A	13.08.2021	238.392		238.075	238.072	238.064	238.063								IG_BH05_PW017-A	238.392	238.063
IG_BH05_PW017-B	13.08.2021	170.551		170.34	172.334	170.329	170.327								IG_BH05_PW017-B	170.551	170.327
IG_BH05_PW018-A	13.08.2021	224.328		223.942	223.927	223.918	223.912	223.911							IG_BH05_PW018-A	224.328	223.911
IG_BH05_PW018-B	13.08.2021	173.288		172.992	172.979	172.968	172.963	172.961							IG_BH05_PW018-B	173.288	172.961
IG_BH05_PW019-A	13.08.2021	285.865		285.396	285.378	285.368	285.364	285.361	285.359						IG_BH05_PW019-A	285.865	285.359
IG_BH05_PW019-B	13.08.2021	196.566		196.26	196.248	196.242	196.237	196.236							IG_BH05_PW019-B	196.566	196.236
IG_BH05_PW023-A	13.08.2021	139.629		139.434	139.427	139.420	139.415	139.415							IG_BH05_PW023-A	139.629	139.415
IG_BH05_PW023-B	13.08.2021	133.248		133.07	133.065	133.059	133.058								IG_BH05_PW023-B	133.248	133.058
IG_BH05_PW024-A	13.08.2021	152.606		152.318	152.295	152.287	152.283	152.279	152.277						IG_BH05_PW024-A	152.606	152.277
IG_BH05_PW024-B	13.08.2021	164.370		164.14	164.126	164.115	164.108	164.106							IG_BH05_PW024-B	164.370	164.106
IG_BH05_PW025-A	13.08.2021	187.783		187.623	187.611	187.604	187.599	187.596	187.594						IG_BH05_PW025-A	187.783	187.594
IG_BH05_PW025-B	13.08.2021	116.634		116.541	116.534	116.526	116.523	116.522							IG_BH05_PW025-B	116.634	116.522
	Set-up date	**m(dry surf)**		**13.09.2021**	**23.09.2021**	**07.10.2021**	**21.10.2021**	**04.11.2021**	**18.11.2021**								
Drying time (days)				11	21	35	49	63	77								
IG_BH05_PW026-A	02.09.2021	167.513		167.298	167.282	167.277	167.267	167.263	167.261						IG_BH05_PW026-A	167.513	167.261
IG_BH05_PW026-B	02.09.2021	129.632		129.479	129.47	129.467	129.463	129.459	129.459						IG_BH05_PW026-B	129.632	129.459
IG_BH05_PW027-A	02.09.2021	227.077		226.909	226.899	226.892	226.885	226.881	226.88						IG_BH05_PW027-A	227.077	226.88
IG_BH05_PW027-B	02.09.2021	138.084		137.993	137.984	137.98	137.974	137.952	137.951						IG_BH05_PW027-B	138.084	137.951
IG_BH05_PW028-A	02.09.2021	212.555		212.29	212.278	212.273	212.27	212.265	212.264						IG_BH05_PW028-A	212.555	212.264
IG_BH05_PW028-B	02.09.2021	130.414		130.255	130.246	130.243	130.239	130.233	130.234						IG_BH05_PW028-B	130.414	130.233
IG_BH05_PW029-A	02.09.2021	223.648		223.258	223.247	223.239	223.234	223.227	223.229						IG_BH05_PW029-A	223.648	223.227
IG_BH05_PW029-B	02.09.2021	144.155		143.917	143.909	143.9	143.898								IG_BH05_PW029-B	144.155	143.898
	Set-up date	**m(dry surf)**		**23.03.2022**	**06.04.2022**	**20.04.2022**	**04.05.2022**	**18.05.2022**	**01.06.2022**								
Drying time (days)				9	23	37	51	65	79								
IG_BH05_AR033-A	14.03.2022	226.480		226.055	226.050	226.028	226.038	226.040							IG_BH05_AR033-A	226.480	226.028
IG_BH05_AR033-B	14.03.2022	376.999		376.248	376.238	376.225	376.235	376.241	376.236						IG_BH05_AR033-B	376.999	376.225
IG_BH05_AR052-A	14.03.2022	192.251		192.220	192.217	192.203	192.208	192.210							IG_BH05_AR052-A	192.251	192.203
IG_BH05_AR052-B	14.03.2022	135.558		135.533	135.532	135.517	135.524	135.527	135.526						IG_BH05_AR052-B	135.558	135.517
IG_BH05_AR059-A	14.03.2022	175.005		174.931	174.918	174.902	174.900								IG_BH05_AR059-A	175.005	174.9
IG_BH05_AR059-B	14.03.2022	275.875		275.783	275.766	275.760	275.765	275.766							IG_BH05_AR059-B	275.875	275.76

Table B-1.3: Determination of gravimetric water content; sample weights, drying times and calculated water contents of core pieces used for isotope diffusive exchange experiments

Sample	Date start drying	Drying times (days	m (cryst.dish)	m (cryst+ rock)	13.09.2021	27.09.2021	12.10.2021	27.10.2021	09.11.2021	23.11.2021	07.12.2021		mass dry	m rock wet	m rock dry
IG_BH05_PW001 LAB	25.08.2021	33	89.131	437.260	436.657	436.655							436.655	348.129	347.524
IG_BH05_PW001 ICE	25.08.2021	33	89.020	436.933	436.338	436.339							436.338	347.913	347.318
IG_BH05_PW002 LAB	25.08.2021	104	85.213	487.081	486.567	486.561	486.550	486.540	486.526	486.535	486.536		486.526	401.868	401.313
IG_BH05_PW002 ICE	25.08.2021	104	93.905	493.990	493.483	493.477	493.458	493.450	493.435	493.444	493.446		493.435	400.085	399.530
IG_BH05_PW003 LAB	25.08.2021	33	86.940	490.470	489.814	489.812							489.812	403.53	402.872
IG_BH05_PW003 ICE	25.08.2021	63	87.203	488.100	487.379	487.369	487.364	487.366					487.364	400.897	400.161
Sample	**Date start drying**	**Drying times (days**	**m (cryst.dish)**	**m (cryst+ rock)**	**28.09.2021**	**12.10.2021**	**27.10.2021**	**09.11.2021**	**23.11.2021**	**07.12.2021**	**21.12.2021**		**mass dry**	**m rock wet**	**m rock dry**
IG_BH05_PW004 LAB	13.09.2021	99	87.221	454.416	453.392	453.300	453.274	453.203	453.221	453.211	453.211		453.203	367.195	365.982
IG_BH05_PW004 ICE	13.09.2021	99	92.973	464.661	463.633	463.542	463.521	463.444	463.464	463.453	463.452		463.444	371.688	370.471
IG_BH05_PW005 LAB	13.09.2021	85	91.801	489.887	489.313	489.304	489.299	489.276	489.287	489.289			489.276	398.086	397.475
IG_BH05_PW005 ICE	13.09.2021	85	85.982	484.548	483.987	483.980	483.972	483.953	483.960	483.960			483.953	398.566	397.971
Sample	**Date start drying**	**Drying times (days**	**m (cryst.dish)**	**m (cryst+ rock)**	**28.09.2021**	**12.10.2021**	**27.10.2021**	**09.11.2021**	**23.11.2021**	**07.12.2021**	**21.12.2021**		**mass dry**	**m rock wet**	**m rock dry**
IG_BH05_PW006 LAB	21.09.2021	36	89.840	548.281	547.616	547.608	547.606						547.606	458.441	457.766
IG_BH05_PW006 ICE	21.09.2021	36	86.934	545.639	544.952	544.945	544.943						544.943	458.705	458.009
IG_BH05_PW007 LAB	21.09.2021	36	88.823	596.363	595.612	595.604	595.604						595.604	507.54	506.781
IG_BH05_PW007 ICE	21.09.2021	36	91.268	599.006	598.239	598.232	598.232						598.232	507.738	506.964
IG_BH05_PW008 LAB	21.09.2021	91	92.200	566.696	566.207	566.191	566.175	566.153	566.164	566.167	566.162		566.153	474.496	473.953
IG_BH05_PW008 ICE	21.09.2021	63	88.670	564.233	563.767	563.746	563.739	563.725	563.727				563.725	475.563	475.055
IG_BH05_PW009 LAB	21.09.2021	91	83.821	607.474	606.516	606.500	606.489	606.476	606.481	606.485	606.482		606.476	523.653	522.655
IG_BH05_PW009 ICE	21.09.2021	63	91.201	615.519	614.748	614.720	614.706	614.697	614.698				614.697	524.318	523.496
IG_BH05_PW010 LAB	21.09.2021	91	86.036	530.763	530.190	530.171	530.163	530.145	530.154	530.159	530.154		530.145	444.727	444.109
IG_BH05_PW010 ICE	21.09.2021	91	88.788	535.572	535.000	534.981	534.969	534.953	534.962	534.967	534.963		534.953	446.784	446.165
IG_BH05_PW011 LAB	21.09.2021	91	87.602	556.009	555.428	555.408	555.400	555.379	555.386	555.390	555.385		555.379	468.407	467.777
IG_BH05_PW011 ICE	21.09.2021	77	90.365	560.827	560.230	560.209	560.195	560.183	560.187	560.188			560.183	470.462	469.818
Sample	**Date start drying**	**Drying times (days**	**m (cryst.dish)**	**m (cryst+ rock)**	**07.10.2021**	**21.10.2021**	**04.11.2021**	**18.11.2021**	**02.12.2021**	**16.12.2021**	**22.12.2021**		**mass dry**	**m rock wet**	**m rock dry**
IG_BH05_PW015 LAB	30.09.2021	63	93.453	575.459	574.767	574.756	574.746	574.756	574.758				574.746	482.006	481.293
IG_BH05_PW015 ICE	30.09.2021	63	87.007	570.495	569.801	569.792	569.782	569.790	569.792				569.782	483.488	482.775
IG_BH05_PW016 LAB	30.09.2021	83	89.549	484.176	483.711	483.699	483.694	483.697	483.700	483.688	483.689		483.688	394.627	394.139
IG_BH05_PW016 ICE	30.09.2021	49	91.519	487.493	487.014	487.005	487.002	487.002					487.002	395.974	395.483

Table B-1.3: Continued

Sample	Date start drying	Drying times (days	m (cryst.dish)	m (cryst+ rock)	27.10.2021	10.11.2021	24.11.2021	08.12.2021	22.12.2021	13.01.2022	26.01.2022		mass dry	m rock wet	m rock dry
IG_BH05_PW012 LAB	19.10.2021	99	94.267	578.268	577.712	577.709	577.701	577.688	577.683	577.677	577.676		577.676	484.001	483.409
IG_BH05_PW012 ICE	19.10.2021	22	81.089	554.300	553.740	553.739							553.739	473.211	472.650
IG_BH05_PW013 LAB	19.10.2021	22	87.591	487.313	486.818	486.819							486.818	399.722	399.227
IG_BH05_PW013 ICE	19.10.2021	64	87.839	485.271	484.753	484.757	484.754	484.743	484.741				484.741	397.432	396.902
IG_BH05_PW014 LAB	19.10.2021	64	88.441	522.110	521.619	521.616	521.612	521.597	521.599				521.597	433.669	433.156
IG_BH05_PW014 ICE	19.10.2021	22	88.790	521.092	520.576	520.574							520.574	432.302	431.784
IG_BH05_PW017 LAB	19.10.2021	36	89.356	544.151	543.623	543.630	543.629						543.623	454.795	454.267
IG_BH05_PW017 ICE	19.10.2021	99	87.170	539.297	538.778	538.787	538.771	538.762	538.766	538.757	538.759		538.757	452.127	451.587
IG_BH05_PW018 LAB	19.10.2021	64	87.842	552.772	552.203	552.209	552.202	552.191	552.193				552.191	464.93	464.349
IG_BH05_PW018 ICE	19.10.2021	22	90.678	557.507	556.946	556.946							556.946	466.829	466.268
IG_BH05_PW019 LAB	19.10.2021	22	83.845	519.790	519.178	519.177							519.177	435.945	435.332
IG_BH05_PW019 ICE	19.10.2021	64	88.639	524.756	524.154	524.157	524.152	524.141	524.140				524.140	436.117	435.501
IG_BH05_PW020 LAB	19.10.2021	64	84.294	637.533	636.900	636.896	636.889	636.875	636.873				636.873	553.239	552.579
IG_BH05_PW020 ICE	19.10.2021	22	93.404	647.993	647.342	647.340							647.340	554.589	553.936
IG_BH05_PW021 LAB	19.10.2021	64	86.535	558.354	557.723	557.719	557.716	557.703	557.704				557.703	471.819	471.168
IG_BH05_PW021 ICE	19.10.2021	64	90.029	558.933	558.314	558.310	558.303	558.294	558.292				558.292	468.904	468.263
IG_BH05_PW022 LAB	19.10.2021	86	88.044	534.279	533.479	533.477	533.470	533.454	533.461	533.452			533.452	446.235	445.408
IG_BH05_PW022 ICE	19.10.2021	22	87.939	536.033	535.297	535.298							535.297	448.094	447.358
IG_BH05_PW023 LAB	19.10.2021	64	89.520	511.696	511.119	511.120	511.115	511.103	511.103				511.103	422.176	421.583
IG_BH05_PW023 ICE	19.10.2021	99	89.022	512.127	511.525	511.520	511.515	511.505		511.499	511.500		511.499	423.105	422.477
IG_BH05_PW024 LAB	19.10.2021	99	94.763	448.100	447.592	447.581	447.572	447.554		447.550	447.550		447.550	353.337	352.787
IG_BH05_PW024 ICE	19.10.2021	99	86.416	444.454	443.903	443.892	443.884	443.868	443.864	443.857	443.858		443.857	358.038	357.441
IG_BH05_PW025 LAB	19.10.2021	64	87.507	526.459	526.076	526.068	526.059	526.049	526.048				526.048	438.952	438.541
IG_BH05_PW025 ICE	19.10.2021	99	89.342	524.624	524.233	524.226	524.218	524.207	524.203	524.196	524.197		524.196	435.282	434.854

Sample	Date start drying	Drying times (days	m (cryst.dish)	m (cryst+ rock)	10.11.2021	24.11.2021	08.12.2021	22.12.2021	13.01.2022	26.01.2022			mass dry	m rock wet	m rock dry
IG_BH05_PW026 LAB	02.11.2021	50	85.366	466.718	466.402	466.392	466.375	466.375					466.375	381.352	381.009
IG_BH05_PW026 ICE	02.11.2021	50	87.824	466.222	465.861	465.848	465.835	465.837					465.835	378.398	378.011
IG_BH05_PW027 LAB	02.11.2021	50	87.552	568.017	567.611	567.592	567.579	567.577					567.577	480.465	480.025
IG_BH05_PW027 ICE	02.11.2021	50	88.079	565.846	565.395	565.377	565.365	565.363					565.363	477.767	477.284
IG_BH05_PW028 LAB	02.11.2021	50	86.261	469.461	468.995	468.978	468.967	468.968					468.967	383.2	382.706
IG_BH05_PW028 ICE	02.11.2021	50	88.445	473.226	472.723	472.709	472.696	472.696					472.696	384.781	384.251
IG_BH05_PW029 LAB	02.11.2021	50	88.241	557.975	557.090	557.069	557.049	557.048					557.048	469.734	468.807
IG_BH05_PW029 ICE	02.11.2021	85	91.125	558.252	557.330	557.307	557.289	557.284	557.269	557.267			557.267	467.127	466.142

Sample	Date start drying	Drying times (days	m (cryst.dish)	m (cryst+ rock)	31.05.2022	14.06.2022	29.06.2022	13.07.2022	28.07.2022	10.08.2022			mass dry	m rock wet	m rock dry
IG_BH05_AR059 LAB	24.05.2022	78	88.081	391.181	390.905	390.900	390.906	390.898	390.907	390.894			390.894	303.100	302.813
IG_BH05_AR059 ICE	24.05.2022	78	89.016	390.174	389.879	389.884	389.888	389.882	389.891	389.875			389.875	301.158	300.859

Table B-1.4: Determination of gravimetric water content; sample weights, drying times and calculated water contents of core pieces used for out-diffusion experiments

Sample	Date start drying	Drying times (days)	m wet surface	m dry surface	m wet surf	m dry surf	18.11.2021	02.12.2021	16.12.2021	05.01.2022	19.01.2022	03.02.2022	16.02.2022	02.03.2022	17.03.2022	31.03.2022	19.04.2022	03.05.2022	18.05.2022	31.05.2022	14.06.2022	29.06.2022	13.07.2022	28.07.2022	m (dry)	m(PW) b.e.	m(PW) a.e.
			g	g	g	g	g	g	g	g	g	g	g	g	g	g	g	g	g	g	g	g	g	g	g	g	g
Drying time (days)																											
PW001	12.11.2021	125	1433.106	1433.079	1433.672	1433.082	1430.922	1430.574	1430.451	1430.455	1430.402	1430.394	1430.387	1430.362	1430.364										1430.362	2.717	2.720
PW002	12.11.2021	54	1439.948	1439.895	1440.054	1439.823	1437.603	1437.486	1437.412	1437.414															1437.412	2.483	2.411
PW003	12.11.2021	172	1424.088	1423.929	1424.097	1423.880	1421.522	1421.250	1421.161	1421.178	1421.116	1421.108	1421.102	1421.072	1421.076	1421.083	1421.061	1421.070							1421.061	2.868	2.819
PW004	12.11.2021	258	1639.730	1639.730	1639.696	1639.631	1638.328	1637.678	1637.191	1636.864	1636.652	1636.478	1636.374	1636.274	1636.194	1636.148	1636.048	1636.030	1636.019	1636.006	1635.980	1635.994	1635.949	1635.948	1636.030	3.700	3.601
PW005	12.11.2021	172	1427.112	1427.080	1427.116	1427.027	1425.248	1424.962	1424.877	1424.883	1424.838	1424.834	1424.822	1424.799	1424.802	1424.815	1424.795	1424.803							1424.799	2.281	2.228
Sample	**Date start drying**	**Drying times (days)**	**m wet surface**	**m dry surface**	**m wet surf**	**m dry surf**	**07.12.2021**	**22.11.2021**	**05.01.2022**	**19.01.2022**	**03.02.2022**	**17.02.2022**	**03.03.2022**	**17.03.2022**	**31.03.2022**	**19.04.2022**	**03.05.2022**	**18.05.2022**									
			g	g	g	g	g	g	g	g	g	g	g	g	g	g	g	g									
Drying time (days)																											
PW006	30.11.2021	169	1427.611	1427.555	1427.651	1427.455	1424.961	1424.902	1424.913	1424.872	1424.864	1424.859	1424.807	1424.822	1424.832	1424.801	1424.816	1424.821							1424.801	2.754	2.654
PW007	30.11.2021	65	1394.153	1394.110	1394.316	1394.155	1391.901	1391.853	1391.873	1391.832	1391.832														1391.832	2.278	2.323
PW008	30.11.2021	36	1465.364	1465.295	1465.486	1465.301	1463.544	1463.455	1463.457																1463.455	1.840	1.846
PW009	30.11.2021	65	1473.619	1473.535	1474.209	1473.780	1470.843	1470.807	1470.817	1470.771	1470.770														1470.770	2.765	3.010
PW010	30.11.2021	36	1449.523	1449.520	1449.933	1449.735	1447.579	1447.511	1447.513																1447.511	2.009	2.224
PW011	30.11.2021	79	1464.240	1464.205	1464.501	1464.318	1462.311	1462.221	1462.186	1462.177	1462.172	1462.174													1462.172	2.033	2.146
PW012	30.11.2021	65	1511.679	1511.659	1511.952	1511.800	1509.757	1509.669	1509.635	1509.621	1509.620														1509.620	2.039	2.180
PW013	30.11.2021	79	1467.226	1467.202	1467.906	1467.530	1465.027	1464.974	1464.954	1464.940	1464.932	1464.932													1464.932	2.270	2.598
PW014	30.11.2021	65	1485.278	1485.270	1485.655	1485.471	1483.528	1483.440	1483.410	1483.395	1483.393														1483.393	1.877	2.078
PW015	30.11.2021	79	1477.526	1477.510	1477.590	1477.475	1475.524	1475.250	1475.222	1475.218	1475.205	1475.203													1475.203	2.307	2.272
PW016	30.11.2021	79	1447.520	1447.505	1447.680	1447.525	1445.537	1445.457	1445.438	1445.432	1445.428	1445.429													1445.428	2.077	2.097
Sample	**Date start drying**	**Drying times (days)**	**m wet surface**	**m dry surface**	**m wet surf**	**m dry surf**	**21.01.2022**	**03.02.2022**	**17.02.2022**	**03.03.2022**	**17.03.2022**	**31.03.2022**	**19.04.2022**	**03.05.2022**	**18.05.2022**												
			g	g	g	g	g	g	g	g	g	g	g	g	g												
Drying time (days)																											
PW017	12.01.2022	64	1428.345	1428.345	1428.480	1428.314	1426.428	1426.389	1426.375	1426.336	1426.336														1426.336	2.009	1.978
PW018	12.01.2022	64	1353.747	1353.657	1353.892	1353.561	1351.474	1351.439	1351.426	1351.384	1351.385														1351.384	2.273	2.177
PW019	12.01.2022	64	1446.181	1446.155	1446.232	1446.070	1443.802	1443.711	1443.693	1443.648	1443.647														1443.647	2.508	2.423
PW020	12.01.2022	111	1402.935	1402.924	1403.257	1403.086	1401.104	1401.071	1401.054	1401.016	1401.012	1401.029	1401.002	1401.016											1401.002	1.922	2.084
PW021	12.01.2022	64	1427.583	1427.565	1427.927	1427.729	1425.676	1425.639	1425.623	1425.587	1425.587														1425.587	1.978	2.142
PW022	12.01.2022	64	1423.297	1423.230	1423.664	1423.247	1419.698	1419.678	1419.657	1419.607	1419.608														1419.607	3.623	3.640
PW023	12.01.2022	64	1405.199	1405.170	1405.635	1405.331	1403.008	1402.985	1402.972	1402.927	1402.925														1402.925	2.245	2.406
PW024	12.01.2022	64	1460.157	1460.094	1460.144	1460.027	1458.197	1458.051	1457.993	1457.936	1457.937														1457.936	2.158	2.091
PW025	12.01.2022	126	1420.961	1420.928	1421.088	1420.948	1419.755	1419.713	1419.684	1419.636	1419.640	1419.650	1419.617	1419.631	1419.637										1419.617	1.311	1.331
Sample	**Date start drying**	**Drying times (days)**	**m wet surface**	**m dry surface**	**m wet surf**	**m dry surf**	**11.05.2022**	**18.05.2022**																			
			g	g	g	g	g	g																			
Drying time (days)																											
PW026	02.02.2022	105	1445.716	1445.630	1446.090	1445.920	1444.136	1444.137																	1444.136	1.494	1.784
PW027	02.02.2022	105	1450.834	1450.818	1450.967	1450.782	1449.527	1449.525																	1449.525	1.293	1.257
PW028	02.02.2022	105	1465.159	1465.130	1465.330	1465.145	1463.010	1463.008																	1463.008	2.122	2.137
PW029	02.02.2022	105	1440.303	1440.235	1440.942	1440.570	1437.439	1437.441																	1437.439	2.796	3.131
Sample	**Date start drying**	**Drying times (days)**	**m wet surface**	**m dry surface**	**m wet surf**	**m dry surf**	**01.12.2022**	**15.12.2022**	**03.01.2023**	**12.01.2023**	**25.01.2023**	**08.02.2023**	**21.02.2023**	**07.03.2023**	**21.03.2023**												
			g	g	g	g	g	g	g	g	g	g	g	g	g												
Drying time (days)																											
AR033	22.11.2022	119	1032.833	1032.790	1032.993	1032.822	1030.653	1030.619	1030.614	1030.609	1030.590	1030.592	1030.587	1030.587	1030.588										1030.587	2.203	2.235
AR052	22.11.2022	119	1523.570	1523.566	1524.116	1524.016	1523.216	1523.112	1523.082	1523.079	1523.049	1523.032	1523.039	1523.041	1523.044										1523.032	0.534	0.984
AR059	22.11.2022	105	1173.639	1173.639	1174.060	1173.950	1173.242	1173.126	1173.069	1173.045	1173.011	1172.993	1172.987	1172.986											1172.986	0.653	0.964

Table B-1.5: Determination of gravimetric water content; sample weights, drying times and calculated water contents of core sections used for out-gassing experiments (DG)

Sample ID	Date (start drying)	drying time	Lab Nr.	m(core) on site	m(core) after exp.	m(dust) in cyl	m (core final, corr.)	Δ ini-end	19.07.2023	26.07.2023	02.08.2023	10.08.2023	17.08.2023	22.08.2023
		days		g	g	g	g	g	g	g	g	g	g	g
IG_BH05_DG001	05.07.2023	98	378510	1642.44	1641.49	0.078	1641.568	0.794	1639.654	1639.612	1639.488	1639.386	1639.399	1639.394
IG_BH05_DG002	05.07.2023	133	378511	1762.77	1762.512	0.002	1762.514	0.254	1759.767	1759.737	1759.702	1759.641	1759.648	1759.653
IG_BH05_DG003	05.07.2023	98	378512	1754.05	1752.933	0.004	1752.937	1.109	1751.023	1751.002	1750.967	1750.921	1750.947	1750.942
IG_BH05_DG004	05.07.2023	106	378513	1620.37	1619.657	0.032	1619.689	0.649	1617.772	1617.726	1617.722	1617.682	1617.695	1617.690
IG_BH05_DG005	05.07.2023	106	378514	1778.30	1777.07	0.32	1777.39	0.593	1775.922	1775.871	1775.833	1775.798	1775.806	1775.803

Table B-1.5: Continued

28.08.2023	05.09.2023	12.09.2023	20.09.2023	26.09.2023	05.10.2023	11.10.2023	19.10.2023	26.10.2023	30.10.2023	07.11.2023	15.11.2023		Final weight	m(PW) core b.e.	m(PW) core a.e.	WC (mcore b.e.)	WC (mcore a.e.)
g	g	g	g	g	g	g	g	g	g	g	g		g	g	g	wt. %	wt. %
1639.440	1639.348	1639.316	1639.302	1639.273	1639.253	1639.253							1639.253	3.109	2.237	0.19	0.14
1759.704	1759.601	1759.554	1759.548	1759.518	1759.513	1759.505	1759.494	1759.491	1759.491	1795.469	1759.460		1759.460	3.308	3.052	0.19	0.17
1751.020	1750.919	1750.867	1750.855	1750.825	1750.805	1750.803							1750.803	3.243	2.130	0.18	0.12
1617.740	1617.649	1617.610	1617.608	1617.575	1617.562	1617.556	1617.554						1617.554	2.784	2.103	0.17	0.13
1775.853	1775.765	1775.718	1775.721	1775.696	1775.676	1775.667	1775.665						1775.665	2.318	1.408	0.13	0.08

Table B-1.6: Determination of gravimetric water content; sample weights, drying times and calculated water contents of core sections used for out-gassing experiments (NG)

Sample ID	date (drying start)	drying time	m (core)ini	m (core final)	m (powder)	m (core final, corr.)	Δ ini-end	17.10.2023	24.10.2023	30.10.2023	07.11.2023	15.11.2023	23.11.2023	07.12.2023	21.12.2023	11.01.2024	25.01.2024
		days	kg	g	g	g	g	g	g	g	g	g	g	g	g	g	g
IG_BH05_NG001	03.10.2023	79	1591.34	1590.296	0.095	1590.391	0.854	1588.505	1588.490	1588.473	1588.429	1588.398	1588.384	1588.361	1588.363		
IG_BH05_NG003	03.10.2023	79	1588.75	1587.750	0.034	1587.784	0.966	1586.039	1586.008	1585.976	1585.951	1585.938	1585.844	1585.822	1585.822		
IG_BH05_NG005	03.10.2023	114	1794.00	1794.400	0.021	1794.421	-0.421	1792.516	1792.501	1792.463	1792.427	1792.409	1792.384	1792.335	1792.338	1792.288	1792.276
IG_BH05_NG007	03.10.2023	114	1716.69	1714.990	0.093	1715.083	1.607	1713.186	1713.177	1713.124	1713.091	1713.078	1713.046	1712.941	1712.95	1712.892	1712.893
IG_BH05_NG009	03.10.2023	79	1720.37	1718.870	0.440	1719.310	1.060	1717.609	1717.605	1717.575	1717.536	1717.506	1717.494	1717.448	1717.448		

Table B-1.6: Continued

Final weight	m(PW) core b.e.	m(PW) core a.e.	WC (mcore b.e.)	WC (mcore a.e.)
g	g	g	wt. %	wt. %
1588.361	2.88	1.93	0.18	0.12
1585.822	2.89	1.93	0.18	0.12
1792.276	1.70	2.12	0.09	0.12
1712.892	3.70	2.10	0.22	0.12
1717.448	2.48	1.42	0.14	0.08

APPENDIX B-2

Determination of Bulk Wet and Dry Density: Raw Data

Table B-2.1: Determination of bulk wet and dry density; sample dimensions, weights and density results

Sample	m (core) wet	diameter core	height core	Volume core	bulk, wet density	bulk, dry density
	g	cm	cm	ccm	g/ccm	g/ccm
IG_BH05_AQ001	435.669	6.06	5.65	163.0	2.67	2.67
IG_BH05_AQ002	378.792	6.07	4.95	143.2	2.64	2.64
IG_BH05_AQ003	458.372	6.06	6.02	173.6	2.64	2.64
IG_BH05_AQ004	437.750	6.08	5.03	146.0	3.00	3.00
IG_BH05_AQ005	465.358	6.09	6.03	175.6	2.65	2.65
IG_BH05_AQ006	516.497	6.09	6.73	196.0	2.63	2.63
IG_BH05_AQ007	456.800	6.08	5.92	171.9	2.66	2.66
IG_BH05_AQ008	480.475	6.11	6.14	180.0	2.67	2.67
IG_BH05_AQ009	485.967	6.10	6.31	184.4	2.64	2.64
IG_BH05_AQ010	453.553	6.10	5.78	168.9	2.69	2.69
IG_BH05_AQ011	429.000	6.09	5.49	159.9	2.68	2.68
IG_BH05_AQ012	424.920	6.10	5.38	157.2	2.70	2.70
IG_BH05_AQ013	432.194	6.08	5.58	162.0	2.67	2.67
IG_BH05_AQ014	553.942	6.09	7.20	209.7	2.64	2.64
IG_BH05_AQ015	441.573	6.09	5.75	167.5	2.64	2.64
IG_BH05_AQ016	425.458	6.09	5.47	159.3	2.67	2.67
IG_BH05_AQ017	460.909	6.08	5.92	171.9	2.68	2.68
IG_BH05_AQ018	519.254	6.08	6.72	195.1	2.66	2.66
IG_BH05_AQ019	500.848	6.08	6.50	188.7	2.65	2.65
IG_BH05_AQ020	528.319	6.10	6.73	196.7	2.69	2.69
IG_BH05_AQ021	456.652	6.11	5.82	170.6	2.68	2.68
IG_BH05_AQ022	433.723	6.09	5.69	165.7	2.62	2.62
IG_BH05_AQ023	384.385	6.09	4.97	144.8	2.66	2.66
IG_BH05_AQ024	393.617	6.10	4.96	145.0	2.72	2.72
IG_BH05_AQ025	434.766	6.09	5.51	160.5	2.71	2.71
IG_BH05_AQ026	500.756	6.09	6.33	184.4	2.72	2.72
IG_BH05_AQ027	544.318	6.07	6.90	199.7	2.73	2.73
IG_BH05_AQ028	420.331	6.09	5.36	156.1	2.69	2.69
IG_BH05_AQ029	523.936	6.10	6.65	194.3	2.70	2.70

Table B-2.1: Continued

Sample	m (core a.e.) wet	m (core a.e.) dry	diameter core	height core	Volume core	bulk, wet density	bulk, dry density
	g	g	cm	cm	ccm	g/ccm	g/ccm
IG_BH05_PW001	1433.672	1433.082	6.06	18.58	535.9	2.68	2.67
IG_BH05_PW002	1440.054	1439.823	6.07	18.70	541.1	2.66	2.66
IG_BH05_PW003	1424.097	1423.880	6.05	18.60	534.7	2.66	2.66
IG_BH05_PW004	1639.696	1639.631	6.10	18.63	544.5	3.01	3.01
IG_BH05_PW005	1427.116	1427.027	6.10	18.25	533.4	2.68	2.68
IG_BH05_PW006	1427.651	1427.455	6.08	18.65	541.5	2.64	2.64
IG_BH05_PW007	1394.316	1394.155	6.06	18.30	527.8	2.64	2.64
IG_BH05_PW008	1465.486	1465.301	6.11	18.81	551.5	2.66	2.66
IG_BH05_PW009	1474.209	1473.780	6.11	19.00	557.1	2.65	2.65
IG_BH05_PW010	1449.933	1449.735	6.09	18.47	538.0	2.69	2.69
IG_BH05_PW011	1464.501	1464.318	6.10	18.61	543.9	2.69	2.69
IG_BH05_PW012	1511.952	1511.800	6.10	19.17	560.2	2.70	2.70
IG_BH05_PW013	1467.906	1467.530	6.08	18.87	547.9	2.68	2.68
IG_BH05_PW014	1485.655	1485.471	6.11	18.92	554.7	2.68	2.68
IG_BH05_PW015	1477.590	1477.475	6.09	18.90	550.5	2.68	2.68
IG_BH05_PW016	1447.680	1447.525	6.10	18.72	547.1	2.65	2.65
IG_BH05_PW017	1428.480	1428.314	6.08	18.55	538.6	2.65	2.65
IG_BH05_PW018	1353.892	1353.561	6.08	17.55	509.5	2.66	2.66
IG_BH05_PW019	1446.232	1446.070	6.08	18.63	540.9	2.67	2.67
IG_BH05_PW020	1403.257	1403.086	6.10	17.89	522.8	2.68	2.68
IG_BH05_PW021	1427.927	1427.729	6.10	18.29	534.5	2.67	2.67
IG_BH05_PW022	1423.664	1423.247	6.11	18.43	540.4	2.63	2.63
IG_BH05_PW023	1405.635	1405.331	6.11	18.18	533.0	2.64	2.64
IG_BH05_PW024	1460.144	1460.027	6.11	18.37	538.6	2.71	2.71
IG_BH05_PW025	1421.088	1420.948	6.10	18.04	527.2	2.70	2.70
IG_BH05_PW026	1348.090	1347.920	6.10	18.23	532.8	2.53	2.53
IG_BH05_PW027	1450.967	1450.782	6.07	18.45	533.9	2.72	2.72
IG_BH05_PW028	1465.330	1465.145	6.10	18.68	545.9	2.68	2.68
IG_BH05_PW029	1440.942	1440.570	6.10	18.44	538.9	2.67	2.67
IG_BH05_AR033	1032.993	1032.822	6.04	12.23	350.4	2.95	2.95
IG_BH05_AR052	1524.116	1524.016	6.10	17.83	521.1	2.92	2.92
IG_BH05_AR059	1174.060	1173.95	6.05	14.77	424.6	2.77	2.76

APPENDIX B-3

Aqueous Extraction Experiments: Raw Data

Table B-3.1: Experimental data of aqueous extraction experiments

Sample	Depth	m (bottle)	m (bottle + rock)	m (rock)	m (H2O)	m (tot)	water:rock
	m a.b.	g	g	g	g	g	
IG_BH05_AQ001	166.4	19.356	121.985	102.629	62.581	184.566	0.61
IG_BH05_AQ002	221.1	18.730	122.889	104.159	66.198	189.087	0.64
IG_BH05_AQ003	253.2	18.233	128.173	109.940	70.390	198.563	0.64
IG_BH05_AQ004	290.0	18.315	112.543	94.228	74.310	186.853	0.79
IG_BH05_AQ005	343.2	18.014	124.164	106.150	67.112	191.276	0.63
IG_BH05_AQ006	387.4	17.987	124.886	106.899	67.690	192.576	0.63
IG_BH05_AQ007	399.9	19.407	128.401	108.994	66.957	195.358	0.61
IG_BH05_AQ008	427.0	17.982	117.780	99.798	65.171	182.951	0.65
IG_BH05_AQ009	453.6	18.022	131.119	113.097	57.424	188.543	0.51
IG_BH05_AQ010	480.1	17.990	124.943	106.953	66.779	191.722	0.62
IG_BH05_AQ011	507.1	18.159	116.854	98.695	64.104	180.958	0.65
IG_BH05_AQ012	525.7	18.767	120.78	102.013	61.540	182.32	0.60
IG_BH05_AQ013	560.4	18.024	131.959	113.935	60.720	192.679	0.53
IG_BH05_AQ014	588.2	18.748	130.018	111.270	62.037	192.055	0.56
IG_BH05_AQ015	612.8	18.310	99.818	81.508	76.096	175.914	0.93
IG_BH05_AQ016	640.4	18.009	126.64	108.631	64.903	191.543	0.60
IG_BH05_AQ017	664.6	18.017	139.827	121.810	55.015	194.842	0.45
IG_BH05_AQ018	694.2	18.761	140.536	121.775	46.259	186.795	0.38
IG_BH05_AQ019	720.7	18.040	135.186	117.146	50.457	185.643	0.43
IG_BH05_AQ020	750.3	18.117	121.011	102.894	65.923	186.934	0.64
IG_BH05_AQ021	773.3	18.010	124.375	106.365	67.092	191.467	0.63
IG_BH05_AQ022	801.8	18.039	99.618	81.579	70.688	170.306	0.87
IG_BH05_AQ023	827.9	18.049	140.195	122.146	50.211	190.406	0.41
IG_BH05_AQ024	849.3	18.017	125.662	107.645	56.987	182.649	0.53
IG_BH05_AQ025	881.8	18.735	117.949	99.214	62.457	180.406	0.63
IG_BH05_AQ026	906.7	15.141	135.587	120.446	69.03	204.617	0.57
IG_BH05_AQ027	937.0	15.158	113.015	97.857	76.789	189.804	0.78
IG_BH05_AQ028	963.4	15.151	139.303	124.152	59.684	198.987	0.48
IG_BH05_AQ029	982.3	15.155	136.195	121.040	63.348	199.543	0.52

APPENDIX B-4

Isotope Diffusive Exchange Experiments: Raw Data

Table B-4.1: Experimental data of isotope diffusive exchange experiments

Sample		Date Experiment Start	Date Experiment End	Weight container	Weight container and rock	Cryst. dish	Cryst Dish + H2O	Total weight container	Weight rock	Weight test solution	Total weight container after experiment	Weight test solution after experiment	Weight container and rock after experiment	Weight test solution after experiment	Weight rock after experiment	mass (PW)	mass TW+PW after exp.	Δ total weight before & after	Δ weight rock before & after	Δ weight test solution before & after	Δ weight rock and test solution	Δ weight rock and test solution - Δ total weight before and after	Δ weight rock and test solution	Δ water loss (total weight)	remaining water fraction
				g	g	g	g	g	g	g	g	g	g	g	g	g	g	g	g	g	g	g	% of TW	% of TW+PW	
PW001	LAB	25.06.2021	25.08.2021	523.972	872.166	15.007	16.840	889.000	348.194	1.833	888.972	16.678	872.289	1.671	348.317	0.605	2.276	-0.028	0.123	-0.162	-0.039	-0.011	2.1	1.2	0.99
PW002	LAB	25.06.2021	25.08.2021	516.442	918.468	12.865	14.697	933.161	402.026	1.832	933.128	14.584	918.544	1.719	402.102	0.555	2.274	-0.033	0.076	-0.113	-0.037	-0.004	2.0	1.5	0.99
PW003	LAB	25.06.2021	25.08.2021	524.163	928.340	14.379	16.196	944.527	404.177	1.817	944.493	16.047	928.447	1.668	404.284	0.658	2.326	-0.034	0.107	-0.149	-0.042	-0.008	2.3	1.5	0.99
PW004	LAB	06.07.2021	13.09.2021	521.601	888.791	14.029	15.782	904.572	367.190	1.753	904.594	15.692	888.910	1.663	367.309	1.213	2.876	0.022	0.119	-0.090	0.029	0.007	-1.7	-0.8	1.01
PW005	LAB	06.07.2021	13.09.2021	524.009	922.207	13.234	15.011	937.211	398.198	1.777	937.236	14.963	922.279	1.729	398.270	0.611	2.340	0.025	0.072	-0.048	0.024	-0.001	-1.4	-1.1	1.01
PW006	LAB	19.07.2021	21.09.2021	514.985	974.116	15.410	17.216	991.327	459.131	1.806	991.303	17.104	974.204	1.694	459.219	0.675	2.369	-0.024	0.088	-0.112	-0.024	0.000	1.3	1.0	0.99
PW007	LAB	19.07.2021	21.09.2021	518.880	1026.894	12.962	14.759	1041.648	508.014	1.797	1041.620	14.623	1027.004	1.661	508.124	0.759	2.420	-0.028	0.110	-0.136	-0.026	0.002	1.4	1.2	0.99
PW008	LAB	19.07.2021	21.09.2021	520.526	995.306	15.369	17.162	1012.456	474.780	1.793	1012.458	17.105	995.365	1.736	474.839	0.543	2.279	0.002	0.059	-0.057	0.002	0.000	-0.1	-0.1	1.00
PW009	LAB	19.07.2021	21.09.2021	523.355	1048.407	14.832	16.629	1065.023	525.052	1.797	1065.028	16.736	1048.301	1.904	524.946	0.998	2.902	0.005	-0.106	0.107	0.001	-0.004	-0.1	-0.2	1.00
PW010	LAB	19.07.2021	21.09.2021	516.307	961.256	15.160	16.947	978.194	444.949	1.787	978.189	16.839	961.364	1.679	445.057	0.618	2.297	-0.005	0.108	-0.108	0.000	0.005	0.0	0.2	1.00
PW011	LAB	19.07.2021	21.09.2021	513.949	982.570	14.653	16.441	999.002	468.621	1.788	999.004	16.337	982.676	1.684	468.727	0.63	2.314	0.002	0.106	-0.104	0.002	0.000	-0.1	-0.1	1.00
PW012	LAB	09.08.2021	19.10.2021	524.953	1009.206	14.934	16.736	1025.931	484.253	1.802	1025.900	16.542	1009.353	1.608	484.400	0.592	2.200	-0.031	0.147	-0.194	-0.047	-0.016	2.6	1.4	0.99
PW013	LAB	09.08.2021	19.10.2021	523.922	923.819	14.793	16.565	940.376	399.897	1.772	940.346	16.430	923.912	1.637	399.990	0.495	2.132	-0.030	0.093	-0.135	-0.042	-0.012	2.4	1.4	0.99
PW014	LAB	09.08.2021	19.10.2021	513.652	947.513	14.133	15.932	963.435	433.861	1.799	963.406	15.746	947.656	1.613	434.004	0.513	2.126	-0.029	0.143	-0.186	-0.043	-0.014	2.4	1.4	0.99
PW015	LAB	29.07.2021	30.09.3021	521.128	1003.324	13.409	15.205	1018.525	482.196	1.796	1018.488	15.052	1003.437	1.643	482.309	0.713	2.356	-0.037	0.113	-0.153	-0.040	-0.003	2.2	1.6	0.98
PW016	LAB	29.07.2021	30.09.2021	523.610	918.461	15.167	16.911	935.367	394.851	1.744	935.329	16.772	918.563	1.605	394.953	0.488	2.093	-0.038	0.102	-0.139	-0.037	0.001	2.1	1.8	0.98
PW017	LAB	13.08.2021	19.10.2021	523.847	978.939	14.946	16.770	995.701	455.092	1.824	995.671	16.611	979.058	1.665	455.211	0.528	2.193	-0.030	0.119	-0.159	-0.040	-0.010	2.2	1.4	0.99
PW018	LAB	13.08.2021	19.10.2021	515.080	980.829	13.393	15.123	995.947	465.749	1.730	995.916	15.020	980.898	1.627	465.818	0.581	2.208	-0.031	0.069	-0.103	-0.034	-0.003	2.0	1.4	0.99
PW019	LAB	13.08.2021	19.10.2021	516.210	952.534	14.818	16.623	969.148	436.324	1.805	969.119	16.483	952.638	1.665	436.428	0.613	2.278	-0.029	0.104	-0.140	-0.036	-0.007	2.0	1.3	0.99
PW020	LAB	09.08.2021	19.10.2021	516.431	1070.091	14.813	16.576	1086.658	553.660	1.763	1086.636	16.401	1070.228	1.588	553.797	0.66	2.248	-0.022	0.137	-0.175	-0.038	-0.016	2.2	1.0	0.99
PW021	LAB	09.08.2021	19.10.2021	523.286	995.408	12.945	14.588	1009.990	472.122	1.643	1009.968	14.404	995.563	1.459	472.277	0.651	2.110	-0.022	0.155	-0.184	-0.029	-0.007	1.8	1.0	0.99
PW022	LAB	09.08.2021	19.10.2021	522.551	969.044	13.584	15.129	984.162	446.493	1.545	984.135	15.002	969.128	1.418	446.577	0.827	2.245	-0.027	0.084	-0.127	-0.043	-0.016	2.8	1.2	0.99
PW023	LAB	13.08.2021	19.10.2021	523.703	946.325	14.436	16.248	962.562	422.622	1.812	962.527	16.090	946.439	1.654	422.736	0.593	2.247	-0.035	0.114	-0.158	-0.044	-0.009	2.4	1.6	0.98
PW024	LAB	13.08.2021	19.10.2021	522.834	876.499	13.572	15.397	891.891	353.665	1.825	891.857	15.240	876.620	1.668	353.786	0.55	2.218	-0.034	0.121	-0.157	-0.036	-0.002	2.0	1.5	0.98
PW025	LAB	13.08.2021	19.10.2021	524.637	963.930	13.696	15.507	979.432	439.293	1.811	979.400	15.278	964.122	1.582	439.485	0.411	1.993	-0.032	0.192	-0.229	-0.037	-0.005	2.0	1.6	0.98
PW026	LAB	02.09.2021	02.11.2021	522.235	904.011	15.007	16.798	920.796	381.776	1.791	920.791	16.644	904.129	1.637	381.894	0.343	1.980	-0.005	0.118	-0.154	-0.036	-0.031	2.0	0.3	1.00
PW027	LAB	02.09.2021	02.11.2021	517.948	998.672	13.994	15.727	1014.389	480.724	1.733	1014.380	15.482	998.882	1.488	480.934	0.44	1.928	-0.009	0.210	-0.245	-0.035	-0.026	2.0	0.5	1.00
PW028	LAB	02.09.2021	02.11.2021	523.079	906.402	13.648	15.130	921.527	383.323	1.482	921.513	14.984	906.553	1.336	383.474	0.494	1.830	-0.014	0.151	-0.146	0.005	0.019	-0.3	0.8	0.99
PW029	LAB	02.09.2021	02.11.2021	517.317	987.222	14.691	16.477	1003.692	469.905	1.786	1003.676	16.197	987.459	1.506	470.142	0.927	2.433	-0.016	0.237	-0.280	-0.043	-0.027	2.4	0.7	0.99
AR059	LAB	14.03.2022	24.05.2022	516.272	819.281	13.233	14.760	834.038	303.009	1.527	834.037	14.413	819.594	1.180	303.322	0.287	1.467	-0.001	0.313	-0.347	-0.034	-0.033	2.2	0.1	1.00
PW001	ICE	25.06.2021	25.08.2021	524.348	872.308	13.894	15.647	887.950	347.960	1.753	887.917	15.458	872.454	1.564	348.106	0.595	2.159	-0.033	0.146	-0.189	-0.043	-0.010	2.5	1.5	0.98
PW002	ICE	25.06.2021	25.08.2021	517.574	917.835	12.522	14.329	932.162	400.261	1.807	932.126	14.213	917.911	1.691	400.337	0.555	2.246	-0.036	0.076	-0.116	-0.040	-0.004	2.2	1.6	0.98
PW003	ICE	25.06.2021	25.08.2021	575.977	977.072	14.105	15.930	992.991	401.095	1.825	992.969	15.801	977.166	1.696	401.189	0.736	2.432	-0.022	0.094	-0.129	-0.035	-0.013	1.9	0.9	0.99
PW004	ICE	06.07.2021	13.09.2021	516.959	888.695	13.844	15.620	904.312	371.736	1.776	904.333	15.525	888.814	1.681	371.855	1.217	2.898	0.021	0.119	-0.095	0.024	0.003	-1.4	-0.7	1.01
PW005	ICE	06.07.2021	13.09.2021	515.109	913.861	12.324	14.134	927.989	398.752	1.810	928.006	14.075	913.935	1.751	398.826	0.595	2.346	0.017	0.074	-0.059	0.015	-0.002	-0.8	-0.7	1.01
PW006	ICE	19.07.2021	21.09.2021	514.884	974.091	14.478	16.264	990.345	459.207	1.786	990.322	16.147	974.177	1.669	459.293	0.696	2.365	-0.023	0.086	-0.117	-0.031	-0.008	1.7	1.0	0.99
PW007	ICE	19.07.2021	21.09.2021	514.639	1023.219	13.565	15.353	1038.560	508.580	1.788	1038.529	15.215	1023.320	1.650	508.681	0.774	2.424	-0.031	0.101	-0.138	-0.037	-0.006	2.1	1.3	0.99
PW008	ICE	19.07.2021	21.09.2021	522.484	998.864	13.141	14.919	1013.767	476.380	1.778	1013.741	14.758	998.992	1.617	476.508	0.508	2.125	-0.026	0.128	-0.161	-0.033	-0.007	1.9	1.2	0.99
PW009	ICE	19.07.2021	21.09.2021	521.637	1046.652	14.819	16.585	1063.220	525.015	1.766	1063.226	16.618	1046.611	1.799	524.974	0.822	2.621	0.006	-0.041	0.033	-0.008	-0.014	0.5	-0.2	1.00
PW010	ICE	19.07.2021	21.09.2021	517.867	965.136	15.066	16.837	981.965	447.269	1.771	981.965	16.721	965.250	1.655	447.383	0.619	2.274	0.000	0.114	-0.116	-0.002	-0.002	0.1	0.0	1.00
PW011	ICE	19.07.2021	21.09.2021	522.917	993.713	14.373	16.142	1009.839	470.796	1.769	1009.836	16.022	993.828	1.649	470.911	0.644	2.293	-0.003	0.115	-0.120	-0.005	-0.002	0.3	0.1	1.00
PW012	ICE	09.08.2021	19.10.2021	529.086	1002.484	13.575	15.196	1017.667	473.398	1.621	1017.638	15.008	1002.626	1.433	473.540	0.561	1.994	-0.029	0.142	-0.188	-0.046	-0.017	2.8	1.5	0.99
PW013	ICE	09.08.2021	19.10.2021	516.009	913.641	14.104	15.822	929.457	397.632	1.718	929.424	15.651	913.768	1.547	397.759	0.530	2.077	-0.033	0.127	-0.171	-0.044	-0.011	2.6	1.6	0.98
PW014	ICE	09.08.2021	19.10.2021	517.601	950.143	14.755	16.507	966.637	432.542	1.752	966.604	16.277	950.323	1.522	432.722	0.518	2.040	-0.033	0.180	-0.230	-0.050	-0.017	2.9	1.6	0.98
PW015	ICE	29.07.2021	30.09.3021	518.391	1002.445	15.040	16.680	1019.123	484.054	1.640	1019.081	16.501	1002.585	1.461	484.194	0.713	2.174	-0.042	0.140	-0.179	-0.039	0.003	2.4	1.9	0.98
PW016	ICE	29.07.2021	30.09.2021	517.438	913.913	13.946	15.682	929.587	396.475	1.736	929.549	15.523	914.031	1.577	396.593	0.491	2.068	-0.038	0.118	-0.159	-0.041	-0.003	2.4	1.8	0.98
PW017	ICE	13.08.2021	19.10.2021	522.211	974.803	14.119	15.824	990.617	452.592	1.705	990.586	15.652	974.932	1.533	452.721	0.528	2.061	-0.031	0.129	-0.172	-0.043	-0.012	2.5	1.5	0.98
PW018	ICE	13.08.2021	19.10.2021	519.979	987.496	14.909	16.536	1004.026	467.517	1.627	1003.993	16.405	987.589	1.496	467.610	0.540	2.036	-0.033	0.093	-0.131	-0.038	-0.005	2.3	1.6	0.98
PW019	ICE	13.08.2021	19.10.2021	521.770	958.491	14.275	16.084	974.564	436.721	1.809	974.538	15.920	958.616	1.645	436.846	0.581	2.226	-0.026	0.125	-0.164	-0.039	-0.013	2.2	1.2	0.99
PW020	ICE	09.08.2021	19.10.2021	523.869	1079.083	13.421	15.182	1094.255	555.214	1.761	1094.233	14.967	1079.261	1.546	555.392	0.561	2.107	-0.022	0.178	-0.215	-0.037	-0.015	2.1	1.0	0.99
PW021	ICE	09.08.2021	19.10.2021	516.316	985.849	12.968	14.445	1000.287	469.533	1.477	1000.259	14.230	986.023	1.262	469.707	0.641	1.903	-0.028	0.174	-0.215	-0.041	-0.013	2.8	1.5	0.99
PW022	ICE	09.08.2021	19.10.2021	514.684	964.489	16.551	18.300	982.785	449.805	1.749	982.745	18.161	964.581	1.610	449.897	0.736	2.346	-0.040	0.092	-0.139	-0.047	-0.007	2.7	1.7	0.98
PW023	ICE	13.08.2021	19.10.2021	524.752	948.213	14.267	16.056	964.258	423.461	1.789	964.224	15.891	948.339	1.624	423.587	0.628	2.252	-0.034	0.126	-0.165	-0.039	-0.005	2.2	1.5	0.98
PW024	ICE	13.08.2021	19.10.2021	514.715	872.954	12.720	14.509	887.458	358.239	1.789	887.426	14.333	873.095	1.613	358.380	0.597	2.210	-0.032	0.141	-0.176	-0.035	-0.003	2.0	1.4	0.99
PW025	ICE	13.08.2021	19.10.2021	524.922	960.627	12.846	14.660	975.295	435.705	1.814	975.248	14.408	960.839	1.562	435.917	0.428	1.990	-0.047	0.212	-0.252	-0.040	0.007	2.2	2.4	0.98
PW026	ICE	02.09.2021	02.11.2021	516.343	894.895	14.06	15.677	910.563	378.552	1.617	910.551	15.485	895.052	1.425	378.709	0.387	1.812	-0.012	0.157	-0.192	-0.035	-0.023	2.2	0.7	0.99
PW027	ICE	02.09.2021	02.11.2021	523.637	1001.514	14.293	15.989	1017.496	477.877	1.696	1017.482	15.680	1001.791	1.387	478.154	0.483	1.870	-0.014	0.277	-0.309	-0.032	-0.018	1.9	0.7	0.99
PW028	ICE	02.09.2021	02.11.2021	516.722	901.592	12.981	14.743	916.319	384.87	1.762	916.308	14.505	901.785	1.524	385.063	0.530	2.054	-0.011	0.193	-0.238	-0.045	-0.034	2.6	0.5	0.99
PW029	ICE	02.09.2021	02.11.2021	517.691	984.987	13.389	15.188	1000.163	467.296	1.799	1000.148	14.846	985.275	1.457	467.584	0.985	2.442	-0.015	0.288	-0.342	-0.054	-0.039	3.0	0.6	0.99
AR059	ICE	14.03.2022	24.05.2022	517.847	818.981	13.267	14.785	833.766	301.134	1.518	833.815	14.547	819.240	1.280	301.393	0.299	1.579	0.049	0.259	-0.238	0.021	-0.028	-1.4	-3.1	1.03

Table B-4.2: Analytical raw data of isotope diffusive exchange experiments

Sample	Test water	Initial $\delta^{18}O$ TW	Initial $\delta^{2}H$ TW	Final $\delta^{18}O$ TW	Final $\delta^{2}H$ TW
		Permill VSMOW	Permill VSMOW	Permill VSMOW	Permill VSMOW
PW001	LAB	-10.25	-74.0	-10.74	-79.6
PW002	LAB	-10.25	-74.0	-9.95	-73.3
PW003	LAB	-10.25	-74.0	-10.43	-76.5
PW004	LAB	-10.30	-73.2	-11.70	-85.9
PW005	LAB	-10.30	-73.2	-10.60	-77.4
PW006	LAB	-10.30	-73.2	-10.23	-74.7
PW007	LAB	-10.30	-73.2	-10.38	-76.0
PW008	LAB	-10.30	-73.2	-10.01	-72.0
PW009	LAB	-10.30	-73.2	-9.71	-70.6
PW010	LAB	-10.30	-73.2	-9.87	-70.2
PW011	LAB	-10.30	-73.2	-9.83	-69.9
PW012	LAB	-10.13	-72.6	-9.11	-66.9
PW013	LAB	-10.13	-72.6	-8.97	-66.9
PW014	LAB	-10.13	-72.6	-9.21	-68.2
PW015	LAB	-10.16	-72.8	-9.82	-72.2
PW016	LAB	-10.16	-72.8	-9.75	-71.5
PW017	LAB	-10.06	-72.5	-9.59	-70.9
PW018	LAB	-10.06	-72.5	-9.27	-69.5
PW019	LAB	-10.06	-72.5	-9.70	-71.4
PW020	LAB	-10.13	-72.6	-9.57	-70.7
PW021	LAB	-10.13	-72.6	-9.65	-71.4
PW022	LAB	-10.13	-72.6	-10.23	-75.6
PW023	LAB	-10.06	-72.5	-9.76	-71.6
PW024	LAB	-10.06	-72.5	-9.76	-71.3
PW025	LAB	-10.06	-72.5	-9.35	-68.6
PW026	LAB	-10.00	-72.1	-9.16	-67.8
PW027	LAB	-10.00	-72.1	-9.10	-67.8
PW028	LAB	-10.00	-72.1	-9.20	-67.8
PW029	LAB	-10.00	-72.1	-9.32	-67.9
AR059	LAB	-10.16	-72.8	-8.34	-65.1
PW001	ICE	-31.63	-247.3	-25.46	-196.5
PW002	ICE	-31.63	-247.3	-26.26	-205.5
PW003	ICE	-31.63	-247.3	-25.16	-196.1
PW004	ICE	-31.85	-248.2	-23.80	-184.4
PW005	ICE	-31.85	-248.2	-26.47	-206.2
PW006	ICE	-31.85	-248.2	-24.84	-195.0
PW007	ICE	-31.85	-248.2	-24.42	-191.3
PW008	ICE	-31.85	-248.2	-26.45	-208.0
PW009	ICE	-31.85	-248.2	-23.94	-187.2
PW010	ICE	-31.85	-248.2	-26.46	-205.6
PW011	ICE	-31.85	-248.2	-26.33	-204.1
PW012	ICE	-31.73	-248.1	-25.19	-198.7
PW013	ICE	-31.73	-248.1	-25.06	-198.2
PW014	ICE	-31.73	-248.1	-26.18	-207.0
PW015	ICE	-31.50	-247.1	-24.33	-191.6
PW016	ICE	-31.50	-247.1	-26.14	-205.2
PW017	ICE	-31.68	-248.4	-25.49	-201.2
PW018	ICE	-31.68	-248.4	-24.64	-195.4
PW019	ICE	-31.68	-248.4	-25.72	-202.1
PW020	ICE	-31.73	-248.1	-25.43	-200.9
PW021	ICE	-31.73	-248.1	-25.12	-198.4
PW022	ICE	-31.73	-248.1	-23.97	-189.0
PW023	ICE	-31.68	-248.4	-25.63	-201.2
PW024	ICE	-31.68	-248.4	-26.16	-205.5
PW025	ICE	-31.68	-248.4	-27.47	-216.5
PW026	ICE	-31.44	-245.4	-26.41	-208.0
PW027	ICE	-31.44	-245.4	-26.91	-211.4
PW028	ICE	-31.44	-245.4	-26.06	-204.6
PW029	ICE	-31.44	-245.4	-24.02	-188.1
AR059	ICE	-31.59	-247.3	-27.09	-215.5

APPENDIX B-5

Out-diffusion Experiments: Raw Data

Table B-5.1: Experimental data of out-diffusion experiments

Sample		IG_BH05_Blank	IG_BH05_PW001	IG_BH05_PW002	IG_BH05_PW003	IG_BH05_PW004	IG_BH05_PW005	IG_BH05_PW006	IG_BH05_PW007	IG_BH05_PW008	IG_BH05_PW009	IG_BH05_PW010
Depth	m		171.4	219.1	253.5	290.2	341.7	386.7	398.5	426.3	454.3	479.4
start experiment		25.06.2021	25.06.2021	25.06.2021	25.06.2021	06.07.2021	06.07.2021	19.07.2021	19.07.2021	19.07.2021	19.07.2021	19.07.2021
Initial Rock Mass (as received, +/- mountain wet)	g		1433.106	1439.948	1424.088	1639.730	1427.112	1427.611	1394.153	1465.364	1473.619	1449.523
Initial Rock Mass (start experiment)	g		1433.079	1439.895	1423.929	1639.730	1427.080	1427.555	1394.110	1465.295	1473.535	1449.520
Final Rock Mass (resaturated)	g		1433.082	1439.823	1423.880	1639.631	1427.027	1427.455	1394.155	1465.301	1473.780	1449.735
Uptake of water	g		-0.02	-0.13	-0.21	-0.10	-0.09	-0.16	0.00	-0.06	0.16	0.21
Saturation	%		100.002	100.009	100.015	100.006	100.006	100.011	100.000	100.004	99.989	99.985
Core Diametre	cm		6.06	6.07	6.05	6.10	6.10	6.08	6.06	6.11	6.11	6.09
Core Length	cm		18.58	18.7	18.6	18.63	18.25	18.65	18.3	18.81	19	18.47
Volume of Rock Sample	cm3		535.90	541.14	534.70	544.46	533.35	541.47	527.82	551.52	557.09	538.01
Density (calculated from volume & mass)	g/cm3		2.67	2.66	2.66	3.01	2.68	2.64	2.64	2.66	2.65	2.69
Mass of Rock (calculated from volume and density)			1433.11	1439.95	1424.09	1639.73	1427.11	1427.61	1394.15	1465.36	1473.62	1449.52
Masses before experiment												
Mass cylinder	g	380.492	382.186	362.041	356.014	381.694	360.872	357.522	361.624	380.536	361.404	379.447
Mass cylinder + core	g		1815.278	1801.896	1779.945	2021.438	1787.935	1785.062	1755.735	1845.832	1834.910	1828.963
Mass cylinder + core + H2O	g	839.661	1958.439	1946.814	1923.894	2159.922	1928.233	1948.897	1906.412	1983.217	1986.396	1979.224
Mass tot start	g	839.661	1958.399	1946.786	1923.890	2160.050	1928.252	1948.900	1906.401	1983.211	1986.398	1979.222
Initial Water Mass	ml	459.169	143.161	144.918	143.949	138.484	140.298	163.835	150.677	137.385	151.486	150.261
Ratio Exp.Water : Rock			0.100	0.101	0.101	0.084	0.098	0.115	0.108	0.094	0.103	0.104
End Experiment		12.11.2021	12.11.2021	12.11.2021	12.11.2021	12.11.2021	12.11.2021	30.11.2021	30.11.2021	30.11.2021	30.11.2021	30.11.2021
Mass cylinder + core + H2O final	g		1951.074	1939.298	1916.343	2152.552	1920.409	1939.721	1898.135	1975.130	1978.053	1971.265
Final Water Mass (measured, not all recoverable)	ml	112.774	133.003	134.291	133.211	131.984	129.438	150.848	139.092	126.654	139.554	139.393
Time Experiment	days	140	140	140	140	129	129	134	134	134	134	134
Volume of samples for Cl-measurements												
sample A	ml	0.5	0.5	0.5	0.5	0.5	0.6	0.5	0.7	0.5	0.6	0.5
sample B	ml	0.5	0.5	0.5	0.5	0.5	0.5	0.5	0.5	0.5	0.6	0.5
sample C	ml	0.6	0.5	0.5	0.5	0.5	0.5	0.5	0.5	0.5	0.6	0.5
sample D	ml	0.5	0.5	0.5	0.5	0.5	0.5	0.5	0.5	0.5	0.6	0.5
sample E	ml	0.5	0.5	0.5	0.5	0.5	0.5	0.5	0.5	0.5	0.6	0.5
sample F	ml	0.5	0.5	0.5	0.5	0.5	0.5	0.5	0.5	0.5	0.5	0.5
sample G	ml	0.5	0.5	0.5	0.5	0.5	0.5	0.5	0.5	0.5	0.5	0.5
sample H-1	ml	0.5	0.5	0.5	0.5	0.5	0.5	1.0	1.0	1.0	1.0	1.0
sample H-2	ml											
sample I	ml	0.5	0.5	0.5	0.5	0.5	0.5	0.5	0.5	0.5	0.5	0.5
sample K	ml	0.5	0.5	0.5	0.5	0.5	0.5	0.5	0.5	0.5	0.5	0.5
sample L	ml	0.5	0.5	0.5	0.5	0.5	0.5	0.5	0.5	0.5	0.5	0.5
sample M	ml	0.5	0.5	0.5	0.5	0.5	0.5	0.5	0.5	0.5	0.5	0.5
sample N	ml	0.5	0.5	0.5	0.5	0.5	0.5	0.5	0.5	0.5	0.5	0.5
total volume subsamples		6.6	6.5	6.5	6.5	6.5	6.6	7.0	7.2	7.0	7.5	7.0
Volumen TS calculated cyl (ini-final)	ml		7.3	7.5	7.5	7.5	7.8	9.2	8.3	8.1	8.3	8.0
Difference V(ss) - V(calc)	ml		0.825	0.988	1.047	0.998	1.243	2.179	1.066	1.081	0.845	0.957
Difference % of TS	%		0.6	0.7	0.7	0.7	0.9	1.3	0.7	0.8	0.6	0.6

Table B-5.1: Continued

Sample		IG_BH05_PW011	IG_BH05_PW012	IG_BH05_PW013	IG_BH05_PW014	IG_BH05_PW015	IG_BH05_PW016	IG_BH05_PW017	IG_BH05_PW018	IG_BH05_PW019	IG_BH05_PW020	IG_BH05_PW021
Depth	m	506.4	525.1	560.1	587.1	612.1	637.4	665.3	692.4	722.2	749.6	774.5
start experiment		19.07.2021	09.08.2021	09.08.2021	09.08.2021	29.07.2021	29.07.2021	13.08.2021	13.08.2021	13.08.2021	09.08.2021	09.08.2021
Initial Rock Mass (as received, +/- mountain wet)	g	1464.240	1511.679	1467.226	1485.278	1477.526	1447.520	1428.345	1353.747	1446.181	1402.935	1427.583
Initial Rock Mass (start experiment)	g	1464.205	1511.659	1467.202	1485.270	1477.510	1447.505	1428.345	1353.657	1446.155	1402.924	1427.565
Final Rock Mass (resaturated)	g	1464.318	1511.800	1467.530	1485.471	1477.475	1447.525	1428.314	1353.561	1446.070	1403.086	1427.729
Uptake of water	g	0.08	0.12	0.30	0.19	-0.05	0.01	-0.03	-0.19	-0.11	0.15	0.15
Saturation	%	99.995	99.992	99.979	99.987	100.003	100.000	100.002	100.014	100.008	99.989	99.990
Core Diametre	cm	6.10	6.10	6.08	6.11	6.09	6.10	6.08	6.08	6.08	6.1	6.1
Core Length	cm	18.61	19.17	18.87	18.92	18.90	18.72	18.55	17.55	18.63	17.89	18.29
Volume of Rock Sample	cm3	543.87	560.24	547.86	554.75	550.54	547.09	538.57	509.54	540.89	522.83	534.52
Density (calculated from volume & mass)	g/cm3	2.69	2.70	2.68	2.68	2.68	2.65	2.65	2.66	2.67	2.68	2.67
Mass of Rock (calculated from volume and density)		1464.24	1511.68	1467.23	1485.28	1477.53	1447.52	1428.35	1353.75	1446.18	1402.94	1427.58
Masses before experiment												
Mass cylinder	g	380.872	382.357	381.181	379.326	382.744	381.568	383.336	380.603	359.540	380.090	357.144
Mass cylinder + core	g	1845.083	1894.012	1848.395	1864.629	1860.240	1829.068	1811.689	1734.251	1805.713	1783.015	1784.703
Mass cylinder + core + H2O	g	1991.696	2028.312	1989.737	2001.013	2001.812	1970.021	1950.219	1870.413	1944.974	1938.206	1931.560
Mass tot start	g	1991.689	2028.299	1989.737	2000.986	2001.812	1970.019	1950.346	1870.428	1944.953	1938.216	1931.605
Initial Water Mass	ml	146.613	134.300	141.342	136.384	141.572	140.953	138.530	136.162	139.261	155.191	146.857
Ratio Exp.Water : Rock		0.100	0.089	0.096	0.092	0.096	0.097	0.097	0.101	0.096	0.111	0.103
End Experiment		30.11.2021	30.11.2021	30.11.2021	30.11.2021	30.11.2021	30.11.2021	12.01.2022	12.01.2022	12.01.2022	12.01.2022	12.01.2022
Mass cylinder + core + H2O final	g	1983.756	2021.500	1982.943	1994.237	1994.079	1962.654	1942.043	1862.208	1937.095	1930.810	1924.122
Final Water Mass (measured, not all recoverable)	ml	135.857	124.527	131.478	126.793	130.591	130.815	127.003	124.783	128.619	144.661	136.107
Time Experiment	days	134	113	113	113	124	124	152	152	152	156	156
Volume of samples for Cl-measurements												
sample A	ml	0.5	0.5	0.5	0.5	0.5	0.5	0.5	0.5	0.5	0.5	0.5
sample B	ml	0.5	0.5	0.5	0.5	0.5	0.5	0.5	0.6	0.5	0.5	0.5
sample C	ml	0.5	0.5	0.5	0.5	0.5	0.5	0.5	0.9	0.5	0.5	0.5
sample D	ml	0.5	0.5	0.5	0.5	0.5	0.5	0.5	0.5	0.5	0.5	0.5
sample E	ml	0.5	0.5	0.5	0.5	0.5	0.5	0.5	0.5	0.5	0.5	0.5
sample F	ml	0.5	0.5	0.5	0.5	0.5	0.5	0.5	0.5	0.5	0.5	0.5
sample G	ml	0.5	0.5	0.5	0.5	0.5	0.5	0.5	0.5	0.5	0.5	0.5
sample H-1	ml	1.0	0.5	0.5	0.5	0.5	0.5	0.5	0.5	0.5	0.5	0.5
sample H-2	ml											
sample I	ml	0.5	0.5	0.5	0.5	0.5	0.5	0.5	0.5	0.5	0.5	0.5
sample K	ml	0.5	0.5	0.5	0.5	0.5	0.5	0.5	0.5	0.5	0.5	0.5
sample L	ml	0.5	0.5	0.5	0.5	0.5	0.5	0.5	0.5	0.5	0.5	0.5
sample M	ml	0.5	0.5	0.5	0.5	0.5	0.5	0.5	0.5	0.5	0.5	0.5
sample N	ml	0.5				0.5	0.5	0.5	0.5	0.5	0.5	0.5
total volume subsamples		7.0	6.0	6.0	6.0	6.5	6.5	6.5	7.0	6.5	6.5	6.5
Volumen TS calculated cyl (ini-final)	ml	7.9	6.8	6.8	6.7	7.7	7.4	8.3	8.2	7.9	7.4	7.5
Difference V(ss) - V(calc)	ml	0.933	0.799	0.794	0.749	1.233	0.865	1.803	1.220	1.358	0.906	0.983
Difference % of TS	%	0.6	0.6	0.6	0.5	0.9	0.6	1.3	0.9	1.0	0.6	0.7

Table B-5.1: Continued

Sample		IG_BH05_PW022	IG_BH05_PW023	IG_BH05_PW024	IG_BH05_PW025	IG_BH05_PW026	IG_BH05_PW027	IG_BH05_PW028	IG_BH05_PW029	IG_BH05_AR033	IG_BH05_AR052	IG_BH05_AR059
Depth	m	797.3	827.2	848.7	881.5	906.1	936.8	963.0	986.5	717.4	856.0	979.0
start experiment		09.08.2021	13.08.2021	13.08.2021	13.08.2021	02.09.2021	02.09.2021	02.09.2021	02.09.2021	14.03.2022	14.03.2022	14.03.2022
Initial Rock Mass (as received, +/- mountain wet)	g	1423.297	1405.199	1460.157	1420.961	1445.716	1450.834	1465.159	1440.303	1032.833	1523.570	1173.639
Initial Rock Mass (start experiment)	g	1423.230	1405.170	1460.094	1420.928	1445.630	1450.818	1465.130	1440.235	1032.790	1523.566	1173.639
Final Rock Mass (resaturated)	g	1423.247	1405.331	1460.027	1420.948	1445.920	1450.782	1465.145	1440.570	1032.822	1524.016	1173.950
Uptake of water	g	-0.05	0.13	-0.13	-0.01	0.20	-0.05	-0.01	0.27	-0.01	0.45	0.31
Saturation	%	100.004	99.991	100.009	100.001	99.986	100.004	100.001	99.981	100.001	99.971	99.974
Core Diametre	cm	6.11	6.11	6.11	6.10	6.10	6.07	6.10	6.10	6.04	6.10	6.05
Core Length	cm	18.43	18.18	18.37	18.04	18.23	18.45	18.68	18.44	12.23	17.83	14.77
Volume of Rock Sample	cm3	540.38	533.05	538.62	527.21	532.77	533.90	545.92	538.90	350.42	521.08	424.60
Density (calculated from volume & mass)	g/cm3	2.63	2.64	2.71	2.70	2.71	2.72	2.68	2.67	2.95	2.92	2.76
Mass of Rock (calculated from volume and density)		1423.30	1405.20	1460.16	1420.96	1445.72	1450.83	1465.16	1440.30	1032.83	1523.57	1173.64
Masses before experiment												
Mass cylinder	g	381.407	381.465	381.034	354.716	357.070	381.486	361.770	376.902	362.381	376.629	383.385
Mass cylinder + core	g	1804.623	1786.632	1841.136	1775.656	1802.697	1832.313	1826.906	1817.131	1395.273	1900.287	1557.015
Mass cylinder + core + H2O	g	1945.843	1924.912	1979.208	1913.249	1941.151	1986.891	1967.458	1953.880	1513.166	2033.359	1699.618
Mass tot start	g	1945.926	1924.925	1979.224	1913.252	1941.154	1986.902	1967.482	1953.899	1513.055	2033.296	1699.629
Initial Water Mass	ml	141.220	138.280	138.072	137.593	138.454	154.578	140.552	136.749	117.893	133.072	142.603
Ratio Exp.Water : Rock		0.099	0.098	0.095	0.097	0.096	0.107	0.096	0.095	0.114	0.087	0.122
End Experiment		12.01.2022	12.01.2022	12.01.2022	12.01.2022	02.02.2022	02.02.2022	02.02.2022	02.02.2022	22.11.2022	22.11.2022	22.11.2022
Mass cylinder + core + H2O final	g	1938.359	1917.401	1971.113	1905.542	1933.505	1979.301	1960.050	1946.123	1505.481	2025.969	1691.003
Final Water Mass (measured, not all recoverable)	ml	130.272	127.438	135.105	127.041	127.861	138.022	129.954	125.461	106.492	121.895	129.901
Time Experiment	days	156	152	152	152	153	153	153	153	253	253	253
Volume of samples for Cl-measurements												
sample A	ml	0.5	0.5	0.5	0.5	0.7	0.5	0.5	0.6	0.5	0.5	0.7
sample B	ml	0.5	0.5	0.6	0.5	0.5	0.5	0.5	0.5	0.5	0.5	0.7
sample C	ml	0.5	0.5	0.5	0.5	0.5	0.5	0.5	0.5	0.5	0.5	0.7
sample D	ml	0.5	0.5	0.5	0.5	0.5	0.5	0.5	0.5	0.5	0.5	0.7
sample E	ml	0.5	0.5	0.5	0.5	0.5	0.5	0.5	0.5	0.5	0.5	0.7
sample F	ml	0.5	0.5	0.5	0.5	0.5	0.5	0.5	0.5	0.5	0.5	0.7
sample G	ml	0.5	0.5	0.6	0.5	0.5	0.5	0.5	0.5	0.5	0.5	0.5
sample H-1	ml	0.5	0.5	0.6	0.5	0.5	0.5	0.5	0.5	0.5	0.5	0.5
sample H-2	ml			0.6								
sample I	ml	0.5	0.5	0.5	0.5	0.5	0.5	0.5	0.5	0.5	0.5	0.5
sample K	ml	0.5	0.5	0.5	0.5	0.5	0.5	0.5	0.5	0.5	0.5	0.5
sample L	ml	0.5	0.5	0.5	0.5	0.5	0.5	0.5	0.5	0.5	0.5	0.5
sample M	ml	0.5	0.5	0.5	0.5	0.5	0.5	0.5	0.5	0.5	0.5	0.5
sample N	ml	0.5	0.5	0.5	0.5	0.5	0.5	0.5	0.5	0.5	0.5	0.5
total volume subsamples		6.5	6.5	7.4	6.5	6.7	6.5	6.5	6.6	6.5	6.5	7.7
Volumen TS calculated cyl (ini-final)	ml	7.6	7.5	8.1	7.7	7.6	7.6	7.4	7.8	7.574	7.327	8.626
Difference V(ss) - V(calc)	ml	1.067	1.024	0.711	1.210	0.949	1.101	0.932	1.176	1.074	0.827	0.926
Difference % of TS	%	0.8	0.7	0.5	0.9	0.7	0.7	0.7	0.9	0.9	0.6	0.6

Table B-5.2: Chemical composition of time series samples taken during out-diffusion experiments

Sample			IG_BH05_PW001											IG_BH05_PW002										
Sub-samples	Time	Date	Na	K	Ca	Mg	Sr	F	Cl	SO4	NO3	Br	Br/Cl	Na	K	Ca	Mg	Sr	F	Cl	SO4	NO3	Br	Br/Cl
	days		mg/l	mg/l	mg/l	mg/l	mg/l	mg/l	mg/l	mg/l	mg/l	mg/l		mg/l	mg/l	mg/l	mg/l	mg/l	mg/l	mg/l	mg/l	mg/l	mg/l	
Preparation		25.06.2021																						
A	1	26.06.2021	2.9	0.45	0.67	<0.2	<0.1	<0.1	0.46	<0.5	1.2	<0.05		3.9	1.5	2.0	<0.2	<0.1	<0.1	1.6	<0.5	<0.2	<0.05	
B	3	28.06.2021	4.6	0.63	0.73	<0.2	<0.1	<0.1	0.56	<0.5	1.3	<0.05		6.3	2.1	3.2	<0.2	<0.1	<0.1	3.5	<0.5	<0.2	0.06	17
C	4	29.06.2021	5.0	0.71	0.75	<0.2	<0.1	<0.1	0.61	<0.5	1.1	<0.05		7.1	2.2	3.5	<0.2	<0.1	<0.1	4.0	<0.5	<0.2	0.06	15
D	7	02.07.2021	6.1	0.83	0.81	<0.2	<0.1	0.11	0.66	<0.5	0.9	<0.05		8.8	2.3	4.1	<0.2	<0.1	0.17	4.6	<0.5	<0.2	0.06	13
E	12	07.07.2021	7.2	0.91	0.95	<0.2	<0.1	0.12	0.73	<0.5	0.92	<0.05		10.4	2.4	4.5	<0.2	<0.1	0.22	5.0	<0.5	<0.2	0.06	12
F	14	09.07.2021	7.7	0.92	0.97	<0.2	<0.1	0.13	0.77	<0.5	0.81	<0.05		11.2	2.4	4.7	<0.2	<0.1	0.27	5.3	<0.5	<0.2	0.06	11
G	21	16.07.2021	8.8	0.96	1.1	<0.2	<0.1	0.15	0.90	<0.5	0.71	<0.05		13.4	2.6	5.3	<0.2	<0.1	0.39	5.7	<0.5	<0.2	0.06	11
H	28	23.07.2021	9.6	1.0	1.2	<0.2	<0.1	0.18	0.96	<0.5	0.95	<0.05		14.3	2.7	5.6	<0.2	<0.1	0.46	6.3	0.55	<0.2	0.06	10
I	48	12.08.2021	11.0	1.1	1.2	<0.2	<0.1	0.23	1.0	0.53	0.50	<0.05		17.4	2.8	5.8	<0.2	<0.1	0.58	6.8	0.80	<0.2	0.06	9
K	61	25.08.2021	11.8	1.2	1.2	<0.2	<0.1	0.25	1.0	0.83	0.32	<0.05		19.2	2.8	5.9	<0.2	<0.1	0.62	6.8	0.95	<0.2	0.06	9
L	77	10.09.2021	12.3	1.2	1.2	<0.2	<0.1	0.28	1.0	1.2	<0.2	<0.05		20.5	2.8	6	<0.2	<0.1	0.79	6.8	1.1	<0.2	0.06	9
M	91	24.09.2021	13.2	1.3	1.2	<0.2	<0.1	0.30	1.0	1.7	<0.2	<0.05		21.7	2.8	6.20	<0.2	<0.1	0.83	6.8	1.3	<0.2	0.06	9
N	119	22.10.2021	15.3	1.4	1.2	<0.2	<0.1	0.38	1.0	2.6	<0.2	<0.05		24.3	2.9	6.3	<0.2	<0.1	0.97	6.8	1.6	<0.2	0.06	9
FINAL	140	12.11.2021	16.0	1.4	1.2	<0.2	<0.1	0.37	1.0	2.6	<0.2	<0.05		26.8	2.9	6.3	<0.2	<0.1	0.97	6.8	1.6	<0.2	0.06	9
Sample			IG_BH05_PW003																					
Sub-samples	Time	Date	Na	K	Ca	Mg	Sr	F	Cl	SO4	NO3	Br	Br/Cl											
	days		mg/l	mg/l	mg/l	mg/l	mg/l	mg/l	mg/l	mg/l	mg/l	mg/l												
Preparation		25.06.2021																						
A	1	26.06.2021	4.6	1.5	2.1	<0.2	<0.1	<0.1	1.7	<0.5	1.6	<0.05												
B	3	28.06.2021	7.5	2.0	3.0	<0.2	<0.1	<0.1	2.3	<0.5	1.8	<0.05												
C	4	29.06.2021	8.3	2.1	3.3	<0.2	<0.1	<0.1	2.4	<0.5	2.0	0.05	21											
D	7	02.07.2021	10.2	2.2	3.6	<0.2	<0.1	0.11	2.6	<0.5	1.6	0.06	23											
E	12	07.07.2021	12.2	2.3	3.9	<0.2	<0.1	0.17	2.8	<0.5	1.5	0.07	25											
F	14	09.07.2021	12.8	2.3	4.0	<0.2	<0.1	0.19	2.9	0.60	1.3	0.08	28											
G	21	16.07.2021	15.2	2.5	4.3	<0.2	<0.1	0.21	3.1	0.68	1.3	0.08	26											
H	28	23.07.2021	16.4	2.5	4.6	<0.2	<0.1	0.25	3.2	0.75	1.3	0.08	25											
I	48	12.08.2021	20.3	2.5	5.1	<0.2	<0.1	0.28	3.4	0.81	1.3	0.08	24											
K	61	25.08.2021	22.5	2.5	5.6	<0.2	<0.1	0.30	3.5	0.94	1.3	0.08	23											
L	77	10.09.2021	23.7	2.5	5.8	<0.2	<0.1	0.37	3.5	0.97	1.3	0.08	23											
M	91	24.09.2021	25.5	2.5	6	<0.2	<0.1	0.40	3.5	1.1	1.3	0.08	23											
N	119	22.10.2021	29.7	2.5	6	<0.2	<0.1	0.45	3.5	1.3	1.3	0.08	23											
FINAL	140	12.11.2021	30.2	2.5	6.1	<0.2	<0.1	0.5	3.5	1.5	1.3	0.08	23											
Sample			IG_BH05_PW004											IG_BH05_PW005										
Sub-samples	Time	Date	Na	K	Ca	Mg	Sr	F	Cl	SO4	NO3	Br	Br/Cl	Na	K	Ca	Mg	Sr	F	Cl	SO4	NO3	Br	Br/Cl
	days		mg/l	mg/l	mg/l	mg/l	mg/l	mg/l	mg/l	mg/l	mg/l	mg/l		mg/l	mg/l	mg/l	mg/l	mg/l	mg/l	mg/l	mg/l	mg/l	mg/l	
Preparation		06.07.2021																						
A	1	07.07.2021	13.3	0.40	1.3	<0.2	<0.1	<0.1	0.55	1.0	<0.2	<0.05		3.1	1.0	1.1	<0.2	<0.1	<0.1	0.79	<0.5	<0.2	<0.05	
B	3	09.07.2021	17.6	0.44	1.4	<0.2	<0.1	<0.1	0.67	1.2	<0.2	<0.05		4.4	1.5	1.7	<0.2	<0.1	0.11	2.1	<0.5	<0.2	<0.05	
C	4	10.07.2021	19.3	0.46	1.5	<0.2	<0.1	<0.1	0.71	1.3	<0.2	<0.05		4.9	1.6	2.0	<0.2	<0.1	0.12	2.4	<0.5	<0.2	<0.05	
D	7	13.07.2021	22.6	0.49	1.6	<0.2	<0.1	<0.1	0.78	1.8	<0.2	<0.05		5.9	1.8	2.2	<0.2	<0.1	0.13	2.6	0.53	<0.2	<0.05	
E	14	20.07.2021	25.6	0.52	1.8	<0.2	<0.1	<0.1	0.84	2.7	<0.2	<0.05		7.4	1.8	2.5	<0.2	<0.1	0.16	3.0	0.70	<0.2	<0.05	
F	16	22.07.2021	27.8	0.54	2.0	<0.2	<0.1	<0.1		3.6	<0.2	<0.05		7.6	1.8	2.7	<0.2	<0.1	0.17	3.1	0.75	<0.2	<0.05	
G	21	27.07.2021	30.5	0.60	2.2	<0.2	<0.1	<0.1	0.9	5.1	<0.2	<0.05		8.3	1.8	2.9	<0.2	<0.1	0.18	3.3	0.97	<0.2	<0.05	
H	29	04.08.2021	35.6	0.66	2.4	<0.2	<0.1	<0.1	0.94	6.4	<0.2	<0.05		9.7	2.0	3.1	<0.2	<0.1	0.20	3.6	1.2	<0.2	<0.05	
I	48	23.08.2021	40.7	0.7	2.5	<0.2	<0.1	0.1	0.94	8.2	<0.2	<0.05		11.5	2.0	3.2	<0.2	<0.1	0.23	3.9	1.7	<0.2	<0.05	
K	62	06.09.2021	44.5	0.72	2.6	<0.2	<0.1	0.12	0.94	10.5	<0.2	<0.05		12.2	2.0	3.3	<0.2	<0.1	0.28	4.1	2.0	<0.2	<0.05	
L	76	20.09.2021	48.6	0.75	2.6	<0.2	<0.1	0.16	0.94	11.8	<0.2	<0.05		13.2	2.0	3.4	<0.2	<0.1	0.33	4.1	2.3	<0.2	0.07	17
M	90	04.10.2021	50.2	0.77	2.6	<0.2	<0.1	0.18	0.94	13.1	<0.2	<0.05		14.3	2.0	3.6	<0.2	<0.1	0.35	4.1	2.7	<0.2	0.07	17
N	120	03.11.2021	53.2	0.78	2.7	<0.2	<0.1	0.22	0.94	15.9	<0.2	<0.05		16.3	2.0	4.0	<0.2	<0.1	0.38	4.1	3.7	<0.2	0.07	17
FINAL	129	12.11.2021	53.7	0.79	2.7	<0.2	<0.1	0.23	0.94	15.9	<0.2	<0.05		16.9	2.0	4.0	<0.2	<0.1	0.38	4.1	3.7	<0.2	<0.05	

Table B-5.2: Continued

Sample			IG_BH05_PW006											IG_BH05_PW007										
Sub-samples	Time	Date	Na	K	Ca	Mg	Sr	F	Cl	SO4	NO3	Br	Br/Cl	Na	K	Ca	Mg	Sr	F	Cl	SO4	NO3	Br	Br/Cl
	days		mg/l	mg/l	mg/l	mg/l	mg/l	mg/l	mg/l	mg/l	mg/l	mg/l		mg/l	mg/l	mg/l	mg/l	mg/l	mg/l	mg/l	mg/l	mg/l	mg/l	
Preparation		19.07.2021																						
A	1	20.07.2021	3.7	1.3	2.8	<0.2	<0.1	0.12	1.9	<0.5	<0.2	<0.05		3.9	1.2	2.5	<0.2	<0.1	<0.1	4.0	<0.5	<0.2	0.07	18
B	3	22.07.2021	5.2	1.4	3.9	<0.2	<0.1	0.22	2.7	<0.5	<0.2	<0.05		5.9	1.6	3.4	<0.2	<0.1	<0.1	6.2	<0.5	0.25	0.09	15
C	4	23.07.2021	5.6	1.5	4.4	<0.2	<0.1	0.43	2.9	<0.5	<0.2	<0.05		6.6	1.7	3.8	<0.2	<0.1	<0.1	6.8	<0.5	0.27	0.10	15
D	7	26.07.2021	6.9	1.7	5.3	<0.2	<0.1	0.61	3.6	<0.5	<0.2	<0.05		8.1	1.9	4.4	<0.2	<0.1	0.14	8.2	<0.5	<0.2	0.11	13
E	13	01.08.2021	9.0	2.0	6.0	<0.2	<0.1	0.74	4.2	0.52	<0.2	0.05	12	10.4	2.2	5.2	<0.2	<0.1	0.15	9.9	0.33	<0.2	0.13	13
F	16	04.08.2021	9.9	2.1	6.5	<0.2	<0.1	1.0	4.5	0.60	<0.2	0.05	11	11.5	2.3	5.6	<0.2	<0.1	0.18	10.7	0.45	0.22	0.15	14
G	21	09.08.2021	10.7	2.2	6.9	<0.2	<0.1	1.2	4.7	0.76	<0.2	0.05	11	12.1	2.3	5.9	<0.2	<0.1	0.25	11.0	0.55	<0.2	0.16	15
H	31	19.08.2021	11.8	2.3	7.6	<0.2	<0.1	1.3	4.8	0.92	<0.2	0.05	10	13.4	2.3	6.1	<0.2	<0.1	0.29	11.0	0.63	<0.2	0.16	15
I	49	06.09.2021	14.2	2.4	7.9	<0.2	<0.1	1.5	4.9	1.4	<0.2	0.05	10	15.2	2.3	6.3	<0.2	<0.1	0.33	11.0	0.80	0.22	0.16	15
K	63	20.09.2021	15.7	2.5	8.2	<0.2	<0.1	1.7	4.9	1.7	<0.2	0.05	10	16.4	2.3	6.4	<0.2	<0.1	0.40	11.0	0.91	<0.2	0.16	15
L	77	04.10.2021	16.7	2.5	8.6	<0.2	<0.1	1.8	4.9	2.0	<0.2	0.05	10	17.5	2.3	6.5	<0.2	<0.1	0.45	11.0	1.1	<0.2	0.16	15
M	91	18.10.2021	17.6	2.5	9.0	<0.2	<0.1	1.9	4.9	2.1	<0.2	0.05	10	18.6	2.3	6.6	<0.2	<0.1	0.49	11.0	1.4	<0.2	0.16	15
N	113	09.11.2021	19.1	2.7	10.4	<0.2	<0.1	2.1	4.9	2.5	<0.2	<0.05		19.6	2.3	6.6	<0.2	<0.1	0.54	11.0	1.7	<0.2	0.16	15
FINAL	134	30.11.2021	20.1	2.7	10.6	<0.2	<0.1	2.1	4.9	2.5	<0.2	<0.05		21.5	2.3	6.6	<0.2	<0.1	0.55	11.0	1.7	<0.2	0.16	15
Sample			IG_BH05_PW008											IG_BH05_PW009										
Sub-samples	Time	Date	Na	K	Ca	Mg	Sr	F	Cl	SO4	NO3	Br	Br/Cl	Na	K	Ca	Mg	Sr	F	Cl	SO4	NO3	Br	Br/Cl
	days		mg/l	mg/l	mg/l	mg/l	mg/l	mg/l	mg/l	mg/l	mg/l	mg/l		mg/l	mg/l	mg/l	mg/l	mg/l	mg/l	mg/l	mg/l	mg/l	mg/l	
Preparation		19.07.2021																						
A	1	20.07.2021	6.5	2.7	3.0	<0.2	<0.1	<0.1	11.0	<0.5	<0.2	0.47	43	8.4	2.3	6.6	<0.2	<0.1	<0.1	20.0	0.50	<0.2	0.46	23
B	3	22.07.2021	9.6	3.3	4.8	<0.2	<0.1	<0.1	17.2	<0.5	<0.2	0.66	38	13.2	2.7	10.5	<0.2	<0.1	0.16	34.8	0.68	<0.2	0.63	18
C	4	23.07.2021	10.3	3.4	5.4	<0.2	<0.1	<0.1	18.7	<0.5	<0.2	0.72	39	14.7	2.8	13.2	<0.2	<0.1	0.21	39.3	0.76	<0.2	0.71	18
D	7	26.07.2021	12.7	3.7	6.4	<0.2	<0.1	<0.1	22.5	<0.5	<0.2	0.95	42	18.0	3.2	14.4	<0.2	<0.1	0.28	47.3	0.99	<0.2	0.85	18
E	13	01.08.2021	15.9	4.1	7.9	<0.2	<0.1	<0.1	27.5	0.55	<0.2	1.2	44	21.7	3.7	16.8	<0.2	<0.1	0.46	53.6	1.4	<0.2	0.92	17
F	16	04.08.2021	16.8	4.2	8.3	<0.2	<0.1	<0.1	29.3	0.73	<0.2	1.3	44	23.2	3.7	18.3	<0.2	<0.1	0.68	54.4	1.7	<0.2	0.95	17
G	21	09.08.2021	17.8	4.2	8.7	<0.2	<0.1	0.11	30.2	0.93	<0.2	1.4	46	23.4	3.7	20.1	<0.2	<0.1	0.89	54.7	2.1	<0.2	0.95	17
H	31	19.08.2021	18.9	4.2	9.1	<0.2	<0.1	0.12	30.5	1.1	<0.2	1.4	46	24.3	3.7	21.3	<0.2	<0.1	1.1	54.8	2.3	<0.2	0.95	17
I	49	06.09.2021	20.8	4.2	9.8	<0.2	<0.1	0.13	30.5	1.5	<0.2	1.4	46	25.7	3.7	21.6	<0.2	<0.1	1.5	54.8	2.8	<0.2	0.95	17
K	63	20.09.2021	22.2	4.2	10.2	<0.2	<0.1	0.14	30.5	1.8	<0.2	1.4	46	26.4	3.7	22.8	<0.2	<0.1	1.7	54.8	3.1	<0.2	0.95	17
L	77	04.10.2021	22.9	4.2	10.4	<0.2	<0.1	0.15	30.5	2.1	<0.2	1.4	46	26.8	3.7	22.8	<0.2	<0.1	1.8	54.8	3.8	<0.2	0.95	17
M	91	18.10.2021	24.1	4.2	10.9	<0.2	<0.1	0.15	30.5	2.7	<0.2	1.4	46	27.3	3.7	22.8	<0.2	<0.1	2.0	54.8	4.3	<0.2	0.95	17
N	113	09.11.2021	25.1	4.2	11.2	<0.2	<0.1	0.15	30.5	2.7	<0.2	1.4	46	28.4	3.7	24.3	<0.2	<0.1	2.0	54.8	4.3	<0.2	0.95	17
FINAL	134	30.11.2021	27.2	4.4	12.6	<0.2	<0.1	0.15	30.5	2.7	<0.2	1.4	46	29.9	3.7	25.7	<0.2	<0.1	2.0	54.8	4.3	<0.2	0.95	17
Sample			IG_BH05_PW010											IG_BH05_PW011										
Sub-samples	Time	Date	Na	K	Ca	Mg	Sr	F	Cl	SO4	NO3	Br	Br/Cl	Na	K	Ca	Mg	Sr	F	Cl	SO4	NO3	Br	Br/Cl
	days		mg/l	mg/l	mg/l	mg/l	mg/l	mg/l	mg/l	mg/l	mg/l	mg/l		mg/l	mg/l	mg/l	mg/l	mg/l	mg/l	mg/l	mg/l	mg/l	mg/l	
Preparation		19.07.2021																						
A	1	20.07.2021	5.5	3.6	6.7	<0.2	<0.1	<0.1	16.2	<0.5	<0.2	0.35	22	5.8	4.5	7.3	<0.2	<0.1	<0.1	19.9	<0.5	<0.2	0.43	22
B	3	22.07.2021	8.9	4.7	10.8	<0.2	<0.1	<0.1	28.6	<0.5	<0.2	0.59	21	8.4	4.7	11.8	<0.2	<0.1	<0.1	31.3	<0.5	<0.2	0.72	23
C	4	23.07.2021	9.9	5.0	12.4	<0.2	<0.1	<0.1	33.0	<0.5	<0.2	0.63	19	9.4	5.0	12.8	<0.2	<0.1	<0.1	35.5	<0.5	<0.2	0.77	22
D	7	26.07.2021	12.4	5.6	17.3	<0.2	<0.1	<0.1	39.3	0.74	<0.2	0.85	22	11.3	5.5	17.3	<0.2	<0.1	<0.1	46.1	0.78	<0.2	0.87	19
E	13	01.08.2021	16.5	6.8	22.9	0.21	<0.1	<0.1	51.9	0.86	0.26	0.99	19	15.0	6.7	22.4	0.20	<0.1	<0.1	53.3	1.0	<0.2	1.1	21
F	16	04.08.2021	17.9	6.9	24.6	0.20	<0.1	<0.1	56.4	0.93	0.36	1.1	20	16.1	7.0	23.9	0.20	<0.1	<0.1	57.8	1.2	<0.2	1.2	21
G	21	09.08.2021	18.7	7.0	28.0	<0.2	<0.1	<0.1	59.3	1.4	0.42	1.2	20	16.8	7.1	25.6	<0.2	<0.1	<0.1	60.7	1.5	<0.2	1.3	21
H	31	19.08.2021	20.4	7.1	28.3	0.21	<0.1	<0.1	63.0	1.6	0.37	1.3	21	18.1	7.3	27.8	0.20	<0.1	<0.1	63.0	1.7	<0.2	1.3	21
I	49	06.09.2021	22.2	7.1	28.8	<0.2	<0.1	<0.1	65.9	2.0	0.32	1.4	21	19.5	7.4	28.4	<0.2	<0.1	<0.1	66.6	2.2	<0.2	1.3	20
K	63	20.09.2021	23.4	7.1	29.4	<0.2	<0.1	<0.1	65.9	2.5	<0.2	1.4	21	20.9	7.6	29.3	<0.2	<0.1	<0.1	66.6	2.5	<0.2	1.3	20
L	77	04.10.2021	24.1	7.1	29.8	<0.2	<0.1	<0.1	65.9	3.0	0.38	1.4	21	21.5	7.8	30.0	<0.2	<0.1	<0.1	66.6	3.1	<0.2	1.3	20
M	91	18.10.2021	24.8	7.1	30.4	<0.2	<0.1	0.10	65.9	3.5	0.23	1.4	21	22.2	7.8	30.9	<0.2	<0.1	<0.1	66.6	3.5	<0.2	1.3	20
N	113	09.11.2021	26.0	7.1	32.4	<0.2	<0.1	0.10	65.9	4.0	0.37	1.4	21	23.7	8.4	31.6	<0.2	<0.1	<0.1	66.6	3.8	<0.2	1.3	20
FINAL	134	30.11.2021	27.6	7.1	32.5	<0.2	<0.1	<0.1	65.9	4.1	<0.2	1.4	21	25.1	8.2	31.9	<0.2	<0.1	<0.1	66.6	3.8	<0.2	1.3	20

Table B-5.2: Continued

Sample			IG_BH05_PW012											IG_BH05_PW013										
Sub-samples	Time	Date	Na	K	Ca	Mg	Sr	F	Cl	SO4	NO3	Br	Br/Cl	Na	K	Ca	Mg	Sr	F	Cl	SO4	NO3	Br	Br/Cl
	days		mg/l	mg/l	mg/l	mg/l	mg/l	mg/l	mg/l	mg/l	mg/l	mg/l		mg/l	mg/l	mg/l	mg/l	mg/l	mg/l	mg/l	mg/l	mg/l	mg/l	
Preparation		09.08.2021																						
A	1	10.08.2021	6.8	3.9	8.0	<0.2	<0.1	<0.1	21.2	0.29	<0.2	0.55	26	9.6	4.2	13.0	<0.2	<0.1	<0.1	38.9	0.33	<0.2	0.78	20
B	3	12.08.2021	10.0	5.0	12.6	<0.2	<0.1	<0.1	33.6	0.31	<0.2	0.70	21	14.5	5.2	22.0	0.20	<0.1	<0.1	57.1	0.63	0.23	1.1	19
C	4	13.08.2021	11.5	5.4	14.2	<0.2	<0.1	<0.1	40.3	0.5	<0.2	0.86	21	16.9	5.6	26.0	0.22	<0.1	<0.1	69.1	0.74	<0.2	1.5	22
D	7	16.08.2021	14.4	6.4	20.2	<0.2	<0.1	<0.1	48.3	0.9	<0.2	0.94	19	20.4	6.2	31.8	0.24	<0.1	<0.1	77.8	1.1	<0.2	1.8	23
E	11	20.08.2021	16.6	6.7	22.1	<0.2	<0.1	<0.1	53.4	1.1	<0.2	1.1	21	23.0	6.4	33.7	0.22	<0.1	<0.1	85.5	1.4	<0.2	1.9	22
F	14	23.08.2021	17.5	6.8	23.8	<0.2	<0.1	<0.1	56.6	1.2	<0.2	1.2	21	24.4	6.5	35.6	0.24	<0.1	<0.1	89.6	1.7	<0.2	2.0	22
G	21	30.08.2021	20.0	7.2	25.2	<0.2	<0.1	<0.1	63.8	1.5	<0.2	1.3	20	26.4	6.5	37.1	0.25	<0.1	<0.1	98.7	1.9	<0.2	2.1	21
H	29	07.09.2021	21.5	7.4	26.9	<0.2	<0.1	<0.1	71.4	1.7	<0.2	1.4	20	27.0	6.5	38.5	0.20	<0.1	0.11	102	2.2	<0.2	2.2	22
I	49	27.09.2021	23.5	7.6	28.0	<0.2	<0.1	<0.1	75.9	2.2	<0.2	1.4	18	29.2	6.5	40.8	<0.2	<0.1	0.13	102	2.8	<0.2	2.2	22
K	63	11.10.2021	25.3	7.8	29.8	<0.2	<0.1	<0.1	75.9	2.9	<0.2	1.4	18	29.5	6.5	42.0	<0.2	<0.1	0.14	102	3.1	<0.2	2.2	22
L	74	22.10.2021	26.3	8.0	31.0	<0.2	<0.1	<0.1	75.9	3.4	<0.2	1.4	18	30.5	6.5	43.0	0.23	<0.1	0.18	102	3.9	<0.2	2.2	22
M	92	09.11.2021	26.5	7.9	31.9	<0.2	<0.1	<0.1	75.9	3.4	<0.2	1.4	18	31.4	6.7	43.7	0.23	<0.1	0.14	102	3.9	<0.2	2.2	22
N													/											/
FINAL	113	30.11.2021	33.5	8.3	32.3	<0.2	<0.1	<0.1	75.9	3.4	<0.2	1.4	18	33.0	6.5	43.6	0.22	<0.1	0.18	102	3.9	<0.2	2.2	22
Sample			IG_BH05_PW014																					
Sub-samples	Time	Date	Na	K	Ca	Mg	Sr	F	Cl	SO4	NO3	Br	Br/Cl											
	days		mg/l	mg/l	mg/l	mg/l	mg/l	mg/l	mg/l	mg/l	mg/l	mg/l												
Preparation		09.08.2021																						
A	1	10.08.2021	5.5	3.5	7.2	<0.2	<0.1	<0.1	14.3	0.26	<0.2	0.22	15											
B	3	12.08.2021	7.9	3.8	10.1	<0.2	<0.1	<0.1	21.4	0.38	<0.2	0.30	14											
C	4	13.08.2021	9.3	4.0	11.5	<0.2	<0.1	<0.1	25.8	0.49	<0.2	0.42	16											
D	7	16.08.2021	11.6	4.5	14.1	<0.2	<0.1	<0.1	31.1	0.58	<0.2	0.55	18											
E	11	20.08.2021	13.4	4.8	15.8	<0.2	<0.1	<0.1	35.0	0.9	<0.2	0.64	18											
F	14	23.08.2021	14.6	5.1	17.3	<0.2	<0.1	<0.1	37.9	1.1	<0.2	0.70	18											
G	21	30.08.2021	16.6	5.3	18.9	<0.2	<0.1	<0.1	43.9	1.4	<0.2	0.84	19											
H	29	07.09.2021	18.1	5.5	20.8	<0.2	<0.1	<0.1	47.7	1.7	<0.2	0.92	19											
I	49	27.09.2021	20.4	5.8	22.8	<0.2	<0.1	<0.1	50.1	2.0	<0.2	0.95	19											
K	63	11.10.2021	21.8	6.1	24.3	<0.2	<0.1	<0.1	50.1	2.4	<0.2	0.95	19											
L	74	22.10.2021	24.5	6.4	26.3	<0.2	<0.1	<0.1	50.1	2.8	<0.2	0.95	19											
M	92	09.11.2021	24.2	6.4	26.3	<0.2	<0.1	<0.1	50.1	2.9	<0.2	0.95	19											
N													/											
FINAL	113	30.11.2021	26.2	6.3	26.6	<0.2	<0.1	<0.1	50.1	3	<0.2	0.95	19											
Sample			IG_BH05_PW015											IG_BH05_PW016										
Sub-samples	Time	Date	Na	K	Ca	Mg	Sr	F	Cl	SO4	NO3	Br	Br/Cl	Na	K	Ca	Mg	Sr	F	Cl	SO4	NO3	Br	Br/Cl
	days		mg/l	mg/l	mg/l	mg/l	mg/l	mg/l	mg/l	mg/l	mg/l	mg/l		mg/l	mg/l	mg/l	mg/l	mg/l	mg/l	mg/l	mg/l	mg/l	mg/l	
Preparation		29.07.2021																						
A	1	30.07.2021	4.3	2.8	5.0	<0.2	<0.1	<0.1	8.6	0.17	<0.2	0.23	27	4.3	2.5	8.4	<0.2	<0.1	<0.1	11.6	0.25	<0.2	0.26	22
B	3	01.08.2021	5.9	3.4	6.2	<0.2	<0.1	<0.1	11.8	0.19	<0.2	0.27	23	5.9	2.7	10.4	<0.2	<0.1	<0.1	16.8	0.29	<0.2	0.35	21
C	4	02.08.2021	6.3	3.6	6.7	<0.2	<0.1	<0.1	12.8	0.21	<0.2	0.30	23	6.6	3.0	12.1	<0.2	<0.1	0.14	19.0	0.34	<0.2	0.38	20
D	7	05.08.2021	7.9	4.0	8.6	<0.2	<0.1	<0.1	16.2	0.25	<0.2	0.40	25	7.7	3.3	15.8	<0.2	<0.1	0.32	22.9	0.39	<0.2	0.46	20
E	12	10.08.2021	9.6	4.3	9.8	<0.2	<0.1	<0.1	19.9	0.41	<0.2	0.58	29	9.3	3.6	18.6	<0.2	<0.1	0.47	27.9	0.55	<0.2	0.53	19
F	14	12.08.2021	10.5	4.6	10.5	<0.2	<0.1	<0.1	21.6	0.50	<0.2	0.63	29	9.9	3.8	19.3	<0.2	<0.1	0.53	29.4	0.68	<0.2	0.55	19
G	21	19.08.2021	11.8	4.8	11.4	<0.2	<0.1	0.10	24.0	0.70	<0.2	0.66	28	11.3	4.1	22.1	<0.2	<0.1	0.57	31.7	0.99	<0.2	0.63	20
H	29	27.08.2021	13.8	5.0	12.0	<0.2	<0.1	0.13	25.7	0.96	<0.2	0.66	26	12.9	4.2	23.3	<0.2	<0.1	0.62	34.8	1.2	<0.2	0.70	20
I	48	15.09.2021	15.4	5.1	12.6	<0.2	<0.1	0.17	27.0	1.3	<0.2	0.66	24	13.5	4.3	24.8	<0.2	<0.1	0.72	34.8	1.8	<0.2	0.72	21
K	61	28.09.2021	16.7	5.2	13.1	<0.2	<0.1	0.19	27.0	1.6	<0.2	0.66	24	14.3	4.3	25.5	<0.2	<0.1	0.75	34.8	2.4	<0.2	0.72	21
L	76	13.10.2021	18.1	5.2	13.8	<0.2	<0.1	0.20	27.0	2.0	<0.2	0.66	24	15.3	4.4	26.5	<0.2	<0.1	0.78	34.8	2.7	0.22	0.72	21
M	91	28.10.2021	19.6	5.2	14.3	<0.2	<0.1	0.23	27.0	2.5	<0.2	0.66	24	16.4	4.4	27.5	0.20	<0.1	0.85	34.8	3.4	<0.2	0.72	21
N	123	29.11.2021	21.2	5.2	14.4	<0.2	<0.1	0.23	27.0	2.6	<0.2	0.66	24	17.4	4.4	27.9	<0.2	<0.1	0.87	34.8	3.5	<0.2	0.72	21
FINAL	124	30.11.2021	21.3	5.2	14.5	<0.2	<0.1	0.25	27.0	2.6	<0.2	0.66	24	17.5	4.4	27.9	0.20	<0.1	0.88	34.8	3.5	<0.2	0.72	21

Table B-5.2: Continued

Sample			IG_BH05_PW017											IG_BH05_PW018										
Sub-samples	Time	Date	Na	K	Ca	Mg	Sr	F	Cl	SO4	NO3	Br	Br/Cl	Na	K	Ca	Mg	Sr	F	Cl	SO4	NO3	Br	Br/Cl
	days		mg/l	mg/l	mg/l	mg/l	mg/l	mg/l	mg/l	mg/l	mg/l	mg/l		mg/l	mg/l	mg/l	mg/l	mg/l	mg/l	mg/l	mg/l	mg/l	mg/l	
Preparation		16.08.2021																						
A	1	17.08.2021	2.7	1.8	6.2	<0.2	<0.1	<0.1	5.9	0.13	<0.2	0.09	15	4.0	1.7	4.7	<0.2	<0.1	0.14	9.9	0.17	<0.2	0.22	22
B	3	19.08.2021	5.6	2.4	10.0	<0.2	<0.1	<0.1	13.1	0.18	<0.2	0.30	23	8.6	2.6	9.3	<0.2	<0.1	0.24	22.0	0.32	<0.2	0.63	29
C	4	20.08.2021	6.4	2.5	10.8	<0.2	<0.1	0.10	14.4	0.21	<0.2	0.34	24	10.1	2.7	10.8	<0.2	<0.1	0.27	27.5	0.41	<0.2	0.83	30
D	7	23.08.2021	8.2	2.7	13.2	<0.2	<0.1	0.16	19.3	0.35	<0.2	0.40	21	12.9	3.0	13.1	<0.2	<0.1	0.38	31.6	0.52	<0.2	0.93	29
E	11	27.08.2021	9.9	2.8	15.1	<0.2	<0.1	0.25	23.9	0.43	<0.2	0.50	21	14.9	3.3	14.9	<0.2	<0.1	0.72	35.1	0.66	<0.2	1.0	28
F	14	30.08.2021	10.6	2.9	16.5	<0.2	<0.1	0.30	25.9	0.57	<0.2	0.58	22	16.3	3.4	15.9	<0.2	<0.1	0.93	39.3	0.76	<0.2	1.1	28
G	21	06.09.2021	12.1	3.0	17.9	<0.2	<0.1	0.51	28.6	0.65	<0.2	0.62	22	17.9	3.4	16.8	<0.2	<0.1	1.0	42.9	0.86	<0.2	1.2	28
H-1	25	10.09.2021											/											/
H-2	29	14.09.2021	13.2	3.0	18.7	<0.2	<0.1	0.53	30.0	0.83	<0.2	0.66	22	19	3.4	17.6	<0.2	<0.1	1.2	43.4	1.1	<0.2	1.2	
I	49	04.10.2021	15.3	3.0	20.0	<0.2	<0.1	0.56	33.0	1.2	<0.2	0.71	22	21.5	3.4	18.5	<0.2	<0.1	1.5	43.9	1.5	<0.2	1.2	27
K	63	18.10.2021	16.5	3.0	21.2	<0.2	<0.1	0.58	34.7	1.6	<0.2	0.71	20	22.9	3.4	19.0	<0.2	<0.1	1.6	43.9	2.1	<0.2	1.2	27
L	78	02.11.2021	18.1	3.0	23	<0.2	<0.1	0.69	34.7	2.0	<0.2	0.71	20	24.4	3.4	19.4	<0.2	<0.1	1.7	43.9	2.4	<0.2	1.2	27
M	91	15.11.2021	18.0	3.0	23.4	<0.2	<0.1	0.56	34.7	2.2	<0.2	0.71	20	24.3	3.4	19.8	<0.2	<0.1	1.8	43.9	2.6	<0.2	1.2	27
N	121	15.12.2021	19.1	3.0	24.0	<0.2	<0.1	0.67	34.7	2.2	<0.2	0.71	20	25.7	3.5	20.8	<0.2	<0.1	2.3	43.9	2.6	<0.2	1.2	27
FINAL	149	12.01.2022	20.4	3.0	24.1	<0.2	<0.1	0.70	34.7	2.5	<0.2	0.71	20	26.3	3.2	20.8	<0.2	<0.1	2.5	43.9	2.8	<0.2	1.2	27
Sample			IG_BH05_PW019																					
Sub-samples	Time	Date	Na	K	Ca	Mg	Sr	F	Cl	SO4	NO3	Br	Br/Cl											
	days		mg/l	mg/l	mg/l	mg/l	mg/l	mg/l	mg/l	mg/l	mg/l	mg/l												
Preparation		16.08.2021																						
A	1	17.08.2021	3.2	1.8	4.6	<0.2	<0.1	<0.1	8.4	0.31	<0.2	0.12	14											
B	3	19.08.2021	6.1	2.3	8.5	<0.2	<0.1	<0.1	17.1	0.38	<0.2	0.25	15											
C	4	20.08.2021	7.0	2.4	9.6	<0.2	<0.1	0.10	20.0	0.56	<0.2	0.38	19											
D	7	23.08.2021	8.8	2.6	11.8	<0.2	<0.1	0.11	24.3	0.67	<0.2	0.46	19											
E	11	27.08.2021	10.3	2.7	12.9	<0.2	<0.1	0.16	28.5	0.95	<0.2	0.55	19											
F	14	30.08.2021	11.2	2.7	13.9	<0.2	<0.1	0.20	31.7	1.2	<0.2	0.62	20											
G	21	06.09.2021	13.1	2.8	15.6	<0.2	<0.1	0.27	35.5	1.5	<0.2	0.67	19											
H-1	25	10.09.2021											/											
H-2	29	14.09.2021	13.9	2.8	16.4	<0.2	<0.1	0.33	36.9	1.9	<0.2	0.69	19											
I	49	04.10.2021	16.5	2.8	17.9	<0.2	<0.1	0.40	39.7	2.9	<0.2	0.69	17											
K	63	18.10.2021	17.4	2.8	19.1	<0.2	<0.1	0.41	40.2	3.5	<0.2	0.69	17											
L	78	02.11.2021	18.7	2.8	20.0	0.27	<0.1	0.46	40.2	4.1	<0.2	0.69	17											
M	91	15.11.2021	18.9	2.9	20.0	0.25	<0.1	0.51	40.2	4.2	<0.2	0.69	17											
N	121	15.12.2021	20.0	2.9	21.0	0.25	<0.1	0.57	40.2	4.5	<0.2	0.69	17											
FINAL	149	12.01.2022	20.9	2.9	21.0	0.29	<0.1	0.64	40.2	4.6	<0.2	0.69	17											
Sample			IG_BH05_PW020											IG_BH05_PW021										
Sub-samples	Time	Date	Na	K	Ca	Mg	Sr	F	Cl	SO4	NO3	Br	Br/Cl	Na	K	Ca	Mg	Sr	F	Cl	SO4	NO3	Br	Br/Cl
	days		mg/l	mg/l	mg/l	mg/l	mg/l	mg/l	mg/l	mg/l	mg/l	mg/l		mg/l	mg/l	mg/l	mg/l	mg/l	mg/l	mg/l	mg/l	mg/l	mg/l	
Preparation		09.08.2021																						
A	1	10.08.2021	3.8	3.0	8.5	<0.2	<0.1	<0.1	14.9	0.30	<0.2	0.27	18	4.4	2.4	7.2	<0.2	<0.1	<0.1	15.1	0.25	<0.2	0.36	24
B	3	12.08.2021	5.6	3.6	12.6	<0.2	<0.1	<0.1	22.8	0.48	<0.2	0.35	15	6.8	3.3	11.7	<0.2	<0.1	0.11	24.4	0.38	<0.2	0.48	20
C	4	13.08.2021	6.3	3.8	14.0	<0.2	<0.1	<0.1	27.0	0.59	0.24	0.41	15	7.7	3.5	12.8	<0.2	<0.1	0.16	27.3	0.51	<0.2	0.53	19
D	7	16.08.2021	7.9	4.3	17.4	<0.2	<0.1	<0.1	32.9	0.67	0.27	0.62	19	9.7	4.0	16.2	<0.2	<0.1	0.18	33.7	0.60	<0.2	0.79	23
E	11	20.08.2021	9.2	4.5	19.4	<0.2	<0.1	<0.1	35.8	0.92	0.38	0.70	20	11.1	4.1	18.2	<0.2	<0.1	0.19	38.0	0.82	<0.2	0.92	24
F	14	23.08.2021	9.9	4.6	20.8	<0.2	<0.1	<0.1	39.1	1.2	0.50	0.78	20	12.2	4.2	20.1	<0.2	<0.1	0.21	39.9	1.0	<0.2	1.1	28
G	21	30.08.2021	11.0	4.8	22.7	<0.2	<0.1	0.13	44.9	1.6	0.50	0.89	20	13.6	4.3	22.0	<0.2	<0.1	0.25	46.3	1.2	<0.2	1.2	26
H	29	07.09.2021	11.7	4.9	24.0	<0.2	<0.1	0.15	46.6	1.9	0.47	0.92	20	14.4	4.3	23.2	<0.2	<0.1	0.35	49.9	1.4	<0.2	1.2	24
I	49	27.09.2021	12.9	5.1	26.8	<0.2	<0.1	0.16	50.0	2.3	0.52	0.94	19	16.2	4.3	25.0	<0.2	<0.1	0.39	53.4	1.9	<0.2	1.2	22
K	63	11.10.2021	14.0	5.2	28.1	<0.2	<0.1	0.17	50.0	2.9	0.54	0.94	19	16.9	4.3	26.2	<0.2	<0.1	0.41	53.4	2.4	<0.2	1.2	22
L	74	22.10.2021	15.2	5.3	30.3	<0.2	<0.1	0.19	50.0	3.2	0.89	0.94	19	18.1	4.3	27.3	<0.2	<0.1	0.50	53.4	2.7	0.22	1.2	22
M	92	09.11.2021	14.8	5.0	30.3	<0.2	<0.1	0.19	50.0	3.3	0.56	0.94	19	18.6	4.3	28.0	<0.2	<0.1	0.33	53.2	2.7	0.22	1.2	23
N	120	07.12.2021	15.5	5.2	30.9	<0.2	<0.1	0.19	50.0	3.3	0.69	0.94	19	18.9	4.3	28.2	<0.2	<0.1	0.53	53.2	2.7	<0.2	1.2	23
FINAL	156	12.01.2022	16.0	4.9	31.6	0.26	<0.1	0.2	50	3.3	0.54	0.94	19	20.1	4.3	30.3	<0.2	<0.1	0.76	53.4	2.7	<0.2	1.2	22

Table B-5.2: Continued

Sample			IG_BH05_PW022										
Sub-samples	Time	Date	Na	K	Ca	Mg	Sr	F	Cl	SO4	NO3	Br	Br/Cl
	days		mg/l	mg/l	mg/l	mg/l	mg/l	mg/l	mg/l	mg/l	mg/l	mg/l	
Preparation		09.08.2021											
A	1	10.08.2021	10.0	1.9	16.3	<0.2	<0.1	0.13	40.4	0.64	<0.2	2.1	52
B	3	12.08.2021	13.9	2.3	25.3	0.25	<0.1	0.22	52.4	0.88	<0.2	2.8	53
C	4	13.08.2021	16.1	2.6	29.4	0.27	<0.1	0.27	62.4	1.2	<0.2	3.1	50
D	7	16.08.2021	18.7	2.7	33.7	0.28	<0.1	0.41	68.0	1.8	<0.2	3.4	50
E	11	20.08.2021	21.0	2.8	35.6	0.28	<0.1	0.53	72.6	2.2	<0.2	3.6	50
F	14	23.08.2021	22.3	2.9	38.2	0.30	<0.1	0.56	77.6	2.6	<0.2	3.8	49
G	21	30.08.2021	24.0	2.9	40.1	0.32	<0.1	0.65	83.9	2.9	<0.2	4.0	48
H	29	07.09.2021	25.2	2.9	43.1	0.27	<0.1	0.79	87.6	3.5	<0.2	4.1	47
I	49	27.09.2021	27.4	2.9	45.9	0.29	<0.1	0.95	88.3	4.4	<0.2	4.1	46
K	63	11.10.2021	28.4	2.9	48.3	0.32	<0.1	1.1	88.3	5.1	<0.2	4.1	46
L	75	23.10.2021	30.5	2.9	51.0	0.38	<0.1	1.3	88.3	5.6	<0.2	4.1	46
M	91	08.11.2021	30.5	2.9	51.1	0.38	<0.1	1.3	88.3	5.6	<0.2	4.1	46
N	120	07.12.2021	31.6	2.9	52.1	0.38	<0.1	1.3	88.3	5.8	<0.2	4.1	46
FINAL	156	12.01.2022	32.3	2.9	52.9	0.53	<0.1	1.9	88.3	6.5	<0.2	4.1	46

Sample			IG_BH05_PW023											IG_BH05_PW024										
Sub-samples	Time	Date	Na	K	Ca	Mg	Sr	F	Cl	SO4	NO3	Br	Br/Cl	Na	K	Ca	Mg	Sr	F	Cl	SO4	NO3	Br	Br/Cl
	days		mg/l	mg/l	mg/l	mg/l	mg/l	mg/l	mg/l	mg/l	mg/l	mg/l		mg/l	mg/l	mg/l	mg/l	mg/l	mg/l	mg/l	mg/l	mg/l	mg/l	
Preparation		16.08.2021																						
A	1	17.08.2021	2.9	1.4	4.4	<0.2	<0.1	<0.1	8.9	0.24	<0.2	0.15	17	2.7	2.3	4.2	<0.2	<0,1	<0,1	7.1	0.25	<0.2	0.10	14
B	3	19.08.2021	7.1	2.4	11.9	<0.2	<0.1	0.16	25.6	0.55	<0.2	0.62	24	5.3	3.2	8.5	<0.2	<0,1	<0,1	15.2	0.46	<0.2	0.26	17
C	4	20.08.2021	8.3	2.6	13.7	<0.2	<0.1	0.18	29.6	0.76	<0.2	0.7	25	6.1	3.4	9.5	<0.2	<0,1	<0,1	17.2	0.52	<0.2	0.30	17
D	7	23.08.2021	10.8	3.0	18.3	0.23	<0.1	0.27	40.1	0.92	<0.2	0.9	23	7.6	3.5	11.7	<0.2	<0,1	<0,1	22.2	0.61	<0.2	0.36	16
E	11	27.08.2021	12.7	3.4	21.6	0.32	<0.1	0.44	45.4	1.3	<0.2	1.0	22	9.1	3.7	13.1	<0.2	<0,1	<0,1	26.9	0.71	<0.2	0.44	16
F	14	30.08.2021	13.9	3.5	23.8	0.39	<0.1	0.69	51.1	1.5	<0.2	1.1	22	10.2	3.9	14.4	<0.2	<0,1	<0,1	30.9	0.87	<0.2	0.54	17
G	21	06.09.2021	15.1	3.6	24.2	0.40	<0.1	0.88	54.6	2.0	<0.2	1.2	22	11.6	4.5	17.3	<0.2	<0,1	<0,1	36	0.99	<0.2	0.65	18
H-1	25	10.09.2021											/	14.5	5.3	21.8	<0.2	<0,1	<0,1	41.7	1.6	<0.2	0.78	19
H-2	29	14.09.2021	16.2	3.6	24.8	0.40	<0.1	1.0	55.4	2.6	<0.2	1.3	23	17.1	6.7	24.9	<0.2	<0,1	<0,1	45.8	2.3	<0.2	0.85	18
I	49	04.10.2021	17.9	3.6	25.1	0.40	<0.1	1.3	56.2	3.3	<0.2	1.3	23	22.5	8.3	29.6	<0.2	<0,1	0.1	56.4	4.9	<0.2	1.01	18
K	63	18.10.2021	18.7	3.6	28.4	0.43	<0.1	1.5	56.2	3.6	<0.2	1.3	23	25.1	8.8	33.8	<0.2	<0,1	0.2	57.3	6.8	<0.2	1.06	18
L	78	02.11.2021	19.7	3.6	29.4	0.50	<0.1	1.7	56.2	4.3	0.26	1.3	23	28.4	8.8	37.1	<0.2	<0,1	0.3	58.3	7.5	0.24	1.11	19
M	91	15.11.2021	19.6	3.6	30.2	0.46	<0.1	1.7	56.1	4.6	<0.2	1.3	23	28.4	8.8	37.1	<0.2	<0,1	0.4	58.7	7.5	<0.2	1.11	19
N	121	15.12.2021	20.1	3.6	31.2	0.44	<0.1	2.0	56.2	4.6	<0.2	1.3	23	31.0	8.8	38.5	<0.2	<0,1	0.3	61.6	7.7	<0.2	1.11	18
FINAL	149	12.01.2022	21.2	3.6	32.5	0.47	<0.1	2.4	56.2	4.9	<0.2	1.3	23	34.3	8.8	40.4	<0.2	<0,1	0.3	61.6	8.0	<0.2	1.11	18

Sample			IG_BH05_PW025										
Sub-samples	Time	Date	Na	K	Ca	Mg	Sr	F	Cl	SO4	NO3	Br	Br/Cl
	days		mg/l	mg/l	mg/l	mg/l	mg/l	mg/l	mg/l	mg/l	mg/l	mg/l	
Preparation		16.08.2021											
A	1	17.08.2021	3.5	3	6.2	<0.2	<0.1	<0.1	13.7	0.18	<0.2	0.29	21
B	3	19.08.2021	7.7	4.8	15.1	<0.2	<0.1	<0.1	35.0	0.24	<0.2	0.94	27
C	4	20.08.2021	8.9	5.3	17.5	<0.2	<0.1	<0.1	39.7	0.36	<0.2	1.0	25
D	7	23.08.2021	11.4	6.2	23.2	0.20	<0.1	<0.1	53.3	0.49	<0.2	1.4	26
E	11	27.08.2021	13.3	6.8	27.2	0.22	<0.1	<0.1	60.0	0.56	<0.2	1.6	27
F	14	30.08.2021	14.7	7.3	29.0	0.23	<0.1	<0.1	65.5	0.64	<0.2	1.8	27
G	21	06.09.2021	15.7	7.5	31.4	0.24	<0.1	<0.1	70.7	0.78	<0.2	1.9	27
H-1	25	10.09.2021											/
H-2	29	14.09.2021	16.7	7.5	33.6	0.23	<0.1	<0.1	73.3	1.0	<0.2	2.0	27
I	49	04.10.2021	18.5	7.5	35.9	0.26	<0.1	<0.1	76.6	1.6	<0.2	2.1	27
K	63	18.10.2021	19.0	7.5	38.9	0.27	<0.1	<0.1	76.6	2.1	<0.2	2.1	27
L	78	02.11.2021	19.7	7.5	40.3	0.34	<0.1	0.17	76.6	3.4	<0.2	2.1	27
M	91	15.11.2021	20.1	7.5	40.3	0.33	<0.1	0.17	76.6	3.5	<0.2	2.1	27
N	121	15.12.2021	20.6	7.5	40.3	0.34	<0.1	<0.1	76.6	3.6	<0.2	2.1	27
FINAL	149	12.01.2022	21.3	7.5	43.1	0.38	<0.1	0.17	76.6	3.7	<0.2	2.1	27

Table B-5.2: Continued

Sample			IG_BH05_PW026											IG_BH05_PW027										
Sub-samples	Time	Date	Na	K	Ca	Mg	Sr	F	Cl	SO4	NO3	Br	Br/Cl	Na	K	Ca	Mg	Sr	F	Cl	SO4	NO3	Br	Br/Cl
	days		mg/l	mg/l	mg/l	mg/l	mg/l	mg/l	mg/l	mg/l	mg/l	mg/l		mg/l	mg/l	mg/l	mg/l	mg/l	mg/l	mg/l	mg/l	mg/l	mg/l	
Preparation		02.09.2021																						
A	1	03.09.2021	6,6	4,4	8,3	<0.2	<0.1	<0.1	25,1	0,30	<0.2	0,96	38	5,4	5,2	10,9	<0.2	<0.1	<0.1	29,7	0,19	<0.2	0,97	33
B	3	05.09.2021	9,3	4,9	12,3	<0.2	<0.1	<0.1	33,2	0,40	<0.2	1,4	42	7,8	5,2	16,5	0,22	<0.1	<0.1	43,7	0,28	<0.2	1,3	30
C	4	06.09.2021	10,1	5,1	13,2	<0.2	<0.1	<0.1	36,5	0,53	<0.2	1,5	41	8,8	5,4	18,0	0,24	<0.1	<0.1	46,4	0,42	<0.2	1,5	32
D	8	10.09.2021	12,3	5,4	16,0	0,22	<0.1	<0.1	44,5	0,66	<0.2	1,9	43	10,9	5,7	22,8	0,30	<0.1	<0.1	56,0	0,61	<0.2	1,7	30
E	12	14.09.2021	13,8	5,6	17,5	0,24	<0.1	<0.1	48,3	0,81	<0.2	2,2	46	12,4	6,0	25,8	0,35	<0.1	<0.1	63,6	0,74	<0.2	1,9	30
F	14	16.09.2021	14,5	5,7	18,6	0,26	<0.1	<0.1	51,6	0,98	0,28	2,3	45	13,0	6,1	27,1	0,37	<0.1	<0.1	68,1	0,85	<0.2	2,0	29
G	21	23.09.2021	15,5	5,7	19,9	0,23	<0.1	0,10	53,8	1,3	<0.2	2,3	43	14,4	6,2	30,0	0,35	<0.1	<0.1	72,3	1,2	<0.2	2,2	30
H	29	01.10.2021	16,6	5,7	21,1	0,24	<0.1	0,12	55,7	1,7	<0.2	2,3	41	15,0	6,5	33,2	0,39	<0.1	<0.1	76,5	1,7	<0.2	2,3	30
I	48	20.10.2021	18,3	5,7	23,2	0,30	<0.1	0,13	55,7	2,3	0,29	2,3	41	16,5	7,0	36,1	0,50	<0.1	<0.1	76,6	2,9	0,22	2,3	30
K	61	02.11.2021	19,8	5,7	23,8	0,34	<0.1	0,16	55,7	2,7	<0.2	2,3	41	18,1	7,2	37,2	0,68	0,10	0,13	76,6	3,3	<0.2	2,3	30
L	75	16.11.2021	20,2	5,7	23,8	0,34	<0.1	0,18	55,7	2,9	<0.2	2,3	41	17,8	7,2	37,1	0,60	<0.1	0,13	76,6	4,0	<0.2	2,3	30
M	91	02.12.2021	20,4	5,7	23,8	0,34	<0.1	0,19	55,7	3,0	<0.2	2,3	41	18,6	7,3	37,2	0,59	<0.1	<0.1	76,7	4,0	<0.2	2,3	30
N	120	31.12.2021	22,2	5,7	25,1	0,34	<0.1	0,19	55,7	3,2	<0.2	2,3	41	18,9	7,5	37,5	0,59	<0.1	<0.1	76,7	4,0	<0.2	2,3	30
FINAL	153	02.02.2022	22,4	5,6	25,5	0,34	<0.1	0,19	55,7	3,4	<0.2	2,3	41	19,9	7,2	37,2	0,61	<0.1	<0.1	76,7	4,0	<0.2	2,3	30
Sample			**IG_BH05_PW028**											**IG_BH05_PW029**										
Sub-samples	**Time**	**Date**	**Na**	**K**	**Ca**	**Mg**	**Sr**	**F**	**Cl**	**SO4**	**NO3**	**Br**	**Br/Cl**	**Na**	**K**	**Ca**	**Mg**	**Sr**	**F**	**Cl**	**SO4**	**NO3**	**Br**	**Br/Cl**
	days		**mg/l**	**mg/l**	**mg/l**	**mg/l**	**mg/l**	**mg/l**	**mg/l**	**mg/l**	**mg/l**	**mg/l**		**mg/l**	**mg/l**	**mg/l**	**mg/l**	**mg/l**	**mg/l**	**mg/l**	**mg/l**	**mg/l**	**mg/l**	
Preparation		02.09.2021																						
A	1	03.09.2021	8,1	4,2	13,0	0,20	<0.1	<0.1	37,5	0,40	<0.2	0,64	17	15,3	6,7	40,7	<0.2	<0.5	<0.1	98,9	0,62	<0.2	3,8	38
B	3	05.09.2021	11,7	5,2	19,4	0,26	<0.1	<0.1	51,1	0,50	<0.2	0,75	15	23,8	8,4	63,6	0,20	<0.5	0,15	160	0,92	<0.2	5,8	36
C	4	06.09.2021	13,1	5,5	22,0	0,27	<0.1	0,10	57,8	0,60	<0.2	0,85	15	25,4	8,6	68,8	0,22	<0.5	0,19	177	1,1	<0.2	6,4	36
D	8	10.09.2021	16,2	6,0	26,6	0,31	<0.1	0,23	71,9	0,70	<0.2	1,1	15	32,8	9,9	91,0	0,25	<0.5	0,29	216	1,4	<0.2	8,5	39
E	12	14.09.2021	18,5	6,2	30,5	0,34	<0.1	0,25	78,5	0,81	<0.2	1,2	15	35,5	10	98,2	0,29	<0.5	0,52	242	1,6	<0.2	9,4	39
F	14	16.09.2021	19,2	6,3	31,7	0,35	<0.1	0,29	83,8	1,0	<0.2	1,3	16	36,6	10,1	102	0,31	<0.5	0,56	250	1,8	<0.2	9,6	38
G	21	23.09.2021	21,2	6,3	33,0	0,31	<0.1	0,31	90,8	1,3	<0.2	1,4	15	39,4	10,1	106	0,27	<0.5	0,59	257	2,7	<0.2	9,6	37
H	29	01.10.2021	23,3	6,4	36,9	0,32	<0.1	0,34	94,0	1,8	<0.2	1,5	16	40,1	10,2	108	0,30	<0.5	0,67	261	3,3	<0.2	9,6	37
I	48	20.10.2021	26,9	6,4	38,2	0,40	<0.1	0,43	98,0	3,2	<0.2	1,5	15	42,5	10,3	116	0,38	<0.5	0,75	263	4,7	<0.2	9,6	37
K	61	02.11.2021	28,2	6,4	40,4	0,56	<0.1	0,42	98,0	3,6	<0.2	1,5	15	44	10,3	116	0,47	<0.5	0,78	264	5,4	<0.2	9,6	36
L	75	16.11.2021	27,7	6,4	40,5	0,49	<0.1	0,42	98,0	3,7	<0.2	1,5	15	44,1	10,3	116	0,46	<0.5	0,99	264	5,7	<0.2	9,6	36
M	91	02.12.2021	30,2	6,5	42,2	0,50	<0.1	0,42	98,0	3,7	<0.2	1,5	15	44,1	10,4	118	0,45	<0.5	1,0	267	5,7	<0.2	9,6	36
N	120	31.12.2021	29,6	6,5	42,1	0,50	<0.1	0,42	98,0	3,7	<0.2	1,5	15	44,6	10,4	121	0,47	<0.5	1,0		5,7	<0.2	9,6	
FINAL	153	02.02.2022	30,3	6,5	42,1	0,53	<0.1	0,42	98,0	3,7	<0.2	1,5	15	45,4	10,4	121	0,47	<0.5	1,0	269	5,7	<0.2	9,6	36

Table B-5.2: Continued

Sample			IG_BH05_AR033											IG_BH05_AR052										
Sub-samples	Time	Date	Na	K	Ca	Mg	Sr	F	Cl	SO4	NO3	Br	Br/Cl	Na	K	Ca	Mg	Sr	F	Cl	SO4	NO3	Br	Br/Cl
	days		mg/l	mg/l	mg/l	mg/l	mg/l	mg/l	mg/l	mg/l	mg/l	mg/l		mg/l	mg/l	mg/l	mg/l	mg/l	mg/l	mg/l	mg/l	mg/l	mg/l	
Preparation		14.03.2022																						
A	1	15.03.2022	9.3	1.4	30.9	0.64	<0.1	0.58	35.4	3.5	0.94	0.74	21	3.1	4.4	8.2	0.17	<0.1	0.17	2.1	2.1	<0.2	<0.05	
B	3	17.03.2022	11.5	1.5	33.7	0.66	<0.1	0.74	48.5	3.9	0.88	0.99	20	4.7	4.6	9.8	0.20	<0.1	0.24	3.0	3.5	<0.2	<0.05	
C	4	18.03.2022	15.5	1.5	40.1	0.72	<0.1	0.72	64.1	4.7	1.9	1.41	22	4.9	4.9	9.9	0.20	<0.1	0.26	3.3	3.6	<0.2	<0.05	
D	7	21.03.2022	15.8	1.9	41.1	0.76	<0.1	0.74	64.9	5.2	2.2	1.51	23	5.9	4.9	11.6	0.27	<0.1	0.30	4.7	4.7	<0.2	0.12	26
E	12	26.03.2022	19.2	1.9	52.9	0.85	<0.1	0.97	72.1	6.8	2.8	1.52	21	7.0	5.0	13.6	0.31	<0.1	0.40	7.2	5.9	<0.2	0.14	19
F	14	28.03.2022	22.1	2.1	59.1	0.86	<0.1	0.97	87.5	7.4	3.2	1.52	17	10.1	6.2	19.2	0.45	<0.1	0.40	10.7	8.9	<0.2	0.23	21
G	22	05.04.2022	24.6	2.2	59.4	0.86	<0.1	0.97	92.5	7.9	3.8	1.53	17	10.4	6.2	20.0	0.48	<0.1	0.42	12.6	9.2	<0.2	0.26	21
H	30	13.04.2022	26.2	2.2	60.7	0.95	<0.1	1.1	97.8	9.4	4.0	1.54	16	11.4	6.5	22.5	0.54	<0.1	0.43	14.1	10.7	<0.2	0.32	23
I	50	03.05.2022	28.1	2.3	61.6	0.97	<0.1	1.2	103	11.5	4.2	1.57	15	14.0	6.9	31.1	0.74	<0.1	0.44	15.6	15.2	<0.2	0.39	25
K	63	16.05.2022	30.3	2.4	62.5	1.0	<0.1	1.3	105	12.9	4.9	1.64	16	14.7	7.2	31.9	0.77	<0.1	0.45	16.7	15.6	<0.2	0.40	24
L	78	31.05.2022	31.7	2.6	63.2	1.1	<0.1	1.5	108	14.7	5.0	1.68	16	18.6	7.9	34.1	0.89	<0.1	0.46	18.4	20.3	<0.2	0.40	22
M	92	14.06.2022	32.5	2.7	63.4	1.1	<0.1	1.6	108	16.0	5.0	1.69	16	18.6	8.2	36.4	0.92	<0.1	0.48	18.4	20.4	<0.2	0.40	22
N	126	18.07.2022	34.2	3.1	64.0	1.2	<0.1	1.6	109	19.0	5.1	1.69	16	19.6	8.3	37.0	0.96	<0.1	0.50	18.4	22.4	<0.2	0.40	22
FINAL	253	22.11.2022	34.8	3.1	65.5	1.2	0.75	1.6	109	19.0	5.1	1.69	16	19.9	8.4	37.2	0.99	0.38	0.60	18.4	27.4	<0.2	0.40	22

Sample			IG_BH05_AR059										
Sub-samples	Time	Date	Na	K	Ca	Mg	Sr	F	Cl	SO4	NO3	Br	Br/Cl
	days		mg/l	mg/l	mg/l	mg/l	mg/l	mg/l	mg/l	mg/l	mg/l	mg/l	
Preparation		14.03.2022											
A	1	15.03.2022	4.3	3.7	11.5	0.22	<0.1	0.19	8.6	1.7	<0.2	0.12	14
B	3	17.03.2022	5.0	3.8	11.8	0.26	<0.1	0.20	8.8	1.8	<0.2	0.14	16
C	4	18.03.2022	5.8	3.9	13.0	0.29	<0.1	0.21	9.9	1.9	<0.2	0.22	22
D	7	21.03.2022	8.8	4.1	18.6	0.42	<0.1	0.22	12.9	2.8	<0.2	0.25	19
E	12	26.03.2022	8.8	4.3	18.6	0.44	<0.1	0.23	13.9	3.1	<0.2	0.29	21
F	14	28.03.2022	9.6	4.3	18.6	0.44	<0.1	0.24	14.6	3.4	<0.2	0.33	23
G	22	05.04.2022	12.2	4.3	21.8	0.52	<0.1	0.25	18.3	4.1	<0.2	0.35	19
H	30	13.04.2022	13.7	4.4	24.7	0.61	<0.1	0.25	20.4	4.6	<0.2	0.38	19
I	50	03.05.2022	16.9	4.6	27.6	0.90	<0.1	0.27	24.5	6.7	<0.2	0.39	16
K	63	16.05.2022	18.8	4.7	28.8	0.94	<0.1	0.44	24.9	7.4	<0.2	0.41	16
L	78	31.05.2022	19.0	5.0	29.7	0.99	<0.1	0.44	25.1	7.7	<0.2	0.41	16
M	92	14.06.2022	20.8	5.2	29.7	1.1	<0.1	0.44	25.2	9.0	<0.2	0.41	16
N	126	18.07.2022	22.1	5.3	31.1	1.2	<0.1	0.44	25.2	10.0	<0.2	0.41	16
FINAL	253	22.11.2022	24.6	5.4	33.3	1.3	0.40	0.44	25.4	10.5	<0.2	0.41	16

APPENDIX B-6

Out-Gassing Experiments: Raw Data

Table B-6.1: Analytical detection limits and analytical errors of gases determined by GC-FID and GC-WLD

Gas species	Analytical method	Detection Limit	Analytical error
Hydrocarbons		vpm	%
Methane (CH_4)	GC-FID	1.0	3
Ethane (C_2H_6)	GC-FID	1.0	5
Propane (C_3H_8)	GC-FID	1.0	5
i-Butane (i-C_4H_{10})	GC-FID	1.0	5
n-Butane (n-C_4H_{10})	GC-FID	1.0	5
i-Pentane (i-C_5H_{12})	GC-FID	1.0	5
n-Butane (n-C_5H_{12})	GC-FID	1.0	5
Ethene (C_2H_4)	GC-FID	1.0	5
Propene (C_3H_6)	GC-FID	1.0	5
Butene (C_4H_8)	GC-FID	1.0	5
Normal Gases		Vol. %	%
Nitrogen (N_2)	GC-WLD	0.01	2
Oxygen (O_2)	GC-WLD	0.01	2
Carbon dioxide (CO_2)	GC-WLD	0.01	3
Argon (Ar)	GC-WLD	0.01	5
Helium (He)	GC-WLD	0.01	5
Hydrogen (H_2)	GC-WLD	0.01	3

Table B-6.2: Composition of air used for correction (Ozima & Podosek, 2002)

Gas species		Unit	Conc. In air
Oxygen	O_2	%	20.94
Nitrogen	N_2	%	78.08
Carbon dioxide	CO_2	%	0.038
Methane	CH_4	%	0.000176
Helium	He	%	0.000524
Argon	Ar	%	0.934
Krypton	Kr	%	0.000114
Neon	Ne	%	0.00182
Xenon	Xe	%	8.70E-06
Atomic abundances of NG isotopes			
36Ar		%	0.3364
40Ar		%	99.6
3He		%	0.000138
4He		%	99.999862
84Kr		%	57
20Ne		%	90.5
22Ne		%	9.23
132Xe		%	26.9

Table B-6.3: Raw Data of gas chromatographic measurements

Labor-Nr.		**378510**	**378511**	**378512**	**378513**	**378514**
		IG_BH05_DG001	**IG_BH05_DG002**	**IG_BH05_DG003**	**IG_BH05_DG004**	**IG_BH05_DG005**
Depth	**mbgs**	**431,2**	**536,4**	**634,2**	**744,3**	**879,3**
Sampling date		**01.07.2021**	**05.07.2021**	**10.07.2021**	**18.07.2021**	**27.07.2021**
Sampling time		**16:00**	**15:02**	**16:32**	**05:07**	**17:41**
Temperatur Lab	°C	21	21	21	21	21
Final Pressure	mbar	31	33	35	31	32
Void Volume	ml	252	207	211	260	202
Helium	Vol. %	12,5	8,7	2,5	3,3	1,6
Argon	Vol. %	1,9	2,0	2,2	2,3	2,2
Oxygen	Vol. %	1,0	0,8	1,4	1,3	0,6
Nitrogen	Vol. %	75,8	74,1	87,6	82	89,8
Carbondioxide	Vol. %	0,18	0,02	< 0,03	< 0,03	< 0,03
Hydrogen	Vol. %	8,4	14	6	9,7	5,5
Methane	vpm	4280	2690	1770	4820	452
Ethane	vpm	43	41	53	142	14
Propane	vpm	12	8	8	20	5
i-Butane	vpm	12	2	4	4	< 1
n-Butane	vpm	27	5	4	16	3
i-Pentane	vpm	< 1	33	8	< 1	< 1
n-Pentane	vpm	24	27	18	70	28
Ethene	vpm	11	10	6	11	9
Propene	vpm	10	11	8	15	10
1-Butene	vpm	9	8	< 1	14	9
SUM	Vol.%	100,2	99,9	99,9	99,1	99,8
Ratios						
C1/(C2+)		29	19	16	17	6
N2/Ar		40	37	40	36	41

Table B-6.3: Experimental data of out-gassing experiments (non-inert (DG) gases)

Sample		IG_BH05_DG001	IG_BH05_DG002	IG_BH05_DG003	IG_BH05_DG004	IG_BH05_DG005
Depth a.b.	**mbgs**	**431,2**	**536,4**	**634,2**	**744,3**	**879,3**
Lab Nr.		**378510**	**378511**	**378512**	**378513**	**378514**
Temperature measurement	°C	21	21	21	21	21
	K	294	294	294	294	294
Pressure (start)	mbar	0	0	0	0	0
Temperature set-up	°C	16	16	16	16	16
	K	289	289	289	289	289
Pressure (start) corrected STP	mbar	0,0	0,0	0,0	0,0	0,0
He Volume (start)	ml	0,00	0,00	0,00	0,00	0,00
Pressure (end)	mbar	31	33	35	31	32
Water vapour pressure (21°C)	mbar	24,8	24,8	24,8	24,8	24,8
Pressure end (without P(WV))		6,2	8,2	10,2	6,2	7,2
Volume corrected for WV	ml	1,6	1,7	2,2	1,6	1,5
Air contamination	%	4,8	3,8	6,7	6,2	2,9
Pressure end corrected for air cont.	**mbar**	**5,9**	**7,9**	**9,5**	**5,8**	**7,0**
Pressure end corr STP	**mbar**	**5,5**	**7,3**	**8,8**	**5,4**	**6,5**
Void Volume	ml	252	207	211	260	202
Water content	wt.%	0,19	0,19	0,18	0,17	0,13
PW volume	ml	3,11	3,31	3,24	2,78	2,32
Ratio V(PW):V(void)		0,0123	0,0160	0,0154	0,0107	0,0115
% of PW of tot Vol	%	1,2	1,6	1,5	1,1	1,1
Gas volume corrected WV, air	ml	1,5	1,6	2,0	1,5	1,4
Gas volume corrected STP	ml	1,4	1,5	1,9	1,4	1,3

Table B-6.4: Noble gas analyses; Inlet parameter and analytical raw data

						Inlet Parameters			
Sample	**Sample ID**	**date (meas.)**	**T (°C)**	**T(K)**	**DT (K)**	**P(mbar)**	**Dp (mbar)**	**V (cc)**	**DV (cc)**
IG_BH05_NG001	**HI_378515**	27.07.2023	22,50	295,65	0,1	30,23	0,060	36,316	0,04
IG_BH05_NG003	**HI_378516**	03.08.2023	23,18	296,33	0,1	31,59	0,063	36,316	0,04
IG_BH05_NG005	**HI_378517**	07.08.2023	22,86	296,01	0,1	32,42	0,065	36,316	0,04
IG_BH05_NG007	**HI_378518**	31.07.2023	23,01	296,16	0,1	28,88	0,058	36,316	0,04
IG_BH05_NG009	**HI_378519**	31.07.2023	22,89	296,04	0,1	31,66	0,063	36,316	0,04

		Isotopes abs. amounts [ccSTP]							
Sample	**Sample ID**	^{3}He	err abs.	^{4}He	err abs.	^{20}Ne	err abs.	^{22}Ne	err abs.
IG_BH05_NG001	HI_378515	4,67E-11	7,31E-13	1,45E-03	9,30E-06	3,94E-07	1,90E-09	4,08E-08	4,19E-10
IG_BH05_NG003	HI_378516	7,25E-11	2,43E-12	2,85E-03	1,89E-05	4,92E-07	2,34E-09	5,07E-08	4,30E-10
IG_BH05_NG005	HI_378517	1,74E-10	3,91E-12	5,33E-03	3,50E-05	8,06E-07	3,77E-09	8,29E-08	5,21E-10
IG_BH05_NG007	HI_378518	6,08E-11	2,17E-12	2,53E-03	1,69E-05	6,42E-08	6,07E-10	7,76E-09	3,87E-10
IG_BH05_NG009	HI_378519	3,01E-11	1,55E-12	2,92E-03	1,93E-05	6,26E-07	2,94E-09	6,51E-08	4,64E-10

		Isotopes abs. amounts [ccSTP]							
Sample	**Sample ID**	^{36}Ar	err abs.	^{40} Ar	err abs.	^{84}Kr	err abs.	^{132}Xe	err abs.
IG_BH05_NG001	HI_378515	1,26E-05	7,59E-07	4,15E-03	1,29E-05	1,16E-06	1,49E-08	2,01E-07	1,95E-09
IG_BH05_NG003	HI_378516	1,62E-05	8,16E-07	5,81E-03	1,76E-05	1,54E-06	2,06E-08	2,55E-07	2,52E-09
IG_BH05_NG005	HI_378517	2,24E-05	9,71E-07	8,23E-03	2,51E-05	1,96E-06	2,84E-08	2,85E-07	2,95E-09
IG_BH05_NG007	HI_378518	1,01E-05	7,18E-07	3,72E-03	1,17E-05	1,05E-06	1,48E-08	2,06E-07	2,02E-09
IG_BH05_NG009	HI_378519	2,07E-05	9,32E-07	7,03E-03	2,14E-05	1,81E-06	2,34E-08	2,86E-07	2,87E-09

		Isotope ratios			
Sample	**Sample ID**	22/20Ne	err abs.	36/40Ar	err abs.
IG_BH05_NG001	HI_378515	1,03E-01	2,61E-04	2,91E-03	1,38E-04
IG_BH05_NG003	HI_378516	1,03E-01	2,20E-04	2,82E-03	1,10E-04
IG_BH05_NG005	HI_378517	1,03E-01	1,18E-04	2,71E-03	1,14E-04
IG_BH05_NG007	HI_378518	1,21E-01	1,32E-03	2,75E-03	1,20E-04
IG_BH05_NG009	HI_378519	1,04E-01	1,30E-04	2,87E-03	1,14E-04

Table B-6.5: Experimental data of out-gassing experiments (noble gases (NG))

Sample		IG_BH05_NG001	IG_BH05_NG003	IG_BH05_NG005	IG_BH05_NG007	IG_BH05_NG009
Depth a.b.	**mbgs**	**428,5**	**533,3**	**630,2**	**747,3**	**872,2**
Lab Nr.		**378515**	**378516**	**378517**	**378518**	**378519**
Temperature measurement	°C	22,5	23,18	22,86	23,01	22,89
	K	295,5	296,18	295,86	296,01	295,89
Pressure (start)	mbar	0	0	0	0	0
Temperature set-up	°C	16	16	16	16	16
	K	289	289	289	289	289
Pressure (start) corrected STP	mbar	0	0	0	0	0
N2 Volume (start)	ml	0	0	0	0	0
Pressure (end)	mbar	30,23	31,59	32,42	28,88	31,66
Water vapour pressure (P(WV))	mbar	27	28	28	28	28
Pressure end (without P(WV))	mbar	3,1	3,3	4,7	0,9	3,9
Volume corrected for WV	ml	0,83	0,89	0,91	0,20	0,86
Void Volume	ml	271	272	196	224	223
Water content	wt.%	0,18	0,18	0,09	0,21	0,14
PW volume	ml	2,86	2,87	1,60	3,55	2,44
Ratio V(PW):V(void)		0,01	0,01	0,01	0,02	0,01
% of PW of tot Vol	%	1,05	1,05	0,81	1,56	1,08

APPENDIX C

Error Calculations

APPENDIX C-1

Gravimetric Water Content

The water content is calculated according to $WC_{grav} = \frac{m_{pw}}{m_{core,wet}}$

Where WC_{grav} = gravimetric water content, m_{pw} = mass of pore water, $m_{core,wet}$ = mass of the wet core sample

Error calculation after Gaussian error propagation

$$\sigma(WC_{grav}) = \sqrt{\left(dWC_{grav}dm_{PW} \times \sigma(m_{PW})\right)^2 + \left(dWC_{grav}dm_{core,wet} \times \sigma(m_{core,wet})\right)^2}$$

Analytical errors (error of measurement)

$s(m_{pw})$ = difference between $m_{core,dry\ surface}$ before and after drying + 0.05 g (=variations at end of drying); The constant of 0.05 g is the empirically derived uncertainty associated to the drying process of the surface, i.e. loss of water from the core surface.

$s(m_{core,wet})$ = difference between $m_{core,dry\ surface}$ before and after experiment

Both uncertainties include the mass difference of the individual cores before and after the experiments (cf. Appendix II).

Derivations

$$dWC_{grav}dm_{pw} = \frac{100}{m_{core,wet}}$$

$$dWC_{grav}dm_{core,wet} = \frac{-100 \times m_{pw}}{(m_{core,wet})^2}$$

APPENDIX C-2

Water Loss Porosity

The water-loss (connected porosity), ϕ_{WL}, is calculated according to

$$\phi_{WL} = WC_{wet} \times \frac{\rho_{bulk,wet}}{\rho_{water}}$$

where WC_{wet} is the water content based on the wet weight of the rock sample and $\rho_{bulk,wet}$ the bulk wet density of the rock. The density of water, ρ_{water}, is assumed to be 1 g/cm^3.

The conversion of the formula leads to

$$\phi_{WL} = \frac{m_{pw} \times 100}{r^2 \times h \times \pi \times \rho_{water}}$$

where r = radius of the core pieces, h = height of the core.

Error calculation after Gaussian error propagation

$$\sigma(\phi_{WL}) = \sqrt{\begin{matrix}\left(d\phi_{WL}dm_{PW} \times \sigma(m_{PW})\right)^2 + \left(d\phi_{WL}dr \times \sigma(r)\right)^2 + \\ \left(d\phi_{WL}dh \times \sigma(h)\right)^2 + \left(d\phi_{WL}d\rho_{water} \times \sigma(\rho_{water})\right)^2\end{matrix}}$$

Analytical errors (error of measurement)

s(m_{pw}) = difference between $m_{core,dry\ surface}$ before and after drying + 0.05 g (=variations at end of drying)

s(r) = 0.02 cm

s(h) = 0.2 cm

s(r_{water}) = 0.03 g/cm^3

Derivations

$$d\phi dm_{pw} = \frac{100}{r^2 \times h \times \pi \times \rho_{water}}$$

$$d\phi dr = \frac{-m_{pw} \times 100 \times 2r \times h \times \pi \times \rho_{water}}{(r^2 \times h \times \pi \times \rho_{water})^2}$$

$$d\phi dh = \frac{-m_{pw} \times 100 \times r^2 \times \pi \times \rho_{water}}{(r^2 \times h \times \pi \times \rho_{water})^2}$$

$$d\phi dh = \frac{-m_{pw} \times 100 \times r^2 \times \pi \times h}{(r^2 \times h \times \pi \times \rho_{water})^2}$$

APPENDIX C-3

Porewater Cl- and Br Concentration

Calculations

$$C_{PW} = \frac{(m_{PW} + m_{TWi} - \sum^{n} m_s) \times C_{TW\infty} - (m_{TWi} \times C_{TWi}) + \sum^{n} m_s \times C_s}{m_{PW}}$$

where C_{pw} = porewater concentration; m_{pw} = mass of porewater; m_{TWi} = initial mass of test water; C_{TWi} = initial Cl-concentration of test water; m_s = mass of sub sample used for time series; C_s = Cl concentration of sub sample used for time series.

Error calculation after Gaussian error propagation

$$\sigma(C_{PW}) = \sqrt{\begin{matrix}(dC_{PW}dm_{PW} \times \sigma(m_{PW}))^2 + (dC_{PW}dm_{TWi} \times \sigma(m_{TWi}))^2 + \\ +(dC_{PW}dC_{TW\infty} \times \sigma(C_{TW\infty}))^2 + (dC_{PW}dC_{TWi} \times \sigma(C_{TWi}))^2 + \\ (\sigma(\sum m_S))^2 + (\sigma(\sum m_S \times c_S))^2\end{matrix}}$$

Analytical errors (error of measurement)

$\sigma(m_{PW})$ = difference between $m_{core,dry\ surface}$ before and after drying + 0.05 g (=variations at end of drying

$\sigma(m_{TWi})$ = difference between $m_{TWi} - m_S - m_{TW\infty}$-2ml (2 ml = remaining water in the cylinder

$\sigma(C_{TWi})$ = 5% (Cl) and 10 % (Br) of the analysed concentration

$\sigma(C_{TW\infty})$ = 5% (Cl) and 10 % (Br) of the analysed concentration

$\sigma(m_S)$ = 0.05 ml

$\sigma(C_S)$ = 5% (Cl) and 10 % (Br) of the analysed concentration

Derivations

$$dC_{PW}dm_{PW} = \frac{C_{TW\infty} * m_{PW} - [C_{TW\infty} * (m_{PW} + m_{TWi}) - C_{TW} * m_{TWi}]}{m_{PW}^2}$$

$$dC_{PW}dm_{TWi} = \frac{(C_{TW\infty} - C_{TWi}) * m_{PW}}{m_{PW}^2}$$

$$dC_{PW}dC_{TW\infty} = \frac{(m_{PW} - m_{TWi}) * m_{PW}}{m_{PW}^2}$$

$$dC_{PW}dC_{TWi} = \frac{-m_{TWi} * m_{PW}}{m_{PW}^2}$$

$$\sigma\left(\sum(m_s)\right) = (Nr_S \times \sigma(m_S))$$

$$\sigma\left(\sum(m_S \times C_S)\right) = (Nr_S \times C_{S,ave} \times \sigma(m_S)) + (Nr_S \times m_S \times \sigma(C_S))$$

APPENDIX C-4

Br*1000/Cl Mass Ratio of Porewater

Br*1000/Cl porewater mass ratio = R

Error calculation after Gaussian error propagation

$$\sigma(R) = \sqrt{\left(dRdC_{Br} \times \sigma(C_{Br})\right)^2 + \left(dRdC_{Cl} \times \sigma(C_{Cl})\right)^2}$$

Analytical errors (error of measurement)

$\sigma(C_{Cl})$ = Error of porewater Cl concentration calculated according to AIII-3

$\sigma(C_{Br})$ = Error of porewater Br concentration calculated according to AIII-3

Derivations

$$dRdC_{Br} = \frac{1000}{C_{Cl}}$$

$$dRdC_{Cl} = \frac{-1000 \times C_{Br}}{C_{Cl}^2}$$

APPENDIX C-5

Calculation of Isotopic Signatures of Matrix Porewater

Calculation

$$C_{PW} = \frac{C_{TW\infty(Std1)} \times m_{TW(Std2)} \times m_{Rock(Std1)} \times (C_{TW\infty(Std2)} - C_{TW^0(Std2)}) - C_{TW\infty(Std2)} \times m_{TW(Std1)} \times m_{Rock(Std2)} \times (C_{TW\infty(Std1)} - C_{TW^0(Std1)})}{m_{TW(Std2)} \times m_{Rock(Std1)} \times (C_{TW\infty(Std2)} - C_{TW^0(Std2)}) - m_{TW(Std1)} \times m_{Rock(Std2)} \times (C_{TW\infty(Std1)} - C_{TW^0(Std1)})}$$

m_{PW} = mass of porewater (g)

m_{TW} = mass of test water (g)

C_{TW} = isotopic signature of test water at the beginning of the experiment (‰)

$C_{TW\infty}$ = isotopic signature of test water after equilibration (‰)

Std 1 = Experiment 1 applying standard 1

Std 2 = Experiment 2 applying standard 2

Error calculation after Gaussian error propagation

$$\sigma(C_{PW}) = \sqrt{\begin{array}{l}\left(dC_{PW}dm_{TW(Std1)} \times \sigma(m_{TW(Std1)})\right)^2 + \left(dC_{PW}dm_{TW(Std2)} \times \sigma(m_{TW(Std2)})\right)^2 + \\ +\left(dC_{PW}dC_{TW(Std1)} \times \sigma(C_{TW(Std1)})\right)^2 + \left(dC_{PW}dC_{TW(Std2)} \times \sigma(C_{TW(Std2)})\right)^2 + \\ +\left(dC_{PW}dC_{TW\infty(Std1)} \times \sigma(C_{TW\infty(Std1)})\right)^2 + \left(dC_{PW}dC_{TW\infty(Std2)} \times \sigma(C_{TW\infty(Std2)})\right)^2\end{array}}$$

Analytical errors (error of measurement)

$\sigma(m_{TW(Std1)})$ = 0.002 g

$\sigma(m_{TW(Std2)})$ = 0.002 g

$\sigma(C_{TW(Std1)})$ = 0.1 ‰ for ^{18}O and 1.0‰ for ^{2}H

$\sigma(C_{TW(Std2)})$ = 0.1 ‰ for ^{18}O and 1.0‰ for ^{2}H

$\sigma(C_{TW\infty(Std1)})$ = 0.1 ‰ for ^{18}O and 1.0‰ for ^{2}H

$\sigma(C_{TW\infty(Std2)})$ = 0.1 ‰ for ^{18}O and 1.0‰ for ^{2}H

Derivations

$$dC_{PW}dm_{TW(Std1)} = \frac{\left(C_{TW(Std1)} - C_{TW\infty(Std1)}\right) \times C_{TW\infty(Std2)}}{\left(m_{TW(Std1)} \times \left(C_{TW(Std1)} - C_{TW\infty(Std1)}\right) - \left(C_{TW(Std2)} - C_{TW\infty(Std2)}\right) \times m_{TW(Std2)}\right)} -$$

$$- \frac{\left(\left(C_{TW(Std1)} - C_{TW\infty(Std1)}\right) \times C_{TW\infty(Std2)} \times m_{TW(Std1)} - \left(C_{TW(Std2)} - C_{TW\infty(Std2)}\right) \times C_{TW\infty(Std1)} \times m_{TW(Std2)}\right) \times \left(C_{TW(Std1)} - C_{TW\infty(Std1)}\right)}{\left(m_{TW(Std1)} \times \left(C_{TW(Std1)} - C_{TW\infty(Std1)}\right) - \left(C_{TW(Std2)} - C_{TW\infty(Std2)}\right) \times m_{TW(Std2)}\right)^2}$$

$$dC_{PW}dm_{TW(Std2)} = \frac{-\left(C_{TW(Std2)} - C_{TW\infty(Std2)}\right) \times C_{TW\infty(Std1)}}{\left(m_{TW(Std1)} \times \left(C_{TW(Std1)} - C_{TW\infty(Std1)}\right) - \left(C_{TW(Std2)} - C_{TW\infty(Std2)}\right) \times m_{TW(Std2)}\right)} +$$

$$+ \frac{\left(\left(C_{TW(Std1)} - C_{TW\infty(Std1)}\right) \times C_{TW\infty(Std2)} \times m_{TW(Std1)} - \left(C_{TW(Std2)} - C_{TW\infty(Std2)}\right) \times C_{TW\infty(Std1)} \times m_{TW(Std2)}\right) \times \left(C_{TW(Std2)} - C_{TW\infty(Std2)}\right)}{\left(m_{TW(Std1)} \times \left(C_{TW(Std1)} - C_{TW\infty(Std1)}\right) - \left(C_{TW(Std2)} - C_{TW\infty(Std2)}\right) \times m_{TW(Std2)}\right)^2}$$

$$dC_{PW}dC_{TW(Std1)} = \frac{C_{TW\infty(Std2)} \times m_{TW(Std1)}}{\left(m_{TW(Std1)} \times \left(C_{TW(Std1)} - C_{TW\infty(Std1)}\right) - \left(C_{TW(Std2)} - C_{TW\infty(Std2)}\right) \times m_{TW(Std2)}\right)} -$$
$$- \frac{\left(\left(C_{TW(Std1)} - C_{TW\infty(Std1)}\right) \times C_{TW\infty(Std2)} \times m_{TW(Std1)} - \left(C_{TW(Std2)} - C_{TW\infty(Std2)}\right) \times C_{TW\infty(Std1)} \times m_{TW(Std2)}\right) \times m_{TW(Std1)}}{\left(m_{TW(Std1)} \times \left(C_{TW(Std1)} - C_{TW\infty(Std1)}\right) - \left(C_{TW(Std2)} - C_{TW\infty(Std2)}\right) \times m_{TW(Std2)}\right)^2}$$

$$dC_{PW}dC_{TW(Std2)} = \frac{-C_{TW\infty(Std1)} \times m_{TW(Std2)}}{\left(m_{TW(Std1)} \times \left(C_{TW(Std1)} - C_{TW\infty(Std1)}\right) - \left(C_{TW(Std2)} - C_{TW\infty(Std2)}\right) \times m_{TW(Std2)}\right)} +$$
$$+ \frac{\left(\left(C_{TW(Std1)} - C_{TW\infty(Std1)}\right) \times C_{TW\infty(Std2)} \times m_{TW(Std1)} - \left(C_{TW(Std2)} - C_{TW\infty(Std2)}\right) \times C_{TW\infty(Std1)} \times m_{TW(Std2)}\right) \times m_{TW(Std2)}}{\left(m_{TW(Std1)} \times \left(C_{TW(Std1)} - C_{TW\infty(Std1)}\right) - \left(C_{TW(Std2)} - C_{TW\infty(Std2)}\right) \times m_{TW(Std2)}\right)^2}$$

$$dC_{PW}dC_{TW\infty(Std1)} = \frac{-\left(C_{TW\infty(Std2)} \times m_{TW(Std1)} + \left(C_{TW(Std2)} - C_{TW\infty(Std2)}\right) \times m_{TW(Std2)}\right)}{\left(m_{TW(Std1)} \times \left(C_{TW(Std1)} - C_{TW\infty(Std1)}\right) - \left(C_{TW(Std2)} - C_{TW\infty(Std2)}\right) \times m_{TW(Std2)}\right)} +$$
$$+ \frac{\left(\left(C_{TW(Std1)} - C_{TW\infty(Std1)}\right) \times C_{TW\infty(Std2)} \times m_{TW(Std1)} - \left(C_{TW(Std2)} - C_{TW\infty(Std2)}\right) \times C_{TW\infty(Std1)} \times m_{TW(Std2)}\right) \times m_{TW(Std1)}}{\left(m_{TW(Std1)} \times \left(C_{TW(Std1)} - C_{TW\infty(Std1)}\right) - \left(C_{TW(Std2)} - C_{TW\infty(Std2)}\right) \times m_{TW(Std2)}\right)^2}$$

$$dC_{PW}dC_{TW\infty(Std1)} = \frac{-\left(C_{TW\infty(Std2)} \times m_{TW(Std1)} + \left(C_{TW(Std2)} - C_{TW\infty(Std2)}\right) \times m_{TW(Std2)}\right)}{\left(m_{TW(Std1)} \times \left(C_{TW(Std1)} - C_{TW\infty(Std1)}\right) - \left(C_{TW(Std2)} - C_{TW\infty(Std2)}\right) \times m_{TW(Std2)}\right)} +$$
$$+ \frac{\left(\left(C_{TW(Std1)} - C_{TW\infty(Std1)}\right) \times C_{TW\infty(Std2)} \times m_{TW(Std1)} - \left(C_{TW(Std2)} - C_{TW\infty(Std2)}\right) \times C_{TW\infty(Std1)} \times m_{TW(Std2)}\right) \times m_{TW(Std1)}}{\left(m_{TW(Std1)} \times \left(C_{TW(Std1)} - C_{TW\infty(Std1)}\right) - \left(C_{TW(Std2)} - C_{TW\infty(Std2)}\right) \times m_{TW(Std2)}\right)^2}$$

$$dC_{PW}dC_{TW\infty(Std2)} = \frac{\left(m_{TW(Std1)} \times \left(C_{TW(Std1)} - C_{TW\infty(Std1)}\right) + C_{TW\infty(Std1)} \times m_{TW(Std2)}\right)}{\left(m_{TW(Std1)} \times \left(C_{TW(Std1)} - C_{TW\infty(Std1)}\right) - \left(C_{TW(Std2)} - C_{TW\infty(Std2)}\right) \times m_{TW(Std2)}\right)} -$$
$$- \frac{\left(\left(C_{TW(Std1)} - C_{TW\infty(Std1)}\right) \times C_{TW\infty(Std2)} \times m_{TW(Std1)} - \left(C_{TW(Std2)} - C_{TW\infty(Std2)}\right) \times C_{TW\infty(Std1)} \times m_{TW(Std2)}\right) \times m_{TW(Std2)}}{\left(m_{TW(Std1)} \times \left(C_{TW(Std1)} - C_{TW\infty(Std1)}\right) - \left(C_{TW(Std2)} - C_{TW\infty(Std2)}\right) \times m_{TW(Std2)}\right)^2}$$

APPENDIX C-6

Calculation of Mass of Porewater by Isotope Diffusive Exchange Technique

Calculation

$$WC_{IsoEx} = \left[\frac{m_{TW(Std\,2)} \times m_{Rock(Std1)} \times (C_{TW^0(Std\,2)} - C_{TW\infty(Std\,2)}) + m_{TW(Std1)} \times m_{Rock(Std\,2)} \times (C_{TW\infty(Std1)} - C_{TW^0(Std1)})}{m_{Rock(Std1)} \times m_{Rock(Std\,2)} \times (C_{TW\infty(Std\,2)} - C_{TW\infty(Std1)})} \right] \times 100$$

m_{PW} = mass of porewater (g)

m_{TW} = mass of test water (g)

C_{TW} = isotopic signature of test water at the beginning of the experiment (‰)

$C_{TW\infty}$ = isotopic signature of test water after equilibration (‰)

Std 1 = Experiment 1 applying standard 1

Std 2 = Experiment 2 applying standard 2

Error calculation after Gaussian error propagation

$$\sigma(m_{PW}) = \sqrt{\begin{aligned} &\left(dm_{PW}dm_{TW(Std1)} \times \sigma(m_{TW(Std1)})\right)^2 + \left(dm_{PW}dm_{TW(Std\,2)} \times \sigma(m_{TW(Std\,2)})\right)^2 + \\ &+\left(dm_{PW}dC_{TW(Std1)} \times \sigma(C_{TW(Std1)})\right)^2 + \left(dm_{PW}dC_{TW(Std\,2)} \times \sigma(C_{TW(Std\,2)})\right)^2 + \\ &+\left(dm_{PW}dC_{TW\infty(Std1)} \times \sigma(C_{TW\infty(Std1)})\right)^2 + \left(dm_{PW}dC_{TW\infty(Std\,2)} \times \sigma(C_{TW\infty(Std\,2)})\right)^2 \end{aligned}}$$

Analytical errors (error of measurement)

$\sigma(m_{TW(Std1)})$ = 0.002 g

$\sigma(m_{TW(Std2)})$ = 0.002 g

$\sigma(C_{TW(Std1)})$ = 0.1 ‰ for ^{18}O and 1.0‰ for ^{2}H

$\sigma(C_{TW(Std2)})$ = 0.1 ‰ for ^{18}O and 1.0‰ for ^{2}H

$\sigma(C_{TW\infty(Std1)})$ = 0.1 ‰ for ^{18}O and 1.0‰ for ^{2}H

$\sigma(C_{TW\infty(Std2)})$ = 0.1 ‰ for ^{18}O and 1.0‰ for ^{2}H

Derivations

$$dm_{PW}dm_{TW(Std1)} = \frac{\left(C_{TW(Std1)} - C_{TW\infty(Std1)}\right)}{\left(C_{TW\infty(Std1)} - C_{TW\infty(Std\,2)}\right)}$$

$$dm_{PW}dm_{TW(Std\,2)} = \frac{-\left(C_{TW(Std\,2)} - C_{TW\infty(Std\,2)}\right)}{\left(C_{TW\infty(Std1)} - C_{TW\infty(Std\,2)}\right)}$$

$$dm_{PW}dC_{TW(Std1)} = \frac{m_{TW(Std1)}}{\left(C_{TW\infty(Std1)} - C_{TW\infty(Std\,2)}\right)}$$

$$dm_{PW}\,dC_{TW(Std\,2)} = \frac{-m_{TW(Std\,2)}}{\left(C_{TW\infty(Std\,1)} - C_{TW\infty(Std\,2)}\right)}$$

$$dm_{PW}\,dC_{TW\infty(Std\,1)} = \left(\frac{-1}{\left(C_{TW\infty(Std\,1)} - C_{TW\infty(Std\,2)}\right)} - \frac{\left(C_{TW(Std\,1)} - C_{TW\infty(Std\,1)}\right)}{\left(C_{TW\infty(Std\,1)} - C_{TW\infty(Std\,2)}\right)^2}\right) \times m_{TW(Std\,1)} + \left(C_{TW(Std\,2)} - C_{TW\infty(Std\,2)}\right) \times m_{TW(Std\,2)}$$

$$dm_{PW}\,dC_{TW\infty(Std\,2)} = \left(\frac{\left(C_{TW(Std\,1)} - C_{TW\infty(Std\,1)}\right) \times m_{TW(Std\,1)}}{\left(C_{TW\infty(Std\,1)} - C_{TW\infty(Std\,2)}\right)^2} + \frac{1}{\left(C_{TW\infty(Std\,1)} - C_{TW\infty(Std\,2)}\right)^2} - \frac{\left(C_{TW(Std\,2)} - C_{TW\infty(Std\,2)}\right)}{\left(C_{TW\infty(Std\,1)} - C_{TW\infty(Std\,2)}\right)^2}\right) \times m_{TW(Std\,2)}$$



wsp.com

